Statistical inference for infectious disease data of animals

Rebecca Namugabwe Nsubuga

Doctor of Philosophy
University of Edinburgh
2003

Declaration

I declare that this thesis was composed by myself and that the work contained therein is my own, except where explicitly stated otherwise in the text.

(*Rebecca Namugabwe Nsubuga*)

Abstract

Efficient parameter estimation is increasingly recognised to be essential in fitting epidemic models to data. This thesis primarily explores parameter estimation methods as applied to data generated from an experimental infection with foot and mouth disease (FMD) virus in sheep. Data were generated from two experiments involving four groups of sheep, housed under restricted mixing, where sheep in the initial group were inoculated with type O FMD virus. The aim of the analysis is to investigate the presence of any trend in the infection rate with increased generation.

The infection process of FMD virus in sheep can be modelled using chain binomial models and generalized linear models. However, application of these methods requires that the epidemic chain of infection pathways be known. The set of true pathways is an unobservable quantity and, in general, infectious disease data will be incomplete because the infection process is only partially observed. One proposed strategy is subjectively to assign an epidemic chain to the data and to analyse it on this basis. This approach is evaluated.

An alternative to modelling the FMD infection process for individual sheep is to consider the transmission among groups of sheep, thus avoiding the need to make inference about individual infection pathways. Martingale methods and maximum likelihood estimation methods are used to estimate the typical infection rate β applying to groups of sheep where the aim is to investigate whether the infection rate changes across groups. The expected total infection exposure for each group is estimated. This entails knowledge of the time of infection, the latent period and the infectious period for each infected sheep. Parameters for the latent period and infectious period distributions are estimated from the data. A joint distribution of time to infection and latent period is formulated from which expected values for time to infection and the latent period for each infected sheep are estimated. The expected infectious period is estimated by fitting the infectious period distribution to the observed data. Estimates of these expectations and of β are calculated iteratively using an analogy of the Expectation Maximization (EM) algorithm until convergence occurs.

Trends in estimates across groups are summarised using weighted linear regression and their significance is tested using bootstrap methods. The power of the methodology is explored using simulated data from a Susceptible-Latent-Infectious-Removed (SLIR) model that reflects the design of the experiments.

In the final part of the thesis, the properties of the confidence interval based on asymptotic likelihood theory are compared with those of the percentile confidence interval generated by parametric and semi-parametric bootstrap methods. Bootstrap calibration is applied to each of these methods. Simulated data are used to explore the coverage properties of different confidence intervals for the basic reproduction ratio (R_0) of a SIR infection process.

Acknowledgements

I would like to thank my supervisors Iain McKendrick and Mark Woolhouse for their patience, encouragement, guidance and support during the course of this work. I am thankful to the late Rob Kempton for paving the way for me to do my PhD in BioSS and for his input in this work. I am grateful to Gareth Hughes and Valerie Mioulet for the data used in this thesis. Thanks must also be given to Dan Haydon for his assistance during the early stages of this work and to the BioSS students for many stimulating discussions. The application of the GLMs in this thesis is down to Mart de Jong and his group in Lelystad, Netherlands therefore many thanks to them. Thanks go to Louise Matthews and Fabian Nabugoomu for proofreading parts of this thesis. I am thankful to Patrick Mangheni for the endless journeys to 'main building' while following up my living expenses from Makerere University. I also appreciate the encouragement and moral support from my parents Benoni and Beatrice Sajjabi, my mother in law Edith Kigobe, Alex, Petero, Eunice, Esther, friends in Edinburgh and all friends and family at home. I acknowledge help received from Vicky Ward and from Ian Stewart & family, especially child minding my son Jethro. Many thanks for the support and for putting up with short notice calls regarding Jethro's care. A special vote of thanks goes to my husband, Saul, for all the support during the course of this work, for taking care of Jethro and Jonathan and for keeping the home running. Thanks to Jethro for being patient while *maama* was working away. To baby Jonathan, I say thank you for being such an understanding little boy while *maama* was doing the final corrections to the thesis. Lastly I am grateful for the funding from UNESCO, BioSS, Makerere University and CTVM that has enabled me to complete this work.

Table of Contents

Chapter 1

Introduction

Efficient parameter estimation is increasingly recognised to be essential in fitting epidemic models to data. This thesis explores parameter estimation methods as applied to infectious disease data, in particular, data about infectious diseases of animals. Animals are a well defined source of a number of infectious diseases in humans. It is known that infectious diseases can easily cross from animals to humans and a sizeable volume of literature exists on the subject. Taylor et al. (2001), in their review involving 1415 species of infectious organisms known to be pathogenic to humans, identified 61% as zoonotic *i.e.* they can be transmitted between humans and animals. According to Weiss (2001), animals have been a major source of human infectious diseases since time immemorial. The author gives examples of infections such as rabies which are caused by direct animal-to-human transmission or of variant Creutzfeldt-Jacob disease (vCJD) which arose from bovine spongiform encephalopathy (BSE) a recent example of direct zoonosis. BSE is caused by prions and was first observed in 1986 in Great Britain. It was presumably spread by trade in feed containing the infectious agent and there is a strong evidence that both the previously unknown human prion disease, new vCJD and BSE are caused by the same agent (Donnelly et al., 1999; Kretzschmar and Lederer, 2002). According to Borchers (2002), there is evidence that in Great Britain by the end of March 2001, 97 young people acquired vCJD due to consumption of food that contained bovine risk material. Erstad (2002) emphasises that ingestion of prion-infected beef remains the only known cause of new vCJD. Weber et al. (1997) and Donnelly et al. (1999) point out that public concern in Great Britain and Northern Ireland remains focused on the probable link between BSE infection in cattle and new vCJD in humans.

Escherichia coli O157 (*E.coli* O157) is another pathogen responsible for the development of a number of syndromes in humans. *E.coli* O157 is found regularly

in faeces of healthy cattle (Synge et al., 2000) and is transmitted to humans through contaminated food, water and direct contact with infected people or animals (Pennington Group, 1997; Shinoda et al., 1997; Mead and Griffin, 1998). *E.coli* O157:H7 is often a cause of serious disease in humans with asymptomatic animal carriers cited as a reservoir of infection (Clifton-Hadley, 2000). Various authors, for example, Richter et al. (1997); Heuvelink et al. (1998); Hu et al. (1999) and Osek (1999) believe that cattle are the main carriers of the pathogenic bacteria, with food of animal origin (especially beef and milk) being important sources of infection. Other zoonoses apart from BSE and *E.coli* O157, mainly transmissible from animal to man through contaminated food are: salmonellosis, listeriosis and campylobacteriosis (Ganiere et al., 2001). Jemmi et al. (2000) point out that the risk of zoonotic disease transmission when handling livestock or animal products is substantial. The authors further point out that in industrialised countries, diseases such as salmonellosis and campylobacteriosis which can cause serious disease in humans have become a major public health problem.

Companion animals are also a potential route of infection from animals to man. According to Kolarova et al. (2002), the development of close contacts between humans and animals that served humans for meat and as guardians encouraged the exchange of microflora between species. By inhalation of aerosol from animal hair or scales and especially by consumption of animal meat, eggs and milk, humans became subject to the natural circulation of animal microorganisms. Geffray and Paris (2001) point out that domestic pets can transmit numerous bacterial, parasitic, fungi and viral infections and the authors highlight the need to improve knowledge about the epidemiology of pet-transmitted zoonoses.

According to Thrusfield (1995), Chapter 20, in western countries, government veterinary services are increasingly required to justify their budgets, as the role of the public sector diminishes. Also, as the importance of agricultural output declines in these countries, the economic justification for animal disease control is queried more closely. With rising incomes and changing social values, attention in the western countries has widened from the initial (relatively narrow) evaluation of disease in farm livestock to address both qualitative aspects of food production and diseases of companion animals. However, diseases of farm livestock, in addition to being sources of infection to humans, are barriers to international trade. There is a current drive to liberalise world trade through the world trade organisation (WTO) and to the problem of livestock diseases has become even more acute. For instance an exporter of infected product may face higher tariff

than would otherwise be the case (Paarlberg and Lee, 1998). The problem of spread of diseases also impacts upon the harmonisation of trade in the EU which requires free movement of commodities (Zwingmann and Fiedler, 2001). In general, animal diseases have economic as well as biological impact on humans. As already noted above, disease in a livestock population poses a risk to humans as a result of consumption of contaminated animal products (Cornick et al., 2000; Phillips et al., 2000; Bouvet et al., 2001; Chapman et al., 2001; Cobbold and Desmarchelier, 2001; Watson, 2001). Disease in livestock population also reduces the quality and/or quantity of livestock products available for human consumption and export. More importantly, from the economic point of view, disease in livestock populations deters people from consuming associated animal products.

According to Baker and Ridley (1996), following a report of 10 cases of new vCJD which precipitated alarm throughout Europe, the beef trade in the UK collapsed. The 2001 UK foot-and-mouth disease epidemic, is the most recent example of the effect of animal diseases on the economy. This epidemic had vast impact on the agricultural and tourism industries. Thompson et al. (2002) estimated losses to agriculture arising from the epidemic at about 3.1 billion pounds. The authors indicate that the majority of the costs were met by government through compensation for slaughter and disposal as well as clean-up costs. Nevertheless, farmers will have suffered losses which the authors estimated at 355 million pounds, representing 20% of the estimated income from farming in 2001. Taylor (2002) points out that the restrictions imposed for more than 10 months throughout the country in 2001 to control and eradicate FMD had damaging effects on tourism and rural businesses. The decision to eradicate the disease by slaughter rather than vaccination saw a huge number of animals destroyed. Davies (2002) estimates that over 4 million animals were slaughtered from 2000 herds and flocks while Scudamore et al. (2002) put the number of slaughtered animals at 6.5 million of which over 4 million were removed as a direct result of the disease, while a further 2.5 million were slaughtered on welfare grounds. Mepham (2001) questions the ethical validity of the procedure *i.e.* the slaughter of millions of animals, to eradicate the disease. According to Cassagne (2002), FMD has devastated animal husbandry in the Netherlands frequently in the past and still constitutes a threat. The author points out that in 2001, the FMD outbreak proved very disruptive to the wider rural economy, such as the recreational and tourism sectors. Garner et al. (2002) in their study of the economic aspects of FMD in Australia emphasize that an outbreak of FMD would have severe economic consequences on the economy. The authors estimate that in an outbreak lasting six months, real gross

domestic product in Australia would fall by an estimated 3.5 billion Australian dollars and point out that much of the impact would be due to loss of export markets. Undoubtedly, the biological and economic problems that result from infections in animals both serve to emphasize the importance of understanding the mechanisms underlying the spread of diseases in animals.

For some diseases *e.g. E.coli* O157, it is very difficult to identify the virulent strains, Karakulska and Nawrotek (1999) emphasize that it is very important to work out diagnostic methods which will detect the pathogens in the environment quickly and effectively. For FMD, there are variations in the indicators of disease, for instance clinical signs may be observed only after viraemia has already commenced (Hughes et al., 2002b) and there is a high risk of infected animals, especially sheep, being misdiagnosed (Dekker and Terpstra, 1999; Blanco et al., 2002). For such a disease it is vital that laboratory diagnostic tests are very sensitive. Molecular biologists, for instance in Paton and Paton (1998); Karakulska and Nawrotek (1999); Reid et al. (2002) and Reid et al. (2003), are carrying out research to try to perfect diagnostic tests.

Mathematical and statistical modelling has been used in efforts to try to understand the spread of diseases and to estimate parameters of biological importance. Mathematical modelling has been widely used to understand the spread of diseases in human populations. Mathematical modelling in epidemiology was pioneered by D. Bernoulli in 1760 in his work demonstrating the effectiveness of the technique of variolation against smallpox (Anderson and May, 1991, Section 1.2; Valleron, 2000). Mathematical modelling in human disease has investigated infectious diseases such as HIV infection (*e.g.* Coutinho et al. (2001); Greenhalgh and Hay (1997); Salomon and Murray (2001)), Prion diseases (Ferguson et al., 1997), amongst others, as well as non-infectious diseases such as cancer (Valleron, 2000). le Corfec et al. (2000) argue that mathematical models have contributed to a better understanding of the pathogenesis of AIDS.

Mathematical and statistical models are now being used to help understand the dynamics of infectious diseases in animals. For example Anderson et al. (1996) use epidemic models to investigate the transmission dynamics and epidemiology of BSE in British cattle. Ferguson et al. (1999) use models in the estimation of the basic reproduction number of BSE in British cattle. Stringer et al. (1998) formulate a mathematical model to assist in the interpretation of field data following an outbreak of scrapie in a single sheep flock. Woolhouse et al. (1998) use a mathematical model to explore the expected course of an outbreak of scrapie in

a sheep flock and the potential impact of different control measures. Matthews et al. (2001) and Woolhouse et al. (1999) use a mathematical model to understand the epidemiology and population dynamics of scrapie following an outbreak in a flock of Cheviot sheep. MacKenzie and Bishop (2001) use a stochastic model to describe disease transmission dynamics on a pig farm. van Nes et al. (2001) use mathematical and statistical models to analyse an outbreak of pseudorabies virus in a vaccinated sow herd. Nodelijk et al. (2000) use stochastic models to analyse observational data of porcine reproductive and respiratory syndrome virus in a Dutch breeding herd. Stegeman et al. (1999) use a model to estimate the period when classical swine fever virus had been introduced into herds where the infection started in the breeding section during the 1997/98 epidemic in The Netherlands. Jalvingh et al. (1999) use spatial-temporal and stochastic simulation models to evaluate the impact of events and control measures in the 1997/98 classical swine fever epidemic in The Netherlands. Woolhouse et al. (1996) use models to evaluate the effectiveness of vaccination in preventing persistent outbreaks of FMD in Saudi Arabian dairy cattle herds. Durand and Mahul (2000) use what they term an extended state-transition model to study FMD epidemics in France. Dexter (2003) uses stochastic models to explore how stochastic variation in the population dynamics of feral pigs in the Australian semi-arid rangelands affects the probability of persistence of an FMD outbreak and its impact on the density of feral pigs. During the 2001 UK foot-and-mouth disease epidemic, mathematical models were used to guide the disease control policy (Woolhouse, 2003). Ferguson et al. (2001b) and Ferguson et al. (2001c) used models to analyse the transmission intensity and impact of control policies on the epidemic. Morris et al. (2001) used a spatial simulation model to evaluate alternative control policies for the epidemic. Keeling et al. (2001) used an individual farm-based model to explore different options of vaccination in advance of a FMD outbreak following the 2001 UK FMD epidemic.

The importance of modelling was underlined in the Royal Society of London's report on the 2001 UK foot-and-mouth disease epidemic, which stated: "*Quantitative modelling is one of the essential tools both for developing strategies in preparation for an outbreak and for predicting and evaluating the effectiveness of control policies during an outbreak*" (Royal Society, 2002). This report emphasises that more work is required to refine the existing models. When investigating disease transmission in animals, surveys and experiments have an important role as they provide quantitative data enabling statistical analyses to be carried out. However, there is a need for more refined analytical techniques which could utilise

smaller numbers of animals in experiments in line with the UK government policy encouraging the 3Rs of refinement, reduction and replacement (Hay, 1998). In the wake of the 2001 UK foot-and-mouth disease epidemic, the UK government has come to appreciate the importance of animal experiments in trying to understand the mechanisms of infectious diseases. Government agencies now believe that animal experiments have a valuable contribution to make in understanding epidemic mechanisms and in developing control strategies (Matfield, 2002; Anonymous, 2003).

1.1 Infectious diseases in animals

An infectious disease is one in which an animal is invaded by a foreign organism such as a virus, bacterium or parasite from another infected animal. Some infectious diseases require intermediary vectors in order to spread from one animal to another. For instance, equine infectious anaemia of horses can only be spread from one animal to another by blood-sucking biting flies (Hunter, 1996). Infectious diseases can also spread between animals without any intermediary agent and these are sometimes referred to as contagious diseases. Contagious diseases can be spread by direct or indirect transmission. Direct transmission occurs mainly with viruses that do not survive long in the environment. Infection in this case only occurs when there is close contact between diseased and healthy animals. Some organisms can infect animals via the skin, usually by contamination of cuts and abrasion. For example, in bovine farcy, a chronic disease of cattle characterised by lesions under the skin, infection occurs via contamination of skin wounds from tick bites and thorn bushes (Hunter, 1996). Indirect transmission occurs in cases where the infectious organism can survive outside the animal and hence be picked up from the environment. Susceptible animals may become infected by ingestion of contaminated food and water (Hinton, 1993). This is an important route of transmission for many infectious organisms. The longer the organism survives in the environment, the greater the chances of susceptible animals becoming infected through this route. For instance FMD spreads rapidly because infected animals discharge large amounts of the infecting virus in saliva, milk, faeces, semen, urine and exhaled breath to the environment where it may survive for several months (Dekker and Terpstra, 1999). The *E.coli* O157 organism can survive in faeces for a long time (Chapman et al., 1993; Pennington Group, 1997). Other infectious diseases may be transmitted through bedding, vehicles, and harness. This route

of infection is referred to as infection from formites (Bartely et al., 2002). For example in sheep and goat pox, animals can become infected by rubbing against contaminated formites such as sheep pens, as the virus can survive for many months in the environment.

Some infectious diseases are associated with environmental and husbandry factors (the way animals are managed by their owners). It is therefore important to understand the nature of livestock management when designing disease control programmes. For example, mastitis in the modern dairy herd is relatively rare in cows which suckle their calves naturally but it is a very serious problem in high producing dairy cows milked by machine (Kruze, 1998). If not carried out properly with high standards of hygiene, the process of machine milking can lead to bacterial infection of the udder and hence to mastitis (Barkema et al., 1999). Another example of infectious diseases triggered off by environmental or husbandry factors are clostridial toxaemias in which animals are poisoned by toxin produced by infecting clostridial bacteria (Hunter, 1996). These bacteria are widespread in nature, being found in soil, organic matter and are natural inhabitants of the intestines of livestock (Levett, 1986; Alsaif and Brazier, 1996). Although infections with these organisms are normally harmless, in the presence of certain predisposing factors *e.g.* a sudden improvement in nutrition or tissue damage, they can multiply rapidly and produce large quantities of toxins which poison the animal. Tetanus is a good example of such an infection; the causative organism, *Clostridium tetani* localises and multiplies in contaminated cuts and wounds producing a toxin which affects the nervous system. Bruggemann et al. (2003) warn that tetanus is one of the most dramatic and globally prevalent diseases of humans and vertebrate animals, and has been reported for over 24 centuries. The authors point out that the main manifestation of the disease, spastic paralysis, is caused by the second most poisonous substance known, the tetanus toxin, with a human lethal dose of approximately $1ng/kg$. Fortunately, the disease can be successfully controlled through immunization with tetanus toxoid (Bruggemann et al., 2003).

In general there are many different routes by which an organism may pass from an infected individual to a non-infected one. Knowledge of these routes is essential in devising methods to prevent infection. It is essential to understand the agents that cause infectious diseases in order to appreciate better the process by which diseases occur. Micro-organisms are defined as being pathogenic and often referred to as pathogens when they cause a range of pathological changes to tis-

sues once they have invaded an animal. In nature there are thousands of different types of micro-organisms but only a small proportion are pathogenic. Infection due to a particular organism can be diagnosed using a number of criteria, which include clinical signs and symptoms, detection of specific agents, reaction to diagnostic tests and identification of lesions (Dekker and Terpstra, 1999; Reid et al., 2001; Hughes et al., 2002b).

With the "reaction to diagnostic tests" criterion, test reactions may be observed, for example, the reading of antibody titres in serological tests. Serological methods involve investigation of disease and infection in animals by measurement of variables present in serum: for instance, the specific antibody activity of immunoglobulin. Antibodies provide evidence of current and previous exposure to the infectious agent. However, because most commonly used diagnostic tests are neither 100% sensitive nor 100% specific, animals may be misdiagnosed. Animals may be recorded as having an infectious agent present or having had exposure to infectious agent when actually no such exposure has occurred. This constitutes a false positive record. Alternatively, an animal may be recorded as having no infectious agent present or not having had exposure to infectious agent when actually the converse is true. This constitutes a false negative record. Such errors lead to misclassification of infected and non-infected animals. There is therefore a need to validate diagnostic tests. Sensitivity, the proportion of true positives that are detected by the test, and specificity, the proportion of true negatives that are detected by the test are indicators of the validity of diagnostic tests. In Figure 1.1, extracted from Hughes et al. (2002b), where the FMD virus infection in sheep was examined experimentally, it is observed that detection of infected sheep would highly depend on the diagnostic criterion used. For instance using virus isolation from blood as the diagnostic criterion yielded a higher proportion of infected sheep than the criterion of antibody detection in serum and that of clinical signs. The results of these experiments have implications for the diagnosis and control of FMD virus infections and estimation of sensitivity and specificity is another important aspect of veterinary infectious disease data.

1.2 Foot-and-mouth disease

Foot-and-mouth disease (FMD) is a very important and extremely infectious viral disease of cloven hoofed animals and occasionally man (Hunter, 1996). FMD virus can be spread via saliva, milk, semen, faeces, urine and exhaled air as well as

Figure 1.1: *Graph illustrating the epidemiology of experimental FMD virus infection is sheep: graph extracted, with permission, from Hughes et al. (2002b).*

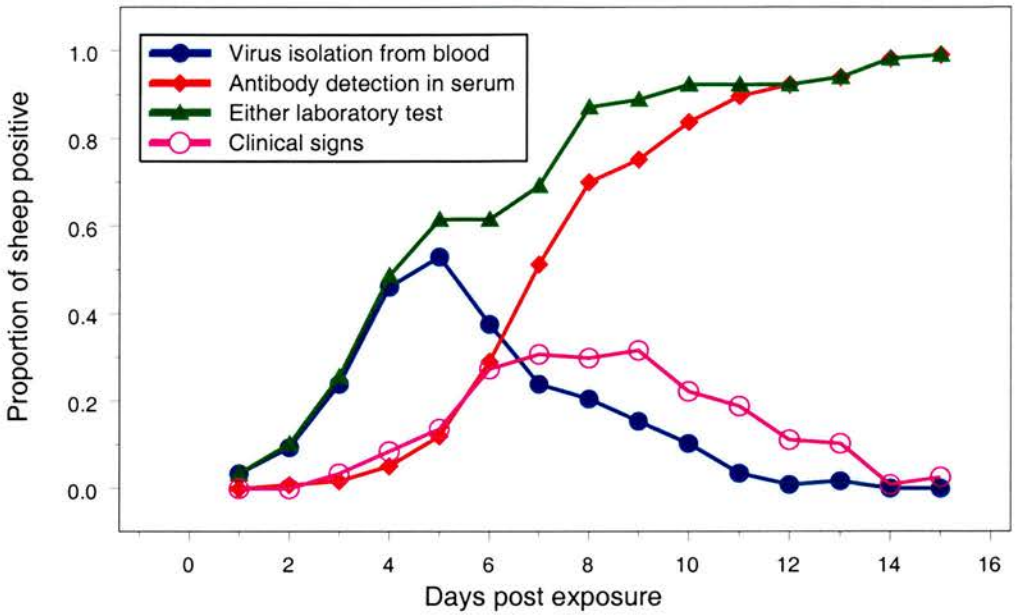

being released directly from ruptured vesicles. The virus is extremely infectious and susceptible animals may be infected by inhalation or ingestion of the virus by various means *e.g.* from nearby infected animals, a virus contaminated environment or in feed, notably uncooked swill containing animal tissues such as lymph nodes, bone marrow and viscera. The virus can also be transferred from location to location on vehicles or clothing, and in cool humid conditions the virus can become wind-borne for long distances. According to Sanson (1994), FMD may well be the most contagious disease known in the animal kingdom. The author attributes this property to the ability of FMD to gain entry and initiate infection through a variety of sites, its small infective dose, short incubation period, the release of virus before the onset of clinical signs, the massive quantities of virus excreted from infected animals, its ability to spread large distances due to airborne dispersal and the persistence of the virus in the environment. The author warns that the above features plus the ability of the virus to be disseminated through movements of animals, animal products, people, plants and equipment all make the disease very difficult to control.

There are seven serotypes of FMD virus, namely A, O, C, SAT 1, SAT 2, SAT 3 and ASIA I and within each serotype there are further sub-types. The disease is enzootic in many parts of the world. In Africa types A, O, SAT 1 and SAT 2 are

widespread while type C is rare and type SAT 3 is mainly present in Southern Africa and Sudan. FMD is absent from North and Central America, Australia, Pacific Islands and most of Europe but endemic in countries bordering continental Europe (Hunter, 1996). Before the 2001 outbreak of FMD in the UK, there had been recent outbreaks in various parts of the world including EU countries (*e.g.* Greece in 1996) Hughes (2001).

Through global trade links, there is always a risk of the virus being exported to virus free countries. Gallagher et al. (2002) on estimating the risk of importation of FMD into Europe concluded that the illegal importation of livestock was the most likely route of introduction of FMD into Europe. Moennig and Kramer (2002) warn that EU member states face a high risk of introduction of FMD through increasing trade and tourism but also through the illegal importation of animals and animal products from all over the world. The 2001 UK FMD epidemic is a concrete example of the disease breaking out in a country after several decades of freedom from FMD. Animal feed is another important source of FMD, for instance the feeding of swill to pigs not only creates a risk of introducing classical swine fever but also of introducing FMD. Indeed, according to Alexandersen et al. (2003), during the 2001 UK FMD epidemic, the first outbreak was at an abattoir which specialised in the processing of culled sows and boars followed by confirmation of the disease at a pig farm fed on waste food. As reported in Bruckner et al. (2002), in 2000 South Africa lost its designation as a zone free from FMD without vaccination in domestic stock attained in 1995 due to the re-introduction of FMD in domestic livestock when the first ever recorded case of serotype O in South Africa was diagnosed in a piggery after the illegal feeding of untreated swill. FMD virus can be moved a big distance by airplanes and boats into a disease free country (de Clercq, 2002).

Moennig and Kramer (2002) highlight that during the 2001 UK FMD epidemic, a rapid spread of the disease became possible through trans-species infection from pigs to sheep. As FMD symptoms are less pronounced in sheep compared to cattle and pigs, this resulted in a late detection of the disease. This factor and the intense trade in animal open markets coupled with numerous long distance animal transports caused the rapid spread of FMD over the country and the export of infection to France and The Netherlands. Moennig and Kramer (2002) also point out that the inadequate hygiene management prevalent in most cattle operations might facilitate the spread of FMD infection, warranting the establishment of legal rules to define an adequate hygiene status for cattle holdings, equivalent to

those criteria implemented for the pig industry. Although not formally confirmed during the UK outbreak, FMD can be transmitted through contact with wildlife (Bruckner et al., 2002). Donaldson (1997) suggests that in the early stages of an outbreak, in a country which is normally free of FMD, before disease control measures have been implemented, FMD can be spread through untreated milk because cattle are not routinely vaccinated.

In endemic areas, the disease in indigenous livestock may follow a mild course with animals recovering in a few days but susceptible animals (*e.g.* exotic cattle) may be severely affected. Although the lesions heal fairly rapidly, convalescence can be prolonged, causing significant losses in milk and meat production and through infertility. Also, draught buffaloes and oxen may be unable to work. Although the disease is generally extremely infectious, less than 5% of affected animals die (Hunter, 1996). FMD causes both clinical and subclinical infection, depending on the natural or acquired immunity of the host. Hutber et al. (1999) point out that within vaccinated dairy herds, FMD may appear as an acute, mild or subclinical infection, depending upon the immune status of the herd, the level of challenge and the efficacy of the vaccine used. The FMD virus can survive outside the infected host for up to several months if not subjected to heat or change in pH, for example, the virus can survive for fifteen weeks on hay and straw (Bartely et al., 2002). In frozen carcasses, the virus can survive for prolonged periods in lymph nodes, viscera and bone marrow.

It is evident from the literature that there is enormous concern about animal diseases, especially those diseases which affect humans medically, socially or economically. It is therefore important that the epidemiology of animal diseases be studied to facilitate the design of control measures. This thesis will investigate statistical inferential techniques as applied to veterinary infectious disease data. It will incorporate a practical component where various inferential methods will be applied to data describing experimental infections of FMD virus in sheep. As discussed earlier in this section, FMD is a highly important disease, and hence it is crucial that the properties of the virus are investigated.

1.3 The foot-and-mouth disease experiments

In this thesis inference will be performed on data generated from experiments infecting sheep with FMD virus. The experiments were inspired by earlier studies

of type O FMD epidemics, which produced unexpected results (Hughes, 2001). These studies followed the outbreaks of FMD in Greece in 1994 and in Tunisia in 1989-90. Results from these studies suggested a marked progressive reduction in the infection potential. The observations made in these studies would suggest that FMD outbreaks could be self-limiting in sheep for some virus strains. The observed epidemiology of the natural outbreaks certainly suggested that some strains of FMD virus were weakly maintained in sheep populations under certain conditions. Such a suggestion if true, would have important implications for the design of FMD control programmes in outbreaks involving sheep as the predominant hosts.

The experiments described in this section were an attempt to assess transmission of the virus through the infection of sequential groups of sheep in a well defined experimental situation. It was crucial to the design of the experiments to ensure a consistent exposure period for sequential groups of sheep. Preliminary experiments (Hughes, 2001) were performed using one animal room within an isolation unit. During these experiments, a group of sheep were initially infected with FMD virus and further susceptible groups of sheep were introduced after the earliest definitive sign of FMD. Analysis of these experiments suggested that due to the early (pre-clinical) excretion of FMD virus by infected sheep, a considerable proportion of the viral excretion was lost before the new susceptible groups of sheep were introduced to the room. Thus it was difficult to expose recipient groups of sheep to the total viral excretion of the donor group while ensuring that the total viral load from these animals is shed in the presence of their (further) recipient group. Subsequent experiments were therefore designed in such a way as to ensure that each recipient group was exposed to the same proportion of the total virus excreted by the donor group. The exposure period was set at 24 hours following another set of preliminary experiments which demonstrated that a 12 hour exposure period was not sufficient to allow transmission to occur beyond the second group. All contact groups of sheep were to be exposed to virus for 24 hours by moving 'up-stream' and following this period, spend 24 hours 'down-stream' potentially donating virus. To ensure that at least some sheep in group 1 had reached peak infectivity when group 2 was brought into contact, inoculation of group 1 was staggered.

1.3.1 Design and objective of experiments

Two identical experiments were carried out within a high security isolation unit at the Institute of Animal Health in Pirbright. The experiments involved four groups (G1-G4) of eight sheep, each group housed in a different room for three days prior to the start of the experiments. All sheep in group 1 were inoculated with the virus, inoculation being staggered in time to ensure a wider distribution of peak infectiousness. Half of group 1 sheep (denoted group $1a$) were inoculated on day 0 while the other half (group $1b$) were moved to a separate room and these were inoculated 24 hours later. All group 1 sheep were inoculated with 10^5 $TCID_{50}$ of FMD virus type O Greece 23/94 in 2ml of M25 buffer intranasally using a 2 inch-length of sterile rubber tubing. Groups of sheep were moved between rooms repeatedly after 24 hours had passed. The movement of groups between rooms are shown in Figure 1.2.

Figure 1.2: *Pattern of movements of groups of sheep in the FMD experiments.*

	MIXING GROUPS			
DAY	Room1	Room2	Room3	Room4
0	G1	G2	G3	G4
1	G1&G2		G3	G4
2	G1	G2&G3		G4
3	G1&G2		G3&G4	
4	G1	G2&G3		G4
5	G1&G2		G3&G4	
6	G1	G2&G3		G4
⋮	⋮	⋮	⋮	⋮
Odd Day	G1&G2		G3&G4	
Even Day	G1	G2&G3		G4

24 hours after the inoculation of group $1a$ sheep, group 2 sheep are moved into the

group 1 room and stay there for 24 hours. They are subsequently moved back to their room and joined by sheep from group 3 for 24 hours. Group 3 sheep are then taken back to their room and joined by group 4 sheep for 24 hours; at the same time group 2 sheep are moved back to the group 1 room where they all remain for 24 hours. After the movement of animals has commenced, sheep repeatedly spend 24 hours in their own room and 24 hours in the preceding room except for group 1 sheep: these remain in their own room throughout the experiment. This process continues until there are no shedding sheep in any groups (7 days after viraemia ceased, see Section 1.3.2 below) and sufficient time had been allowed for any infected but pre-patent animals to become apparent (10 days). All uninfected sheep were challenged at the end of each experiment by intranasal inoculation of 10^5 $TCID_{50}$ of FMD virus type O Greece 23/94 in 2ml of M25 buffer to confirm that they were susceptible to infection.

All sheep movements took place at the same time each morning. Groups of sheep were moved along a 'dirty' corridor, starting with the highest group number. The corridor was disinfected thoroughly after each movement. This ordering should ensure that, should disinfection fail, animals would be typically exposed to virus from a higher passage than that to which they are exposed in their rooms. Following movement, all sheep were sampled, starting with the lowest group. All staff were disinfected thoroughly before moving to a different room.

The main hypothesis to be tested is whether there is an intrinsic diminution in the infectivity of infected animals during the course of successive naturally transmitted infections of FMD virus.

1.3.2 Sampling

On each day of the experiments, blood samples were taken for serology and FMD virus isolation (details found in Hughes (2001)). Throat swabs were also taken every day and were tested for presence of FMD virus using polymerase chain reaction (PCR) (Reid et al., 2001). All sheep were examined daily for clinical signs of FMD in the mouth and on all four feet. Rectal temperatures were recorded daily. Oesophageal-pharyngeal fluid (OPF) was taken from every animal on days estimated as 30 and 33 post-infection for the first experiment and 35 and 38 days post-infection for the second experiment. Animals that did not develop clinical disease at the end of the epidemic were tested for immunity. Processing of samples is described in Hughes (2001).

1.3.3 Observed data from FMD experiments 1 and 2

The observed data as obtained from the experiments is presented in Figures 1.3 and 1.4 for experiments 1 and 2 respectively. The data are viraemic periods, indicating days of detected virus shedding. The 'red' region indicates days when sheep tested positive to FMD virus. For example sheep number 1 from experiment 1 tested positive on days 2, 3 and 4. Methods developed in this thesis will be applied to these data.

Figure 1.3: *Viraemic periods for sheep during serial passage experiment 1. The 'red' bars indicate viraemic periods.*

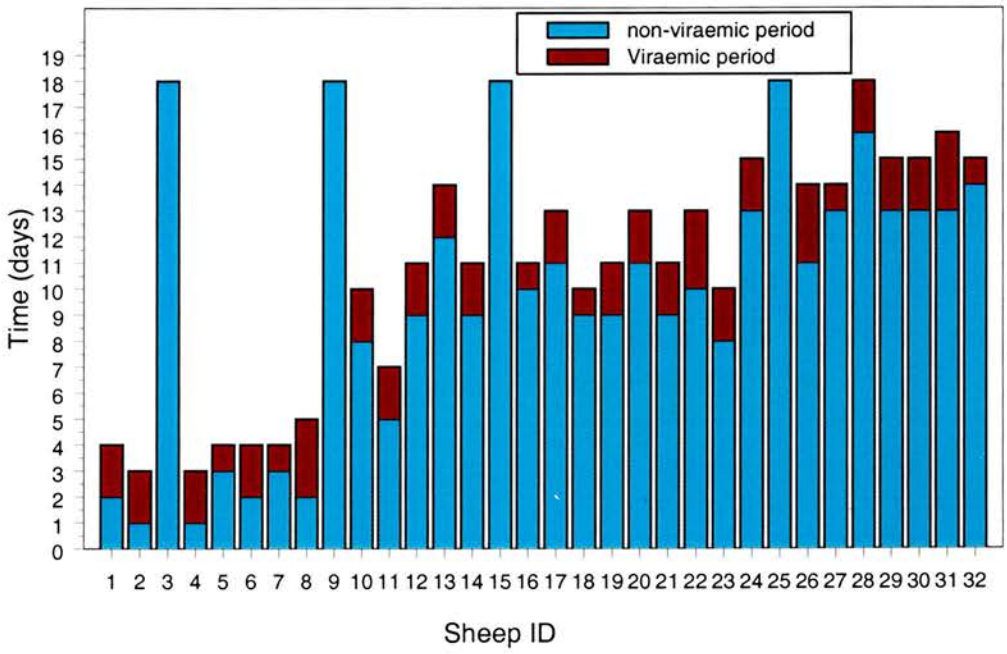

1.4 Infectious disease data

Infectious disease data are usually obtained from epidemics occurring in nature rather than from planned experiments. This fact makes it difficult to accumulate precise and detailed data and often infectious disease data are incomplete due to partial observation of the infection process. For instance, it might be that only the initial and final states of the epidemic are observed or that the data consist of initial values and continuous observation of the removal process, as infected animals are either identified or removed from the population. The number of

Figure 1.4: *Viraemic periods for sheep during serial passage experiment 2. The 'red' bars show viraemic periods.*

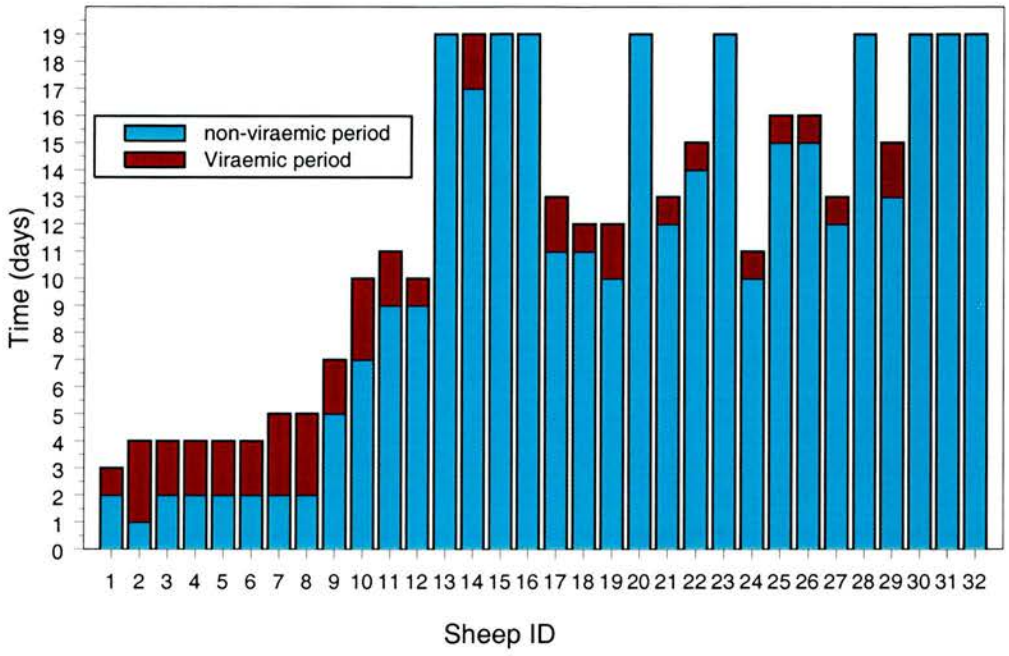

infective and susceptible individuals is not observable at all time points during the period of the epidemic. Usually it is impossible to observe the time at which infections occur or to know which infected individual is responsible for transmitting the disease to a particular susceptible. For some diseases one can hope to have the times at which infected individuals show certain symptoms, this is the most reliable information one can collect about the physical infection process. In practice, one is usually aware of infectives only when they show symptoms but it is sometimes possible to deduce, at least approximately, the times at which infections have occurred and when infected individuals are infectious. For example, Becker (1995) points out that the measles rash erupts about 14 days after infection with relatively little variation and it is reasonable to assume that individuals are infectious during the period immediately prior to the eruption of the rash. However, in the case of animals, it is often not easy to tell if an animal is infected until it finally breaks down or exhibits clinical signs. This is true of FMD in sheep (Sanson, 1994; Hughes et al., 2002b). This makes veterinary infectious disease data even more difficult to analyse. In summary, analysis of these data requires special attention because of the following difficulties:

1. The spread of infection through a community is only partially observable.

2. Dependence in the data usually leads to a likelihood function with an analytically intractable form.

3. Relatively little is known about characteristics that are not directly observable such as the duration of the latent period, which makes it difficult to fit parametric models for the entire progression of the disease as is required for most likelihood-based inference methods.

1.4.1 Issues in the analysis of infectious disease data

The analysis of infectious disease data presents new statistical challenges because standard methods of inference such as those based on likelihood are often too complicated to implement (Becker, 1995). The complexities arise because the infection process is only observed partially leading to the introduction of many integrals into the likelihood function to integrate over unobserved variables. These likelihoods are difficult to analyse and cannot be simplified. Statisticians have devised a number of ways to overcome these difficulties. In human epidemics, for instance, one approach is to restrict the analysis to data summarising outbreaks in households with the assumption that the households are independent *e.g.* in Becker (1968, 1979, 1981), Becker and Hopper (1983) and Becker and Dietz (1995). Further methods to analysis data from independent outbreaks in households are detailed in Bailey (1975), Chapter 14 and Becker (1989), Chapters 2 and 3.

Another way to tackle the difficulties in the likelihood methods is to make additional assumptions which enable the times of infection and the durations of latent and infectiousness periods to be deduced, likelihood methods can then be applied. Another approach has been to use non-likelihood methods. Martingale methods are one such method derived from the theory of martingales. The work of Becker (1989), Chapter 7 highlights that this method has found considerable success in the epidemic context and Becker has applied the method in various papers *e.g.* Becker (1993a), Becker and Hasofer (1997) and Becker and Britton (2001). A more recent approach is the use of Markov Chain Monte Carlo (MCMC) methods where unobservable quantities are estimated along with the desired parameters. Examples where MCMC methods have been applied in the epidemic context are Gibson (1997) for plant epidemics, O'Neill and Roberts (1999) for a smallpox outbreak and O'Neill et al. (2000) for household outbreaks of influenza and measles.

In this thesis inference will be performed on data collected from experiments involving FMD virus in sheep. The rate of infection acting upon groups of sheep will be estimated using martingale and maximum likelihood methods. Estimation will be carried out using an iterative procedure similar to the Expectation-Maximization (EM) algorithm (Dempster et al, 1977; McLachlan and Krishnan, 1997, Section 1.5) to calculate estimates for the unobserved times of infection, times of start of infectiousness, and times of end of infectiousness for infected individuals.

1.5 Thesis outline

In this chapter the main theme of the thesis has been introduced. Biological and socio-economic reasons for interest in infectious diseases in animals have been provided along with an overview of infectious diseases in animals. Particular attention has been paid to FMD virus. A detailed description of the FMD virus infection experiments in sheep has been provided. Some motivation on the use of mathematical and statistical models has also been given.

Chapter 2 presents a review of epidemic models and simulation models. Specific epidemic models such as the general epidemic model and the susceptible-latent-infectious-recovered (SLIR) are described and their application to the experimental FMD design is explored. The simulation models which will be used to generate data for use in other parts of the thesis are described. In addition, the EM algorithm, an inferential method that will be developed later in the thesis to analyse the data is introduced.

Chapter 3 explores specific methods for modelling the FMD experimental infection process on the basis of the infection generation of individual sheep. Chain binomial models suitable for modelling the infection process using infection pathways are described and their application in relation to the FMD experimental data is discussed. Generalized linear models are used to make inference about the generational rate of infection by assigning infection generations to infected individuals. The generalized linear model approach is evaluated using simulated data.

In Chapter 4, methods of parameter estimation using models of the infection process based on average infection rates applying to groups of sheep rather than individual sheep are described. These include maximum likelihood and martingale

methods of estimation. All of these methods require observations which are not available from the experimental data. Hence these estimation methods are to be used within an iterative procedure similar to the EM algorithm to estimate unobserved quantities and hence estimate the rate of infection acting upon groups of sheep.

In Chapter 5, emphasis is placed on modelling the infectiousness period given the observed number of viraemic days without taking into account the time of infection and latent period or the force of infection. This will be referred to as partially modelling an infection process as opposed to fully modelling the entire infection process. If an epidemic does not exhaust the susceptible population in a group of animals, this information will suffice to allow the use of a martingale estimator to estimate the rate of infection parameter. In this chapter, parameters for the estimated distribution of the infectiousness period are estimated based on the observed number of viraemic days. Also estimated is the expected infectiousness period for each infected individual given the number of viraemic days. Martingale estimates for the average rate of infection acting upon groups of sheep are calculated once the expected infectiousness periods for infected individuals have been estimated.

In Chapters 6 and 7, infection process characteristics *i.e.* the time of infection, latent period and infectiousness period are estimated in addition to the rate of infection in what is referred to as a model of the entire infection process. In Chapter 6, distributions for these three infection process characteristics are introduced. From these, expected values of the characteristics are to be estimated. This is achieved directly for the latter variable, while calculations for the expected time to infection and latent period are more complex. These are estimated by considering temporal partitions of constant hazard and then summing up the components from all partitions. The distribution parameters for the latent period distribution are estimated based on the data defining the number of days that group 1 individuals tested negative after inoculation prior to the first positive test result. Also estimated are the average rates of infection applying to groups of sheep. The rates of infection are estimated using martingale (Chapter 6) and maximum likelihood (Chapter 7) estimation methods. The trend in the rate of infection is then summarised. The maximum likelihood estimation methods are carried out to give both unrestricted and restricted estimates for group rates of infection. The estimates for rates of infection and estimates of expected infection process characteristics are calculated alternatingly within an iterative procedure. In Chapter 7, comparisons are made between the martingale, unrestricted and

restricted maximum likelihood based estimates. The statistical significance of the trend in the rate of infection is tested using bootstrap methods.

In Chapter 8, the methods developed in Chapters 6 and 7 are evaluated using simulated epidemic data. Estimation methods based on both martingale and maximum likelihood for the rate of infection are assessed with regard to an existing trend in the rates of infection to investigate if the methods are able to detect the trend. The properties of martingale based methods are further assessed with regard to size of decrease in the rate of infection, size of R_0 and group size.

Chapter 9 is concerned with the exploration of coverage properties of confidence intervals for the reproduction ratio estimated from realisations of a susceptible-infectious-removed (SIR) infection process. Confidence intervals for which the properties depend on asymptotic likelihood theory are evaluated with regard to their appropriateness in situations of small populations and small outbreaks. Asymptotic likelihood theory is shown to give poor results in such situations and therefore ways of improving maximum likelihood estimate statistic based confidence limits are discussed. Bootstrap approaches to the construction of confidence intervals are proposed and evaluated. A bootstrap calibration process is applied to each of the methods with the objective of improving the basic asymptotic likelihood and bootstrap confidence intervals.

In Chapter 10, results derived in the thesis are summarised and possible areas of further work are outlined.

Chapter 2

Epidemic models and simulation modelling

2.1 Introduction

Mathematical and statistical methods have been widely used to contribute to the understanding of the mechanisms underlying the spread of infectious diseases. This has largely been done via the use of epidemic models. Modelling involves the mathematical representation of the physical and biological processes which control infections. The modelling of the processes facilitates the representation of events in quantitative mathematical terms, allowing predictions to be made about future or hypothetical events. Thus epidemic models allow an increased understanding of patterns of disease occurrence. Progress in understanding the nature of epidemic processes has assisted in the prevention of infectious diseases (Anderson and May, 1991, Section 1.3).

In epidemiology, models have been constructed to attempt to predict patterns of disease occurrence and what is likely to happen if specific control strategies are adopted. The modelling of infectious diseases dates back to the 18^{th} century, where Daniel Bernoulli applied a simple life table to French smallpox data (Thrusfield, 1995, Chapter 19). Early models described natural epidemics of human infectious diseases. Thrusfield (1995), Chapter 19, points out that only within the last 30 years has serious attention been paid to the modelling of animal diseases. Early work on the dynamic behavior of theoretical models (for both human and animal diseases) made little attempt to fit models to observational data and was therefore of little direct value to disease control campaigns. However, there has been a trend for subsequent modelling work to become more realistic,

incorporating the effects of control techniques such as vaccination and immunization for human diseases (Halloran et al., 1992; Becker and Hall, 1996; Becker and Utev, 1998). Recent formulations have incorporated the effect of economic constraints and examined the cost-benefit implications of different strategies. Given the trend of increasing computing power, many studies have used computers to simulate situations rather than depending on analytical results. Models can only give useful results if they are biologically valid. Epidemic models therefore should seek to ensure that all known determinants that influence disease occurrence are included, that these factors can be quantified and estimated with accuracy and that the model is biologically meaningful. Mathematical models of the dynamics of communicable diseases have often had a direct bearing on the choice of an immunization programme, the optimal allocation of scarce resources or the best combination of control or eradication techniques (Remme et al., 1995). Most recently, this has been illustrated by the use of mathematical models to drive the governmental response to the 2001 UK FMD epidemic (Green and Medley, 2002).

The epidemic theorem is probably the most important result derived in the theory of epidemic models (Becker, 1989, Section 1.4.1). This theorem quantifies the distribution of the final size of an outbreak of a disease in large closed populations in terms of a parameter R_0 and other aspects of the infection process. By referring to the early stages of an epidemic, R_0 may be loosely defined as the mean number of susceptible individuals infected by a single infected individual introduced into a susceptible population at the beginning of the infected individual's infectious period. R_0 is commonly referred to as the basic reproduction number. The threshold phenomenon frequently associated with R_0 can help explain aspects of disease spread when the disease is endemic in a community. In general terms, where $R_0 < 1$, there is zero probability at the infection giving rise to a major outbreak, affecting the majority of individuals in a population. Where $R_0 > 1$, there is a finite probability, equal to $1 - \frac{1}{R_0}$, of such an outbreak occurring (Bartlett, 1949).

Mathematical epidemic models which are sufficiently simple to provide analytical results may be said to be simplistic and unrealistic, but they can generate useful qualitative predictions about possible modes of behavior (Renshaw, 1991, Section 10.2). Becker (1989), Section 1.4, argues that it is wrong to reject such models on the grounds of their simplicity since therein lies a considerable part of their value. A simple model is more likely to yield to mathematical analysis and hence reveal important characteristics more clearly than a complex model. For example, in a

simple model it is more straightforward to extract estimates of parameters which measure the infectiousness of the disease, the mean duration of the period between infection and infectiousness and similar epidemiologically important parameters.

Bailey (1975), Chapter 1, gives an account of different ways in which mathematical modelling can provide scientific insight into the mechanics of epidemic and endemic processes. Mathematical and statistical studies have an essential role to play in shedding light on the life-cycle of a parasite, the transmission and spread of an infectious disease, the nature of threshold population densities above which an epidemic can flare up and the methods of optimal immunization and control (Renshaw, 1991, Section 10.1).

de Jong (1995) emphasizes that modelling is a useful tool for studying complex phenomena such as the population dynamics of infectious agents, reasoning that models allow disparate measurements to be seen as manifestations of a single underlying process, but warns that a careful choice of model is important. During the UK 2001 foot and mouth disease outbreak government agencies relied heavily on the advise given to them by modellers in the effort to combat the epidemic (Ferguson et al., 2001a; Keeling et al., 2001; Woolhouse, 2003). The importance of modelling during this outbreak in forming efforts to control the epidemic cannot be overestimated.

In the past, it may have been necessary for researchers to develop mathematical models, driven more by the need for mathematical simplicity than biological realism, while the effective fitting of these models to data was sometimes rudimentary. However, research is now being carried out in inferential statistics with the objective of estimating parameters for infectious disease systems *e.g.* in Ferguson et al. (1997, 1999); O'Neill and Roberts (1999); Nodelijk et al. (2000) and Caley and Ramsey (2001). In this thesis, emphasis will be placed on parameter estimation methods as applied to experimental foot-and-mouth disease virus in sheep.

2.2 Types of models

Thrusfield (1995), Chapter 19, points out that veterinary modelling has been focused on infectious diseases. Following earlier work, he classifies infectious agents into two groups according to their generation dynamics. These groups are micro-parasites (*e.g.* viruses and bacteria) and macro-parasites (*e.g.* helminths

and arthropods). These two different groups are associated with two different modelling approaches. One is the density model approach that considers the absolute number of infectious agents in each host, commonly used for macro-parasitic infections where the numbers of infectious organisms can be estimated either in the host or in the environment. A classical example of this approach to modelling is the schistosomes model of MacDonald (1965). The second type is the prevalence model, which is used to model micro-parasites. Since the enumeration of absolute numbers of micro-parasites is usually impracticable, these systems cannot be readily modelled by density models, and so are modelled by prevalence models that consider the presence or absence of infection in the host. Density and prevalence models can be formulated either deterministically or stochastically.

In deterministic models, results obtained do not take account of random variation. It is assumed that the future state of the epidemic process can be determined precisely given the initial numbers of, for example susceptible and infectious individuals as well as the model parameters such as the rate of infection, recovery rate, birth rate or death rate. Stochastic models, however, describe processes or events subject to random variation so that there exists a space of possible epidemic histories, each of which can occur with a certain probability. These models exist within a mathematical structure which allows meaningful confidence intervals to be associated with estimates of model parameters of interest. In this thesis, which is aimed at modelling the infection process of FMD virus in sheep, stochastic models are considered. The model formulations explored are: the general epidemic model, where the infection process is defined in terms of susceptible, infectious and removed/recovered states (SIR), assuming no latent period (the period when an infected individual is not yet infectious after acquiring the infection (Anderson and May, 1991, Section 2.1); a susceptible-latent-infectious-recovered (SLIR) model where infected individuals exhibit a latent period before becoming infectious and then recovering; chain binomial models which involve the explicit identification of infection paths. The thesis also examines how these models relate to generalized linear models where statistical models are fitted to infection data to estimate system parameters.

It is often the case that processes in the real-world that one wishes to investigate are too complicated to fully understand. It is reasonable to strip such processes of less important features and use models of the basic processes (Morgan, 1994, Section 1.2). For many epidemiological processes of interest, assumptions have to be made about the way in which infections occur and develop. These assumptions,

which usually take a mathematical form based on logical relationships, constitute a model that can be used to try to gain more understanding of how the corresponding epidemiological process behaves (Law and Kelton, 2000, Section 1.2). If the model can be understood, then it may provide insight into the process itself. For some processes, the relationships that compose the model may be simple enough to allow the use of analytical methods to obtain exact information about questions of interest. However, most real-world processes are too complicated to map to realistic models which can be evaluated analytically. Models for such processes must be studied by means of simulation.

Often simulation can prove to be a useful tool, not only for describing the properties of the model but also for investigating how the behaviour of the model would change following a change in the model. Which in turn, maps to a possible change in the epidemiological scenario. Features of the model in epidemiological studies that had not previously been anticipated may emerge. In recent years, there has been much interest in mathematical models of the spread of infection (Morgan, 1994, Section 1.3; Renshaw, 1991, Section 10.1). Although the models are often simple, their mathematical solution is not trivial and simulation of the models has frequently been used.

Simulation models for epidemic data are usually constructed on basis of what are commonly known as compartmental models. These models involve categorising the states of individuals over time. Models of this class that will be explored in this thesis are the SIR and SLIR models. These models, as opposed to alternatives such as SIS (Susceptible-Infectious-Susceptible) model will be used on the basis of the results of the FMD experiments. In these experiments there was no evidence of recovered individuals being susceptible to re-infection and, indeed, when they were tested for FMD virus antibodies at the end of the experiments, recovered individuals showed signs of immunity (Hughes, 2001).

In the SIR models, the infectiousness period will be assumed to be negative exponentially distributed with mean $\frac{1}{\lambda}$, where λ is the transition rate to the recovered state. This model is commonly known as the general epidemic model. For the SLIR models, two sub-models will be considered, one which assumes fixed latent and infectiousness periods and another where latent and infectiousness periods are assumed to be variable and are modelled as gamma distributed random variables.

2.2.1 The general epidemic model (SIR)

In the general epidemic model all individuals are initially assumed to be susceptible. Once infected, an individual becomes infectious for a period of time, and is referred to as an infective, after which the individual stops being infectious, recovers and becomes immune or dies. The individual is then said to be removed. Models which assume that individuals pass in turn through the Susceptible, Infective and Removed states are called SIR models and the general epidemic model is defined in these terms. The general epidemic model was first studied in its deterministic form by Kermack and McKendrick (1927) and in its stochastic form it first received attention by Bartlett (1949). The general epidemic model is a memoryless continuous time model describing the spread of a SIR infectious disease in a population of homogeneous individuals that mix uniformly. The infection process is illustrated in Figure 2.1. The model is formulated below, where the Markovian nature of the process is illustrated in that instantaneous probabilities depend only on the current state of the process.

Figure 2.1: *The transition between states in the SIR infection process model, where β is the rate of infection, $\frac{1}{\lambda}$ is the mean infectiousness period, S is the number of susceptible individuals in a mixing group, I is the number of infectious individuals and N is the total number of individuals in a mixing group. R is the number of recovered individuals, and $S + I + R = N$.*

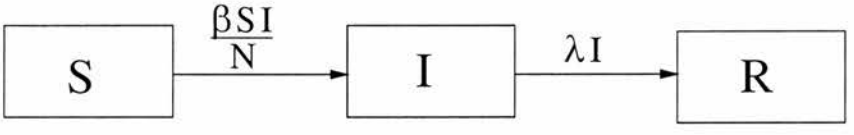

Consider a closed community with N individuals. Let β denote the rate of infection, λ the recovery rate and $S(t)$, $I(t)$, and $R(t)$ denote the number of susceptible, infectious and removed individuals at time t respectively, $R(t) + S(t) + I(t) = N$ holds for all t, where N is the total number of individuals in the population under study.

Under the pseudo mass-action formulation (de Jong et al., 1995) or density dependency formulation of Begon et al. (2002), the general epidemic model is defined by the transition probabilities:

$$\begin{aligned} Pr\{dS(t) = -1, dI(t) = 1, dR(t) = 0\} &= \beta S(t) I(t) dt \\ &\equiv \text{Probability of one new infection in time } dt \end{aligned}$$

$$
\begin{aligned}
Pr\{dS(t) = 0, dI(t) = -1, dR(t) = 1\} &= \lambda I(t)dt \\
&\equiv \text{Probability of one removal in time } dt \\
Pr\{dS(t) = 0, dI(t) = 0, dR(t) = 0\} &= 1 - \beta S(t)I(t)dt - \lambda I(t) \\
&\equiv \text{Probability of no change.}
\end{aligned}
$$

Under the true mass-action formulation (de Jong et al., 1995) or frequency dependency formulation (Begon et al., 2002), which will be used in the rest of the thesis, the general epidemic model is defined by the transition probabilities:

$$
\begin{aligned}
Pr\{dS(t) = -1, dI(t) = 1, dR(t) = 0\} &= \frac{\beta S(t)I(t)dt}{N} \\
Pr\{dS(t) = 0, dI(t) = -1, dR(t) = 1\} &= \lambda I(t)dt \\
Pr\{dS(t) = 0, dI(t) = 0, dR(t) = 0\} &= 1 - \frac{\beta S(t)I(t)dt}{N} - \lambda I(t). \quad (2.1)
\end{aligned}
$$

The choice of true or pseudo-mass action model may sometimes be justified by improvements in fit to data. This will not be possible in this thesis, since the population size is constant for most of the populations under study. The true-mass action formulation will be preferred, on the ground that it has a more intuitive interpretation. $\beta I(t)$ is the force of infection associated with the infective population. If this force is homogeneously distributed through the population, $\frac{S(t)}{N}$ is the fraction of the force applying to susceptibles, the only class able to make the specified transition.

2.2.2 The susceptible-latent-infectious-recovered model

In the SLIR model, the infection process is modelled using four states: the susceptible, latent, infectiousness and removed/recovered (SLIR) states as illustrated in Figure 2.2. Once individuals are infected, they pass through a latent state followed by an infectiousness state and are then removed (no longer infectious with no further effect on the force of infection, and not susceptible).

Figure 2.2: *The transition between states in the SLIR infection process model (Markovian true mass-action formulation).*

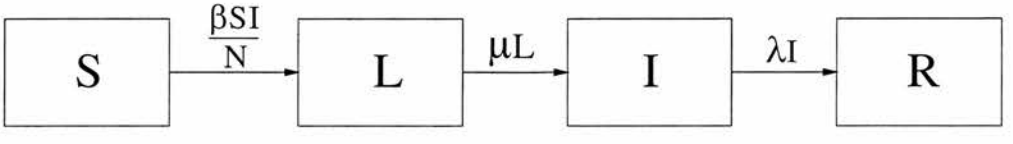

The model latent period corresponds to a period when viral load is low in the animal following initial infection. Only individuals in the infectious state have the potential to infect susceptible individuals. The infectiousness period corresponds to the period when viral load is high and virus is being excreted or is present in damaged epithelial cells at levels such that transmission can occur via physical contacts between individuals. There is usually a rough correspondence between the infectious period and the period during which clinical signs of infection are apparent (Anderson and May, 1991, Section 2.1). End of latency marks the beginning of the infectiousness state and end of infectiousness marks the beginning of the removed state.

Under the Markovian (memoryless) true mass-action formulation the SLIR epidemic model is defined by the following transition probabilities:

$$
\begin{aligned}
Pr\{dS(t) = -1, dL(t) = 1,\ dI(t) = 0,\ dR(t) = 0\} &= \frac{\beta S(t) I(t) dt}{N} \\
Pr\{dS(t) = 0, dL(t) = -1,\ dI(t) = 1,\ dR(t) = 0\} &= \mu L(t) dt \\
Pr\{dS(t) = 0, dL(t) = 0,\ dI(t) = -1,\ dR(t) = 1\} &= \lambda I(t) dt \\
Pr\{dS(t) = 0, dL(t) = 0,\ dI(t) = 0,\ dR(t) = 0\} &= \\
1 - \frac{\beta S(t) I(t) dt}{N} - \mu\, L(t) dt - \lambda\, I(t) dt &
\end{aligned}
$$

where μ is the transition rate between the latency and infectiousness states and λ is the transition rate between the infectiousness and recovery states. It is assumed that the transition times from L to I and from I to R are negative exponentially distributed. This assumption is unrealistic for many applications, and a more appropriate model, based on gamma distributed times to infectiousness and recovery, will be defined in Section 2.4.2.

2.3 Previous applications of epidemic and simulation models

This section will provide a brief review of some recent applications of epidemic models and simulation modelling in the veterinary context. Leslie (1996) uses simulation models to explore the transmission rate of *Salmonella enteriditis* phage type 4 in a flock of laying hens given that experimental work to explore the epidemiology of *Salmonella enteriditis* phage type 4 had left many question relating to the transmission rate unanswered. French et al. (1999) use deterministic and stochastic models to simulate the spread of *Neospora caninum* infection in cattle

to try to understand the effect of various routes of transmission on the efficacy of different control measures of the disease. The authors consider three possible routes of transmission and they argue that the model results for one of the routes of transmission are consistent with what is observed in the field. This highlights the fact that simulation models can yield realistic results. Howard and Donnelly (2000b) use simulations of a SLIR model to evaluate the control policy of slaughtering infected herds on the same day as disease confirmation in a FMD outbreak. This model was also applied to study a classical swine fever outbreak in Taiwan from which the authors concluded that implementation of the proposed policy could have resulted in a smaller number of farms being affected by the outbreak. van Nes et al. (1998) apply an SIR model to experimental and observational data to evaluate the feasibility of eradicating pseudo-rabies virus by vaccination and to determine which factors would hinder such an eradication. van Nes et al. (2001) use SIR models to analyse data summarising a major outbreak of pseudo-rabies virus in a vaccinated sow herd. Nodelijk et al. (2000) use a stochastic SIR model to analyse observational data from a longitudinal study investigating the population dynamics of porcine reproductive and respiratory syndrome virus in a Dutch breeding herd with the aim of quantifying transmission within the herd.

Haydon and Woolhouse (1997) use a SLIR model to generate a set of time varying estimates for the transmission rate for the UK 1967-68 FMD outbreak. These authors assume a fixed latent period and a fixed infectiousness period. Results from their model confirmed the importance of the rapid and effective implementation of control measures to reduce transmission rates during an outbreak. The results in this paper were important during the 2001 UK FMD epidemic. Howard and Donnelly (2000a) use an SLIR model to reconstruct the pattern of infection and estimate a time-varying force of infection and R_0 from observed epidemic data summarising an outbreak of classical swine fever. These authors assume an exponential distribution for the latent and infectiousness periods.

From the literature it is observed that many modellers tend to use the SIR model even in situations where it is not realistic. For most infectious diseases, once an individual is infected it does not become infectious immediately and use of the SLIR model in such situations is more appropriate where the mean length of the latent period is appreciable relative to the length of the mean infectiousness period. However, even in situations where the SLIR model has been used to model the infection process, many researchers have assumed a fixed latent and infectiousness period or an exponential distribution for the latent and infectious-

ness periods (*e.g.* Haydon and Woolhouse (1997); Howard and Donnelly (2000a)). These distributional assumptions are likely to be extremely unrealistic for many infectious diseases. Also, in a number of models, authors have assumed complete observation of data (*e.g.* Becker and Hasofer (1997)). This is never likely to be true in the case of infectious diseases and in some cases, the assumption will give rise to misleading parameter estimates. In this thesis, where the simulation models are used to explore the infection process of FMD in sheep, a random latent period and infectiousness period will be assumed. The unobservable quantities of the infection process will be recognised as such, estimated and not assumed known.

In the next section, the general epidemic model and the SLIR model are described in the context of the experimental FMD infection process.

2.4 Simulation models for experimental FMD virus in sheep

In this section, the general epidemic model and the SLIR model are formulated as applied to the FMD experiments, taking into account the experimental hypothesis of decreasing rate of infection by infection generation. To model the decrease in the rate of infection, a new parameter is introduced. This parameter consistently will be referred to as the passage multiplier. It will usually be denoted by γ. In this formulation, each infected individual has an infection generation number assigned to it and the rate of infection for individuals of infection generation g is given by $\beta_g = \beta\, e^{-\gamma g}$, where β is the rate of infection in the initial group of infectives and $\beta_0 = \beta$. Individuals are assigned infection generation numbers based on the nature of the infection 'donor'. The initial infectives constitute infection generation zero infectives, and an individual who becomes infected from contact with a zero infection generation infectious individual is defined to be a generation one infective. In general, an individual who becomes infected by a generation g infectious individual is assigned an infection generation number of $g + 1$. This is similar to the approach seen in the chain binomial models in Section 3.2 of this thesis. The infection process for the FMD experiments will therefore be modelled based on the properties of individual infectious individuals in the simulation models. Hence, the transition rate between susceptible and infectiousness states in the case of the general epidemic model or between susceptible and latent states for the SLIR model, due to a generation g infectious individual is given by $\frac{\beta_g\, S(t)}{N(t)}$.

Three models were considered for the infection process, namely:

1. A general epidemic model assuming no latent period and exponentially distributed infectiousness period.

2. A model assuming fixed latent and infectiousness periods.

3. A model assuming a random latent period and infectiousness period. These are modelled as independent gamma distributed random variables. The gamma distributions for the two processes are different, with parameters chosen for the latent period distribution to reflect the time elapsing (after inoculation), before viraemia and those for the infectiousness period chosen to reflect the number of observed viraemic days.

2.4.1 The general epidemic model

Each infected individual has a generation number. The generational rate of infection β_g depends on the generation number and is given by $\beta_g = \beta\, e^{-\gamma g}$, where γ is the passage multiplier. Thus the epidemic model is considered separately for each infectious individual such that, in a true-mass action formulation, the transition probability of an infection of a given generation from a g^{th} generation infective individual in a small time period dt is given by $\frac{\beta_g S(t)}{N} dt$. The probability of a removal is the same for each infectious individual and is given by λdt and the probability of no change is given by $1 - \frac{\beta_g S(t)}{N} dt - \lambda dt$. The general epidemic model has two parameters, β, the rate with which an infectious individual makes an infectious contact with another member of the community and λ, the removal rate. The quantity $\frac{\theta=\beta}{\lambda}$, measures the potential that an infective has for infecting a given susceptible. This quantity is called the basic reproduction number, denoted by R_0, and it plays an important role in SIR models.

2.4.1.1 Inter-event times (time to next event)

In the general stochastic epidemic model, the latent period is zero *i.e.* once individuals are infected, they become infectious immediately. The infectiousness period is assumed to be negative exponentially distributed with parameter λ and hence mean infectious period $\frac{1}{\lambda}$. The removal rate is λI, where I is the number of infectious individuals in the system. In the case of non-restricted mixing, there

are two possible events, an infection or a removal. In the situation of restricted mixing due to grouping of individuals, there are three possible events: a new infection, a removal or a change of mixing pattern. Under the assumption of non-restricted mixing, the inter-event times are based on the probabilities of a new infection or a removal. At any moment in time during the infection process, the next event to occur is either a new infection with probability $\frac{NI}{Tt}$ or a removal with probability $\frac{RM}{Tt}$, where $Tt = NI + RM$, NI denotes the instantaneous total infection rate and RM denotes the instantaneous total removal rate. The time to next event, T_e is exponentially distributed with mean $\frac{1}{Tt}$ and random inter-event times can be simulated from this distribution using standard methods (Morgan, 1994, Section 4.3).

2.4.1.2 Simulation of a random time to next event

Random variables from probability distributions can in principal be generated by applying the inverse of the cumulative density function to a uniformly distributed random variable (Morgan, 1994, Section 4.3). The general formula for the probability density function of the uniform distribution is

$$f(x) = \frac{1}{b-a} \text{ for } a \leq x \leq b$$

where a is the location parameter and $b-a$ is the scale parameter. The case where $a = 0$ and $b = 1$ is called the standard uniform distribution with probability density function given by

$$f(x) = 1 \text{ for } 0 \leq x \leq 1$$

and cumulative density function given by

$$F(x) = x \text{ for } 0 \leq x \leq 1.$$

It is important that a reliable source of random uniform numbers is used. This is essential for any kind of stochastic simulation (Press et al., 1992, Section 7.1). In this thesis, a uniform pseudo random number generator $ran1$ from Press et al. (1992), Section 7.1, was used. According to Press et al. (1992), Section 7.1, the routine $ran1$ passes various statistical tests for randomness that the alternative routine $ran0$ is known to fail. Press et al. (1992), Section 7.1, claim that $ran1$ passes all the structural statistical tests for randomness except when the number of calls start to become in the order of the generation period m, say greater than

10^8. Given the total number of random numbers that will be required to simulate the infection process in this thesis, using $ran1$ we are assured of no recycling of numbers, and of the random nature of pseudo random number stream.

To generate a random number from the exponential distribution, the following process is carried out. From standard statistical theory it is known that if a random variable X is uniformly distributed in the range (0, 1), then the random variable $Y = -\lambda\, lnX$ is exponentially distributed with mean λ (Law and Kelton, 2000, Section 8.3.2).

To generate an inter-event time t_e, a uniform random number X, $0 \leq X \leq 1$ is generated, such that $t_e = -\frac{1}{Tt}\, lnX$ is the time to the next event. For each infectious individual, t_e is calculated and the individual responsible for the next event is chosen at random by following the following algorithm:

Algorithm 2.1

1. For each infectious individual generate a uniform random number X,

   $0 \leq X \leq 1$ and calculate t_e;

2. determine the minimum of the t_es denoted $min(t_e)$ and refer to the corresponding individual as the event individual;

3. determine the nature of the next event (refer to Algorithm 2.2 Section 2.4.1.4);

4. if next event is a removal then the event individual will be removed at

   next time = current time + $min(t_e)$

   else event individual will make an infectious contact and the new infected individual will be of generation 'generation of event individual plus 1';.

5. if next event is an infection, use Algorithm 2.3 to choose an individual to be infected;

6. return to step 1 until all infected individuals are removed.

2.4.1.3 Probability of next event

For each infected individual, the force of infection is calculated as $NI = \frac{\beta_q S}{N}$, where S is the number of susceptible individuals mixing with the infected individual. The rate of removal is calculated as $RM = \lambda$. Thus the rate of new infection $= \frac{\beta_q S}{N}$ and rate of removal $= \lambda$.
Let $Tt = NI + RM = \frac{\beta_q S}{N} + \lambda$; the probability of the next event being a new infection is equal to $\frac{NI}{Tt} = \frac{\frac{\beta_q S}{N}}{\frac{\beta_q S}{N}+\lambda}$ and the probability of the next event being a removal is equal to $\frac{RM}{Tt} = \frac{\lambda}{\frac{\beta_q S}{N}+\lambda}$. Based on these probabilities, a choice is made of which event is to occur next.

2.4.1.4 Choice of next event under non-restricted mixing

At time t, the time of next event applying to an individual, it is known that the rate of new infection is NI and the rate of removal is RM. The next event will either be a new infection with probability $\frac{NI}{Tt}$ or a removal with probability $\frac{RM}{Tt}$, where $Tt = NI + RM$.

The procedure to choose the next event involves the following steps:

Algorithm 2.2

1. calculate the rates NI and RM;
2. generate a uniform $(0, 1)$ random number x;
3. if $0 \leq x \leq \frac{NI}{Tt}$ then the next event is a new infection otherwise it is a removal;
4. update $I = I + 1$ and $S = S - 1$ if the next event is a new infection or $R = R + 1$ and $I = I - 1$ if the event is a removal, where I is the number of infectious individuals, S is the number of susceptible individuals and R is the number of removed individuals;
5. go to step 4 of Algorithm 2.1.

2.4.1.5 Choice of individual to infect

The process of selecting the susceptible individual to become infected during the next infectious contact is outlined in the algorithm below; where each susceptible has an equal chance of being selected:

Algorithm 2.3

1. generate a uniform $(0, 1)$ random number x;
2. define tester = (int)$(x \times S) + 1$;
3. set $j = 0$ and $sum = 0$;
4. test whether $sum <$ tester; if true go to step 5, otherwise go to step 7;
5. update j to $j + 1$;
6. iterate through the individuals sequentially, if individual with identity (ID) number j is a susceptible, update sum to $sum+1$ and go to step 4, otherwise go to step 5;
7. return individual with ID $= j$ as new infection, and assign it a generation number equal to generation number of event individual plus 1;
8. go to step 6 of Algorithm 2.1.

2.4.1.6 Restricted mixing in the general epidemic model

Within a model with restricted mixing, the rate of new infection NI from a single infection of generation g depends on the number of susceptible individuals, S_{mix}, and the total number of individuals, N_{mix}, in the mixing groups and is given by $\frac{\beta_g S_{mix}}{N_{mix}}$. The daily change in the mixing pattern is another event in addition to events of new infection and removal. The time to the next event is calculated as in the non-restricted mixing situation. The event which may take place, however, depends on whether the time t_{next} = current time t plus the time to next event is less or greater than t_m, the next time of change of mixing pattern. If t_{next} is less than t_m then the next event is either a new infection or removal (as specified in earlier sections), otherwise the next event is the change of mixing pattern.

If the next event is a removal, then the infectious individual associated with the minimum time of next event is the one to be removed. If, however, the next event is a new infection, then the individual associated with the minimum time of next event is the one 'responsible' for the new infectious contact. The susceptible individual which becomes infected is chosen randomly among the susceptibles currently mixing with the 'donor' individual. The process of selecting a susceptible to make an infectious contact is as described in Section 2.4.1.5 with $S = S_{mix}$, the number of susceptibles in the mixing group.

As discussed in Section 2.2.2, in so far as the general epidemic model does not incorporate a latent state, it is unrealistic for many epidemics. For most diseases, when an individual is infected, infectiousness does not start immediately. There is a period when infected individuals are not yet infectious after acquiring the infection *i.e.* the latent period. For a disease such as FMD, where this time period is appreciable relative to the mean length of infectiousness period, such a model is inappropriate. In the next section infection processes where infected individuals pass through a latent state before becoming infectious are considered. Two situations are considered:

1. latent and infectiousness periods are assumed to be fixed;
2. latent and infectiousness periods are assumed to be gamma distributed random variables.

2.4.2 Models incorporating a latent state in the infection process

2.4.2.1 Structure

The experiments involved 32 sheep in 4 groups of 8 sheep. From the experimental studies, sheep were not re-infected, thus it is assumed that removed/recovered sheep have permanent immunity. Group 1 sheep which are infected at time $t = 0$, the start of the epidemic (experiment) immediately enter the latent state. Sheep in groups 2 to 4 are in the susceptible state at the start of the experiment (time $t = 0$). Sheep in the latent state are infected but not infectious.

2.4.2.2 The model

The rate of infection for an infected sheep is given by β_g where g is the infection generation of the infected sheep. The overall transition rate from susceptible state to latent state is given by $\frac{\beta_g SI}{N}$. However, this is implemented on the basis of individual infectious sheep, *i.e.* $I = 1$ such that the individual transition rate arising from each individual of infection generation g is given by $\frac{\beta_g S}{N}$. The transition rates from latent state to infectious state and from infectious state to removed state could be thought of as time-dependent functions such that the length of the latent period and infectiousness period are either fixed or gamma distributed. A gamma or point distribution was used to model both the latent and the infectiousness periods, and in practice, the algorithm was implemented by assigning projected latency and infectious time periods with the associated distributions to each individual on entry to the associated state.

2.4.2.3 Inter-event times

In addition to the events of infection *i.e.* transition to latent, infectious and removal states, the system incorporates an intrinsic mixing pattern. The change of mixing groups occurs on a daily basis (every 24 hours), thus the maximum inter-event period is 1 day. For each infectious individual, a uniform random number is selected using the *ran*1 random number generator from Press et al. (1992), Section 7.1, as discussed in Section 2.4.1.2 above, following which the time the individual will make an infectious contact with a susceptible individual is calculated as

$$\text{sheep-inf-time} = \frac{-ln(\text{uniform random number})}{\text{infection potential}}$$

where the infection potential is given by $\frac{\beta_g S_{mix}}{N_{mix}}$.
An individual could cease to be infectious before reaching its sheep-inf-time. Hence the time at which the next infection event occurs due to a particular infectious individual is calculated as

$$\text{next-inf-time} = \text{current time } (t) + \text{sheep-inf-time.}$$

The individual with the minimum next-inf-time among the infected individuals, subject to it still being infectious by the associated next-inf-time is selected as the one to make an infectious contact with a susceptible individual at time

next-inf-time. Only the time of a hypothetical next infection event has been determined. Four possible types of events may take place. These are infection, end of latency (start of infectiousness), removal (end of infectiousness) and change of mixing pattern. The time for the next event (denoted next-event-time) and the nature of the next event to take place are determined by choosing the minimum of: next-inf-time, the time of the end of latency for all individuals in the latent state in the mixing group and the time of the end of infectiousness for all individuals in the infectious state in the mixing group. If the minimum of these times, *i.e.* next-event-time is within the current day, then the next event is the one determined by next-event-time, otherwise the next event is a change of mixing pattern and the next-event-time is t = end of current day.

2.4.2.4 Model assuming fixed latent and infectiousness periods

The length of the latent period is based on expert knowledge which suggests that the latent period for experimentally inoculated FMD virus in sheep is between 1 day (24 hours) and 2 days (48 hours). An average value of $1\frac{1}{2}$ days was taken as the fixed latent period for infected individuals. The length of the infectiousness period was determined from the data, and assumed to equal the average length of viraemic period, which was approximately 2.8 days.

Since the latent and infectiousness periods are fixed, the only random event which is modelled is new infection. The other events namely transition from latency to infectiousness, infectiousness to removed and change of mixing pattern in the case of restricted mixing, are not random. The time to a new infection event is based only on the rate of infection NI. Thus, given a uniform $(0, 1)$ random variable X, the random variable of the time to the next event $T_e = -\frac{1}{NI} lnX$ is exponentially distributed with mean $\frac{1}{NI}$. The time to the next event t_e is determined for each infectious individual and the individual with minimum t_e is selected as the one provisionally associated with the next infection. The time

current time $t + t_e$

is compared with the times of the end of latency for all currently latent individuals, the times of removal for all infectious individuals and the time of the next change of mixing pattern (at the end of the current day). The minimum of these times is the time of the next event and determines the nature of the next event. This procedure is repeated until there are no latent or infectious individuals remaining in the system.

2.4.2.5 Infection event in model assuming random latent and infectious periods

A susceptible individual to become infected during the next infectious contact is randomly selected as described in Section 2.4.1.5 with $S = S_{mix}$, the number of susceptibles in the mixing group. Once a susceptible individual has been selected to make an infectious contact *i.e.* to become infected, the 'donor' infectious individual is already known and hence the infection generation is also known. To each newly infected individual

1. an infection generation number is assigned;
2. a latent period is randomly generated as sheep-latent = $\lambda_{lat} \times$ gamran(ν_{lat}), a random variable generated from a gamma distribution with shape parameter ν_{lat} and scale parameter λ_{lat};
3. an infectiousness period is randomly generated from a gamma distribution with shape parameter ν_{inf} and scale parameter λ_{inf} using sheep-inf-period $= \lambda_{inf} \times$ gamran(ν_{inf}).

gamran(ν) is a function that generates random numbers from a gamma distribution with shape parameter ν and scale parameter 1 (Law and Kelton, 2000, Section 8.3.3).

Thus, once infected, an individual has all current and future transition time points (*i.e.* time of infection (start of latency), start of infectiousness and time of recovery) determined.

2.5 The effect of restricted mixing on infection process

The effect of restricted mixing on the infection process in groups of sheep was assessed using simulations. Preliminary simulation studies were performed to identify whether restricted mixing would have an effect on the progress of the infection through groups of sheep. The simulations were performed for both restricted mixing and non-restricted mixing. The assessment was based on the following quantities estimated over 1000 realisations: the average number of secondary infections; the mean instantaneous force of infection and the average cumulative number of secondary infections. Values for these quantities were compared for

Figure 2.3: *The effect of restricted mixing on an infection process in groups of sheep based on (a) the average number of secondary infections, (b) the average cumulative force of infection, and (c) the average cumulative number of secondary infections.*

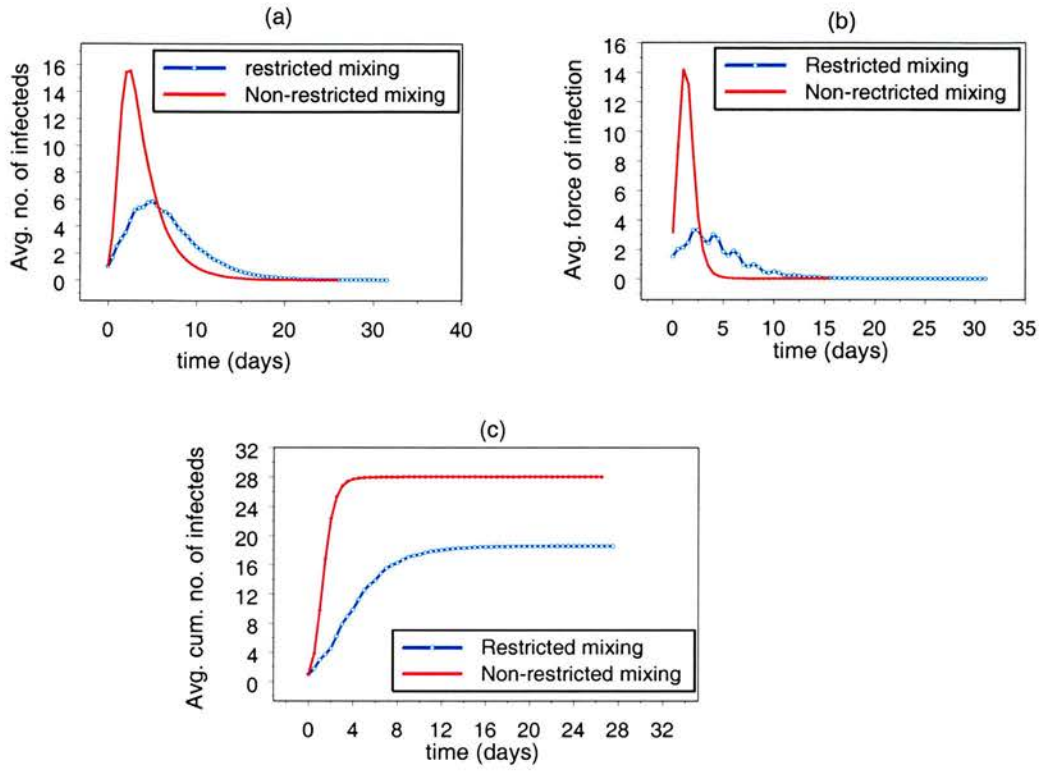

both restricted mixing and non-restricted mixing. These results are summarised in Figure 2.3 and these confirm that restricted mixing has an effect on the infection process across groups. The distribution of the average number of secondary infections and of the average force of infection has a much lower peak under restricted mixing than under non-restricted mixing (Figure 2.3(a) and (b)). The plots also show that the epidemics, on average, tend to last longer under restricted mixing. Figure 2.3(c) shows that the average cumulative number of secondary infections is higher under non-restricted mixing than under restricted mixing.

2.6 Methods of parameter estimation for epidemic models

Maximum likelihood estimation methods are widely used in parameter estimation and hence would normally be the first method considered for parametric infer-

ence. However, for epidemic models, parametric inference based on likelihood is often difficult because the likelihood functions associated with epidemic data are often very complicated as a consequence of the fact that the infection process is only partially observed. In particular, the epidemic pathway is unknown. Likelihood-based inference would be more straightforward if there was a more complete observation of the epidemic process. The complexity of likelihood-based inference applied to incidence data has generated interest in alternative methods of inference for epidemiological parameters.

For closed communities (*i.e.* those with a fixed population), likelihood inference can be based on data summarising the size of independent outbreaks. The most basic model for the size of an outbreak in a closed community is the chain binomial model. However, Becker (1993b) warns that the probability distribution of the size of epidemic is very complicated even under the simplest assumptions. Thus, the method is tenable only in groups of very small sizes, *e.g.* household data. The likelihood for chain binomial models rapidly becomes complicated as the household size increases. These methods will be explored in Chapter 3.

Martingale methods of estimation provide an alternative to the complexity of likelihood-based inference. These methods are derived from the theory of martingales. Martingale theory applied to counting processes provides useful mathematical results to define estimating equations for some of the parameters which define epidemic models (Becker, 1989, Section 7.1; 1993a). These methods will be described in detail in Chapter 4. Under the assumptions of the general epidemic model and SLIR model, martingales corresponding to the process that counts the number of infection and removal events, can be constructed, from which estimates of the desired parameters may be obtained.

Another estimation method which allows for the fact that infectious disease data are typically incompletely observed is the Markov Chain Monte Carlo (MCMC) method. The MCMC method is used to make inference about missing data as well as parameters of interest. For example, Gibson and Renshaw (1998) present MCMC methods used to estimate parameters in stochastic compartmental models from incomplete observation of the corresponding Markov process. This thesis will not investigate the MCMC methodology, but rather concentrate on classical frequentist methods of inference.

2.7 Approaches developed in this thesis

In exploring the infection process of experimental FMD virus in sheep, the main emphasis in this thesis will be on estimating rates of infection in groups of sheep and estimating unobserved infection process characteristics *i.e.* time of infection, length of latent period and length of infectious period for infected individuals (Chapters 5, 6 and 7). The distribution of time to infection will involve a hazard function which depends on the average group rates of infection. The latent and infectiousness period distributions will be assumed to be gamma distributed with parameters estimated from the observed data. The expected times of infection and expected lengths of latent period will be estimated jointly for each individual, since, although the underlying random variables are independent, the inability to observe the nature of the pre-infectious individuals creates a correlation in any estimates. Estimation of the rate of infection in groups of sheep will use both maximum likelihood and martingale methods. The expected time of infection, expected length of latent period and expected length of infectious period based on the assumed distributions and the observed data will be estimated alternately with the average group rates of infection using an iterative scheme similar to the EM algorithm. The EM algorithm is a method which may be used to obtain estimates of parameters and other quantities in situations where there is incomplete data (Dempster et al., 1977; McLachlan and Krishnan, 1997, Section 1.5).

2.7.1 The Expectation-Maximisation (EM) algorithm

The EM algorithm was formally defined by Dempster et al. (1977), although the algorithm had been proposed many times previously to deal with particular methodological problems. It provides a general approach to iterative computation of maximum likelihood estimates where the data can be regarded, in some sense, as incomplete. The concept of 'incomplete data' can be formally defined in terms of two sample spaces $\mathcal{Y}$ and $\mathcal{X}$ where the observed data $\mathbf{y}$ are a sample from $\mathcal{Y}$ and there is a corresponding set of observed and unobserved random variables $\mathbf{x}$ which have been sampled from $\mathcal{X}$. In general the set $\mathcal{X}$ is referred to as the complete data. Different sets of complete values $\mathbf{x}$ can correspond to the observed data set $\mathbf{y}$, but it is assumed that there is a mapping $\mathbf{x} \rightarrow \mathbf{y}(\mathbf{x})$ from $\mathcal{X}$ to $\mathcal{Y}$ and that $\mathbf{x}$ lies in $\mathcal{X}(\mathbf{y})$, the subset of $\mathcal{X}$ determined by the equation $\mathbf{y} = \mathbf{y}(\mathbf{x})$. A family of probability densities $f(\mathbf{x}|\phi)$ is assumed for the complete data depending on the vector of parameters $\phi \in \Omega$. In general, the likelihood for the incomplete

data $g(\mathbf{y}|\phi)$ is more complex than that for the complete data. However, given the result $g(\mathbf{y}|\phi) = \int_{\mathcal{X}(\mathbf{y})} f(\mathbf{x}|\phi)dx$, the EM algorithm proceeds to maximise $g(\mathbf{y}|\phi)$ using the associated family of densities $f(\mathbf{x}|\phi)$. It does this using a pair of iterative procedures, one of which can be thought of as a conditional expectation, and the other as a maximisation.

The general definition of the EM algorithm is based on the function $E[\ln f(\mathbf{x}|\phi')|\mathbf{y}, \phi]$, the expectation of the log-likelihood of the complete data, given the observed data $\mathbf{y}$ and the current parameter estimates $\phi \in \Omega$. The algorithm proceeds by iteration between the two steps:
Expectation-step:

Compute $E[\ln f(\mathbf{x}|\phi')|\mathbf{y}, \phi^{(p)}]$.

Maximisation-step:

Chose $\phi^{(p+1)}$ to be a value $\phi \in \Omega$ maximising

$$E[\ln f(\mathbf{x}|\phi)|\mathbf{y}, \phi^{(p)}]. \tag{2.2}$$

$\phi^{(\mathbf{p})}$ will converge to the parameter value which maximises $g(\mathbf{y}|\phi)$, although convergence may be slow (McLachlan and Krishnan, 1997, Section 4.1).

It will be useful at this point to define a more general class of algorithm. Where $\mathbf{M}()$ is a mapping from $\Omega \to \Omega$, and $\phi^{(p+1)} = \mathbf{M}(\phi^{(p)})$, then if

$$E[\ln f(\mathbf{x}|\mathbf{M}(\phi))|\mathbf{y}, \phi] \geq E[\ln f(\mathbf{x}|\phi)|\mathbf{y}, \phi], \ \forall \phi \in \Omega,$$

then the mapping defines a Generalized Expectation-Maximisation algorithm (GEM). Intuitively, this represents a relaxation of the maximisation rule in the EM algorithm, where $\phi^{(p+1)}$ no longer needs to maximise $E[\ln f(\mathbf{x}|\phi^{(p+1)})|\mathbf{y}, \phi^{(p)}]$, rather

$$E[\ln f(\mathbf{x}|\phi^{(p+1)})|\mathbf{y}, \phi^{(p)}] \geq E[\ln f(\mathbf{x}|\phi^{(p)})|\mathbf{y}, \phi^{(p)}].$$

Dempster et al. (1977) show that this is sufficient to ensure that the log-likelihood on the incomplete data is also non-decreasing. They also propose a further pair of constraints which they believed would guarantee convergence of $\phi^{(p+1)}$ to a single point. In fact, these conditions are not sufficient (McLachlan and Krishnan, 1997, Section 3.6).

The EM algorithm simplifies when applied to a complete-data likelihood derived from distribution functions in the regular exponential family. By definition

(Dempster et al., 1977), the density for a data set $\mathbf{x}$, with parameters $\phi \in \Omega$, can be written in the form,

$$f(\mathbf{x}|\phi) = \frac{b(\mathbf{x}) \exp\{\phi\, \mathbf{t}(\mathbf{x})^T\}}{a(\phi)},$$

where $\mathbf{t}(\mathbf{x})$ is a vector of sufficient statistics for ϕ (with the same dimensionality as ϕ), depending on the complete data $\mathbf{x}$. In general, the EM algorithm simplifies to an iterative estimation of the sufficient statistic with steps:
Expectation-step: Compute $\mathbf{t}^{(p)} = E[\mathbf{t}(\mathbf{x})|\mathbf{y}, \phi^{(p)}]$.
Maximisation-step: $\phi^{(p+1)}$ is the solution of $E[\mathbf{t}(\mathbf{x})|\phi] = \mathbf{t}^{(p)}$.
The expectation step simplifies to the calculation of the expected value of the sufficient statistics for the complete specification given the observed values and the current parameter estimates. The maximisation step is identical to that defined earlier. The maximisation will give a meaningful result whether or not $\mathbf{t}^{(p)}$ can actually be mapped to any complete data set $\mathbf{x}$ in the sample space $\mathcal{X}$. As long as the maximisation step is solvable for $\phi \in \Omega$, this formulation of the EM algorithm will be valid.

In the case where the sufficient statistic $\mathbf{t}(\mathbf{x})$ is linear in the unobserved terms, this process is equivalent to calculating the expected values of each unobserved term, given $\mathbf{y}$ and the current parameter estimate, and using these values in $\mathbf{t}(\mathbf{x})$ instead of the unobserved terms.

In the case of the experimental FMD infection process, it will be shown (Section 4.4) that implementation of the EM algorithm would require use of the most general definition (Equation (2.2)). The resulting algorithm would be computationally prohibitive. Instead, a non-EM iterative algorithm is proposed in Section 4.4, which it is anticipated will give rise to acceptable estimates of the unknown variables of interest, while not being computationally impractical.

2.7.2 Previous applications of the EM algorithm

Since the presentation of its general formulation by Dempster et al. (1977), the EM algorithm has been used as a general-purpose algorithm for MLE in a wide range of situations which are best described as incomplete-data problems. Examples of fields where the EM algorithm has been employed as an estimation procedure are survival analysis (Ng and McLachlan, 1998; Slasor and Laird, 2003), studies involving genetic data (Shoukri and McLachlan, 1994) and medical image

processing (Liang et al., 1992) amongst others. When reviewing the literature citing the EM algorithm, it is striking that the algorithm has mostly been used in problems described by mixture distributions (Ng et al., 1999; McLachlan et al., 1996; Jones and McLachlan, 1991). In the context of epidemic data analysis, however, a literature search does not identify much published work where the EM algorithm has been used. Most of the literature appears only to have mentioned that the EM algorithm could be used as a parameter estimation tool. Only two papers, Becker (1993b) and Becker (1997), are relevant when reviewing the use of the EM algorithm in the epidemic context. Becker (1993b) gives an illustration of how the EM algorithm can be used to simplify likelihood inference. The author demonstrates how the algorithm can be used to estimate a parameter, q, the probability of a susceptible escaping infection when exposed to an infectious individual for the duration of the latter's entire infectious period. The analysis uses size of outbreak data modelled using the chain binomial model (Section 3.2). The E-step involves estimation of the number of outbreaks of a particular epidemic size and in the M-step, the parameter q is estimated. The implementation of the EM algorithm was possible in this context because ML estimates corresponding to specific epidemic chains data had closed analytic forms. Becker (1997) gives an illustration of how the EM algorithm can be used in the analysis of HIV/AIDS data and other infectious diseases in general.

The analysis of infectious disease data is a natural setting for applications of the EM algorithm because the infection process is only partially observed in practice (Becker, 1997). However, the added complication of interactions between infective and susceptible individuals whose numbers change over time make it difficult to compute the expectation in the E-step of the EM algorithm (O'Neill, 2002). The E-step is straightforward for epidemic chain binomial models, but for most transmission models no way has yet been found to effect the E-step directly (Becker, 1997). Instead, for example in applications of HIV/AIDS data in Becker (1997), transmission models have been replaced by pragmatic models which capture only part of the mechanism that generates the data and uses what he calls an EM algorithm with smoothing. This enables reconstruction of the unobserved HIV infection curve as well as the estimation of the distribution for the incubation period until AIDS, amongst other quantities. Due to the difficulties in the E-step, for data on other infectious diseases other than AIDS data, application of the EM algorithm has so far been restricted to the size of outbreaks in households (Becker, 1993b, 1997). In general, for non-chain binomial models, any ML estimate for the parameters will have to be obtained numerically as the likelihood

function becomes complicated. Similar issues apply to the experimental FMD data, and these are discussed in Section 2.7.1, where a different iterative scheme is proposed for the analysis of the experimental FMD data.

2.8 Summary

A review of epidemic models and simulation models has been provided. The SIR and SLIR models have been described and their application to the experimental FMD design has been described. The effect of the restricted mixing imposed by the design of the experiments was explored and it was confirmed that this will have an effect on the infection process across the groups when compared to the equivalent non-restricted mixing model. A description of the EM algorithm has been given and potential difficulties in its implementation in the epidemic context discussed.

The SLIR model with random latent and random infectiousness periods will play a large role in the exploration and evaluation of methods to model the experimental FMD infection process. The model will be used to generate data to evaluate inferential methods and to generate bootstrap epidemic realisations in Chapters 6, 7 and 8. The SIR model will be used to generate data in the simple case of homogenous mixing with no restrictions or sub-groups, to explore the properties of confidence intervals for infection process parameter estimates in Chapter 9. These models have all been formally defined, and the methods used to produce simulated realisations of the processes fully specified.

Chapter 3

Modelling the FMD infection process using infection generation information

3.1 Introduction

In the current and subsequent chapters, specific models suited to the data generated from the FMD experiments are explored. Two scenarios are considered, the first involves modelling the infection process on the basis of infection pathways, *i.e.* modelling the infection process by explicitly considering the likely development of the epidemic between different individuals across the groups. This approach requires knowledge of individual infection generations. The second scenario involves modelling the infection process on the basis of 'average' infection rates in groups of sheep, and this is the subject of Chapters 4, 5, 6 and 7.

Bearing the main objective of the experiments in mind, the infection pathway models considered should aim to estimate infection rates for each infection generation. Two types of model are considered to describe the infection process using infection pathways. These are the chain binomial model (Becker, 1989, Section 2.3), and the generalized linear model (McCullagh and Nelder, 1983, Section 2.2).

3.2 Chain binomial models

Developing a model in terms of epidemic chains would suit the desired objective of investigating whether there is an intrinsic diminution in the infectivity of infected individuals during the course of successive naturally transmitted infections of

FMD virus. These types of models are called chain binomial models. The models are based on epidemic chains where, by specifying the chain type of an epidemic, one specifies the progress of the disease spread among the susceptibles of a group. This can be presented more precisely in terms of generations. Considering the case of introduction of an infectious disease in a community, the first generation of cases consists of those individuals infected by making an infectious contact with one of the introductory cases (cases of generation 0). The second generation of cases consists of those infected by making an infectious contact with one of the first generation cases. The t^{th} generation of cases consists of those individuals infected by making an infectious contact with one of the $(t-1)^{th}$ generation cases. Thus an epidemic chain for an affected group is the enumeration of the number of cases in each generation. For example, $1 \longrightarrow 1 \longrightarrow 2$, denotes the chain consisting of 1 introductory case, 1 first generation case, 2 second generation cases and no cases in third or later generations. Generally, $i_0 \longrightarrow i_1 \longrightarrow \ldots \longrightarrow i_r$ has i_t cases (infectives) in generation t, where $t = 0, 1, 2, \ldots, r$, and no cases thereafter. In most cases the available data do not contain sufficient detail to enable the classification of outbreaks into separate epidemic chains. However, it is useful to formulate epidemic chain models as they lead to outbreak size distributions in terms of parameters that have clear and useful interpretations (Becker, 1989, Section 2.2). The chain binomial model is then formulated by attaching probabilities to each possible epidemic chain. This requires some additional assumptions. Becker (1989), Section 2.3, outlines the necessary assumption namely:

1. Susceptibles make infectious contacts independently of one another and each remaining susceptible has the same probability of making an infectious contact with the infectives of a given generation.

2. The probability q_i that a given susceptible escapes infection when exposed to i infectives of a specific generation does not vary from generation to generation.

For $t = 0, 1, 2, \ldots$, the probability that there are x infectives of generation $t+1$ in a group, given that S_t, susceptibles have been exposed to I_t infectives of generation t, is given by:

$$Pr\left(I_{t+1} = x | S_t = s, I_t = i\right) = \frac{s!}{x!(s-x)!} {p_i}^x {q_i}^{s-x}; \quad x = 0, 1, \ldots, s$$

and $p_i = 1 - q_i$. Then the probability of a specified epidemic chain is the product of probability terms from different binomial distributions.

Generally, the probability of the complete epidemic chain $i_0 \longrightarrow i_1 \longrightarrow \ldots \longrightarrow i_r$ is given by:

$$Pr\left(i_0 \longrightarrow i_1 \longrightarrow \ldots \longrightarrow i_r\right) = \frac{s_0!}{i_1!i_2!\ldots i_r!s_r!} \prod_{t=0}^{r} {p_{i_t}}^{i_{t+1}} {q_{i_t}}^{s_{t+1}}$$

with $i_{r+1} = 0$ and $s_{r+1} = s_r$, *i.e.* there are no more infectives after the r^{th} generation of infectives.

Epidemic chain probabilities are conditional on the number of introductory cases. In order to apply the chain binomial model in practice, the number of infectives and the number of susceptibles present need to be known for each generation. This can be ensured by making the further assumptions that all infectives can be recognized and that, after their infectious period, the infectives are removed or become immune for the remaining period of the epidemic. These assumptions allow the deduction of the number of individuals who remain susceptible at the end of each generation and this is given by $S_{t+1} = S_t - I_{t+1}$, $t = 0, 1, 2, \ldots$, with the initial values $I_0 = i_0$, and $S_0 = s_0$ assumed known.

Becker (1989), Section 2.4, emphasizes that whenever possible one should seek to obtain data in sufficient detail to enable the epidemic chain to be identifiable. In humans, where infectious disease data are generally observational, the most readily available data are data on size of outbreak in, say, households or units like schools and hospitals. These data do not enable the epidemic chain to be identifiable. Epidemic models have been used in the analysis of the size of outbreak (Bailey, 1953a; Longini and Koopman, 1982; Ball, 1986; Addy et al., 1991; Ball and Clancy, 1995; Ball and O'Neill, 1999). The probability of a given size of outbreak can be expressed in terms of the $q_i s$ and the additional assumptions made in the chain binomial model do result in some reduction in the number of parameters to be estimated. Assuming data are sufficiently detailed to determine the number of introductory cases and the initial number of susceptibles, the distribution of the outbreak size can be determined by accumulating the appropriate chain probabilities. However, Becker (1989), Section 2.4, points out that such an analysis is more tedious and less effective than the analysis of epidemic chain data.

There are two specific chain binomial models, the Reed-Frost model and the Greenwood model. These models are obtained by being more specific about the way in which the probability q_i depends on the number of infectives i. Reed and Frost in 1928 formulated a chain binomial model, making the assumption

that $q_i = {q_1}^i$, $i = 1, 2, \ldots$. This assumption stipulates that the event of escaping infection when exposed simultaneously to i infectives of one generation is equivalent to escaping infection when exposed to a single infective in each of i separate generations. In other words, each of the infectives of a group of i infectives from the same generation creates infectious contacts independently. This assumption is appropriate for diseases which are transmitted primarily by close individual-to-individual contacts and hence is appropriate for diseases that are spread by direct transmission.

Greenwood (1931) formulated an alternative chain binomial model by assuming that $q_i = q, \forall i \geq 1$ and $q_0 = 1$. This assumption stipulates that the chance of infection when exposed to 1 infective is identical to that when more than 1 infective is present. This assumption is appropriate when the environment is saturated with infectious material even if only 1 infective is present and the chance of a susceptible being infected depends more on the behaviour of the susceptible individual in the environment. This assumption is appropriate for diseases that are spread by indirect transmission. The two models represent alternative extremes of the range of possible modes of infection. The advantage of both models is that each contains only one parameter.

Chain binomial models have been used in the modelling of infectious disease data for many decades now. Bailey (1953b), describes chain binomial models applied to the analysis of intra-household epidemics involving households of size 3 and 4. Bailey (1956c), illustrates how significance tests can be performed to test for variation in q_i. Bailey (1956a,b), estimates the latent and infectiousness periods of measles by constructing chain binomial models for 2 or 3 cases from families of 3 or more susceptibles, while in Bailey and Alff-Steinberger (1970), the authors give an improved estimation method for latent and infectious periods of a contagious disease by constructing chains from households of size 2 and 3. In general, chain binomial models have mostly been applied to household data, the methodology being easiest to implement when the populations are relatively small.

3.2.1 Application of chain binomial models to FMD experiments

Formulating the model in terms of epidemic chains for the FMD experimental data, group 1 infectives constitute the introductory cases, *i.e.* cases of generation 0 with associated rate of infection β_0. The first generation of cases consists of those

individuals infected by making an infectious contact with one of the introductory cases and their rate of infection is denoted by β_1. The second generation of cases consists of those infected by making an infectious contact with one of the first generation cases and their rate of infection is denoted by β_2. The g^{th} generation of cases consists of those individuals infected by making an infectious contact with one of the $(g-1)^{th}$ generation cases and their rate of infection is denoted by β_g. The objective then is to estimate the different generation rates of infection. A possible alternative would be to think of the problem in terms of a passage multiplier, assuming a constant drop in infectivity on each passage, and hence having only 2 parameters to estimate.

Let β be the rate of making an infectious contact for any infectious individual and γ be the passage multiplier. Then the rate of infection for a g^{th} generation infective is assumed to be:

$$\beta_g = \beta e^{-\gamma g}, \quad 0 \leq \gamma < \infty.$$

The hypothesis to be tested would be whether $\gamma = 0$ or whether $\gamma > 0$.

However, there are potential difficulties with an epidemic chain based model. For instance, observed infectious individuals in group 2 are not necessarily all generation 1 cases as infection can also occur from a group 2 individual to another group 2 individual and also from group 3 to group 2 individuals. However, the first infection to occur in group 2 is definitely due to group 1 infectives and is thus definitely a generation 1 case. For groups 3 and 4, the first infection to occur is not necessarily of generation 2 and 3 respectively. However, group 3 has generation 2 as the possible lowest generation and group 4 has generation 3 as the possible lowest infection generation. For any group $j, j \neq 1$, the first infection to occur in the group must be due to contact with infectious individuals in group $j-1$. Other observed infections in group j could be due to contact with infectious individuals of groups $j-1$, j or $j+1$. Thus at any given time when two groups are mixing, the total hazard due to infectious individuals is a mixture of that arising from different infection generations as the infectious individuals will not necessarily all be of the same generation. The most crucial issue is that the source of infection for each infected sheep will have to be known in order to assign a generation to it. This issue makes inference for epidemic chain models very complicated.

3.2.1.1 Formulation of the likelihood function

Information about the times at which animals tested positive is used to model and make inference about the characteristics of the infection. These characteristics include the duration of the latent period (time between infectious contact and testing positive to infection), the duration of the infectious period and the instantaneous rate of spread of disease β_g. It is assumed that for each infective, the beginning and end points of the infectiousness period can be deduced. The first point in time at which the animal tested positive is used to indicate the beginning of the infectiousness period and the first point at which it subsequently tested negative to indicate the end of the infectious period. The infectiousness process is assumed to be fully specified. This will be a valid approximation if the time between sampling is small, relative to the length of the infectious period. The analysis should make inference about the initial rate of infection, β, the passage multiplier, γ, and about the distribution function for the duration of the latent period. Inference about the characteristics of the latent period is less straightforward because the precise time at which the infectious contacts occur is not observable except for individuals in group 1. It is assumed that the force of infection associated with an infected individual takes non-zero values only on the interval over which the individual is infectious.

The application of epidemic chain models to the FMD data requires consideration of the mixing structures in the experiments. These complicate the equations immensely, but a possible formulation is given below.

Let a_j be an indexing variable for an infected individual in group j; a_j may take values from 1 to I_j, where I_j is the number of infectives in group j at a particular time. Also, let $({u_j}^{a_j}, {w_j}^{a_j})$ be the observed infectious period for infectious individual a_j of group j, where ${u_j}^{a_j}$ marks the beginning of the infectious period of individual animal a_j of group j and ${w_j}^{a_j}$ marks the end of the infectious period for individual a_j.

Without loss of generality, individual $a_j = 1$ will be the first animal in group j to become infectious, $a_j = 2$ will be the second, and so on. Individual I_j is the ${I_j}^{th}$ animal in group j to become infectious, and hence ${u_j}^1 \leq {u_j}^2 \leq \ldots \leq {u_j}^{I_j}$.

Let

$$\delta_{jk}(t) = \begin{cases} 1 & \text{if group } j \text{ and } k \text{ are mixing at time } t \\ 0 & \text{otherwise} \end{cases}$$

Let t denote the time of infection for a new infected individual by infectious individual a_j. For t in $[{u_j}^{a_j}, {w_j}^{a_j}]$, there exists a set $T_{jk} = \{t_1, t_2, \ldots, t_{n_{jk}}\}$, of

size n_{jk}, of transition time points indicating the time points during the infectious period of individual a_j when groups j and k start or cease to mix.

Let ${}^{a_j}h^g{}_{jk}(t)$ be the hazard function at time t, posed by a g^{th} generation infective individual a_j of group j, against susceptible individuals in groups j and k. Hazard function, $h(t)$, is the risk that an individual experiences an event (infection in this case) in a small time interval given that the individual has survived up to the beginning of the interval. $\int_0^t h(u)du$ is also known as the cumulative hazard function and the survivor function, $S(t)$, the probability that the time to infection is greater than or equal to t is given by $S(t) = \exp\{-\int_0^t h(u)du\}$ (Collett, 1994, Section 1.3).
For an observed infectious period $({u_j}^{a_j}, {w_j}^{a_j})$ of a g^{th} generation infectious individual a_j of group j and assuming that $\delta_{jk}({u_j}^{a_j}) = 0$, *i.e.* the groups j and k are not mixing at the start of infectiousness period of individual a_j,

$${}^{a_j}h^g{}_{jk}(t) = \begin{cases} \beta_{g(a_j)}\delta_{jk}(t) & \text{if } {u_j}^{a_j} < t < {w_j}^{a_j} \\ 0 & \text{otherwise} \end{cases}$$

Using indicator function notation,

$${}^{a_j}h^g{}_{jk}(t) = \beta_{g(a_j)} \sum_{i=1}^{\lceil \frac{n_{jk}}{2} \rceil} 1_{[t_{2i-1}, t_{2i}]}(t)$$

and the cumulative hazard function is given by:

$${}^{a_j}H^g{}_{jk}(t) = \int_{{u_j}^{a_j}}^{t} {}^{a_j}h^g{}_{jk}(v)dv = \beta_{g(a_j)} \sum_{i=1}^{\lceil \frac{n_{jk}}{2} \rceil} \int_{{u_j}^{a_j}}^{t} 1_{[t_{2i-1}, t_{2i}]}(v)dv$$

$$= \begin{cases} \beta_{g(a_j)} \sum_{i=1}^{n_{jk}/2} (\min\{t_{2i}, t\} - \min\{t_{2i-1}, t\}) & \text{when } n_{jk} \text{ is even} \\ \beta_{g(a_j)} \sum_{i=1}^{(n_{jk}+1)/2} (\min\{t_{2i}, t\} - \min\{t_{2i-1}, t\}) & \text{when } n_{jk} \text{ is odd.} \end{cases}$$

Then given the set, $I_{jk}(t) = I_j(t) \cup I_k(t)$, of infectious individuals in groups j and k at time t, the total instantaneous hazard is given by:

$$h_{jk}(t) = \sum_{a_{jk} \in I_{jk}(t)} {}^{a_{jk}}h^g{}_{jk}(t)$$

and the cumulative hazard up to time t over all infectious animals is

$$H_{jk}(t) = \sum_{a_{jk} \in I_{jk}(t)} {}^{a_{jk}}H^g{}_{jk}(t).$$

The probability P_{escape}, that any individual remaining susceptible at time τ_1 in groups j and k escapes infection when exposed to the total hazard $h_{jk}(\tau_2)$ up to time τ_2 $(\tau_1 < \tau_2)$ is given by:

$$\begin{aligned} P_{escape} &= \exp\{-\sum_{a_{jk} \in I_{jk}(\tau_2)} \int_{\max\{u_j{}^{a_{jk}}, \tau_1\}}^{\min\{w_j{}^{a_{jk}}, \tau_2\}} a_{jk} h^g{}_{jk}(t) dt\} \\ &= \exp\{-\sum_{a_{jk} \in I_{jk}(\tau_2)} [\ \beta_{g(a_{jk})}\ (\ \min\{w_j{}^{a_{jk}}, \tau_2\} - \max\{u_j{}^{a_{jk}}, \tau_1\}\ )\ ]\ \}, \end{aligned}$$

using the definition of the survivor function above.
Hence, the probability that an initially susceptible individual is infected when exposed to the total hazard $h_{jk}(\tau_2)$ up to time τ_2 is given by $1 - P_{escape}$.

Suppose for a given path of infection, an individual a_k is infected by individual a_j when groups j and k are mixing. Let z be the time it takes for an individual a_k to be infected by individual a_j when groups j and k are mixing during the infectiousness period of a_j, i.e. z is measured from $u_j{}^{a_j}$. The time point when infection takes place, $z^* = u_j{}^{a_j} + z$.
It is desired to determine the conditional density of Z, the time to infection, given that infection did occur and infectious periods $(u_j{}^{a_j}, w_j{}^{a_j})$ and $(u_k{}^{a_k}, w_k{}^{a_k})$ were observed. The conditional density of Z is given by:

$$f_Z(z \mid \text{infection occurs}) =$$

$$\frac{\sum_{a_{jk} \in I_{jk}(z^*)} a_{jk} h^g{}_{jk}(z^*) exp\{-\sum_{a_{jk} \in I_{jk}(z^*)} \int_{u_j{}^{a_j}}^{z^*} a_{jk} h^g{}_{jk}(t) dt\}}{1 - P_{escape}}.$$

Let $x_k{}^{a_k}$ be the latent period for individual a_k infected by individual a_j and $f_X(x)$ be the density of the latent period, then $u_k{}^{a_k} - u_j{}^{a_j} = z + x_k{}^{a_k}$, the time to infection plus the latent period of individual a_k.
The distribution of $U_k{}^{a_k} - U_j{}^{a_j}$ given the infection path and the infectious periods can be determined in terms of the density of Z and that of the latent period. This is given by

$$\int_0^{u_k{}^{a_k} - u_j{}^{a_j}} f_Z(z) f_X(u_k{}^{a_k} - u_j{}^{a_j} - z) dz.$$

Hence, an epidemic with a specific path of infection such that it is individual a_j that makes an infectious contact with individual a_k and observed infectious periods $(u_{jk}{}^{a_{jk}}, w_{jk}{}^{a_{jk}})$ for all $a_{jk} \in I_{jk}(t)$ makes a contribution to the likelihood function of the form:

$$\int_0^{{u_k}^{a_k} - {u_j}^{a_j}} f_Z(z) f_X({u_k}^{a_k} - {u_j}^{a_j} - z)dz \times (1 - P_{escape})$$

$$= \int_0^{{u_k}^{a_k} - {u_j}^{a_j}} [\sum_{a_{jk} \in I_{jk}(z^*)} {}^{a_{jk}} h^g{}_{jk}(z^*) exp\{ - \sum_{a_{jk} \in I_{jk}(z^*)} \int_{{u_j}^{u_j}}^{z^*} {}^{a_{jk}} h^g{}_{jk}(t)dt \} \times$$
$$f_X({u_k}^{a_k} - {u_j}^{a_j} - z)] \, dz.$$

To make inference about the infection rate β, the passage multiplier γ and the characteristics of the latent period, all possible infection paths (epidemic chains) for the observed infections must be considered. Infection in groups of size greater than 1 have more than one possible infection path. Thus the likelihood function will be a sum of contributions from all different paths. It is assumed that infections within groups evolve independently of each other. Finally, the likelihood function formulated must be maximized with respect to the parameters using an appropriate computer algorithm. The EM algorithm (McLachlan and Krishnan, 1997, Section 1.5) is a possible algorithm particularly suitable for problems such as this (Becker, 1993b).

3.2.1.2 The likelihood function

The contribution to the likelihood function of a given infection path can consist of three types of factor. Each type equates to the contribution to the likelihood of an individual which has a particular combination of status and observed data. The factoring of the likelihood into components from single individuals is only possible because of conditional independence. The infection times of individuals are not independent because individuals in the same group are exposed to the same infection challenge (same force of infection) and hence one will tend to observe clustering of infections. However, conditional on the force of infection, the chance of an individual becoming infected is independent of the other individuals. The three classes of factor are:

1. A factor determined by the latent period of infectious individuals in group 1, since these latent periods are known.

2. A factor determined by probabilities of escaping infection for those individuals who were exposed to infection but did not become infected.

3. A third factor determined by the convolution of the time to infection and the latent period for individuals that became infectious after exposure to the virus, coupled with a factor containing the probabilities that these infected individuals escaped infection from any other infectious individuals with which they have been in contact.

Depending on the path of infection, the subset of the likelihood determined by probabilities of escaping infection (2, above), consists of the product of these probabilities over all exposed individuals who escaped infection in all groups. These quantities, however, depend on the mixing pattern. The non-infection probability for an individual depends on the number of infectious individuals to which this individual was exposed, given the mixing pattern. The convolution factor (3, above) is a product of these integrals over all individuals which were infected by the end of the experiment. The limits of the component integrals depend on the conditional path of infection, as will be explained below.

A mathematical formulation for the likelihood function for a given infection path is now developed. Let S_j be the number of susceptible individuals in group j at the end of the epidemic, m be the number of groups that were mixed during the course of the epidemic, I_j be the number of infectives in group j, I be the total number of secondary infections in all groups and $a_j \in I_{jk}(t)$ be the individual that makes an infectious contact with a susceptible individual $a_k \in I_{jk}(t)$, where $I_{jk}(t)$ is the set of infected individual in mixing groups j and k at time t.

Then the contribution to the likelihood function for a given path takes the general form given below.

$$\prod_{a_1=1}^{I_1} f_X({u_1}^{a_1}) \times \prod_{\text{group } j=2}^{m} [\, \exp\{- \sum_{a_{jk} \in I_{jk}(t)} \int_{{u_{jk}}^{a_{jk}}}^{{w_{jk}}^{a_{jk}}} {a_{jk}} {h^g}_{jk}(t) dt\} \,]^{S_j} \times$$

$$\prod_{a_k=1}^{I} \int_0^{{u_k}^{a_k} - {u_j}^{a_j}} [\sum_{a_{jk} \in I_{jk}(z^*)} {a_{jk}} {h^g}_{jk}(z^*) \; exp\{- \sum_{a_{jk} \in I_{jk}(z^*)} \int_{{u_j}^{a_j}}^{{u_j}^{a_j}+z} {a_{jk}} {h^g}_{jk}(t) dt \} \times$$
$$f_X({u_k}^{a_k} - {u_j}^{a_j} - z) \,]\, dz.$$

An illustration is given for 1 path of an observed epidemic in groups of size 2. This is an outbreak in four groups of size 2 consisting of 2 initial (primary) infectious individuals in group 1, 2 secondary infections in group 2, 1 secondary infection in group 3 and no infections in group 4.

Consider an outbreak of the form given in Table 3.1.

Table 3.1: *An epidemic in four groups of size 2.*

Group	1	2	3	4
Infections	2	2	1	0

This observed outbreak could correspond to three possible scenarios defining the number of infected individuals in each infection generation, namely:

1. 2 infecteds of generation 0, 2 infecteds of generation 1, and 1 infected of generation 2.

2. 2 infecteds of generation 0, 1 infected of generation 1, and 2 infecteds of generation 2.

3. 2 infecteds of generation 0, 1 infected of generation 1, 1 infected of generation 2 and 1 infected of generation 3.

The scenarios are illustrated in Figure 3.1. The second scenario could occur in two possible ways, as illustrated in Figure 3.1(c and d). Each scenario can be mapped to various pathways by which it could have arisen, as shown in Figures 3.2 and 3.3.
For instance, in the first scenario, with 2 infecteds of generation 0, 2 infecteds of generation 1 and 1 infected of generation 2, there are 8 possible infection pathways that could have yielded this realisation, considering choices of each individual as a possible donor of infection. These pathways are given in Figure 3.2. In the second scenario, with 2 infecteds of generation 0, 1 of generation 1 and 2 infected of generation 2, there are four possible infection pathways that could have yielded this realisation, as illustrated in Figure 3.3. In the last scenario, with 2 infecteds of generation 0, 1 infected of generation 1, 1 infected of generation 2, and 1 infected of generation 3, there are eight possible infection pathways that could have yielded this realisation, four for each of the two possible scenarios in Figure 3.1(c) and (d), and these are given in Figure 3.3.

For illustrative purposes, to explore the nature of the likelihood function, only 1 infection path from the scenario in Figure 3.1(d) is considered. The scenario comprises 2 generation 0 infectives of group 1, 1 generation 1 infective of group 2, 1 generation 2 infective in group 3 and 1 generation 3 infective in group 2. It is assumed that this realisation is associated with path number 5 from Figure 3.3, which indicates that infection is from individual 1 of group 1 to individual 1 of group 2 to individual 1 of group 3 and then to individual 2 of group 2, *i.e* $Y_{11} \rightarrow Y_{21} \rightarrow Y_{31} \rightarrow Y_{22}$.

Figure 3.1: *Possible scenarios defining number of infecteds per generation. The arrows indicate the infection process through the groups for chain types (a)* $2 \to 2 \to 1$, *(b)* $2 \to 1 \to 2$ *and (c) and (d)* $2 \to 1 \to 1 \to 1$.

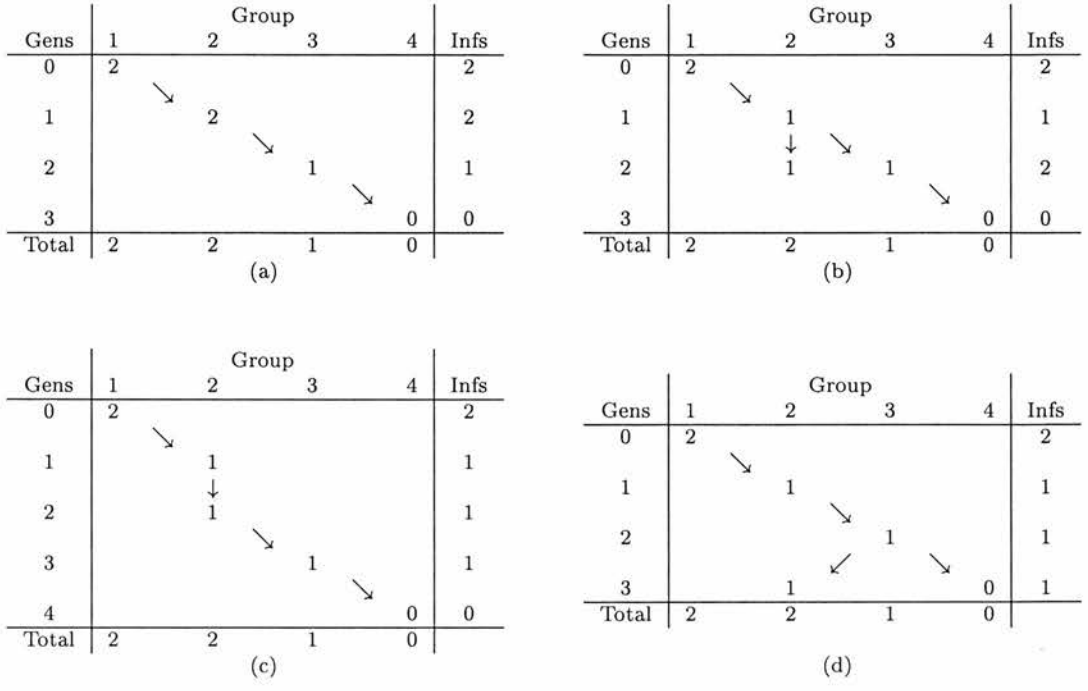

The contribution of path number 5 for scenario 3 in Figure 3.3 to the likelihood function is:

$$\prod_{a_1=1}^{2} f_X({u_1}^{a_1})[\ \exp\{-\int_{u_2^1}^{w_2^1} {}^1h^1{}_{23}(t)dt - \int_{u_3^1}^{w_3^1} {}^1h^2{}_{33}(t)dt - \int_{u_2^2}^{w_2^2} {}^2h^3{}_{23}(t)dt\ \}]^{1(S_3=1)} \times$$

$$[\exp\{-\int_{u_3^1}^{w_3^1} {}^1h^2{}_{34}(t)dt\}\ ]^{2(S_4=2)} \times$$

$$\prod_{a_2=1}^{1} \int_0^{{u_2}^{a_2}-{u_1}^1} \sum_{a_1=1}^{2} {}^{a_1}h^0{}_{12}({u_1}^{a_1}+z) \exp\{-\sum_{a_1=1}^{2} \int_{u_1^{a_1}}^{{u_1}^{a_1}+z} {}^{a_1}h^0{}_{12}(t)dt\} f_X({u_2}^{a_2}-{u_1}^1-z)dz \times$$

$$\prod_{a_3=1}^{1} \int_0^{{u_3}^{a_3}-{u_2}^1} {}^1h^1{}_{23}({u_2}^1+z) \exp\{-\int_{u_2^1}^{u_2^1+z} {}^1h^1{}_{23}(t)dt\} f_X({u_3}^{a_3}-{u_2}^1-z)dz \times$$

$$\prod_{a_2=2}^{2} \int_0^{{u_2}^{a_2}-{u_3}^1} [\ \left({}^1h^1{}_{22}({u_2}^1+z) + {}^1h^2{}_{32}({u_3}^1+z)\right) \exp\{-\sum_{a_1=1}^{2} \int_{u_1^{a_1}}^{{u_1}^{a_1}+z} {}^{a_1}h^0{}_{12}(t)dt\} \times$$

$$\exp\{-\int_{u_2^1}^{u_2^1+z} {}^1h^1{}_{22}(t)dt\} \exp\{-\int_{u_3^1}^{u_3^1+z} {}^1h^2{}_{32}(t)dt\} f_X({u_2}^{a_2}-{u_3}^1-z)\ ]dz.$$

The likelihood function involves unknown components, in particular, the infection path, and hence the generation number of infected individuals. The path can

Figure 3.2: *Possible infection pathways (paths) for scenario 1 given the number of infecteds (Infs) in each infection generation (Gen). $Y_{gi} \equiv$ infected individual i of group g. Arrows indicate the 'donor' and 'recipient' infected individuals.*

	Gen	0		1		2	3
	Infs	2		2		1	0
Paths	1	Y_{11}	$\longrightarrow$	Y_{21}	$\longrightarrow$	Y_{31}	
			$\searrow$				
		Y_{12}		Y_{22}			
	2	Y_{11}	$\longrightarrow$	Y_{21}			
			$\searrow$				
		Y_{12}		Y_{22}	$\longrightarrow$	Y_{31}	
	3	Y_{11}		Y_{21}	$\longrightarrow$	Y_{31}	
			$\nearrow$				
		Y_{12}	$\longrightarrow$	Y_{22}			
	4	Y_{11}		Y_{21}			
			$\nearrow$				
		Y_{12}	$\longrightarrow$	Y_{22}	$\longrightarrow$	Y_{31}	
	5	Y_{11}	$\longrightarrow$	Y_{21}	$\longrightarrow$	Y_{31}	
		Y_{12}	$\longrightarrow$	Y_{22}			
	6	Y_{11}	$\longrightarrow$	Y_{21}			
		Y_{12}	$\longrightarrow$	Y_{22}	$\longrightarrow$	Y_{31}	
	7	Y_{11}	$\longrightarrow$	Y_{22}			
		Y_{12}	$\longrightarrow$	Y_{21}	$\longrightarrow$	Y_{31}	
	8	Y_{11}	$\longrightarrow$	Y_{22}	$\longrightarrow$	Y_{31}	
		Y_{12}	$\longrightarrow$	Y_{21}			

Figure 3.3: *Possible infection pathways (paths) for scenarios 2 and 3 given the number of infecteds (Infs) in each infection generation (Gen). $Y_{gi} \equiv$ infected individual i of group g. Arrows indicate the 'donor' and 'recipient' infected individuals.*

		Scenario 2					Scenario 3							
	Gen	0		1		2	0		1		2		3	
	Infs	2		1		2	2		1		1		1	
Paths	1	Y_{11}	$\longrightarrow$	Y_{21}	$\longrightarrow$	Y_{22}, Y_{31}	Y_{11}	$\longrightarrow$	Y_{21}	$\longrightarrow$	Y_{22}	$\longrightarrow$	Y_{31}	
		Y_{12}					Y_{12}							
	2	Y_{11}	$\longrightarrow$	Y_{22}	$\longrightarrow$	Y_{21}, Y_{31}	Y_{11}	$\longrightarrow$	Y_{22}	$\longrightarrow$	Y_{21}	$\longrightarrow$	Y_{31}	
		Y_{12}					Y_{12}							
	3	Y_{11}					Y_{11}							
		Y_{12}	$\longrightarrow$	Y_{21}	$\longrightarrow$	Y_{22}, Y_{31}	Y_{12}	$\longrightarrow$	Y_{21}	$\longrightarrow$	Y_{22}	$\longrightarrow$	Y_{31}	
	4	Y_{11}					Y_{11}							
		Y_{12}	$\longrightarrow$	Y_{22}	$\longrightarrow$	Y_{21}, Y_{31}	Y_{12}	$\longrightarrow$	Y_{22}	$\longrightarrow$	Y_{21}	$\longrightarrow$	Y_{31}	
	5						Y_{11}	$\longrightarrow$	Y_{21}	$\longrightarrow$	Y_{31}	$\longrightarrow$	Y_{22}	
							Y_{12}							
	6						Y_{11}	$\longrightarrow$	Y_{22}	$\longrightarrow$	Y_{31}	$\longrightarrow$	Y_{21}	
							Y_{12}							
	7						Y_{11}							
							Y_{12}	$\longrightarrow$	Y_{21}	$\longrightarrow$	Y_{31}	$\longrightarrow$	Y_{22}	
	8						Y_{11}							
							Y_{12}	$\longrightarrow$	Y_{22}	$\longrightarrow$	Y_{31}	$\longrightarrow$	Y_{21}	

either be 'made up' given the observed data or summed into the likelihood as an unknown component. The distribution for the latent period has to be assumed in order to be able to evaluate the likelihood function. In addition, it was assumed that the infectiousness period is known precisely but there is a portion of unobserved infectiousness period prior to the first observed time and after the last observed time of infectiousness. If the uncertainty in the infectiousness period is also modelled, the likelihood function will become even more complicated.

It is noticeable that the number of possible infection pathways depends on the group size and how many infected individuals are in each group. The higher the number of infected individuals in each group, the higher the number of possible infection pathways. In the example given above, with just 2 individuals per group and with 2 infectives in group 1, 2 in group 2, 1 in group 3 and none in group 4, the total number of possible infection pathways is twenty. In a situation with group size 8 and with at least 4 infected individuals in each group, the number of possible pathways is very high. For instance, in experiment 1 of the FMD experiments, there are 8 infected individuals in group 1, 6 out of 8 infected individuals in group 2, 8 infected individuals in group 3 and 7 infected individuals in group 4. Restrictions on possible sources of infection may be imposed, for example an assumption of a fixed 1 day latent period would ensure that an individual first observed to be shedding virus on, say, day 4 could not be a possible source of infection for individuals first observed to be shedding on days beyond day 4. Also we could take the mixing pattern into consideration, so that, for example, an individual from group 1 could not be a possible source of infection for an individual in groups 3 and 4. Nevertheless, the number of possible paths would still remain very high.

Depending on the distribution assumed for the latent period, the likelihood function could be complicated since it could involve integrals that are analytically intractable. In the illustration above, it is assumed that the length of the infectious period is known, which is a major assumption. Even if one uses the observed viraemic periods or duration of symptoms to signify the infectious period, there is always an unobserved period of 'infectiousness' especially when sampling has occurred at discrete times, which is usually the case when collecting infectious disease data. The number of generations is also an unknown quantity because the exact times of infection and source of infection are unobservable. It can be appreciated that modelling the FMD experimental infection process using chain binomial models would involve making so many assumptions that the results ob-

tained would be unreliable. Therefore this thesis will not focus on models of individual infection pathways; instead, the average infection process within groups of sheep will be modelled. However, a published (de Jong et al., 1996) approach to modelling FMD experimental data while considering infection pathways using generalized linear models is evaluated, since, of necessity, it incorporates many of the simplifying assumptions listed above.

3.3 Generalized linear models

Generalized linear models (GLMs) are an extension of the classical linear model. A GLM is made up of three components namely, the random component which may be normally distributed (as in ANOVA) or may follow any distribution in the exponential family; the systematic component which models the effect of covariates; and the link function, a monotonic differentiable function which provides the link between the random and systematic components (McCullagh and Nelder, 1983, Section 2.2).

The GLM approach is straightforward when all aspects of the infection process are observable. However, in practice, no genuine infectious disease data set is ever likely to be so complete. There are two sets of circumstances when the approach can be applied, namely:

1. When the disease is such that the latent and infectiousness periods are essentially of fixed duration, *i.e.* random variation in the duration of latent and infectiousness periods is negligible.

2. When the infectiousness period is indicated by observable symptoms or signs. Although there may be variation in the duration of infectiousness period among infectives, one is able to determine the infectiousness period for each infective by the show of symptoms or signs.

Thus, in order to apply the GLM approach to infectious disease data, a number of assumptions have to be made. In particular, it is assumed that the numbers of infectives and susceptibles are observable over time. This is a drawback in the approach as it will limit the applicability of the method. However the method may still answer important epidemiological questions even though the underlying assumptions are only approximately true.

The GLM approach has been used by several authors to estimate infection process parameters in epidemic studies. Becker (1989), Section 6.4, applies the approach to data from a smallpox outbreak in a closed community of Abakaliki in south-eastern Nigeria to estimate the rate of infection, while assuming fixed latent and infectious periods. Becker (1989), Section 6.5, also uses the approach to analyse respiratory disease data to estimate the rate of infection both within a household and between households. Nodelijk et al. (2000), use a GLM to estimate the transmission parameter for respiratory syndrome virus in a Dutch breeding herd of pigs, while van Nes et al. (2001) use a GLM to estimate the reproduction ratio as a measure of transmission of pseudo rabies virus in a vaccinated sow herd.

3.3.1 Formulation of the GLM as applied to epidemic data

Suppose the duration of the latent period is μ_x for each infected individual and that properties of the disease are sufficiently well known that a value can be assigned a *priori* to the constant μ_x, *e.g.* 1 day in the case of the FMD experimental data. Suppose further that the infectious period can be deduced for each infected individual. The aim of the analysis is to study the characteristics of the spread of the disease through a population.
Let λ denote the risk of infection for susceptible individuals due to infectious individuals. Attention is focused on the form of λ and inference about its parameters, where in general,

$$\Pr[\, S(t+\delta) = s-1 | I(t) = i, S(t) = s \,] \;=\; \lambda(i,s)\delta + o(\delta),$$

where $S(t)$ is the number of susceptibles at time t, $I(t)$ is the number of infectives at time t and δ is a small increment in time.
To introduce the generalized linear model, it is convenient to formulate the assumptions about the risk of infection in terms of the individual susceptibles. A given individual, who is still susceptible at time t, may be infected during the time increment $(t, t+\delta)$ with probability $\lambda(I(t))\,\delta + o(\delta)$, where λ is a specified function of $I(t)$ and other epidemiological factors and is assumed to involve only a small number of unknown parameters. It is assumed that each susceptible individual is subjected to the risk of infection independently of other susceptibles, with $\lambda(i) = \frac{\beta i}{N}$, $i = 0, 1, 2, \ldots$, where β is the rate of infection, i is the number of infectious individuals and N is the total number of individuals in the study population.

For the purposes of the present analysis, it is convenient to partition the continuous absolute time scale into a succession of time intervals, in this case, days, *i.e.* to evaluate the process on a day-to-day basis. Partitioning of the time interval is not merely a mathematical convenience but also a reflection of the nature of infectious disease data. Such data are normally available in terms of discrete time units. The time unit is usually chosen in such a way to ensure that only a small number of cases occur in one unit of time. As a results, the conditional probability of a given susceptible escaping infection during the time interval $(t, t+1)$ given $\lambda(I(u))$ for $u \in (t, t+1)$, is approximately equal to $e^{-\int_t^{t+1} \lambda(I(u))du}$. This conditional probability may be approximated by $e^{-\lambda(I(u))}$, for some $u \in (t, t+1)$ if the value of λ does not vary appreciably during the time interval $(t, t+1)$.

3.3.1.1 Analysis of epidemic data based on the GLM approach

Assume that during a given time unit, susceptibles either escape infection or become infected independently of each other. Let $C(t)$ denote the number of individuals infected (cases) during the time interval $(t, t+1]$, $t = 0, 1, 2, \ldots$. The conditional distribution of $C(t)$ given $S(t)$ and $\lambda(I(u))$ for $u \in (t, t+1]$, is approximately a binomial distribution with index $S(t)$ and parameter $1 - e^{-\lambda(I(t))}$, *i.e.* conditional on $S(t)$ and $\lambda(I(u))$,

$$C(t) \sim Bin(S(t),\, 1 - e^{-\lambda(I(t))})$$

and the expected value $E(C(t)) = S(t)\, e^{-\lambda(I(t))}$ from which

$$\lambda(I(t)) \;=\; -\ln\left(1 - \frac{E(C(t))}{S(t)}\right). \tag{3.1}$$

Although $C(0), C(1), C(2), \ldots$ are not independent random variables, it can be claimed that the respective observations $c(0), c(1), c(2), \ldots$, provide essentially independent information about the parameters contained in the specification of λ, when they are treated as conditional on the size of the susceptible population at the start of each day. Thus inference about these parameters should proceed as though $C(0), C(1), C(2), \ldots$ were independent.

If $\lambda(I(t))$ in Equation (3.1) can be linearized by log-transformation such that $\ln[\lambda(I(t))] = \ln\left[-\ln\left(1 - \frac{E(C(t))}{S(t)}\right)\right]$ is linear in the parameters defining $\lambda(I(t))$, then a generalized linear model for the number of new cases $C(t)$ with a complementary log-log link function (McCullagh and Nelder, 1983, Section 2.2.3) has

been specified and can easily be fitted in standard statistical packages, for example Genstat (Genstat 5 Committee, 1993) or S-Plus (MathSoft, 1999), to obtain ML estimates for the parameters involved. Where $\lambda(I(t)) = \frac{\beta I(t)}{N(t)}$, this is indeed the case.

3.3.2 GLMs applied to FMD experimental data

For the FMD experimental data, the aim is to estimate the rate of infection β_g for each infection generation g. Thus the risk of infection at time t is given by:

$$\lambda(I(t)) = \sum_{g=0}^{G} \frac{\beta_g I_g(t)}{N(t)}, \tag{3.2}$$

where G is the total number of infection generations, $I_g(t)$ is the number of generation g infectious individuals at time t and $N(t)$ is the number of individuals mixing in a given group at time t.

From Equation (3.2),

$$\ln\left[-\ln\left(1 - \frac{E(C(t))}{S(t)}\right)\right] = \ln[\lambda(I(t))] = \ln\left[\sum_{g=0}^{G} \frac{\beta_g I_g(t)}{N(t)}\right].$$

However, $\ln[\lambda(I(t))]$ is not linear in the parameters β_g hence a GLM can not be fitted to generate estimates of β_g.

One alternative is to re-parameterise λ in a way similar to that proposed by de Jong et al. (1996). These authors set out to investigate population persistence and recurrent outbreaks of bovine respiratory syncytial virus on dairy farms. Based on the assumption that both seronegative and seropositive cattle can become infected, de Jong et al. (1996) investigate whether infectivity and rate of recovery may differ depending on whether the animal was seronegative or seropositive when infected. They also investigate whether susceptibility to infection may differ between seronegative and seropositive cattle. The authors use GLMs to estimate the different rates of infection namely; β_{nn}, the rate at which seronegative cattle become infected by seronegative infectious cattle, β_{np}, the rate at which seronegative cattle become infected by seropositive infectious cattle, β_{pn}, the rate at which seropositive cattle become infected by seronegative infectious cattle and β_{pp}, the rate at which seropositive cattle become infected by seropositive infectious cattle. In order to be able to apply a GLM to the data, the following expected value equation was used for the case of susceptible seronegative cattle:

$$E[dI_n] = \exp[a + bq]\,\frac{S_n(I_n + I_p)}{N},$$

where S_n is the average number of seronegative cattle, dI_n is the average daily incidence of primary infections, I_n is the number of seronegative infectious cattle, I_p is the number of seropositive infectious cattle, N is the total cattle population under study, the covariate $q = \frac{I_n}{I_n+I_p}$ is the fraction of infectious animals that are seronegative and where a and b are parameters to be estimated from the GLM. Taking $\ln[S_n(\frac{I_n+I_p}{N})]$ as an offset, $\hat{a}$ and $\hat{b}$ were estimated and from these the transmission rate parameters β_{np} and β_{nn} were computed by $\beta_{np} = e^{\hat{a}}$ and $\beta_{nn} = e^{\hat{a}+\hat{b}}$ yielding separate estimates for the rate at which seronegative animals become infected by seronegative infectious animals and the rate at which seronegative animals become infected by seropositive infectious animals. Similarly, the corresponding estimates for seropositive animals were estimated. The technique is exact if over the time period, there is only one category of infectious individuals such that on each sampling day q is either equal to 0 or 1.

Formally, the method makes the approximation that

$$\beta_{nn}\, q + \beta_{np}\,(1-q) \;\simeq\; \beta_{nn}^{q}\, \beta_{np}^{1-q}$$

the equality being true iff $q = 0$ or $q = 1$. Hence the parameterisation assumes that during any sampling day, q is consistently close to either 0 or 1. It is arguable how valid this assumption might be in the original application; it is certainly not especially credible when applied to the FMD experimental data, where there are several generations to be modelled, and a relatively small group size.

Following the parameterisation in de Jong et al. (1996), $\lambda[I(t)]$ in Equation (3.2) can be reparameterised such that

$$\sum_{g=0}^{G} \frac{\beta_g\, I_g(t)}{N(t)} \;\equiv\; \exp[a_0 + \sum_{k=0}^{G} a_k\, q_k] \sum_{g=0}^{G} \frac{I_g(t)}{N(t)}$$

with

$$\beta_0 = e^{a_0},\ \beta_g = e^{a_0 + a_g\, q_g},\ g \geq 1 \ \text{ and } \ q_k = \frac{I_k(t)}{\sum_{g=0}^{G} I_g(t)},\ k \geq 1. \qquad (3.3)$$

Then

$$\ln\left[-\ln\left(1 - \frac{E(C(t))}{S(t)}\right)\right] \;=\; \ln[\lambda(I(t))] \;=\; a_0 + \sum_{k=0}^{G} a_k\, q_k + \ln\left(\sum_{g=0}^{G} \frac{I_g(t)}{N(t)}\right)$$

is linear in the parameters a_g and hence a GLM with complementary log-log link function and $\ln\left(\sum_{g=0}^{G} \frac{I_g(t)}{N(t)}\right)$ as an offset can be fitted to the data to yield the estimates and estimates of standard errors for the a_g.

Estimates for the β_g are then determined from estimates of a_g using Equation (3.3) and estimates of the corresponding standard errors are calculated using the δ method (Becker, 1989, Appendix). The δ method involves expansion of a function of a random variable about its mean, usually with a one-step Taylor approximation, and calculation of the variances of the approximation. For instance, if it is desired to approximate the variance of a function $G(x)$, where X is a random variable with mean μ_x and $G(x)$ is differentiable, then

$$G(x) \simeq G(\mu_x) + (x - \mu_x) G'(\mu_x) = G(\mu_x) + x G'(\mu_x) - \mu_x G'(\mu_x)$$

such that

$$Var(G(x)) \simeq Var(X G'(\mu_x)) \simeq [G'(\mu_x)]^2 Var(X) \tag{3.4}$$

where $G'() = \frac{dG()}{dx}$.

For vector-valued functions of random variables,

$$Var(G(x)) = G'(\mu_x) Var(X) [G'(\mu_x)]^T \tag{3.5}$$

and this in fact is the basis for deriving the asymptotic variance of maximum likelihood estimators. In Equation (3.5), X is a $1 \times m$ vector, $Var(X)$ its $m \times m$ variance-covariance matrix, $G(x)$ is a vector function returning a $1 \times n$ column vector, $G'(x)$ is its $n \times m$ matrix of first derivatives, T is the transpose operator and $Var(G(x))$ is the resulting $n \times n$ variance-covariance matrix of $G(x)$.

An alternative to the de Jong et al. (1996) parameterisation approach is the direct maximization of the likelihood. The likelihood (L) and log-likelihood (l) functions for the cases are given by:

$$\begin{aligned} L &= \prod_{days(t)} \left\{ \binom{S}{C} \left(1 - e^{-\sum_{g=0}^{G} \frac{\beta_g I_g}{N}}\right)^C \left(e^{-\sum_{g=0}^{G} \frac{\beta_g I_g}{N}}\right)^{S-C} \right\} \\ l &= \sum_{days} \ln \binom{S}{C} + \sum_{days(t)} C \ln \left(1 - e^{-\sum_{g=0}^{G} \frac{\beta_g I_g}{N}}\right) + (S - C) \left(-\sum_{g=0}^{G} \frac{\beta_g I_g}{N}\right), \end{aligned} \tag{3.6}$$

where S, C, I_g, and N, all depend on the day t.

The re-parameterisation of the rate of infection proposed to allow fitting via a GLM will yield estimates equal to the estimates obtained by direct maximisation of the likelihood if at any one moment there is only one generation of infectious individuals, *i.e.* infectious individuals in higher generations are detected only when the preceding generation of infections has ceased to be infectious, so that if $I_k(t) > 0$ then $I_g(t)$ should be equal to zero for all $g \neq k$.

3.3.2.1 The data

The de Jong et al. (1996) approach is applied to data from FMD experiment 1. For each day between the start and the end of the experiment, the number of sheep that were viraemic is noted. In this study viraemia is used as an indicator for infectiousness. This is a major assumption, but studies have shown that peak viraemia coincides with high infectiousness (Hughes et al., 2002a). The data extracted from the full experimental data as required to fit the model in Genstat is presented in Table 3.2. Data are presented only for days where the mixing groups have at least 1 infectious individual *i.e* $I(t) > 0$. The data required to fit the GLM was extracted from the observed viraemia experimental data in Figure 1.3. The data previously have been described in Sections 1.3.1 and 1.3.3.

An individual was assumed to have become a case 1 day before it was observed to be shedding virus, *i.e.*, a 1 day fixed latent period was assumed. The basis for this assumption was that if the individual had detectable viraemia on any previous sampling day, then it would have been identified as being viraemic. The assignment of cases to donors and hence cases to generation numbers, was done by 'eye' depending on the most likely donor among the present infectives and the mixing pattern. Four infection generations are assumed, such that all infected individuals that would have been assigned infection generation numbers of 3 or higher are all assigned to infection generation 3. This is on assumption that any passage effects will have largely occurred by generation 3, and in practical terms it ensures an adequate sample size of generation 3 observations. Thus there are four rates of infection parameters to be estimated, *i.e.* β_0, β_1, β_2 and β_3 for infection generations 0 to 3 respectively.

3.3.2.2 Results from the analysis of experimental data

A GLM was fitted to the data in Genstat and the results presented in Table 3.3 were obtained. Group 1 infected individuals which are generation 0 infectives have an estimated rate of infection of 0.14 ($s.e = 0.147$), generation 1 infectives have an estimated rate of infection of 0.86 ($s.e = 0.636$), generation 2 infectives have their rate of infection estimated to be 3.56 ($s.e = 1.724$) and generation 3 and higher infectives have an estimated rate of infection of 0.73 ($s.e = 0.242$).

It is observed that the initial infected individuals have a very low rate of infection. Indeed from the criterion used to define the cases, only 1 generation 1

Table 3.2: *Data from experiment 1 required to fit the generalised linear model where $C_g(t)$ is the number of generation g cases on day t, $C(t) = \sum_{g=0}^{3} C_g(t)$, $I_g(t)$ is the number of generation g infecteds on day t, $I(t) = \sum_{g=0}^{3} I_g(t)$, and $R(t)$ is the number of recovered individuals on day t.*

Day t	Room	$N(t)$	$S(t)$	$C_1(t)$	$C_2(t)$	$C_3(t)$	$C(t)$	$I_0(t)$	$I_1(t)$	$I_2(t)$	$I_3(t)$	$I(t)$	$R(t)$
1	1	16	11	0	0	0	0	5	0	0	0	5	0
2	1	8	1	0	0	0	0	7	0	0	0	7	0
3	1	16	9	1	0	0	1	5	0	0	0	5	2
4	1	8	1	0	0	0	0	1	0	0	0	1	6
4	2	16	15	0	0	0	0	0	1	0	0	1	0
5	1	16	8	0	0	0	0	0	1	0	0	1	7
6	2	16	15	0	2	0	2	0	1	0	0	1	0
7	1	16	7	0	0	2	2	0	0	1	0	1	8
7	3	16	15	0	0	3	3	0	0	1	0	1	0
8	2	16	8	0	0	2	2	0	0	2	5	7	1
9	1	16	4	0	0	0	0	0	0	1	3	4	8
9	3	16	11	0	0	3	3	0	0	1	4	5	0
10	2	16	4	0	0	1	1	0	0	0	8	8	4
10	4	8	7	0	0	0	0	0	0	0	1	1	0
11	1	16	3	0	0	0	0	0	0	0	1	1	12
11	3	16	8	0	0	5	5	0	0	0	4	4	4
12	2	16	2	0	0	0	0	0	0	0	5	5	9
12	4	8	3	0	0	1	1	0	0	0	5	5	0
13	1	16	3	0	0	0	0	0	0	0	1	1	12
13	3	16	2	0	0	0	0	0	0	0	7	7	7
14	2	16	2	0	0	0	0	0	0	0	1	1	13
14	4	8	2	0	0	1	1	0	0	0	4	4	2
15	3	16	1	0	0	0	0	0	0	0	2	2	13
16	4	8	1	0	0	0	0	0	0	0	1	1	6
17	3	16	1	0	0	0	0	0	0	0	1	1	14
18	4	8	1	0	0	0	0	0	0	0	1	1	6

infective was identified. 7 of the 8 initially inoculated sheep became viraemic, but managed to generate only 1 secondary infection. These results do seem to indicate that the inoculated sheep had very low potential to cause infection in group 2 individuals. The estimated rate of infection increases between generation 0 and 1 and between generation 1 and 2 and drops in generation 3. Generation 2 infectives have the highest estimated rate of infection and this could be because of the natural infection exposure from generation 1 infective. The estimated rate of infection drops between generation 2 and 3 infectives and it could be possible that this is associated with the hypothesis of rate of infection dropping through passage. Performing an analysis with only two levels of rate of infection, *i.e.* one rate of infection assumed for the generation 0 *i.e.* infection due to inoculation and one infection rate assumed for all secondary infections (natural infections), yielded an estimated generation zero rate of infection of 0.14 and rate of infection for secondary infections of 1.06. Comparing the model with two levels of rate of infection with a model where only one rate of infection is assumed for all infections, the two models were statistically significantly different (p-value = 0.03,

Table 3.3: *Results obtained from the generalized linear model fitted to data in Table 3.2.*

Infection generation g	$\hat{a}_g$	$s.e(\hat{a}_g)$	$\hat{\beta}_g$	$s.e(\hat{\beta}_g)$
0	-1.96	1.04	0.14	0.147
1	1.81	1.28	0.86	0.636
2	3.23	1.15	3.56	1.724
3	1.64	1.09	0.73	0.242

based on the F test using the change in deviance). The model assuming three different rates of infection, one rate for generations 0 and 1 combined, another rate for generation 2 and one rate for generation 3 and higher generations, provided a better fit to the data compared to the model with one rate of infection. The results indicate that the rate of infection in inoculated sheep is lower than the rate of infection in naturally infected sheep.

As pointed out earlier, the re-parameterisation of the rate of infection proposed in the de Jong et al. (1996) parameterisation would yield estimates equal to estimates obtained by direct maximisation of the likelihood if in any one time period there is only one generation of infectious individuals. However, this may not be the case and indeed from the FMD experimental data it is true for generation 0 and 1 but not for generations 2 and 3. The rates of infection estimates obtained from the GLM have a similar trend to those obtained by direct maximisation, however, the GLM yielded a higher generation 2 rate of infection and a lower generation 3 rate of infection compared to the ML estimates. The estimates obtained by direct maximisation of the likelihood are: $\hat{\beta}_0 = 0.14\,(s.e = 0.199)$, $\hat{\beta}_1 = 0.86\,(s.e = 0.864)$, $\hat{\beta}_2 = 2.58\,(s.e = 1.480)$ and $\hat{\beta}_3 = 0.77\,(s.e = 0.364)$. These differences are probably due to the inadequacies of the de Jong et al. (1996) approximation in this application.

The GLM approach works on the assumption that the infection generation is known for each infected individual. Generally, assignment of infection generation number to individuals is very subjective. For the FMD experimental data, it was assumed that individuals became cases on the day before they tested positive to FMD virus and on that assumption, given the generation of infected individuals with which any particular individual sheep was mixing when it is assumed to have become a case, an infection generation number was assigned to it. In the next section, therefore, the de Jong et al. (1996) approach as applied to data from the FMD experiments is evaluated using simulated data from a model that incorporates the design of the experiment.

3.3.3 Evaluation of the GLM approach using simulated data

Simulation models that reflect the design of the experiment, based on a susceptible-latent-infectious-recovered (SLIR) infection process as described in Section 2.4 were used to generate epidemic data. Data were generated from two models, namely:

1. A model assuming a gamma distributed latent period with distribution mean equal to 1.5 days (based on a *p*riori expert knowledge) and a gamma distributed infectiousness period with distribution mean equal to 2.8 days (calculated from the number of viraemic days observed in experiment 1).

2. A model assuming a fixed latent period of 1.5 days and a fixed infectiousness period of 2.8 days.

The input parameters in the models were a rate of infection set equal to 0.86 for the initially infected individuals of group 1 and a passage multiplier of zero such that the true rates of infection for all infection generations were equal to 0.86. 0.86 is the β_0 estimate from the GLM estimated in Section 3.3.2.2.

From each run of the model, two data sets were generated to evaluate the GLM approach. One is where the analysis can be based on true infection generation. Within the model, the 'donor' for each infected individual is known and hence the true infection generation number will be known. The other data set, based on the same realisation of the process, is the more realistic model of data, where analysis would be based on assigning infected individuals infection generation numbers (referred to as pseudo infection generations) using some criteria as though the truth was not known. These models of infection assignment are outlined below.

Within realisation from the model assuming random latent and random infectiousness periods, an infected individual was identified as having become a case 1 day or 2 days before it was first observed to be infectious based on certain probabilities. Let $p_{-\tau}$ denote the probability of an infective being observed on day d given that it became a case on day $d-\tau$, $I_{-\tau}$ denote the number of infectious individuals on day $d-\tau$ and β the rate of infection.
On making some simplifying assumptions we have:
Pr(individual became exposed on day $d-\tau$ | individual was observed to be positive on day d) is approximately equal to

$$\frac{p_{-\tau}\, I_{-\tau}}{\sum_{i=1}^{\infty} p_{-i}\, I_{-i}}.$$

The approximation is not particularly valid, but it is likely to correspond to the type of simplifying assumption made by a person attempting mentally to assign an infection path to an observed data set.

Restricting τ to only 2 days before observation of infection yields:
Pr(individual became case on day $d - \tau$ | individual was susceptible prior to day $d - \tau$ and was observed to be infectious on day d)

$$\simeq \frac{p_{-\tau} I_{-\tau}}{p_{-1} I_{-1} + p_{-2} I_{-2}}, \quad \text{for } \tau = 1, 2.$$

For the data modelled here, p_{-1} and p_{-2} were set equal to 0.5, *i.e.* equal probabilities of becoming a case either 1 or 2 days before being observed as infectious.

Within realisations from the model assuming fixed latent and infectiousness periods, infection generation numbers for infected individuals were assigned on the basis of when the individuals became infections. This was done by assuming that individuals became cases 1 day before first being observed to be infectious and randomly assigning an infection generation number calculated from the generations of infectious individuals mixing on that day. However, due to the mixing pattern, a situation frequently arose where on that day, the individual in question was not mixing with any infectious individuals and hence it could not have become a case on that day. In such situations the individual was defined as having become a case 2 days before it was observed as being infectious and a generation number was assigned randomly calculated from the generation numbers of infectives mixing on that day.

Thus four different categories of data were analysed, namely:

1. That based on true allocation of infection generation numbers, with random latent and random infectiousness periods.

2. That with random latent and random infectiousness periods with allocated pseudo infection generations based on probabilities.

3. That with fixed latent and infectiousness periods with true allocation of infection generations.

4. That with fixed latent and infectiousness periods with pseudo infection generations derived by assuming infection either 1 or 2 days previously, depending on the presence or absence of candidate individuals.

100 sets of epidemic data in each category were analysed using a GLM to yield estimates for the rate of infection for different infection generations. 95% confidence intervals for each $\hat{\beta}_g$ were constructed and the proportion of intervals, denoted by P(fail), that failed to cover the true value $\beta_g = 0.86$ was determined. For each P(fail), exact 95% confidence intervals were calculated based on the formulae in Armitage and Berry (1994), Section 4.7, to determine whether the approach gave rise to confidence intervals with 95% confidence. The results are summarised in Table 3.4. For some realisations the total number of infection generations inferred was as high as thirteen (generation 0 to 12), however, only results for the first four generations are presented. For each of infection generations 0 to 3, results presented include the mean of $\hat{\beta}_g$ for the 100 realisations, P(fail) and the 95% confidence intervals of P(fail).

Table 3.4: *Summary of results for the power study of the GLM approach based on simulated data.*

Lat/ InfP type	Gen (g)	True infection generation			Pseudo infection generation		
		$\hat{\beta}_g$ mean	P(fail)	95% CIs	$\hat{\beta}_g$ mean	P(fail)	95% CIs
Random	0	0.902	0.117	(0.062, 0.195)	0.621	0.194	(0.123, 0.284)
	1	0.897	0.107	(0.055, 0.183)	1.617	0.117	(0.062, 0.195)
	2	0.975	0.097	(0.048, 0.171)	1.346	0.087	(0.041, 0.159)
	3	0.976	0.126	(0.069, 0.206)	1.248	0.126	(0.069, 0.206)
Fixed	0	0.898	0.050	(0.018, 0.105)	0.393	0.481	(0.383, 0.580)
	1	0.634	0.190	(0.125, 0.271)	1.553	0.038	(0.010, 0.094)
	2	1.015	0.099	(0.052, 0.167)	1.523	0.123	(0.067, 0.201)
	3	0.723	0.248	(0.174, 0.335)	2.210	0.057	(0.021, 0.119)

For all the four categories, apart from estimates of $\hat{\beta}_1$ from the model with fixed latent and infectiousness periods with pseudo generation infection, all estimates have P(fail) greater than the notional 5%. The GLM approach performs poorly in all categories. It is also notable that the pseudo infection generations have inflated estimates of rate of infection compared to the true infection generation, except estimates for the generation 0 parameter. P(fail) is higher for pseudo infection generations for a majority of estimates than in the equivalent true infection generations. However, this effect is not as pronounced as might have been expected. Examining the confidence intervals for P(fail), it is clear that almost all of the true generation infections based intervals do not cover the notional P(fail) of 5%. Thus, it is concluded that the type of re-parameterisation proposed by de Jong

et al. (1996) does not perform well in the particular situation of multiple generation parameter estimation arising from the design of the FMD experiments. Also, the use of informally inferred epidemic paths clearly produces inflated estimates of infection parameters and conservative confidence intervals. The latter effect is inevitable, given the failure to account for the potential variability in the infection path.

3.4 Summary

The use of chain binomial models and generalized linear models as applied to epidemic data have been reviewed and their application to the FMD experimental data evaluated. It was concluded that the chain binomial model would be very difficult to implement in this situation, where the group size is higher than the usual household size in the context where the chain binomial model has been most frequently applied. Evaluation of the GLM approach revealed that the method performs poorly for these data and is highly sensitive to knowledge of individual infection generation numbers. Thus modelling the infection process for the FMD experiments based on individual infection pathways using classical methods appears impractical given the obstacle of having to know the true infection paths. An alternative to the models considered in this chapter is to model the infection process on the basis of average infection rate in groups of sheep rather than in individuals. This approach uses the fact that any decreasing rate of infection across groups is most probably due to the presence of more higher generation infected individuals in higher groups. Modelling the infection process on the basis of groups and the methods for estimating the associated parameters on are the subject of Chapters 4, 5, 6 and 7.

Chapter 4

Group parameter estimation methods for FMD infection process models

4.1 Introduction

In the analysis of the infection dynamics of experimental FMD in sheep, for the rest of this thesis, the focus will be on modelling the infection process in groups of sheep rather than in individual sheep. In the previous chapter it became apparent that formulation of models in terms of infection generations makes inference difficult. The source of infection for each infected individual needs to be known to determine the generation number of an infected individual. Only group 1 infected individuals which were artificially infected and the first group 2 infected individual have a known generation. Modelling the infection process in groups of sheep rather than individuals avoids the need to know individual infection generations and full infection pathways. Models fitted at group level will aim to estimate the typical infection rate, β, acting upon different groups of sheep *i.e.* the rates at which groups of sheep acquire infection. Once a set of β estimates for each group has been calculated, if there is a genuinely decreasing trend, the only possible cause is a drop in infectivity with increased generation. This follows from the consideration that the mixing strategy ensures that an infection in a higher numbered group will tend to be of a higher generation. In the current chapter, methods for estimating β for groups 2 to 4 are described. These include maximum likelihood and martingale estimation methods. β estimates will be calculated together with estimates for the expected characteristics of the infection process in an iterative scheme. The mechanism for the proposed iterative scheme

is described and the justification, mentioned in Section 2.7.1, for using a non-EM algorithm is given.

4.2 Maximum likelihood estimation methods

One of the methods that will be used to estimate the βs is the maximum likelihood estimation (MLE) method. The likelihood and log-likelihood functions are the basis for deriving estimators for parameters from data. While the shapes of these two functions are different, they have their maximum point at the same value of the parameter. The value of the parameter that corresponds to the maximum point of the log-likelihood function is defined to be the ML estimate. In other words, the ML estimate of the unknown parameter in the model is the value that maximizes the log-likelihood for the observed data. The log-likelihood links the data, unknown model parameters and model assumptions and allows rigorous statistical inference. It is of fundamental importance in the theory of inference and in all of statistics.

Generally, calculus is used to find the maximum point of the log-likelihood function and obtain ML estimates in closed form. However, in some cases a closed form solution is unattainable and numerical methods have to be used in order to attain the desired ML estimates. Assuming a model has k parameters $\theta_1, \theta_2, \ldots, \theta_k$, then the log-likelihood $Log_e(L(\theta_1, \theta_2, \ldots, \theta_k|\text{data}) \equiv log_e(L)$ and k log-likelihood equations can be defined:

$$\frac{dlogL}{d\theta_1} = 0, \ \frac{dlogL}{d\theta_2} = 0, \ \ldots, \ \frac{dlogL}{d\theta_k} = 0.$$

The solution of these equations gives ML estimates $\hat{\theta_1}, \hat{\theta_2}, \ldots, \hat{\theta_k}$.

In estimating parameters for the FMD infection process, two sets of estimates of β will be considered using MLE methods applied to two different models, namely, unrestricted ML estimates of β and restricted ML estimates of β. For the unrestricted model (also under martingale methods), the estimates of β in groups 2 to 4 will be unrestricted in the sense that, for instance, the estimate in group 2 can be lower or higher than the estimate in group 3. For the restricted model, however, the estimates of β in groups 3 and 4 will be restricted to ensure that the estimates are non-increasing with respect to increasing group number. This restriction will increase the power to detect a decreasing trend in β if such

a decreasing trend indeed is present. The restriction is justified by the nature of the experimental hypothesis of decreasing infectivity due to passage effect.

4.2.1 Formulation

Let β_g denote the rate of infection to group g.

I_g denote the total number of infected individuals in group g.

N_g denote the total number of individuals in group g.

$n(t)$ denote the total number of mixing individuals at time t.

$I(t)$ denote the total number of infectious individuals in mixing groups at time t.

$I_{gi}(t)$ denote the number of infectious individuals mixing with individual i of group g at time t.

$n_{gi}(t)$ denote the total number of individuals mixing with individual i of group g at time t.

The hazard to which an individual i of group g is exposed at a given time t is given by:

$$h_{gi}(t) = \beta_g \frac{I_{gi}(t)}{n_{gi}(t)}.$$

Then the probability that a susceptible individual i of group g becomes infected at time t_{gi} is given by:

$$\Pr(i \text{ becomes infected at } t_{gi}) = h_{gi}(t_{gi})\, e^{-\int_0^{t_{gi}} h_{gi}(t)\,dt} = \beta_g \frac{I(t_{gi})}{n(t_{gi})} e^{-\beta_g \int_0^{t_{gi}} \frac{I_{gi}(t)}{n_{gi}(t)} dt}$$

and the probability that a susceptible individual s of group g escapes infection during the entire epidemic duration is given by:

$$\Pr(s \text{ escapes infection}) = e^{-\int_0^{t_g^{max}} h_{gs}(t)\,dt} = e^{-\beta_g \int_0^{t_g^{max}} \frac{I_{gs}(t)}{n_{gs}(t)} dt},$$

where t_g^{max} is the time at which virus shedding ceases from the last shedding individual mixing with individuals in group g.

Based on these probabilities, a likelihood function of the infection process given the observed data is formulated and from it parameters will be estimated using MLE.

Let L denote the likelihood function, then:

$$\begin{aligned} L &= \prod_{g=2}^{4} \left\{ \prod_{i=1}^{I_g} \Pr(i \text{ becomes infected at } t_{gi}) \prod_{s=1}^{N_g - I_g} \Pr(s \text{ escapes infection}) \right\} \\ &= \prod_{g=2}^{4} \left\{ \prod_{i=1}^{I_g} \beta_g \frac{I(t_{gi})}{n(t_{gi})} e^{-\beta_g \int_0^{t_{gi}} \frac{I_{gi}(t)}{n_{gi}(t)} dt} \prod_{s=1}^{N_g - I_g} e^{-\beta_g \int_0^{t_g^{max}} \frac{I_{gs}(t)}{n_{gs}(t)} dt} \right\}. \end{aligned} \tag{4.1}$$

Note that the likelihood splits into factors corresponding to infected and non-infected individuals. This arises due to the fact that although the infection times of individuals are not independent, conditional on the force of infection, the probability of an individual becoming infected is independent of that applying to all other individuals.

4.2.2 The likelihood function for unrestricted model MLE

To ensure that the β estimates are non-negative, a re-parameterisation for the βs is proposed such that $\beta_g = e^{\alpha_g}$, $g = 2, 3, 4$, g indicating group number. The likelihood function in Equation (4.1) then becomes:

$$\begin{aligned} L &= \prod_{g=2}^{4} \left\{ \prod_{i=1}^{I_g} e^{\alpha_g} \frac{I(t_{gi})}{n(t_{gi})} e^{-e^{\alpha_g} \int_0^{t_{gi}} \frac{I_{gi}(t)}{n_{gi}(t)} dt} \prod_{s=1}^{N_g - I_g} e^{-e^{\alpha_g} \int_0^{t_g^{max}} \frac{I_{gs}(t)}{n_{gs}(t)} dt} \right\} \\ &= \prod_{i=1}^{I_2} e^{\alpha_2} \frac{I(t_{2i})}{n(t_{2i})} e^{-e^{\alpha_2} \int_0^{t_{2i}} \frac{I_{2i}(t)}{n_{2i}(t)} dt} \prod_{s=1}^{N_2 - I_2} e^{-e^{\alpha_2} \int_0^{t_2^{max}} \frac{I_{2s}(t)}{n_{2s}(t)} dt} \times \\ &\quad \prod_{i=1}^{I_3} e^{\alpha_3} \frac{I(t_{3i})}{n(t_{3i})} e^{-e^{\alpha_3} \int_0^{t_{3i}} \frac{I_{3i}(t)}{n_{3i}(t)} dt} \prod_{s=1}^{N_3 - I_3} e^{-e^{\alpha_3} \int_0^{t_3^{max}} \frac{I_{3s}(t)}{n_{3s}(t)} dt} \times \\ &\quad \prod_{i=1}^{I_4} e^{\alpha_4} \frac{I(t_{4i})}{n(t_{4i})} e^{-e^{\alpha_4} \int_0^{t_{4i}} \frac{I_{4i}(t)}{n_{4i}(t)} dt} \prod_{s=1}^{N_4 - I_4} e^{-e^{\alpha_4} \int_0^{t_4^{max}} \frac{I_{4s}(t)}{n_{4s}(t)} dt}, \end{aligned}$$

where t_{gi} is the time of infection of individual i of group g, $n_{gi}(t)$ is the number of individuals mixing with individual i of group g at time t and $I_{gi}(t)$ is the number of infectious individuals mixing with individual i of group g at time t.

Taking natural logarithms of function L yields a log-likelihood function denoted by l and is given by:

$$\begin{aligned} l &= I_2\,\alpha_2 + \sum_{i=1}^{I_2} \ln\left(\frac{I(t_{2i})}{n(t_{2i})}\right) - e^{\alpha_2} \sum_{i=1}^{I_2} \int_0^{t_{2i}} \frac{I_{2i}(t)}{n_{2i}(t)} dt - e^{\alpha_2} \sum_{s=1}^{N_2 - I_2} \int_0^{t_2^{max}} \frac{I_{2s}(t)}{n_{2s}(t)} dt \; + \\ &\quad I_3\,\alpha_3 + \sum_{i=1}^{I_3} \ln\left(\frac{I(t_{3i})}{n(t_{3i})}\right) - e^{\alpha_3} \sum_{i=1}^{I_3} \int_0^{t_{3i}} \frac{I_{3i}(t)}{n_{3i}(t)} dt - e^{\alpha_3} \sum_{s=1}^{N_3 - I_3} \int_0^{t_3^{max}} \frac{I_{3s}(t)}{n_{3s}(t)} dt \; + \\ &\quad I_4\,\alpha_4 + \sum_{i=1}^{I_4} \ln\left(\frac{I(t_{4i})}{n(t_{4i})}\right) - e^{\alpha_4} \sum_{i=1}^{I_4} \int_0^{t_{4i}} \frac{I_{4i}(t)}{n_{4i}(t)} dt - e^{\alpha_4} \sum_{s=1}^{N_4 - I_4} \int_0^{t_4^{max}} \frac{I_{4s}(t)}{n_{4s}(t)} dt \end{aligned}$$

$$\begin{aligned} &= I_2\,\alpha_2 + I_3\,\alpha_3 + I_4\,\alpha_4 + \sum_{i=1}^{I_2} \ln\left(\frac{I(t_{2i})}{n(t_{2i})}\right) + \sum_{i=1}^{I_3} \ln\left(\frac{I(t_{3i})}{n(t_{3i})}\right) + \sum_{i=1}^{I_4} \ln\left(\frac{I(t_{4i})}{n(t_{4i})}\right) \\ &\quad - e^{\alpha_2} \left[\sum_{i=1}^{I_2} \int_0^{t_{2i}} \frac{I_{2i}(t)}{n_{2i}(t)} dt + \sum_{s=1}^{N_2 - I_2} \int_0^{t_2^{max}} \frac{I_{2s}(t)}{n_{2s}(t)} dt \right] \end{aligned}$$

$$
\begin{aligned}
&- e^{\alpha_3}\left[\sum_{i=1}^{I_3}\int_0^{t_{3i}}\frac{I_{3i}(t)}{n_{3i}(t)}dt \;+\; \sum_{s=1}^{N_3-I_3}\int_0^{t_3^{max}}\frac{I_{3s}(t)}{n_{3s}(t)}dt\right] \\
&- e^{\alpha_4}\left[\sum_{i=1}^{I_4}\int_0^{t_{4i}}\frac{I_{4i}(t)}{n_{4i}(t)}dt \;+\; \sum_{i=1}^{N_4-I_4}\int_0^{t_4^{max}}\frac{I_{4s}(t)}{n_{4s}(t)}dt\right] \\
= \;& I_2\,\alpha_2 + I_3\,\alpha_3 + I_4\,\alpha_4 \;-\; e^{\alpha_2}\,T_2 - \; e^{\alpha_3}\,T_3 - \; e^{\alpha_4}\,T_4 \;+\; W, \qquad (4.2)
\end{aligned}
$$

where

$$
\begin{aligned}
W \;&=\; \sum_{i=1}^{I_2}\ln(\frac{I(t_{2i})}{n(t_{2i})}) + \sum_{i=1}^{I_3}\ln(\frac{I(t_{3i})}{n(t_{3i})}) + \sum_{i=1}^{I_4}\ln(\frac{I(t_{4i})}{n(t_{4i})}) \\
T_g \;&=\; \sum_{i=1}^{I_g}\int_0^{t_{gi}}\frac{I_{gi}(t)}{n_{gi}(t)}dt \;+\; \sum_{s=1}^{N_g-I_g}\int_0^{t_g^{max}}\frac{I_{gs}(t)}{n_{gs}(t)}dt, \qquad g = 2,\,3,\,4.
\end{aligned}
$$

T_g is the total infection exposure time for group g, scaled by the number of mixing individuals and W is a constant term, dependant only on the observed data.

4.2.2.1 Estimation of rate of infection

ML estimates for the rate of infection in terms of the αs are obtained by equating the first derivatives of the log-likelihood in Equation (4.2) to zero and solving for the parameters. Taking derivatives of l in Equation (4.2) with respect to α yields:

$$
\begin{aligned}
\frac{dl}{d\alpha_2} \;&=\; I_2 - e^{\alpha_2}\,T_2; \qquad \frac{d^2l}{d\alpha_2^2} \;=\; -\,e^{\alpha_2}\,T_2, \\
\frac{dl}{d\alpha_3} \;&=\; I_3 - e^{\alpha_3}\,T_3; \qquad \frac{d^2l}{d\alpha_3^2} \;=\; -\,e^{\alpha_3}\,T_3, \\
\frac{dl}{d\alpha_4} \;&=\; I_4 - e^{\alpha_4}\,T_4; \qquad \frac{d^2l}{d\alpha_4^2} \;=\; -\,e^{\alpha_4}\,T_4, \\
\frac{d^2l}{d\alpha_2 d\alpha_3} \;&=\; \frac{d^2l}{d\alpha_2 d\alpha_4} = \frac{d^2l}{d\alpha_3 d\alpha_4} = 0.
\end{aligned}
$$

Equating the first order derivatives to zero yields ML estimators for the α parameters *i.e.*

$$
\begin{aligned}
\frac{dl}{d\alpha_2} = 0 \;&\Rightarrow\; e^{\hat{\alpha}_2} \;=\; \frac{I_2}{T_2} \;\Rightarrow\; \hat{\alpha}_2 \;=\; \ln\left(\frac{I_2}{T_2}\right), \\
\frac{dl}{d\alpha_3} = 0 \;&\Rightarrow\; e^{\hat{\alpha}_3} \;=\; \frac{I_3}{T_3} \;\Rightarrow\; \hat{\alpha}_3 \;=\; \ln\left(\frac{I_3}{T_3}\right), \\
\frac{dl}{d\alpha_4} = 0 \;&\Rightarrow\; e^{\hat{\alpha}_4} \;=\; \frac{I_4}{T_4} \;\Rightarrow\; \hat{\alpha}_4 \;=\; \ln\left(\frac{I_4}{T_4}\right).
\end{aligned}
$$

To ascertain that the estimates attained are unique estimates that give the ML, second order derivatives of the log-likelihood function with respect to α_2, α_3 and α_4 are obtained. The first order derivative with respect to each variable equating to zero is a necessary condition for an extreme value. Each first order derivative has a single zero, therefore the combination of these is the sole extreme value in the space. It remains to show that the $\frac{d^2l}{d\alpha_i^2}$ evaluated at the α ML estimates are all less than zero, which will be sufficient to show that this extremum is a maximum.

The log-likelihood in Equation (4.2) can be viewed as a sum of functions of one variable.
Let $l = l(\alpha_2, \alpha_3, \alpha_4) = l_2(\alpha_2) + l_3(\alpha_3) + l_4(\alpha_4)$, where $l_i(\alpha_i) = I_i\alpha_i - e^{\alpha_i}T_i$, for $i = 2, 3, 4$, then

$$\frac{dl}{d\alpha_i} = \frac{dl_i}{d\alpha_i}, \quad \frac{d^2l}{d\alpha_i^2} = \frac{d^2l_i}{d\alpha_i^2} \quad \text{and} \quad \frac{d^2l}{d\alpha_i d\alpha_j} = 0.$$

Evaluating the second order derivatives $\frac{d^2l_i}{d\alpha_i^2}$ at the ML estimates, $\alpha_i : \frac{dl_i}{d\alpha_i} = 0$ $(\hat{\alpha}_i)$, yields: $\frac{d^2l_i}{d\alpha_i^2} = -I_i \; \forall \; i$. Thus each of the $\frac{d^2l_i}{d\alpha_i^2}$ evaluated at $\hat{\alpha}_i$ is less than zero implying that $l_i(\alpha_i)$ is at a maximum at $\hat{\alpha}_i$, hence $l = \sum l_i(\alpha_i)$ is at a maximum at $\hat{\alpha}_i \; \forall i$, since l is a linear combination of $l_2(\alpha_2)$, $l_3(\alpha_3)$ and $l_4(\alpha_4)$, each of which is a function depending only on α_2, α_3 and α_4 respectively. Hence the attained ML estimates for α correspond to a unique maximum.

After calculating ML estimates for the parameters, it is important to form some idea about the possible deviation between the estimate and the true parameter. From theory by Cramer-Rao (Azzalini, 1996, Section 3.2), the observed information, $\mathcal{I}(\hat{\alpha}) = -\frac{d^2}{d\alpha d\alpha^T} l(\alpha)|_{\alpha=\hat{\alpha}}$ can be used to estimate the standard error of the parameter estimates, where α is the vector of parameters of interest and $\hat{\alpha}$ is the vector of the attained parameter estimates. Using Cramer-Rao's inequality, if $T(y)$ is an unbiased estimator for α and assuming that the expected information matrix, $I(\alpha)$ is positive definite, then

$$var[T(Y)] \geq [I(\alpha)]^{-1}.$$

The expected information matrix, $I(\alpha) = -E\left[\frac{d^2}{d\alpha d\alpha^T} l(\alpha)\right]$, can be estimated by the observed information matrix $\mathcal{I}(\hat{\alpha})$, such that

$$var[T(Y)] \geq [\mathcal{I}(\hat{\alpha})]^{-1} = \left[\frac{d^2}{d\alpha d\alpha^T} l(\alpha)|_{\alpha=\hat{\alpha}}\right]^{-1}.$$

If the estimator attains the minimum variance estimate, then

$$var[T(Y)] = \left[\frac{d^2}{d\alpha d\alpha^T} l(\alpha)|_{\alpha=\hat{\alpha}}\right]^{-1}.$$

Information matrix

The information matrix is the matrix whose elements are the second order derivatives of the log-likelihood function evaluated at the ML estimates. It will be denoted by H and its inverse denoted H^{-1} such that:

$$H = \begin{pmatrix} -I_2 & 0 & 0 \\ 0 & -I_3 & 0 \\ 0 & 0 & -I_4 \end{pmatrix} \text{ and } H^{-1} = \begin{pmatrix} -\frac{1}{I_2} & 0 & 0 \\ 0 & -\frac{1}{I_3} & 0 \\ 0 & 0 & -\frac{1}{I_4} \end{pmatrix}.$$

From the inverse of the information matrix, standard error estimates for the parameter estimates are obtained.
Let $\alpha = (\alpha_2, \alpha_3, \alpha_4)$, then $var(\hat{\alpha}) = -\left[\frac{d^2 l}{d\alpha d\alpha^T}\right]^{-1}_{\alpha=\hat{\alpha}} = -H^{-1}$.

Thus standard error estimates for the $\hat{\alpha}$s are given by:

$$s.e(\hat{\alpha}_2) = \sqrt{-H^{-1}[1,1]} = \sqrt{\frac{1}{I_2}},$$

$$s.e(\hat{\alpha}_3) = \sqrt{-H^{-1}[2,2]} = \sqrt{\frac{1}{I_3}},$$

$$s.e(\hat{\alpha}_4) = \sqrt{-H^{-1}[3,3]} = \sqrt{\frac{1}{I_4}}.$$

Estimates for the rate of infection in terms of β

The estimates for the β_g are as follows:

$$\hat{\beta}_2 = e^{\hat{\alpha}_2} = \frac{I_2}{T_2}, \quad \hat{\beta}_3 = e^{\hat{\alpha}_3} = \frac{I_3}{T_3} \text{ and } \hat{\beta}_4 = e^{\hat{\alpha}_4} = \frac{I_4}{T_4}. \tag{4.3}$$

Standard error estimates for the $\hat{\beta}_g$ are obtained based on the standard error estimates of the αs using the δ method (Becker, 1989, Appendix). The δ method stipulates that if estimators M_j of parameter θ_j have variances $var(M_j)$, $j = 1, \ldots, r$, then for $M = g(M_1, \ldots, M_r)$,

$$var(M) \simeq \sum\sum \frac{dg}{d\theta_i}\frac{dg}{d\theta_j} cov(M_i, M_j).$$

It follows that:
if $r = 1$, $s.e\{g(M_1)\} \simeq |g'(M_1)|\, s.e(M_1)$, and
If $r = 2$,

$$var\{g(M_1, M_2)\} \simeq \left(\frac{dg(\theta_1, \theta_2)}{d\theta_1}\right)^2 var(M_1) + \left(\frac{dg(\theta_1, \theta_2)}{d\theta_2}\right)^2 var(M_2) + 2\,\frac{dg(\theta_1, \theta_2)}{d\theta_1}\frac{dg(\theta_1, \theta_2)}{d\theta_2} cov(M_1, M_2).$$

Thus, using the δ method, the standard error estimates for the $\hat{\beta}$s are as follows:

$$\hat{\beta}_g = e^{\hat{\alpha}_g} = y(\alpha_g),\ s.e(\hat{\beta}_g) \simeq |y'(\alpha_g)| s.e(\hat{\alpha}_g) = e^{\hat{\alpha}_g}\sqrt{\frac{1}{I_g}} = \frac{\sqrt{I_g}}{T_g}.$$

Hence

$$s.e(\hat{\beta}_2) = \frac{\sqrt{I_2}}{T_2},\ s.e(\hat{\beta}_3) = \frac{\sqrt{I_3}}{T_3} \text{ and } s.e(\hat{\beta}_4) = \frac{\sqrt{I_4}}{T_4}. \tag{4.4}$$

4.2.3 Parameter estimates for restricted model MLE

When calculating ML estimates for the restricted model, the aim is to estimate rates of infection acting upon groups of sheep while ensuring that these rates decrease or stay the same across groups. Based on the experimental hypothesis of decreasing infectivity due to passage effect, β estimates will not be allowed to increase across groups. This is in contrast to ML estimates made for the unrestricted model where the β estimates are unrestricted, which may potentially result in for example, $\hat{\beta}_3 > \hat{\beta}_2$.

The procedure to estimate parameters in the restricted model MLE situation is as follows. Initially, estimate the unrestricted model parameters (4.3). If the estimates are valid, *i.e.* $\beta_2 > \beta_3 > \beta_4$, then this point will be the maximum in the parameter space. Refer to this as Case 1. If not, then the maximum will be on the boundary of the restricted space (Hatton, 1977, Section 10.12) and the resulting ML estimates may be any among: $\beta_2 = \beta_3 > \beta_4$ (Case 2) or $\beta_2 > \beta_3 = \beta_4$ (Case 3) or $\beta_2 = \beta_3 = \beta_4$ (Case 4). It is useful to think in terms of a nested hierarchy of parametric models. Just as the maxima of likelihoods with 2 effective parameters (with two parameters constrained to be equal) are less than or equal to the maximum of a likelihood with 3 parameters (with no constraints), the maxima of likelihood with 1 effective parameter (with

all three parameters constrained to be equal: Case 4) must be less than or equal to the likelihoods with 2 effective parameters (Cases 2 and 3). It is important to understand that the extrema corresponding to both Cases 2 and 3 may be wholly within the valid space.

Let α_{23} be the α parameter in Case 2 where $\alpha_2 = \alpha_3$ ($\beta_2 = \beta_3$), α_{34} be the α parameter in Case 3 where $\alpha_3 = \alpha_4$ ($\beta_3 = \beta_4$) and α_{234} be the α parameter in Case 4 where $\alpha_2 = \alpha_3 = \alpha_4$ ($\beta_2 = \beta_3 = \beta_4$). The following algorithm is appropriate:

Algorithm 4.1

1. Estimate α_2, α_3 and α_4. If $\alpha_2 \geq \alpha_3 \geq \alpha_4$, use these estimates (Case 1). Goto end.
2. Estimate α_{23} and α_4 (Case 2).
3. Estimate α_2 and α_{34} (Case 3).
4. If $(\alpha_{23} < \alpha_4)$ and $(\alpha_2 < \alpha_{34})$ goto 8.
5. If $(\alpha_{23} \geq \alpha_4)$ and $(\alpha_2 < \alpha_{34})$, use the α_{23} and α_4 estimates (Case 2). Goto end.
6. If $(\alpha_{23} < \alpha_4)$ and $(\alpha_2 \geq \alpha_{34})$, use the α_2 and α_{34} estimates (Case 3). Goto end.
7. If $(\alpha_{23} \geq \alpha_4)$ and $(\alpha_2 \geq \alpha_{34})$, evaluate the maximum log-likelihoods for each pair of parameter estimates. Use the estimates which give rise to the larger maximum log-likelihood (Case 2 or 3). Goto end.
8. Estimate α_{234} and use this estimate (Case 4). Goto end.
9. End.

For Case 1 *i.e.* $\beta_2 \geq \beta_3 \geq \beta_4$, estimates of these parameters and their corresponding standard error estimates are equal to those estimated using unrestricted model MLE. Now we proceed to determine expressions for the α_g and β_g estimates and their associated estimates of standard error for Cases 2, 3 and 4.

4.2.3.1 Case 2: $\beta_2 = \beta_3 > \beta_4$

For Case 2, $\beta_3 = \beta_2$ and $\alpha_3 = \alpha_2$, thus, the log-likelihood function in Equation (4.2) becomes:

$$l \;=\; (I_2 + I_3)\,\alpha_2 + I_4\alpha_4 \;-\; e^{\alpha_2}\,(T_2 + T_3) \;-\; e^{\alpha_4}\,T_4 \;+\; W.$$

Taking first and second order derivatives of the log-likelihood with respect to α_2 and α_4 yields:

$$\begin{aligned}
\frac{dl}{d\alpha_2} &= I_2 + I_3 - e^{\alpha_2}\,(T_2 + T_3); \quad \frac{dl}{d\alpha_4} = e^{\alpha_4}\,I_4 - e^{\alpha_4}\,T_4, \\
\frac{d^2l}{d\alpha_2^2} &= -e^{\alpha_2}\,(T_2 + T_3); \quad \frac{d^2l}{d\alpha_4^2} = -\,e^{\alpha_4}\,T_4; \quad \frac{d^2l}{d\alpha_2 d\alpha_4} = 0.
\end{aligned}$$

Equating the first order derivatives to zero and solving for α_2 and α_4 yields the following likelihood equations and estimates of α:

$$\frac{dl}{d\alpha_2} = 0 \;\Rightarrow\; e^{\hat{\alpha}_2} = \frac{I_2 + I_3}{T_2 + T_3} \;\Rightarrow\; \hat{\alpha}_2 = \ln\left(\frac{I_2 + I_3}{T_2 + T_3}\right). \tag{4.5}$$

$$\frac{dl}{d\alpha_4} = 0 \;\Rightarrow\; e^{\hat{\alpha}_4} = \frac{I_4}{T_4} \;\Rightarrow\; \hat{\alpha}_4 = \ln\left(\frac{I_4}{T_4}\right). \tag{4.6}$$

Evaluating the second order derivatives at $\hat{\alpha}_g$ gives:

$$\frac{d^2l}{d\alpha_2^2} = -e^{\hat{\alpha}_2}\,(T_2 + T_3) = -\,(I_2 + I_3); \quad \frac{d^2l}{d\alpha_4^2} = -e^{\hat{\alpha}_4}\,T_4 = -I_4; \quad \frac{d^2l}{d\alpha_2 d\alpha_4} = 0.$$

The information matrix, denoted H_2, whose elements are the second order derivatives of the log-likelihood evaluated at the ML estimates, and its inverse, H_2^{-1} are then given by:

$$II_2 = \begin{pmatrix} -(I_2 + I_3) & 0 \\ 0 & -I_4 \end{pmatrix} \text{ and } H_2^{-1} = \begin{pmatrix} -\frac{1}{I_2+I_3} & 0 \\ 0 & -\frac{1}{I_4} \end{pmatrix}$$

and the determinant of matrix H_2, denoted by $\det(H_2)$ is equal to $I_4\,(I_2+I_3) > 0$. Each of the first derivatives has a single root and $\det(H_2)$ is positive. Thus the estimated parameters correspond to a unique maximum in the surface.

Standard error estimates for the estimates of the α_g are determined from the inverse of the information matrix based on Cramer-Rao's theory (Azzalini, 1996, Section 3.2) as follows:

$$s.e(\hat{\alpha}_2) \;=\; \sqrt{-H_2^{-1}[1,1]} \;=\; \sqrt{\frac{1}{I_2 + I_3}}; \quad s.e(\hat{\alpha}_4) \;=\; \sqrt{-H_2^{-1}[2,2]} \;=\; \sqrt{\frac{1}{I_4}}. \tag{4.7}$$

4.2.3.2 Estimates of β_g for Case 2

From Equations (4.5) and (4.6) the estimates for the rates of infection are as follows:

$$\hat{\beta}_2 = e^{\hat{\alpha}_2} = \frac{I_2 + I_3}{T_2 + T_3} = \hat{\beta}_3 \text{ and } \hat{\beta}_4 = e^{\hat{\alpha}_4} = \frac{I_4}{T_4}. \tag{4.8}$$

The standard error estimates for the $\hat{\beta}$s are determined based on the δ method (Becker, 1989, Appendix) as follows:

1. For $\hat{\beta}_2 = e^{\hat{\alpha}_2} = g(\alpha_2) = \hat{\beta}_3$,

$$s.e(\hat{\beta}_2) \simeq |g'(\alpha_2)| s.e(\hat{\alpha}_2) = e^{\hat{\alpha}_2}\sqrt{\frac{1}{I_2 + I_3}} = \hat{\beta}_2\sqrt{\frac{1}{I_2 + I_3}}. \tag{4.9}$$

2. For $\hat{\beta}_4 = e^{\hat{\alpha}_4} = g(\alpha_4)$,

$$s.e(\hat{\beta}_4) \simeq |g'(\alpha_4)| s.e(\hat{\alpha}_4) = e^{\hat{\alpha}_4}\sqrt{\frac{1}{I_4}} = \hat{\beta}_4\sqrt{\frac{1}{I_4}}. \tag{4.10}$$

4.2.3.3 Case 3: $\beta_2 > \beta_3 = \beta_4$

By similar methods to those in Section 4.2.3.1 above, it is trivial to show that:

$$\hat{\beta}_2 = \frac{I_2}{T_2},\ s.e(\hat{\beta}_2) \simeq \hat{\beta}_2\sqrt{\frac{1}{I_2}};\ \hat{\beta}_3 = \hat{\beta}_4 = \frac{I_3 + I_4}{T_3 + T_4},\ s.e(\hat{\beta}_3) \simeq \hat{\beta}_3\sqrt{\frac{1}{I_3 + I_4}}. \tag{4.11}$$

4.2.3.4 Case 4: $\beta_2 = \beta_3 = \beta_4$

Using similar methods to those in Section 4.2.3.1, the estimates obtained for the β_g are:

$$\hat{\beta}_2 = \hat{\beta}_3 = \hat{\beta}_4 = e^{\hat{\alpha}_2} = \frac{I_2 + I_3 + I_4}{T_2 + T_3 + T_4},\ s.e(\hat{\beta}_2) \simeq \hat{\beta}_2\sqrt{\frac{1}{I_2 + I_3 + I_4}}. \tag{4.12}$$

4.2.3.5 Likelihood on boundary of parameter space

The properties of estimates of parameters under ML on a restricted parameter space may be problematic. If the unrestricted estimates are outwith the allowable parameter space, the restricted model ML estimates will be on the boundary of

the parameter space (Hatton, 1977, Section 10.12). In this situation, first order approximations to the properties of the likelihood will be invalid, since these depend on the ability to generate valid Taylor Series approximations to the likelihood at values of the parameter equal to the ML. However, the likelihood is discontinuous at the boundary. If a confidence interval was required for the parameter estimates, Barndorff-Nielsen and Cox (1994), Section 3.8, recommend that the confidence interval from the unrestricted case be used, with regions outside the restricted parameter space being made void. Hence, in principle, it would be possible to generate a confidence interval for the ML estimates. However, the dependence of these parameter estimates on a common inferred underlying infection history creates a lack of independence in the estimates, while variability arising from the lack of knowledge of the infection path is not expressed in the log-likelihood of the data. Where the standard EM algorithm has been used to estimate parameters, methods have been proposed to allow the estimation of the covariance matrix of the estimated parameter vector (McLachlan and Krishnan, 1997, Sections 4.2:4.5). However, it is not clear whether these methods will be valid for non-EM iterative algorithms such as those in the current work. In addition, these methods are based on the asymptotic properties of the complete-data log-likelihood, and it seems likely that the relatively small numbers of animals in the experiments will make such asymptotic arguments hard to justify. Because of these factors, it was decided to base the testing of the alternative hypothesis on bootstrap methods (McLachlan and Krishnan, 1997, Section 4.6) rather than on asymptotic likelihood theory. Although no confidence intervals are therefore required for the estimated parameters, it would seem useful to incorporate information about the apparent precision of the estimates into the bootstrapping procedure. Ideally, this requires a point estimate of the variability of the estimates, and this can only be provided from an expected information matrix evaluated at the point estimate. In the situation where the point estimates for the restricted and unrestricted cases are identical, there is no problem: the standard errors derived from the 3 by 3 information matrix are used. Where the point estimates are on the boundary of the restricted parameter space, the appropriate degenerate information (either a 2 by 2 matrix or scalar) is used, as presented in previous Sections 4.2.3.1 to 4.2.3.4. In a sense, the resulting standard errors are conditional on the parameter estimates being degenerate in that particular way (*i.e.*, either $\alpha_2 = \alpha_3$ or $\alpha_3 = \alpha_4$ or $\alpha_2 = \alpha_3 = \alpha_4$). However, it is felt that the resulting standard errors will provide an appropriate measure of the variability of the parameter estimates within the bootstrap procedure.

4.2.4 Estimation of the exposure time, T_g

For each individual the amount of time for which they were exposed to infection is determined. The total group infection exposure time T_g which features in the expression for the log-likelihood function in Equation (4.2) and in the expressions for the estimates of the β_g, is determined by the length of infection exposure of individuals mixing in group g *i.e.*

$$T_g = \sum_{i=1}^{I_g} \int_0^{t_{gi}} \frac{I_{gi}(t)}{n_{gi}(t)}\, dt + \sum_{s=1}^{N_g - I_g} \int_0^{t_g^{max}} \frac{I_{gs}(t)}{n_{gs}(t)}\, dt,$$

where

N_g is the total number of individuals in group g.

I_g is the total number of infected individuals in group g.

$n_{gi}(t)$ is the number of individuals mixing with infected individual i of group g at time t.

$I_{gi}(t)$ is the number of infected individuals mixing with infected individual i of group g at time t.

$n_{gs}(t)$ is the number of individuals mixing with susceptible individual s of group g at time t.

$I_{gs}(t)$ is the number of infected individuals mixing with susceptible individual i of group g at time t and

t_g^{max} is the maximum of the time of end of experiment and the last time of exposure to infection for group g.

Individuals from a single group that each escaped infection were exposed to the same hazard and hence have the same exposure time. The length of exposure time is estimated based on the infectiousness period of infected individuals. By assuming a distribution for the infectiousness period and fitting the distribution to data, the expected infectiousness period will be estimated.

For each infected individual i, the time between the start of the experiment and the individual's expected time of infection t_{gi} is partitioned into regions of constant hazard while taking into account the re-mixing of groups every 24 hours. Thus, the largest interval has a length of 1 day. The time points of change in hazard will be referred to as transition time points.
Let p_i denote the number of transition time points for individual i, and t_{ki} denote the individual partition time points for individual i, $k = 1, 2, \ldots, p_i$ with $t_{1i} = 0$, the start of the experiment and $t_{p_i i} = t_{gi}$, the expected time of infection for individual i.

The probability that an infected individual i of group g becomes infected at time t_{gi} is given by:

$$\begin{aligned}
&\beta_g \frac{I(t_{gi})}{n(t_{gi})} \exp\left\{-\beta_g \int_0^{t_{gi}} \frac{I_{gi}(t)}{n_{gi}(t)}\, dt\right\} \\
&\quad = \beta_g \frac{I(t_{gi})}{n(t_{gi})} \exp\left\{-\beta_g \sum_{k=1}^{p_i-1} \int_{t_{ki}}^{t_{(k+1)\,i}} \frac{I_{gi}(t)}{n_{gi}(t)}\, dt\right\} \\
&\quad = \beta_g \frac{I(t_{gi})}{n(t_{gi})} \exp\left\{-\beta_g \sum_{k=1}^{p_i-1} \frac{I_{gi}(t_{ki})}{n_{gi}(t_{ki})} \left(t_{(k+1)\,i} - t_{k\,i}\right)\right\}. \qquad (4.13)
\end{aligned}$$

$\sum_{k=1}^{p_i-1} \frac{I_{gi}(t_{ki})}{n_{gi}(t_{ki})} \left(t_{(k+1)\,i} - t_{k\,i}\right)$ in Equation (4.13) is the total expected scaled infection exposure time (scaled by the total number of mixing individuals) for individual i of group g by the time it became infected.

Similarly, the time from the start of the experiment up to the time of the end of the experiment or up to the time when a group ceased to be exposed to infection (*i.e.* when there were no more infectious individuals among those mixing with the group), is partitioned into intervals of constant hazard, again taking the group mixing times into consideration. The probability of an individual escaping infection throughout the experiment is calculated based on these partitioned intervals.

The probability that an individual escapes infection throughout the duration of the epidemic is given by

$$e^{-\beta_g \int_0^{t_g^{max}} \frac{I_{gi}(t)}{n_{gi}(t)}\, dt}.$$

The time period $[0,\, t_g^{max}]$ is partitioned into intervals of constant hazard.
Let p_g denote the number of transition time points in the period $[0,\, t_g^{max}]$ for group g individuals that escaped infection. Individuals in the same group that each escape infection have the same transition time points during the period $[0,\, t_g^{max}]$. Also let t_{mg} denote the individual transition time points for group g, $m = 1, 2, \ldots, p_g$, with $t_{1g} = 0$ and $t_{p_g g} = t_g^{max}$. Then the probability that an individual s in group g escapes infection up to the end of the experiment is given by:

$$\begin{aligned}
\exp\left\{-\beta_g \int_0^{t_g^{max}} \frac{I_{gi}(t)}{n_{gi}(t)}\, dt\right\} &= \exp\left\{-\beta_g \sum_{m=1}^{p_g-1} \int_{t_{mg}}^{t_{(m+1)\,g}} \frac{I_{gi}(t)}{n_{gi}(t)}\, dt\right\} \\
&= \exp\left\{-\beta_g \sum_{m=1}^{p_g-1} \frac{I_{gi}(t_{mg})}{n_{gi}(t_{mg})} \left(t_{(m+1)\,g} - t_{m\,g}\right)\right\}. \qquad (4.14)
\end{aligned}$$

$\sum_{m=1}^{p_g-1} \frac{I_{gs}(t_{mg})}{n_{gs}(t_{mg})} (t_{m+1\,g} - t_{m\,g})$ in Equation (4.14) is the total infection exposure time, scaled by the number of mixing individuals $n_{gs}(\cdot)$, for a susceptible individual that escaped infection in group g.

The total group infection exposure time T_g is therefore given by the expression below:

$$\begin{aligned} T_g &= \sum_{i=1}^{I_g} \int_0^{t_{gi}} \frac{I_{gi}(t)}{n_{gi}(t)}\, dt + \sum_{s=1}^{N_g - I_g} \int_0^{t_g^{max}} \frac{I_{gs}(t)}{n_{gs}(t)}\, dt \\ &= \sum_{i=1}^{I_g} \sum_{k=1}^{p_i-1} \frac{I_{gi}(t_{ki})}{n_{gi}(t_{ki})} \left(t_{(k+1)\,i} - t_{k\,i}\right) + \sum_{s=1}^{N_g - I_g} \sum_{m=1}^{p_g-1} \frac{I_{gs}(t_{mg})}{n_{gs}(t_{mg})} \left(t_{(m+1)\,g} - t_{m\,g}\right) \\ &= \sum_{i=1}^{I_g} \sum_{k=1}^{p_i-1} \frac{I_{gi}(t_{ki})}{n_{gi}(t_{ki})} \left(t_{(k+1)\,i} - t_{k\,i}\right) + (N_g - I_g) \sum_{m=1}^{p_g-1} \frac{I_g(t_{mg})}{n_g(t_{mg})} \left(t_{(m+1)\,g} - t_{m\,g}\right). \end{aligned} \tag{4.15}$$

$I_g(t)$ denotes the number of infectious individuals mixing in group g at time t and $n_g(t)$ denotes the total number of individuals mixing in group g at time t.

The number of infectives at a given time t, and the transition points, are of course, unobserved. Where these are replaced with estimated values derived from an iterative algorithm, as described in Section 6.6, the resulting quantity is treated as an estimator for $E[T_g]$.

4.3 Martingale methods

As noted in Section 1.4, infectious disease data present several difficulties in their analysis and in the estimation of parameters. The spread of infection through a community (group in our case) is only partially observable. Relatively little information is available about characteristics such as the duration of latent period that are not directly observable making it difficult to formulate and fit parametric models for the entire disease process. Also, the lack of independence in the data usually leads to likelihood functions with an unmanageable form. To tackle some of these difficulties, alternative methods to MLE have been developed to make statistical inference about relevant epidemiological parameters. One such method is the martingale method of estimation. Becker (1993a) points out that martingale methods have provided methods of inference in a number of situations where no satisfactory method of analysis was previously available. Martingale methods

facilitate the construction of estimating equations and the derivation of parameter estimates and associated standard error estimates.

4.3.1 Previous applications of martingale methods

The use of martingales as a tool to derive methods for nonparametric inference was first illustrated by Aalen in a 1975 Berkeley PhD thesis (Becker, 1989, Section 7.7). Andersen and Borgan (1985) give a review of the methodology. The first application to inference for parameters of an epidemic model is given in Becker (1977). Other illustrations of the use of martingale methods in the analysis of infectious disease data, particularly those involving two types of susceptibles, are given by Becker and Angulo (1981) and Becker (1982). Martingale methods have since been applied to the estimation of epidemiological parameters such as the force of infection, the infection potential, the mean duration of the infectiousness period, and the basic reproduction number, R_0. Becker (1993a) uses martingale methods to estimate the mean infection potential for the general epidemic where the infection process for an individual was defined by Susceptible-Infected-Removed states and the time spent in the infected state was exponentially distributed. Martingale methods have also been used to make inference in populations with varying susceptibility, for instance, in vaccinated and un-vaccinated individuals. This approach enables, for example, the estimation of the degree of protection offered by a vaccine (Becker, 1993a). de Jong and Kimman (1994) use martingale methods to generate estimates for R_0 in vaccinated and un-vaccinated Landrace pigs while investigating the experimental transmission of virus in a population of pigs. The application of martingale methods to infectious disease data, where the rate of infection is allowed to depend on time is discussed by Becker and Yip (1989). Becker and Hasofer (1998) illustrate the use of martingale methods to estimate the transmission rate in a situation where a disease is highly infectious and hence the number of susceptible individuals at the end of the epidemic is likely to be zero. The formulation of martingale methods presented in this thesis develops ideas presented in Becker (1979, 1981); Becker and Hopper (1983) and Becker (1989), Chapter 7.

4.3.2 Martingale methods for epidemic models

In epidemic parameter estimation, interest is focused on martingales arising from counting processes.

A counting process,

$$N = \{N(t); t \geq 0\}$$

is a random process that counts the occurrence of certain events over time, where $N(t)$ is the number of events occurring in the time interval $(0, t]$. N is a piece-wise constant function with jumps of size $+1$. In epidemic studies, the development of the appropriate counting processes is governed by the following transition equations:

$$Pr\{dN(t) = 1 | \mathcal{H}(t)\} = A(t)dt$$
$$Pr\{dN(t) = 0 | \mathcal{H}(t)\} = 1 - A(t)dt$$

where $A(t)$ is the intensity process of $N(t)$, itself often a random process, and $\mathcal{H}(t)$ denotes the history of the process up to time t. Martingales are expressed in terms of a counting process and the associated intensity process. A mathematical definition of a martingale is given below.

Suppose that certain random processes are followed continuously over time beginning at time $t = 0$.
Then a martingale is a random process $M = \{M(t);\ t \geq 0\}$ such that for every $t \geq 0$:

1. The value of $M(t)$ is determined by $\mathcal{H}(t)$
2. $E(|M(t)|) < \infty$
3. $E(M(u)|\mathcal{H}(t)) = M(t)$ for every $u \geq t$.

Property 3 is referred to as the martingale property, which stipulates that the expected value of a martingale at any future point in time is equal to its current value. The concept of a zero mean martingale is then derived from this property:

$E\{M(t)|\mathcal{H}(0)\} = M(0)$ for all $t \geq 0$ and when $M(0) = 0$ this leads to
$E\{M(t)|\mathcal{H}(0)\} = 0$.

In this case $M(t)$ is defined to be a zero mean martingale.
It is also possible to define a variation process on $M(t)$ which describes the variability present in $M(t)$.

The martingale estimate for a parameter of interest is produced by setting the value of an appropriate zero mean martingale at a specified observation time t equal to zero. The resulting estimator is therefore a special case of the method of moments estimator (Becker, 1989, Section 7.1). A useful estimator will be a function of only observed quantities and the parameter(s) of interest.

4.3.2.1 Formulation

Let $N(t)$ denote the number of individuals infected during the time interval $(0, t]$ and assume that individuals are either susceptible, latent, infectious or removed ($SLIR$) at any given moment.
Suppose at time $t = 0$ there are s susceptibles and i infectives in the community. Using the true mass action formulation of an epidemic process (de Jong et al., 1995), the intensity process of $N(t)$ is given by:

$$A(t) = \frac{\beta(t)I(t)S(t)}{n(t)}$$

where $I(t)$ is the number of infectious individuals in the community at time t, $S(t)$ is the number of individuals still susceptible to infection and $n(t)$ is the total number of individuals mixing at time t.
It follows that the process $M(t)$ specified by

$$M(t) = N(t) - \int_0^t A(u)du$$

is a zero mean martingale with respect to the history $\mathcal{H}(t)$.

Although the entire infection process is not observed, martingales can be defined with reference to histories based on incomplete observations of the epidemic. The aim is to develop methods of inference that depend only on observable aspects of the epidemic. Estimating equations are therefore constructed involving only observable aspects of the epidemic and the parameters of interest.

Martingale methods tend to involve only simple computations and often apply in a general fashion as they can be derived to make statistical inference about specific parameters without requiring a complete specification of the epidemic process. In fact the attraction of these methods is that they require only partial specifications of the model. The use of martingale methods is appealing since it also allows derivation of estimates of the standard errors of the parameters and hence construction of confidence intervals, however, these depend on the use of the martingale central limit theorem and hence are only valid for large epidemics.

An important result from the theory of martingales is that integration of certain random processes with respect to a zero mean martingale M leads to processes which are also zero mean martingales. Predictable random processes *i.e.* processes that can be forecast through observable quantities of the infection process, are chosen for this purpose. The fact that a predictable random process can be

specified given observed properties of the infection process makes it possible to evaluate the resulting integrals.
Let B be a predictable random process such that its history $\mathcal{H}(x)$ determines $B(x)$ for every $x \geq 0$.
The new process M^* specified by the stochastic integral

$$M^*(t) = \int_0^t B(x)dM(x) = \int_0^t B(x)dN(x) - \int_0^t B(x)A(x)dx$$

is a zero mean martingale with respect to $\mathcal{H}$ *i.e.* $E\ [dM^*|\mathcal{H}(x)\ ] = 0$, and $Var\,[\int_0^t B(x)dM(x)\,] = E\,[\int_0^t B^2(x)dN(x)\,]$ (Becker, 1989, Section 7.1).
This result is used in formulating martingale estimates for the rate of infection acting upon groups of sheep.

4.3.3 Martingale β estimates from experimental FMD data

It is assumed that the infection process is such that individuals are either susceptible, latent, infectious or removed ($SLIR$) at any given moment. The intensity process for the epidemic is then given by:

$$A(t) = \frac{\beta I(t)S(t)}{n(t)},$$

where β is the infection rate, $I(t)$ is the number of infectious individuals in the community at time t, $S(t)$ is the number of individuals still susceptible to infection and $n(t)$ is the total number of individuals mixing at time t.
The probability of a new infection occurring in a small time interval $(t, t+\delta t)$ is given by:

$$pr\{dN(t) = 1|S(t), L(t), I(t), R(t)\} = \frac{\beta I(t)S(t)}{n(t)}dt$$

and the process,

$$M(t) = N(t) - \int_0^t \frac{\beta I(x)S(x)}{n(x)}dx,$$

is a zero mean martingale.

If the infection process was observable continuously over the duration of the epidemic so that the number of individuals in each epidemic state was known, an estimating equation for β could be obtained by evaluating the martingale M at

the precise end of the epidemic T and equating it to its mean of zero. This would yield an estimate of β:

$$\hat{\beta} = \frac{N(T)}{\int_0^T \frac{I(x)S(x)}{n(x)}dx} \quad \text{and} \quad s.e(\hat{\beta}) = \frac{[N(T)]^{1/2}}{\int_0^T \frac{I(x)S(x)}{n(x)}dx}. \tag{4.16}$$

This estimator, which assumes complete information, is identical to the unrestricted model ML estimator in Equation (4.3).

However, for the experimental FMD data, only daily observations of virus shedding or absence of shedding for any infected individual are available. The use of a zero mean martingale M is proposed using an appropriate predictable process $B(.)$.

The zero mean martingale $M(t)$ has been defined:

$$M(t) = N(t) - \int_0^t \frac{\beta I(x)S(x)}{n(x)}dx.$$

Let $B(x) = \frac{J(x-)}{S(x-)}$ where $J(x) = \begin{cases} 1 & S(x) > 0 \\ 0 & S(x) = 0 \end{cases}$
with $B(x) = 0$ when $J(x-) = 0$.

Integrating $B(x)$ with respect to the martingale M, the zero mean martingale M^*, specified below, is obtained:

$$\begin{aligned} M^*(t) &= \int_0^t B(x)dN(x) - \int_0^t \frac{B(x)\beta I(x)S(x)}{n(x)}dx \\ &= \int_0^t B(x)dN(x) - \int_0^t \frac{\beta I(x)J(x)}{n(x)}dx. \end{aligned}$$

$x-$ used in the definition of B ensures predictability and hence in the computation of integral $\int_0^t B(x)dN(x)$ one inserts the values of S just prior to each of the jump times.

An estimate for β is obtained by solving the method of moments estimating equation for the martingale M^*, namely $E[M^*(T)] = 0$, giving:

$$\hat{\beta} = \frac{\int_0^T B(x)dN(x)}{E[\int_0^T \frac{I(x)J(x)}{n(x)}dx]} \quad \text{and} \quad s.e(\hat{\beta}) = \frac{[\int_0^T B^2(x)dN(x)]^{1/2}}{E[\int_0^T \frac{I(x)J(x)}{n(x)}dx]} \tag{4.17}$$

where

$$\int_0^T B(x)dN(x) = \frac{1}{s} + \frac{1}{(s-1)} + \ldots + \frac{1}{S(T)+1} \quad \text{and}$$

$$\int_0^T B^2(x)dN(x) = \frac{1}{s^2} + \frac{1}{(s-1)^2} + \cdots + \frac{1}{(S(T)+1)^2}.$$

Where $S(x) > 0$ for all $x > 0$, $\frac{I(x)J(x)}{n(x)} = \frac{I(x)}{n(x)}$ and hence

$$E[\int_0^T \frac{I(x)J(x)}{n(x)}dx] = E[\int_0^T \frac{I(x)}{n(x)}dx].$$

In a particular group where all individuals ultimately became infectious we define T_{final} as the time at which the final susceptible became infected. It follows that

$$E[\int_0^T \frac{I(x)J(x)}{n(x)}dx] = E[\int_0^{T_{final}} \frac{I(x)}{n(x)}dx].$$

Sheep are observed to be shedding virus on a certain number of occasions. Where an infective is identified as positive at the beginning and end of a period, it is assumed that it is positive throughout this period (observed infectiousness period), with probability 1. Hence, any problems in applying the expectation operator only arise with respect to the unobserved 'excess' infectiousness periods at the beginning and end of each observed virus shedding period.

The denominator in the expression for the estimator $\hat{\beta}$ (Equation (4.17)) is the total expected infection exposure time for each group, where the total exposure time is scaled by the total number of sheep mixing at any given time in the true mass action formulation. Thus the martingale estimate for β requires an estimate for the expected total infection exposure time for each group. The length of time for which susceptibles were exposed to infection is estimated through consideration of the infectiousness period of infected individuals and the mixing strategy. The complete infectiousness period for any infected individual is, however, an unobserved quantity which has to be estimated. The expected infectiousness period is one of the infection process characteristics which will be estimated via the iterative scheme (Chapters 5 and 6). The estimated expected infectiousness period for each infected sheep will be determined and the contributions of each infected sheep to the total infection exposure time for the relevant group will be summed.

Using both MLE and martingale methods, β estimates will be calculated within an iterative scheme. Also calculated within this scheme are estimates for the expected infection process characteristics, some of which will be required to obtain the β estimates. Throughout the thesis, estimates of β based on expressions in Equation (4.17) will be referred to as arising from the martingale estimator. The martingale estimator for β in the situation with incomplete information (Equation (4.17)) depends to a lesser extent on the estimated unobserved infection process

information than the estimator based on Equation (4.16), which yields identical estimates to the ML estimator obtained from Equation (4.2), which assumes complete observed information and hence uses all of the estimated infection process information. The martingale estimator in Equation (4.17) might therefore be less sensitive to any inadequacies in the estimated pattern of infection arising from the non-EM algorithm nature of the iterative procedure. In contrast, martingale estimates have generally been used where there is incomplete data (*e.g.* in Becker (1993a); Becker and Hasofer (1997, 1998); Britton (1998)), and it is inevitable that the performance of such estimates will be suboptimal when compared with those using complete information such as Equation (4.16). Both approaches require estimates from the iterative procedure, however, the martingale method makes minimal use of the expected pattern of infection, while the MLE approach makes heavy use of these data. In Chapter 7, comparisons of estimates based on the martingale estimate in Equation (4.17) and the unrestricted ML estimates will be made.

4.4 Proposed iterative scheme

Considering the log-likelihood for the complete data (assuming t_{gi} known) in Equation (4.1), it is not possible to formulate the function

$$I_2\alpha_2 + I_3\alpha_3 + I_4\alpha_4 - e^{\alpha_2}T_2 - e^{\alpha_3}T_3 - e^{\alpha_4}T_4 \tag{4.18}$$

in the form $\alpha\mathbf{t}(\mathbf{x})^T + A(\alpha)$, where $A(\alpha)$ does not contain any observed random variables. The density for these data is therefore not a member of the exponential family, and hence the formulation of an EM algorithm to maximise the likelihood of the observed data would involve the maximisation of the expectation of the function in Equation (4.18) conditional on the observed data. I_2, I_3 and I_4 are all observed quantities, so the expectation would apply to the function

$$-e^{\alpha_2}T_2(\mathbf{t}_2, \mathbf{t}_3) - e^{\alpha_3}T_3(\mathbf{t}_2, \mathbf{t}_3, \mathbf{t}_4) - e^{\alpha_4}T_4(\mathbf{t}_3, \mathbf{t}_4) \tag{4.19}$$

where the dependence of the function on the unobserved times of infection in each group $\mathbf{t}_g$ is made explicit. The functions will also depend on the unobserved full length of shedding times, but these estimates are assumed to be conditionally independent of the times at which animals become infected, and will be estimated using the methods described in Sections 5.2, 5.2.1 and 5.2.2. Nevertheless, calculation of the function in Equation (4.19), given the high dimensionality of

the unobserved data, would be computationally prohibitive. Maximisation would have to proceed by numerical means, which would make the entire process even more computationally expensive (O'Neill, 2002). Even use of a GEM algorithm, which would remove much of the computation consequent on a maximisation step, appears to be computationally infeasible.

It should be noted that the log-likelihood (Equation (4.2)) for the complete data set indicates that the vector of statistics (I_2, I_3, I_4, T_2, T_3, T_4) are sufficient for the parameter $(\alpha_2, \alpha_3, \alpha_4)$. I_2, I_3 and I_4 are observed quantities. If the likelihood had been in the regular exponential family form, the EM algorithm would have involved estimation of the expectation values of T_2, T_3, and T_4 given the observed data. This, of course, still presents the same computational difficulties as discussed previously, since T_2, T_3, and T_4 are not linear functions of the unobserved variables t_{gi}. However, it is possible to formulate a feasible, although computationally expensive scheme in which each t_{gi} is estimated by the associated expected value, conditional on the expected shedding periods of those individuals which have previously become infective. In a situation such as this, where the latent period is fairly short with a low variability, and the shedding periods are well defined through frequent sampling, it is hoped that the expected values of T_2, T_3, and T_4 will be well approximated by the proposed scheme. Estimates of $(\alpha_2, \alpha_3, \alpha_4)$ are then made by maximising the 'complete' likelihood, with unobserved values replaced with their expected values.

It should be stressed that the resulting algorithm is not an EM algorithm. Having already abandoned the EM framework, it was considered useful to consider whether other estimates for β might be incorporated. In particular, the martingale estimator for β in the situation with incomplete information (Equation (4.17)) uses much less of the unobserved information from the realisation than the ML estimator obtained from Equation (4.2). It might therefore be less sensitive to any inadequacies in the estimated pattern of infection arising from the expectation step of the iterative procedure. Hence, another algorithm is proposed, where the expectation step proceeds as outlined above, but where the maximisation step is replaced with an 'estimation' step, where the martingale estimator is used to generate an updated estimate for β.

As stated above, neither of these algorithms are EM algorithms. Therefore, there is no guarantee that they will converge to the parameter estimates corresponding to the ML for the complete data.

4.5 Conclusion

The methods that will be used to estimate β in groups of sheep have been described. An iterative scheme has been proposed where the infection process characteristics are estimated alternatingly with the β estimates. The maximisation step in the EM algorithm will be replaced by an 'estimation' step, where the ML or martingale estimator is used to generate an updated estimate for β. The resulting iterative schemes are not EM algorithms, but in a situation where the (unobserved) latent periods are short and have low variability, and where frequent sampling defines the shedding periods fairly accurately, it seems reasonable to believe that the algorithms will give reasonable estimates of the unobserved variables. The experimental FMD infection process will be explored in two ways. Firstly, in Chapter 5, the infection process will be partially modelled, considering only the infectiousness period. In this chapter, only the martingale method of estimation will be used to estimate β for groups of sheep. The second approach will involve modelling the entire infection process where the time of infection and latent period will also be considered in addition to the infectiousness period. The aim here will be to estimate the expected infection process characteristics and the rate of infection acting upon groups of sheep using both MLE and martingale estimation methods (Chapters 6 and 7).

Although not pursued in this thesis, modelling of the infection process in groups of sheep and indeed by individual sheep could be achieved using MCMC methods. These are established Bayesian methods that enable samples to be drawn from some target density that is only known up to an element of proportionality. Introductions to the subject can be found in Gilks et al. (1996) and Gamerman (1997). Brooks (1998) gives a comprehensive review of some of the common areas of research in MCMC methods. Renshaw and Gibson (1998) investigate whether MCMC methods can be usefully applied to stochastic processes with unobserved birth times. O'Neill (2002) gives a tutorial introduction to Bayesian inference for epidemic models using MCMC methods. Examples in epidemic modelling where MCMC methods have been employed are: Gibson (1997), to fit spatiotemporal stochastic models in plant epidemiology, Gibson and Renshaw (1998), for parameter estimation in stochastic compartmental models and O'Neill and Roberts (1999), for inference for partially observed stochastic epidemics applied to household data from a smallpox outbreak. O'Neill et al. (2000), use MCMC to analyses infectious disease data from household outbreaks of influenza and measles and O'Neill and Becker (2001), examine inference for epidemics with variable

susceptibility. Britton and O'Neill (2002), use MCMC to fit models for stochastic epidemics in populations with random social structure and Clough et al. (2003), estimate pathogen prevalence within groups of animals from faecal-pat sampling data. However, given the low volume of data available in the FMD experiments, it was felt most appropriate to investigate classical methods of model fitting.

Chapter 5

Modelling the infectiousness period of infected individuals

5.1 Introduction

The main objective of this chapter is to estimate the expected infectiousness period of infected individuals given data defining the viraemic periods. The modelling here will be referred to as a partial model of the infection process where information about the latent period or the force of infection is not taken into account. Also estimated in this chapter is the martingale rate of infection (β) acting upon groups (2 to 4) of sheep, mainly with the purpose of highlighting the importance of modelling the entire infection process which will be addressed in Chapters 6 and 7. The martingale estimator (Equation (4.17)) requires only the number of infections occurring in the group and an estimate of the total exposure time to infective individuals in the group to generate an estimate of $\hat{\beta}$. The former quantity is immediately available from the data, the latter requires to be estimated. In this chapter, a simple method to estimate the expected infectiousness period for each infective is proposed, which, in principle, allows martingale estimates for $\hat{\beta}$ to be calculated. This method assumes that the estimates of infectiousness periods are conditionally independent of the infection process, and hence of β, given the observed data. This will be a reasonable assumption if the period between observations is short relative to the length of infective periods, since in this situation, knowledge of β, and hence of the distribution of infection times for an individual, is unlikely to change the estimate of total infectiousness time by any great amount.

A gamma distribution is assumed for the infectiousness period and from the observed data the parameters of the distribution are estimated. The expected

infectiousness period is estimated conditional on τ, the number of days for which the individual infected sheep tested positive to FMD virus. From Chapter 4 it was established that in order to be able to calculate a martingale estimate for β for a given group, the expected time of infection exposure for that group has to be estimated (refer to Equation (4.17)). Once an estimate for the expected infectiousness period for each individual has been derived, the total expected time of infection exposure for each group is estimated. This is attained by establishing for how long infected individuals were infectious and how much of the infectiousness period contributed to the time of exposure of infection in different groups. A martingale estimate for β for each group is then calculated. These martingale estimates derived on the basis of the partial information of viraemic periods will be compared with the martingale estimate in Chapter 6 where estimated times for the start of infectiousness are obtained. Considering the objective of the experiments, it is desirable to assess the trend in the estimates of β across groups. This will be done in Chapter 6.

5.2 Distribution of infectiousness period

A gamma distribution with shape parameter ν_{inf} and scale parameter λ_{inf} is assumed for the infectiousness period, T_I, with density given by:

$$f_{\nu_{inf},\lambda_{inf}}(t_I) = \frac{{\lambda_{inf}}^{\nu_{inf}} \; {t_I}^{\nu_{inf}-1} e^{-\lambda_{inf} t_I}}{\Gamma(\nu_{inf})}.$$

It should be noted that the subscript *'inf'* is used to reflect the fact that the parameters, ν_{inf} and λ_{inf}, define the distribution of the infectiousness period. Parameters ν_{inf} and λ_{inf} are to be estimated using maximum likelihood estimation by maximising the likelihood of the infectiousness period given the data. Once the parameter estimates are calculated, expected values of the infectiousness period can then be calculated, from which the amount of infection exposure for a given group is determined.

Often an exponential distributed or a fixed infectiousness period is assumed (Haydon and Woolhouse, 1997; Howard and Donnelly, 2000a). However, for many infection processes, the exponential distribution is not a realistic option for the distribution of the infectiousness period. A gamma distribution is therefore assumed due its wider variability in shape depending on the value of the shape

parameter. The exponential distribution is a special case of a gamma distribution. Figure 5.1 shows different shapes of gamma distribution based on the same value of the scale parameter ($\lambda_{inf} = 1$).

Figure 5.1: *Probability density function for a gamma variate for various values of the shape parameter and scale parameter equal to 1.*

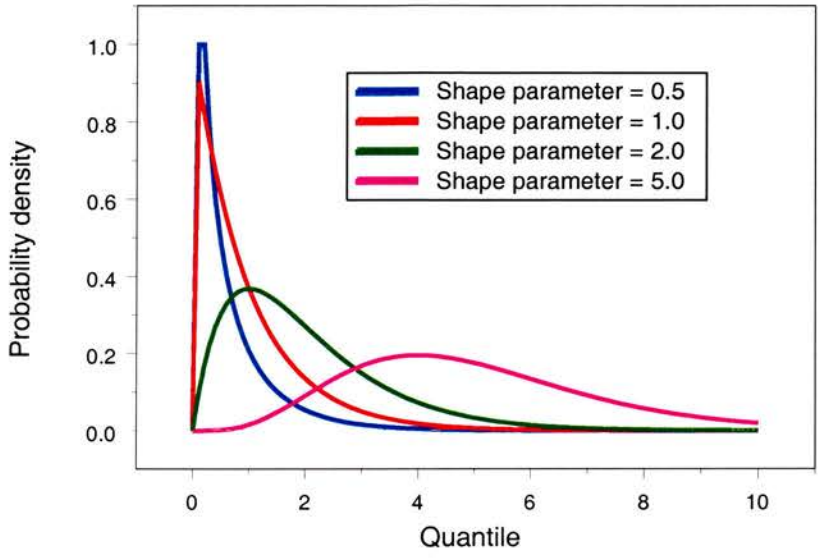

For any infected individual, let

n_e be the number of daily observed test results that were positive ($n_e \geq 0$),

τ be the day of the first observed positive test,

ω be the day of the last observed positive test,

t_I be the infectiousness period for an infected individual.

The aim is to determine the expected length of infectiousness period, t_I, for an infected individual conditional on the number of times the individual tested positive for FMD virus. Let $\Pr(t_I|n_e)$ denote the probability of length of infectiousness period, t_I, given n_e. Using Bayes' rule,

$$\begin{aligned} \Pr(t_I|n_e) &= \frac{\Pr(n_e|t_I)\ \Pr(t_I)}{\Pr(n_e)} \\ \Rightarrow \quad \Pr(n_e)\Pr(t_I|n_e) &= \Pr(n_e|t_I)\Pr(t_I) \end{aligned}$$

where $\Pr(t_I)$ is the probability density function of the infectiousness period and $\Pr(n_e|t_I)$ is the probability of detecting n_e positive observed days given the length of infectiousness period t_I.

If $n_e > 0$ then it is possible for the infectiousness period t_I to have taken any value between $n_e - 1$ and $n_e + 1$. However, conditional on t_I, there are different

probabilities of n_e positive observations having been detected. The distribution of n_e given the various ranges of t_I is given below, assuming that the time of observation and the infectiousness state are independent.

		Range of t_I			
		$0 < t_I < 1$	$1 < t_I < 2$	$2 < t_I < 3$	...
Number	0	$1 - t_I$	0	0	...
of positive	1	t_I	$2 - t_I$	0	...
obs (n_e)	2	0	$t_I - 1$	$3 - t_I$	...
	3	0	0	$t_I - 2$	...
	⋮	⋮	⋮	⋮	...

If $n_e - 1 < t_I < n_e$, the probability of detecting n_e positive tests is equal to $t_I - (n_e - 1) = t_I - n_e + 1$ and if $n_e < t_I < n_e + 1$, the probability of detecting n_e positive tests is $n_e + 1 - t_I$.
Hence,

$$\begin{aligned}\Pr(n_e)\Pr(t_I|n_e) &= \Pr(n_e|t_I)\Pr(t_I) \\ &= \begin{cases} (t_I - n_e + 1) f_{\nu_{inf},\lambda_{inf}}(t_I) & \text{if} \quad n_e - 1 < t_I < n_e \\ (n_e + 1 - t_I) f_{\nu_{inf},\lambda_{inf}}(t_I) & \text{if} \quad n_e < t_I < n_e + 1 \end{cases}\end{aligned}$$

and

$$\begin{aligned}&\int \Pr(n_e)\Pr(t_I|n_e)\,dt_I \\ &\quad = \int_{n_e-1}^{n_e} (t_I - n_e + 1)\, f_{\nu_{inf},\lambda_{inf}}(t_I)\,dt_I + \int_{n_e}^{n_e+1} (n_e + 1 - t_I)\, f_{\nu_{inf},\lambda_{inf}}(t_I)\,dt_I\end{aligned}$$

$$\begin{aligned}&\Rightarrow \Pr(n_e) \int \Pr(t_I|n_e)\,dt_I \\ &\quad = \int_{n_e-1}^{n_e} (t_I - n_e + 1)\, f_{\nu_{inf},\lambda_{inf}}(t_I)\,dt_I + \int_{n_e}^{n_e+1} (n_e + 1 - t_I)\, f_{\nu_{inf},\lambda_{inf}}(t_I)\,dt_I.\end{aligned}$$

But, by definition

$$\int \Pr(t_I|n_e)\,dt_I = 1,$$

hence

$$\Pr(n_e) = \int_{n_e-1}^{n_e} (t_I - n_e + 1)\, f_{\nu_{inf},\lambda_{inf}}(t_I)\,dt_I + \int_{n_e}^{n_e+1} (n_e + 1 - t_I)\, f_{\nu_{inf},\lambda_{inf}}(t_I)\,dt_I$$

allowing the formulation of a likelihood function given the data in the next section and hence parameters ν_{inf} and λ_{inf} can be estimated.

5.2.1 Estimation of parameters ν_{inf} and λ_{inf}

The likelihood function consists of different components which depend on whether the infectiousness period, t_I is between $n_e - 1$ and n_e or between n_e and $n_e + 1$.

For $n_e > 0$, the contribution to the likelihood is:

$$\int_{n_e-1}^{n_e} (t_I - n_e + 1) f_{\nu_{inf},\lambda_{inf}}(t_I) dt_I \; + \; \int_{n_e}^{n_e+1} (n_e + 1 - t_I) f_{\nu_{inf},\lambda_{inf}}(t_I) dt_I.$$

For $n_e = 0$ the contribution to the likelihood for an infected individual is:

$$\int_0^1 (1 - t_I) f_{\nu_{inf},\lambda_{inf}}(t_I) dt_I.$$

Therefore the full log-likelihood function is given by:

$$\begin{aligned} &(\text{freq for } n_e = 0) \times \ln\left[\int_0^1 (1 - t_I) f(t_I)\, dt_I\right] \; + \\ &\sum_{n_e>0} (n_e \text{ freq}) \times \ln\left[\int_{n_e-1}^{n_e} (t_I - n_e + 1)\, f(t_I)\, dt_I + \int_{n_e}^{n_e+1} (n_e + 1 - t_I)\, f(t_I)\, dt_I\right]. \end{aligned} \tag{5.1}$$

Maximisation of the log-likelihood is implemented in the Splus statistical package using the *nlminb* in-built routine to yield the desired parameter estimates $\hat{\nu}_{inf}$ and $\hat{\lambda}_{inf}$ for the gamma distributed infectiousness period. Expected values of the infectiousness period can then be estimated and this is performed in the next section.

The above formulation assumes that infectiousness starts randomly during the unobserved day prior to the day of the first observed positive test. This is not strictly true since infectiousness period is a function of the past time of infection and the latent period distribution but it will be very close to the truth, especially given the relatively dense sampling strategy used in the FMD experiments. In Chapter 6 the model for the entire infection process will address the above issue.

5.2.2 Expected infectiousness period

Once the parameters of the distribution of the infectiousness period have been estimated, estimates for the expected infectiousness period for each infected individual can be calculated.

Let $f(t_I|n_e)$ denote the density of the infectiousness period distribution given n_e. Then,

$$f(t_I|n_e) \propto f_{\nu_{inf},\lambda_{inf}}(t_I)\Pr(n_e|t_I)$$

$$= \begin{cases} (t_I - n_e + 1)f_{\nu_{inf},\lambda_{inf}}(t_I) & \text{if } n_e - 1 < t_I < n_e \\ (n_e + 1 - t_I)f_{\nu_{inf},\lambda_{inf}}(t_I) & \text{if } n_e < t_I < n_e + 1 \end{cases}$$

After rescaling,

$$f(t_I|n_e) = \begin{cases} \frac{(t_I - n_e + 1)f_{\nu_{inf},\lambda_{inf}}(t_I)}{\int_{n_e-1}^{n_e}(t_I - n_e + 1)f(t_I)dt_I + \int_{n_e}^{n_e+1}(n_e + 1 - t_I)f(t_I)dt_I} & \text{if } n_e - 1 < t_I < n_e \\ \frac{(n_e + 1 - t_I)f_{\nu_{inf},\lambda_{inf}}(t_I)}{\int_{n_e-1}^{n_e}(t_I - n_e + 1)f(t_I)dt_I + \int_{n_e}^{n_e+1}(n_e + 1 - t_I)f(t_I)dt_I} & \text{if } n_e < t_I < n_e + 1 \end{cases}$$

For $(n_e > 0)$, the expected infectiousness period for an infected individual is given by:

$$E[T_I|n_e] = \frac{\int_{n_e-1}^{n_e} t_I^2 f(t_I)dt_I - (n_e - 1)\int_{n_e-1}^{n_e} t_I f(t_I)dt_I + (n_e + 1)\int_{n_e}^{n_e+1} t_I f(t_I)dt_I - \int_{n_e}^{n_e+1} t_I^2 f(t_I)dt_I}{\int_{n_e-1}^{n_e} t_I f(t_I)dt_I - (n_e - 1)\int_{n_e-1}^{n_e} f(t_I)dt_I + (n_e + 1)\int_{n_e}^{n_e+1} f(t_I)dt_I - \int_{n_e}^{n_e+1} t_I f(t_I)dt_I} \tag{5.2}$$

For example, for $n_e = 2$,

$$E[T_I|n_e = 2] = \frac{\int_1^2 t_I^2 f(t_I)dt_I - \int_1^2 t_I f(t_I)dt_I + 3\int_2^3 t_I f(t_I)dt_I - \int_2^3 t_I^2 f(t_I)dt_I}{\int_1^2 t_I f(t_I)dt_I - \int_1^2 f(t_I)dt_I + 3\int_2^3 f(t_I)dt_I - \int_2^3 t_I f(t_I)dt_I} \tag{5.3}$$

where $f(t_I)$ is the density for the distribution of the infectiousness period which is gamma with shape parameter ν_{inf} and scale parameter λ_{inf}.

All integrals in Equation (5.2) can be expressed in terms of integrals of a gamma density. For instance, for any arbitrary limits a and b, $f(t)$ a density function and $\mathrm{F}_\gamma(t;\, \nu,\, \lambda)$ the cumulative distribution function for a gamma distributed random variable T, with shape parameter ν and scale parameter λ;

$$\begin{aligned} \int_a^b tf(t)dt &= \int_a^b \frac{t\lambda^\nu t^{\nu-1}e^{-\lambda t}\,dt}{\Gamma(\nu)} = \int_a^b \frac{\lambda^\nu}{\Gamma(\nu)} t^\nu e^{-\lambda t}dt \\ &= \frac{\Gamma(\nu+1)}{\lambda\Gamma(\nu)}\int_a^b \frac{\lambda^{\nu+1}t^\nu e^{-\lambda t}dt}{\Gamma(\nu+1)} \\ &= \frac{\nu}{\lambda}\int_a^b \frac{\lambda^{\nu+1}t^\nu e^{-\lambda t}}{\Gamma(\nu+1)}\,dt \\ &= \frac{\nu}{\lambda}[\ \mathrm{F}_\gamma(b;\nu+1,\lambda) - \mathrm{F}_\gamma(a;\nu+1,\lambda)\ ] \end{aligned} \tag{5.4}$$

and

$$\begin{aligned}\int_a^b t^2 f(t)dt &= \int_a^b \frac{t^2\lambda^\nu t^{\nu-1}e^{-\lambda t}\,dt}{\Gamma(\nu)} = \int_a^b \frac{\lambda^\nu}{\Gamma(\nu)} t^{\nu+1}e^{-\lambda t}dt \\ &= \frac{\Gamma(\nu+2)}{\lambda^2\Gamma(\nu)}\int_a^b \frac{\lambda^{\nu+2}t^{\nu+1}e^{-\lambda t}dt}{\Gamma(\nu+2)} \\ &= \frac{(\nu+1)\nu}{\lambda^2}\int_a^b \frac{\lambda^{\nu+2}t^{\nu+1}e^{-\lambda t}}{\Gamma(\nu+2)}\,dt \\ &= \frac{(\nu+1)\nu}{\lambda^2}[\ \mathrm{F}_\gamma(b;\nu+2,\lambda) - \mathrm{F}_\gamma(a;\nu+2,\lambda)\ ].\end{aligned} \tag{5.5}$$

Hence the expression, in Equation (5.2), for the estimator of the expected infectiousness period given n_e has components that are all analytically tractable and once $\hat{\nu}_{inf}$ and $\hat{\nu}_{inf}$ have been obtained, estimates for the expected infectiousness period can be calculated.

The PCR technique used in detecting virus in the blood samples is considered to be sensitive and specific (Reid et al., 2001; Hughes et al., 2002b). Using the simplifying assumption that a positive test result indicates infectiousness, if sheep had been infectious (had live virus in blood) on day $\tau - 1$, the day before the first positive test was observed, these sheep should have tested positive. Similarly if sheep were still infectious on day $\omega + 1$, the day after the last observed positive test, they should have tested positive to FMD virus presence. Thus infectiousness begins sometime between day $\tau - 1$ and τ and ceases sometime between day ω and $\omega + 1$.

If n_e positive tests have been observed, the observed infectiousness period is equal to $n_e - 1$ days. Thus the expected unobserved infectiousness period, T_u, is the difference between the expected and observed infectiousness periods *i.e.* $T_u = E[T_I|n_e] - (n_e - 1)$. The unobserved period is composed of a portion before τ and after ω. Half of the unobserved infectiousness period is assigned to each portion, since the model provides no basis for preferring one portion over the other.

After estimating the expected infectiousness period for each infected sheep, the amount of expected infectiousness period that each contributes to the expected total infection exposure time for each group can be determined. The expected total infection exposure time is derived and estimates for the β_g can then be calculated.

5.3 Estimation of rate of infection

The rate of infection (β) acting upon groups of sheep is estimated based on expected infectiousness periods and the times when infected individuals test positive. Martingale estimates for β for each group and their respective standard error estimates are calculated based on Equation (4.17) of Chapter 4. Any trend in the estimates of the βs can only be attributable to a drop of infectivity with increased generation, as infected sheep in higher groups will tend to have high infection generations.

The use of the martingale estimates, based on modelling only the expected infectiousness times, depends on the assumption that there is at least one remaining susceptible individual in each group at the end of the epidemic. However, if there are no susceptible individuals left at the end of the epidemic in a group, the martingale estimate for β is an underestimate. There will be an amount of infection exposure time included in the total infection exposure time of the affected group which should not be included because in actual fact this group will have ceased to be influenced by any infection exposure after the infection time of the last susceptible individual in the group.

Modelling only the infectiousness times yields inferential methods that are quite easy to implement and in situations where the group susceptible population is not exhausted, the resulting martingale estimate for β might be sufficient. However, when analysing data from groups where all individuals are infected by the end of the epidemic, it is necessary to use the more appropriate estimate for β, based on an estimate of the time of infection of the last individual to become infected in the group. The problem of underestimation of the β parameters, which arises when all individuals are infected, will be addressed through modelling of the entire infection process. This is the subject of Chapter 6.

5.4 Application to experimental data

For each infected sheep the number of days that the animal tested positive, denoted by n_e, is known. Hence the infectiousness period for an infected sheep is expected to be between $n_e - 1$ and $n_e + 1$ days given an observed infectiousness period of $n_e - 1$ days. Conditioning on the expected infectiousness period t_I, there are different probabilities of n_e positive test days having been detected. If

the infectiousness period, t_I is between $n_e - 1$ and n_e *i.e.* $T_u < 1$, the probability of detecting n_e days of positive tests is equal to $t_I - (n_e - 1)$. Alternatively if t_I is between n_e and $n_e + 1$ *i.e.* $T_u > 1$, the probability of detecting n_e days of positive tests is given by $n_e + 1 - t_I$. Taking the different possibilities into account yielded an estimator for the expected infectiousness period (Equation (5.2)), from which an estimate for the expected infectiousness period for each infected sheep is calculated.

5.4.1 Data from experiments 1 and 2

The experimental data are summarised in Table 5.1, in the form that is required for analysis using a partial model of the infection process. These data consist of the identity of the sheep, sheep ID, the number of days with positive test result n_e, the day of the first positive test result τ, and the day of the last positive test result ω. Sheep with ID $1 - 8$ belong to group 1, ID $9 - 16$ are group 2 sheep, ID $17 - 24$ are in group 3 and sheep with ID $25 - 32$ belong to group 4.

Table 5.1: *Data from experiments* 1 *and* 2 *for each sheep indicating number of days with positive test result,* n_e*, the day of the first positive test result* τ*, and the day of the last positive test result* ω*.*

Experiment 1								Experiment 2							
ID	τ	ω	n_e	ID	τ	ω	n_e	ID	τ	ω	n_e	ID	τ	ω	n_e
1	2	4	3	17	11	13	3	1	2	3	2	17	11	13	3
2	1	3	3	18	9	10	2	2	1	4	4	18	11	12	2
3*	-	-	-	19	9	11	3	3	2	4	3	19	10	12	3
4	1	3	3	20	11	13	3	4	2	4	3	20*	-	-	-
5	3	4	2	21	9	11	3	5	2	4	3	21	12	13	2
6	2	4	3	22	10	13	4	6	2	4	3	22	14	15	2
7	3	4	2	23	8	10	3	7	2	5	4	23*	-	-	-
8	2	5	4	24	13	15	3	8	2	5	4	24	10	11	2
9*	-	-	-	25*	-	-	-	9	5	7	3	25	15	16	2
10	8	10	3	26	11	14	4	10	7	10	4	26	15	16	2
11	5	7	3	27	13	14	2	11	9	11	3	27	12	13	2
12	9	11	3	28	16	18	3	12	9	10	2	28*	-	-	-
13	12	14	3	29	13	15	3	13*	-	-	-	29	13	15	3
14	9	11	3	30	13	15	3	14	17	19	3	30*	-	-	-
15*	-	-	-	31	13	16	4	15*	-	-	-	31*	-	-	-
16	10	11	2	32	14	15	2	16*	-	-	-	32*	-	-	-

**sheep did not shed virus, thus assumed not to be infected.*

From experiment 1, in group 1, sheep 3 did not test positive for FMD virus even though it was inoculated. In groups 2 to 4, sheep 9, 15 and 25 did not test

positive for FMD virus. In group 2, 2 susceptible sheep remained at the end of the epidemic, all group 3 sheep became infected and 1 susceptible individual remained in group 4 at the end of the experiment. There were 21 secondary infectives in groups 2 to 4 from 24 initial susceptibles. In experiment 2, there were 15 secondary infectives from groups 2 to 4 with at least 2 susceptible individuals in each of these groups at the end of the experiment. Sheep with no observed viraemic days were confirmed as uninfected by serology at the end of the experiment (Hughes, 2001).

Sheep with at least 1 positive test result *i.e.* $n_e \geq 1$, are considered to have been infected. For both experiments, n_e takes values 2, 3, and 4 in all groups. In experiment 1 more than half of the infected sheep tested positive on 3 occasions ($n_e = 3$) and in experiment 2, about half of the infected sheep tested positive on 3 occasions. The distribution of n_e is given in Table 5.2.

Table 5.2: *Distribution of n_e for sheep data in Table 5.1.*

n_e	2	3	4	Total
Frequency(expt1)	6	18	4	28
Frequency(expt2)	9	10	4	23

For each value of n_e the expected value of the infectiousness period, $E[T_I|n_e]$, is calculated from expressions in Equations (5.2), (5.4) and (5.5).

5.4.2 Estimates of ν_{inf} and λ_{inf}

The log-likelihood function for the infectiousness process is as given in Equation (5.1) in Section 5.2.1 *i.e.*

$$\begin{aligned} l \;=\; & (\text{freq for } n_e = 0) \;\times\; \ln\left[\int_0^1 (1 - t_I) f(t_I)\, dt_I\right] \;+ \\ & \sum_{n_e > 0} (n_e \text{ freq}) \;\times\; \ln\Bigg[\int_{n_e-1}^{n_e} (t_I - n_e + 1)\, f(t_I)\, dt_I \;+ \\ & \qquad \int_{n_e}^{n_e+1} (n_e + 1 - t_I)\, f(t_I)\, dt_I\Bigg] \\ = \; & \sum_{n_e > 0} (n_e \text{ freq}) \;\times\; \ln\Bigg[\int_{n_e-1}^{n_e} t_I\, f(t_I)\, dt_I \;-\; (n_e - 1)\int_{n_e-1}^{n_e} f(t_I)\, dt_I \;+ \\ & \qquad (n_e + 1)\int_{n_e}^{n_e+1} f(t_I)\, dt_I \;-\; \int_{n_e}^{n_e+1} t_I\, f(t_I)\, dt_I\Bigg]. \end{aligned}$$

Frequency for $n_e = 0$ is zero for both experiments.

Using the property of the gamma density as stated in Equation (5.4) and the fact that the frequency for $n_e = 0$ is zero, the expression for the full log-likelihood function becomes:

$$\begin{aligned} l \;=\; \sum_{n_e>0} (n_e \text{ freq}) \times \ln \Big\{ & \frac{\nu_{inf}}{\lambda_{inf}} \left[\mathrm{F}_\gamma(n_e; \nu_{inf}+1, \lambda_{inf}) - \mathrm{F}_\gamma(n_e-1; \nu_{inf}+1, \lambda_{inf}) \right] \\ & - (n_e-1) \left[\mathrm{F}_\gamma(n_e; \nu_{inf}, \lambda_{inf}) - \mathrm{F}_\gamma(n_e-1; \nu_{inf}, \lambda_{inf}) \right] \\ & + (n_e+1) \left[\mathrm{F}_\gamma(n_e+1; \nu_{inf}, \lambda_{inf}) - \mathrm{F}_\gamma(n_e; \nu_{inf}, \lambda_{inf}) \right] \\ & - \frac{\nu_{inf}}{\lambda_{inf}} \left[\mathrm{F}_\gamma(n_e+1; \nu_{inf}+1, \lambda_{inf}) - \mathrm{F}_\gamma(n_e; \nu_{inf}+1, \lambda_{inf}) \right] \Big\}. \end{aligned} \tag{5.6}$$

The log-likelihood function was maximised using the *nlminb* routine in the Splus statistical package yielding the estimates, below, for the parameters of the distribution of infectiousness period.

Experiment 1

The estimate for the shape parameter $\hat{\nu}_{inf} = 12.6362$ and the estimate for the scale parameter $\hat{\lambda}_{inf} = 4.4952$. Thus the estimate for the mean of the distribution of the infectiousness period for the infected sheep in experiment 1 given by $\frac{\hat{\nu}_{inf}}{\hat{\lambda}_{inf}}$, is 2.81 days, with standard deviation estimated by $\sqrt{\frac{\hat{\nu}_{inf}}{\hat{\lambda}^2_{inf}}} = 0.791$.

Experiment 2

The estimate for the shape parameter $\hat{\nu}_{inf} = 22.7237$ and the estimate for the scale parameter $\hat{\lambda}_{inf} = 8.1539$. Thus the mean of the distribution of the infectiousness period for the infected sheep in experiment 2 is estimated to be equal to 2.79 days, with an estimated standard deviation of 0.585.

From both experiments, results indicate that infected sheep have an estimated infectiousness duration of 2.8 days on average with the variation in infectiousness higher in experiment 1 than in experiment 2, but probably exhibiting no statistically significant difference.

5.4.3 Estimates of expected infectiousness period

For every observed value of n_e, a corresponding estimate for the expected infectiousness period is calculated. For $n_e = 2$, the estimator for the expected infectiousness period is as given in Equation (5.3). For $n_e = 3$ and $n_e = 4$ the expressions are similar. The expressions are further simplified by substituting the

integrals by the equivalent quantities from Equations (5.4) and (5.5). Table 5.3 lists estimates for the expected infectiousness period given n_e. For instance, the results indicate that from experiment 1, if an individual sheep tested positive on 2 sampling days *i.e.* $n_e = 2$, then its expected infectiousness period is estimated to be equal to 2.18 days and from experiment 2, the respective estimate for the infectiousness period is 2.28 days.

Table 5.3: *Expected infectiousness period given n_e for sheep data in Table 5.1.*

n_e	2	3	4
expected inf period (expt1)	2.18	2.92	3.77
expected inf period (expt2)	2.28	2.90	3.65

The consequence of only partially modelling the infection process is that the infectiousness period of a sheep is based on n_e and the infectiousness period distribution only. As a result sheep from the same experiment that have the same n_e be associated with the same estimate for the expected infectiousness period.

Given that an individual sheep tested positive on n_e days, the observed infectiousness period for such an infected sheep is $n_e - 1$ days. Thus there is always an amount of unobserved infectiousness period (T_u). The unobserved amount of infectiousness is composed of a period before the first observed positive test and a period after the last observed positive test. From the results in Table 5.3 giving the estimated expected infectiousness period, $E[T_I|n_e]$ is always greater than the observed infectiousness period $n_e - 1$. Thus $T_u = E[T_I|n_e] - (n_e - 1) > 0$ and the size of T_u for each n_e for both experiments is presented in Table 5.4.

Table 5.4: *Unobserved infectiousness period (T_u).*

n_e	2	3	4
T_u (expt1)	1.18	0.92	0.77
T_u (expt2)	1.28	0.90	0.65

Results indicate that the unobserved infectiousness period is higher for lower n_e. Sheep that tested positive on only 2 sampling days are estimated to have had more than a day of their expected infectiousness period unobserved while sheep that tested positive on 3 sampling days are likely to have had just under a day of unobserved infectiousness. Sheep that tested positive on 4 sampling days, are estimated to have less of their infectiousness period unobserved compared to those with $n_e = 2$ and $n_e = 3$.

Sheep start excreting virus at an unobserved point in time between day $\tau - 1$ and day τ and stop excreting virus sometime between day ω and day $\omega + 1$. In order to assign the estimated expected infectiousness period of each infected sheep, it has to be decided how much of the estimated unobserved expected infectiousness period is before τ and how much is after ω. There is no basis of weighting one over the other, so half of the unobserved expected infectiousness period (T_u) is assigned to the period before τ and half to the period after ω. Thus for each infected sheep, the estimated start of infectiousness is given by $\tau - \frac{1}{2}T_u$ and the estimated end of infectiousness is $\omega + \frac{1}{2}T_u$. For instance for sheep number 1 in experiment 1, its $n_e = 3$, $\tau = 2$, $\omega = 3$ and its expected infectiousness period is estimated to be 2.92 days. Therefore the unobserved expected infectiousness period is estimated to be 0.92 giving $\frac{1}{2}T_u = 0.46$. Hence the estimated start of infectiousness for sheep number 1 is at time $= 2 - 0.46 = 1.54$ and estimated end of infectiousness is at time $4 + 0.46 = 4.46$.

Tables 5.5 and 5.6 give estimates for the time of start of infectiousness and end of infectiousness for each infected sheep from experiments 1 and 2 respectively.

Table 5.5: *Estimates for the expected infectiousness process for infected sheep (Experiment 1).*

ID	Inf.Start	Inf.End	Inf.Period	n_e	ID	Inf.Start	Inf.End	Inf.Period	n_e
1	1.54	4.46	2.92	3	17	10.54	13.46	2.92	3
2	0.54	3.46	2.92	3	18	9.41	11.59	2.18	2
3*	-	-	-	-	19	8.54	11.46	2.92	3
4	0.54	3.46	2.92	3	20	10.54	13.46	2.92	3
5	2.41	4.59	2.18	2	21	8.54	11.46	2.92	3
6	1.54	4.46	2.92	3	22	10.62	14.39	3.77	4
7	2.41	4.59	2.18	2	23	7.54	10.46	2.92	3
8	1.62	5.39	3.77	4	24	12.54	15.46	2.92	3
9*	-	-	-	-	25*	-	-	-	-
10	7.54	10.46	2.92	3	26	10.62	14.39	3.77	4
11	4.54	7.46	2.92	3	27	12.41	14.59	2.18	2
12	8.54	11.46	2.92	3	28	15.54	18.46	2.92	3
13	11.54	14.46	2.92	3	29	12.54	15.46	2.92	3
14	8.54	11.46	2.92	3	30	12.54	15.46	2.92	3
15*	-	-	-	-	31	12.62	16.39	3.77	4
16	9.41	11.59	2.18	2	32	13.41	15.59	2.18	2

* *These sheep did not shed virus, hence assumed not to be infected.*

For both experiments, results indicate that group 1 sheep are estimated to have been infectious between day 0 and day 6. The first group 1 sheep to shed virus is estimated to have entered the infectiousness state at time 0.54 for experiment 1 (time 0.68 for experiment 2) and the last sheep from this group to shed virus is

Table 5.6: *Estimates for the expected infectiousness process for infected sheep (Experiment 2).*

ID	Inf.Start	Inf.End	Inf.Period	n_e	ID	Inf.Start	Inf.End	Inf.Period	n_e
1	1.36	3.64	2.28	2	17	10.55	13.45	2.90	3
2	0.68	4.33	3.65	4	18	10.36	12.64	2.28	2
3	1.55	4.45	2.90	3	19	9.55	12.45	2.90	3
4	1.55	4.45	2.90	3	20*	-	-	-	-
5	1.55	4.45	2.90	3	21	11.36	13.64	2.28	2
6	1.55	4.45	2.90	3	22	13.36	15.64	2.28	2
7	1.68	5.33	3.65	4	23*	-	-	-	-
8	1.68	5.33	3.65	4	24	9.36	11.64	2.28	2
9	4.55	7.45	2.90	3	25	14.36	16.64	2.28	2
10	6.68	10.33	3.65	4	26	14.36	16.64	2.28	2
11	8.55	11.45	2.90	3	27	11.36	13.64	2.28	2
12	8.36	10.64	2.28	2	28*	-	-	-	-
13*	-	-	-	-	29	12.55	15.45	2.90	3
14	16.55	19.45	2.90	3	30*	-	-	-	-
15*	-	-	-	-	31*	-	-	-	-
16*	-	-	-	-	32*	-	-	-	-

** These sheep did not shed virus, hence assumed not infected.*

estimated to have ceased being infectious at time 5.39 for experiment 1 (time 5.33 for experiment 2). For both experiments, only 1 sheep in group 2 was estimated to be infectious during the estimated expected infectiousness period of group 1 sheep. In experiment 2, it is estimated that sheep 14 started shedding virus when all sheep in groups 2 and 3 had ceased to be infectious. Thus, sheep 14 was probably infected due to infected individuals in group 3 and not group 2. The estimated pattern of virus shedding is presented in Figure 5.2.

5.4.4 Estimation of the rate of infection for each group

After deriving estimates for the expected infectiousness period for each infected sheep, the expected total infection exposure time for each of groups 2 to 4 (which is required for the martingale estimate of β, as given in Equation (4.17)), can now be estimated. Taking the mixing of groups into account, the appropriate contribution of expected infection exposure from each infective sheep to the relevant group is calculated.

For example, sheep 1 in experiment 1 is estimated to have excreted virus from time 1.54 to 4.46. During day 1 *i.e.* between day 1 and day 2, group 1 and group 2 sheep were mixing. Thus during this time, any infectious individuals which are present contribute to the expected infection exposure time of group 2. Sheep 1,

Figure 5.2: *Graph showing estimated infectiousness periods in experiments 1 and 2.*

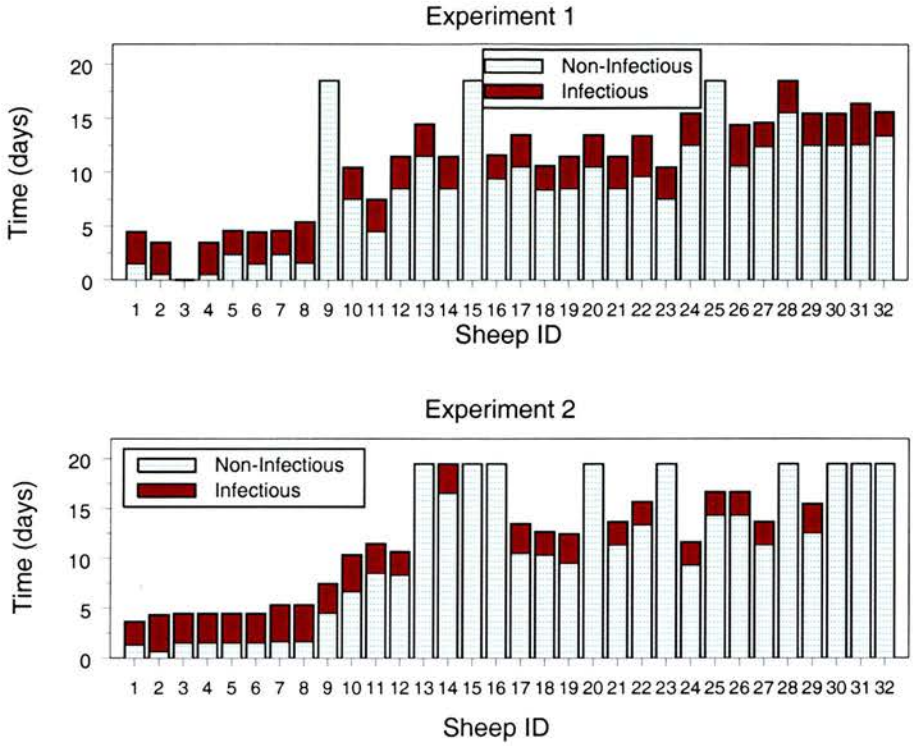

during day 1, contributed $2 - 1.54 = 0.46$ days to group 2 expected infection exposure time. Again during day 3 *i.e.* between day 3 and day 4, group 1 and 2 were mixing during this period, sheep 1 was still infectious, so it contributed a full day of infection time to the expected exposure time of group 2. For the period between day 5 and 6, although group 1 and 2 were mixing, sheep 1 did not contribute to the exposure time because it had ceased excreting virus at the estimated time of 4.46 after the start of experiment. Thus in total, sheep 1 contributed an expected value of 1.46 days of infection exposure to group 2. Because a true mass action model is assumed, the infection time is scaled by the total number of sheep mixing during the contribution period.

For groups 2 and 3, the infection exposure time is divided by 16 because once the experiment has started, these groups are always mixing with another group, making the total number of sheep present always equal to 16. For group 4, however, the scaling number depends on the day of mixing. If the day of mixing is odd, say day 3 *i.e.* between day 3 and 4, then the estimated expected infection time exposure during this period will be divided by 16, the total number of sheep from group 3 and group 4, since on odd days groups 3 and 4 are mixing. However,

if the mixing is on an even day, say day 4 *i.e.* between day 4 and 5, then the total number of sheep will be 8 because group 4 sheep will not be mixing with any other sheep from another group on these days.

All contributions of infection time exposure from each infected sheep are calculated, scaled and summed, yielding an estimate for the total expected infection exposure time for each of groups 2 to 4. The expected infection exposure times for each group are given in Table 5.7 for both experiments.

Table 5.7: *Estimates for expected total group infection exposure time, in days, scaled by the number of mixing individuals.*

group	2	3	4
exposure time (expt1)	2.3952	2.6452*	2.6423
exposure time (expt2)	2.1357	1.6829	1.4060

* *all sheep in group infected*

The numerator in the expression in Equation (4.17) for calculating β estimates is given by:

$$\int_0^T B(x)dN(x) = \frac{1}{s} + \frac{1}{s-1} + \ldots + \frac{1}{S(T)+1}$$

where s is the number of susceptibles in each group at the start of the experiments, which is 8 in this case, T is the time of the end of the epidemic and $S(T)$ is the number of susceptibles remaining in the group at the end of the epidemic. For experiment 1, the number of susceptibles remaining at the end of the experiment (epidemic) are: 2 in group 2, 0 in group 3 and 1 in group 4. For experiment 2, the number of susceptibles remaining at the end of the experiment are: 3 in group 2, 2 in group 3 and 4 in group 4. Thus the value for $\int_0^T B(x)dN(x)$ for each group can be calculated and are presented in Table 5.8.

Table 5.8: *Number of susceptibles at the end of experiments, S(T), and corresponding values for the integral of the B function for each group.*

	Experiment 1		Experiment 2	
Group	S(T)	Integral of B	S(T)	Integral of B
2	2	1.2179	3	0.8845
3	0	2.7179	2	1.2179
4	1	1.7179	4	0.6345

The quantities required for the β estimate are now all known, and hence it is

possible to calculate estimates for β for each group, 2 to 4, with corresponding standard error estimates.
Recall that

$$\hat{\beta} = \frac{\int_0^T B(x)dN(x)}{E[\int_0^T \frac{I(x)J(x)}{n(x)}]dx} \quad \text{and} \quad s.e(\hat{\beta}) = \frac{[\int_0^T B^2(x)dN(x)]^{1/2}}{E[\int_0^T \frac{I(x)J(x)}{n(x)}dx]}.$$

The numerator of $\hat{\beta}$ is the value of the integral of the B function given in Table 5.8 and the denominator is the expected total infection exposure given in Table 5.7. The numerator for the standard error estimate of $\hat{\beta}$ is given by

$$\sqrt{\int_0^T B^2(x)dN(x)} = \sqrt{\frac{1}{s^2} + \frac{1}{(s-1)^2} + \cdots + \frac{1}{(S(T)+1)^2}} \tag{5.7}$$

and is calculated from the values of the number of susceptibles at the start and end of the experiments.

The results for the estimates of β and the corresponding standard error estimates for the three groups are presented in Table 5.9, for both experiments. Group 3 has the highest estimated rate of infection, followed by group 4 and then group 2 which has the lowest β estimate for both experiments. It should be noted that in group 3, all individuals became infected. As a result the rate of infection in this group is underestimated because all of the estimated expected infection exposure time was included in the calculation of the estimate and yet the group was only exposed to infection up to the time of the infection of the last individual to become infected in this group. Although underestimated, group 3 still has the highest estimated rate of infection. In practice, such a risk of systematic underestimation must be regarded as a serious drawback of this approach.

Table 5.9: *Estimates of group rate of infection (β) per day and corresponding standard error estimates.*

		Group		
		2	3	4
Experiment 1	$\hat{\beta}$	0.5085	1.0275*	0.6502
	s.e($\hat{\beta}$)	0.2199	0.4672	0.2749
Experiment 2	$\hat{\beta}$	0.4142	0.7237	0.4513
	s.e($\hat{\beta}$)	0.1910	0.3130	0.2292

**all sheep in group became infected*

Given the experimental hypothesis, it would be expected that group 2 would exhibit the highest rate of infection, followed by group 3 and then group 4. However,

the results do not indicate this. One explanation could be that the inoculated virus does not have as much infection potential as the naturally acquired virus. This would lead to a lower force of infection acting upon group 2 individuals which is the only group that is exposed to group 1 (inoculated) infection. There is a decrease in the estimated rate of infection between groups 3 and 4 by contrast to the increasing trend visible between groups 2 and 3. It would be interesting to see what would happen if there were a greater number of groups to assess if the rate of infection would continue to fall with higher group number. Investigation of significance of trend is addressed in Chapter 6.

5.5 Summary

In this chapter a partial model of the infection process was considered where only the infectiousness periods were modelled. A gamma distribution was assumed to describe the infectiousness period and distribution parameters were estimated conditional on the observed viraemic data. The expected duration of infectiousness period given the number of viraemic days was estimated and hence the infectiousness period for each infected individual was estimated. It was observed that there was an appreciable expected unobserved infectiousness period and that this varied depending on the number of observed viraemic days. Individuals with observed viraemic period of 2 days had more than a day of the expected infectiousness period unobserved while those with 4 days of observed viraemic period have slightly over half a day of unobserved expected infectiousness period.

The expected duration of infection exposure for groups 2 to 4 was estimated and the martingale rate of infection acting upon groups 2 to 4 was estimated. The method described provides an efficient way in which to calculate those β estimates applying to different groups of animals. However, the method has a major drawback. In experiment 1, group 3 had all its members infected and as a result, the martingale estimate for the rate of infection acting upon this group is an underestimate. To correct this, the time of infection for last individual to become infected in this group needs to be estimated so that the appropriate amount of infection exposure is used in calculating the estimate for the rate of infection. Therefore before formally testing whether there is a trend in the estimates for the rate of infection, a more appropriate estimate of β in group 3 of experiment 1 is developed. This will be achieved by modelling the entire infection process (see Chapter 6).

Chapter 6

Full modelling of the infection process: martingale estimation methods

6.1 Introduction

In this chapter, the entire infection process is modelled *i.e.* for each infected individual, the time of infection, latent period and infectiousness period are all considered. Expected values for these quantities are estimated. The time to infection and the latent period are modelled using a joint distribution of the two infection process characteristics conditional on the time (day) of the first positive test (τ) for an infected individual. In Section 6.2, the distribution for the time to infection is derived from survival analysis theory and in Section 6.3, a gamma distribution is proposed for the latent period. Although these two quantities are assumed to be independent, they are modelled jointly due to a correlation in their estimates which arises from the inability to observe the nature of the pre-infectious individuals. The estimates for the expected infection process characteristics are calculated alternately with the rates of infection, β_g, acting upon groups of sheep, using an iterative procedure as discussed in Chapters 2 and 4. In this chapter, martingale based β estimates are calculated, while in Chapter 7, ML estimates are calculated for two different models of β_g.

When all individuals in a group are infected, a cumulative amount of infection is 'wasted' as there are no susceptible individuals left to infect. When this fact is ignored in determining a martingale estimate for the rate of infection for groups where all individuals became infected, the result is an underestimate for the parameter. Estimation of the expected time of infection enables allocation of the

appropriate amount of infection exposure time to the martingale estimate for groups where all individuals become infected. The process of determining estimates for the expected infection process characteristics is described in this chapter in Section 6.4. It should be stressed that this procedure remains unchanged even if the β estimates are derived using MLE methods as in Chapter 7. It is just that a different β estimation method is used in the 'maximisation step' of the iterative scheme. Calculation of martingale β estimates is described in Section 6.5. The algorithm that is used to implement the iterative scheme and to derive estimates for the expected infection process characteristics and β is outlined in Section 6.6. The aim for the FMD experiments was to assess whether FMD infection is sheep is self-limiting. With this aspect in mind, in Section 6.7, the trend in the estimated βs is assessed. For the martingale β estimates, the trend is summarised by a slope estimated using weighted linear regression. The Significance of the estimated slope is tested using bootstrap methods, based on simulated epidemic realisations. In Section 6.9, the proposed method is applied to the experimental FMD data.

6.2 Distribution of time to infection

It is vital to estimate the time at which an infected individual is expected to have made an infectious contact *i.e.* the time at which it became infected. Besides having other uses, knowledge of this quantity, is crucial for martingale based parameter estimation in groups where all sheep became infected. The time to infection is modelled from the start of the experiment (epidemic). In this section the distribution of time to infection for infected individuals is established.

Let X_1 be the time to infection and $f(x_1)$ denote its density function.
Let $S(x_1)$ be the Survivor function *i.e.* the probability that the lifetime T is at least x_1.
Then

$$S(x_1) = Pr(T \geq x_1) = \int_{x_1}^{\infty} f(u)du = 1 - \int_0^{x_1} f(u)du = 1 - F(x_1).$$

Let $h(x_1)$ denote the instantaneous force of infection at time x_1 conditional on survival to time x_1.

From survival analysis theory (Collett, 1994, Section 1.3),

$$S(x_1) = \exp\{-\int_0^{x_1} h(u)du\}.$$

Therefore the density function for X_1 is given by

$$f(x_1) = h(x_1) \exp\{-\int_0^{x_1} h(u)du\}. \tag{6.1}$$

In our case,

$$h(t) = \frac{I(t)}{n(t)}\beta, \tag{6.2}$$

where $I(t)$ is the number of active infectives at time t, $n(t)$ is the total number of individuals in a mixing group at time t, β is the rate of infection and $h(t)$ depends on β.

6.3 Distribution of latent period

It is necessary to model the latency process because for many infectious diseases including FMD, infected individuals pass through a latent state prior to becoming infectious. Proper understanding of this characteristic of the infection process can have an impact on the control policies appropriate during an outbreak of a particular infectious disease. For the FMD experimental infection, a gamma distribution with shape parameter ν_{lat} and scale parameter λ_{lat} is assumed for the latent period. The density is denoted by $g_{\nu_{lat},\lambda_{lat}}(x_2)$, where X_2 denotes the length of the latent period for an infected individual. Thus the density function is given by

$$g_{\nu_{lat},\lambda_{lat}}(x_2) = \frac{{\lambda_{lat}}^{\nu_{lat}} {x_2}^{\nu_{lat}-1} e^{-\lambda_{lat}x_2}}{\Gamma(\nu_{lat})}.$$

For a group 1 individual, suppose n_l negative tests were observed before the first positive test after inoculation. The latent period for an infected individual would be between n_l and $n_l + 1$ days *i.e.* $x_2 \in (n_l, n_l + 1)$.
Using MLE methods, estimators for parameters ν_{lat} and λ_{lat} are calculated by maximising the log-likelihood function given in Equation (6.3) below.
If $n_l < x_2 < n_l + 1$, consideration of all possible values of n_l for all infected sheep, yields a log-likelihood function given by:

$$\sum_{\text{all } n_l} (n_l \text{ freq}) \times \ln \left[\int_{n_l}^{n_l+1} \frac{{\lambda_{lat}}^{\nu_{lat}} {x_2}^{\nu_{lat}-1} e^{-\lambda_{lat}x_2}}{\Gamma(\nu_{lat})} \, dx_2 \right]. \tag{6.3}$$

The log-likelihood function is maximised using in-built routines in the S-Plus statistical package, yielding the required parameter estimates for ν_{lat} and λ_{lat}.

6.4 Estimation of entire infection process

When modelling the entire infection process for experimental FMD, two categories of individuals are considered *viz.* group 1 individuals and groups 2 to 4 individuals. Group 1 sheep were artificially infected with FMD virus at the start of the experiment. The artificial inoculation was staggered, half of group 1 sheep being inoculated on day 0, while 24 hours later the rest of the group 1 sheep were inoculated with the virus. Time $t = 0$ (day 0) is regarded as the time of infection for the first 4 group 1 sheep (ID numbers 1 to 4) and day 1 as the time of infection for the other 4 group 1 sheep (ID numbers 5 to 8). Thus the time of infection for group 1 individuals is known. For these individuals therefore, the aim is to determine estimates for their expected length of latent and infectiousness periods. For groups 2, 3, and 4, there is no explicit information about their time to infection or latent period, all that is observed is the time at which any infected sheep tested positive to FMD virus. Therefore for infected sheep in these groups, the aim is to estimate the expected time of infection, expected latent period and expected infectiousness period. The expected infectiousness period for infected sheep from all groups is estimated as in Section 5.2.2.

6.4.1 Infection process for group 1 sheep

For group 1 sheep the time of infection is assumed to be known, based on the inoculation times. Thus only the latent and infectiousness periods for these sheep require to be estimated.

6.4.1.1 Estimation of expected latent period

Let T_L be the latent period with density given by

$$f(t_L) = \frac{{\lambda_{lat}}^{\nu_{lat}} {t_L}^{\nu_{lat}-1} e^{-\lambda_{lat} t_L}}{\Gamma(\nu_{lat})}. \tag{6.4}$$

If n_l negative tests were observed before τ then $t_L \in (n_l, n_l+1)$ *i.e.* if an individual tested negative n_l times (on n_l days), then the length of the latent period is between n_l and $n_l + 1$ days. In both experiments, group 1 sheep tested negative for either 1 day after inoculation or never tested negative after inoculation, before the first positive test was observed. So n_l takes values 0 and 1 only, implying that the length of the latent period is between 0 and 2 days. The expected length of

the latent period is therefore calculated conditional on the number of negative observed tests, n_l.

After rescaling $f(t_L)$ in Equation (6.4), the conditional density of T_L given n_l is given by:

$$\begin{aligned} f(t_L|n_l) &= \frac{f(t_L)}{\int_{n_l}^{n_l+1} f(t_L)dt_L} \qquad\qquad n_l < t_L < n_l + 1 \\ &= \frac{\frac{{\lambda_{lat}}^{\nu_{lat}}}{\Gamma(\nu_{lat})} {t_L}^{\nu_{lat}-1} e^{-\lambda_{lat} t_L}}{\int_{n_l}^{n_l+1} \frac{{\lambda_{lat}}^{\nu_{lat}}}{\Gamma(\nu_{lat})} {t_L}^{\nu_{lat}-1} e^{-\lambda_{lat} t_L}\, dt_L}. \end{aligned}$$

Thus the expected latent period conditional on n_l is given by:

$$E[T_L|n_l] = \frac{\int_{n_l}^{n_l+1} t_L f(t_L)dt_L}{\int_{n_l}^{n_l+1} f(t_L)dt_L}. \tag{6.5}$$

Once $\hat{\lambda}_{lat}$ and $\hat{\nu}_{lat}$ have been estimated, estimates for the expected latent period for each sheep in the group will be calculated depending on whether the sheep had 0 or 1 negative tests observed prior to testing positive.

6.4.1.2 Estimation of expected infectiousness period

In Chapter 5, it was assumed that infectiousness started randomly some time between day $\tau - 1$ and day τ (τ is the day of the first observed positive test) and that infectiousness ceased between day ω and day $\omega + 1$ (ω is the day of the last observed positive test). However, with time of infection known and estimates for the expected length of latent period obtained, the expected time when infectiousness started can be estimated. Based on the assumed distribution for the infectiousness process, the expected length of the infectiousness period conditional on n_e, the number of observed positive test results and the expected start of infectiousness is estimated. It is known that the latent period ends sometime between day $\tau - 1$ and day τ. If the unobserved infectiousness period before τ is denoted by T_τ and the time of end of latency (start of infectiousness) by z, then T_τ is equal to $\tau - z$. Thus the length of the infectiousness period, denoted by t_I, ranges between the observed period plus T_τ and observed period plus T_τ plus 1 day of unobserved potential infectiousness period after ω, *i.e.*

$$\begin{aligned} & n_e - 1 + T_\tau < t_I < n_e - 1 + T_\tau + 1 \\ \Longrightarrow\ & n_e - 1 + T_\tau < t_I < n_e + T_\tau. \end{aligned}$$

The process is illustrated in Figure 6.1.

Figure 6.1: *Figure to illustrate the infection process.*

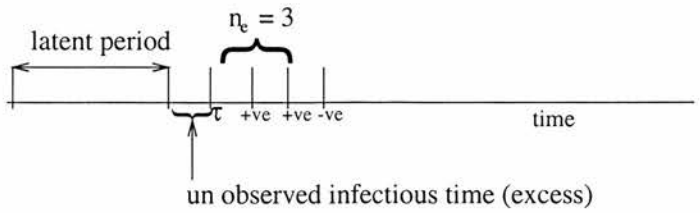

Let T_I denote the length of infectiousness period. The unconditional random variable T_I is gamma distributed with shape parameter ν_{inf} and scale parameter λ_{inf} with density function given by

$$f_{\nu_{inf},\lambda_{inf}}(t_I) = \frac{{\lambda_{inf}}^{\nu_{inf}} \; {t_I}^{\nu_{inf}-1} e^{-\lambda_{inf} t_I}}{\Gamma(\nu_{inf})}.$$

Estimation of the length of infectiousness period is described in Section 5.2.2 and estimation of parameters ν_{inf} and λ_{inf} is described in Section 5.2.1.

The rescaled density function for T_I conditional on the observed data and T_τ is given by:

$$\frac{f(t_I)}{\int f(t_I)dt_I}, \quad n_e - 1 + T_\tau \; < \; t_I \; < \; n_e + T_\tau$$

and hence the expected infectiousness period for an infected individual given that it had n_l negative tested days followed by n_e positive tested days is given by

$$E[T_I|n_e, n_l] = \frac{\int_{n_e-1+T_\tau}^{n_e+T_\tau} t_I f(t_I)dt_I}{\int_{n_e-1+T_\tau}^{n_e+T_\tau} f(t_I)dt_I}. \tag{6.6}$$

Comparing Equation (6.6) with Equation (5.2), one can observe the effect of assuming a random start of infectiousness or of having a known start of infectiousness on the nature of the expression for the expected infectiousness period. In Equation (5.2), the expected infectiousness period depends on whether t_I lies between $n_e - 1$ and n_e or between n_e and $n_e + 1$, however, in Equation (6.6), it is known that t_I lies between $n_e - 1 + T_\tau$ and $n_e + T_\tau$. In practice, T_τ is estimated using $\tau - E[T_L|n_l]$ and n_e is observed. From these data and the estimated density for the infectious period, the expected infectiousness periods for each infected group 1 sheep can be estimated. Group 1 sheep will then each have a complete set of estimates of the unobserved quantities which define the effect of the infection process on each individual. The contribution of these sheep to group 2 total expected infection exposure can then be determined.

6.4.2 Infection process for group 2 to 4 sheep

For groups 2 to 4 the expected time to infection, expected length of latent periods and expected length of infectiousness period need to be estimated for all infected sheep. The expected time to infection and the expected latent period are estimated from the joint distribution of these two infection process characteristics, conditional on τ. The time period from the start of the experiment to the time of infection for each infected sheep, is partitioned into intervals of constant force of infection (hazard), $h(t)$. The partitions are based on changes in hazard arising from changes in the number of infectives (new infections and removals) and also from the mixing patterns which change on a daily basis (every 24 hours). The maximum range for any interval is therefore 1 day (24 hours). Once the partitions are identified, estimates for the expected time of infection, x_1, and expected latent period, x_2, are obtained by summing the components over all possible partitions. Figure 6.2 demonstrates the partitioning.

Figure 6.2: *Sketch of partitioned time scale, where t_T is the time of the most recent change in $h(t)$ prior to the time of infection x_1.*

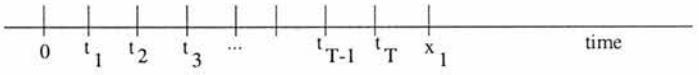

For any arbitrary time point t, between t_i and t_{i+1}, a partitioned interval, the force of infection $h(t)$ is given by:

$$h(t) = \frac{\beta I_i}{n(t)} = h(t_i).$$

which is the instantaneous hazard at time t_i.
I_i is the number of active infectious individuals in interval $[t_i, t_{i+1})$, which is equal to the number of infectious individuals at the start of this interval of time, t_i.
The density for the time to infection X_1 can be given in terms of the hazard in each partitioned interval up to time x_1. The density $f(x_1)$, as given in Equation (6.1), expressed in terms of these intervals becomes

$$\begin{aligned} f(x_1) &= h(x_1)\, \exp\{-\int_0^{x_1} h(u)du\} \\ &= h(x_1)\, \exp\left[-\int_0^{t_1} h(u)du - \int_{t_1}^{t_2} h(u)du - \ldots - \int_{t_{T-1}}^{t_T} h(u)du -\right. \end{aligned}$$

$$\int_{t_T}^{x_1} h(u)du\Big]$$

$$= h(x_1)\exp\{-\int_0^{t_1} h(u)du\}\exp\{-\int_{t_1}^{t_2} h(u)du\}\ldots\exp\{-\int_{t_{T-1}}^{t_T} h(u)du\}\times$$
$$\exp\{-\int_{t_T}^{x_1} h(u)du\}.$$

The hazard at time x_1, $h(x_1)$, is the hazard that has given rise to a new infection whose time of infection is x_1. This is the hazard in interval $[t_T, x_1)$ given by $h(t_T)$. Thus $h(x_1) = h(t_T)$ and $h(t_T)$ will be denoted by h_T for ease of notation. The expression for $f(x_1)$ becomes:

$$\begin{aligned} f(x_1) &= h(t_T)\exp\{-h(0)(t_1-0)\}\exp\{-h(t_1)(t_2-t_1)\}\times\ldots\times \\ &\qquad \exp\{-h(t_{T-1})(t_T-t_{T-1})\}\exp\{-h(t_T)(x_1-t_T)\} \\ &= h_T\exp\left(\sum_{i=0}^{T-1} -h_i\times(t_{i+1}-t_i)+h_T t_T\right)\exp\{-h_T x_1\}. \end{aligned} \tag{6.7}$$

6.4.2.1 Joint distribution of the time to infection, X_1 and the latent period, X_2

Preliminary investigations showed that modelling the time to infection without taking into account the latent period produced very unrealistic estimates of the times of infection. The time of infection converged toward the first exposure time for each individual. The two processes are therefore modelled jointly. A joint distribution of the time to infection and the latent period, conditional on the time of the first observed positive test for an infected individual is considered. Figure 6.3 is a sketch of the infection process from the start of the experiment *i.e.* time 0.

Figure 6.3: *Sketch of infection process.*

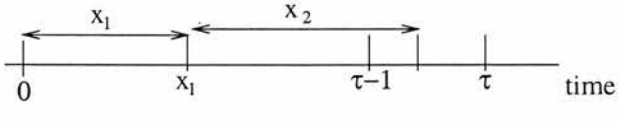

The time to infection (X_1) and latent period (X_2) are assumed to be independent *i.e.* the length of the latent period for an infected individual is not affected by the time taken for the individual to be infected. However, as pointed out earlier, the inability to observe the nature of the pre-infectious individuals creates a correlation in any estimates of the two infection process characteristics. Thus

the two quantities are modelled jointly. A joint distribution of X_1 and X_2 based on partitioned intervals of constant force of infection is formulated below.

Let $f(x_1, x_2)$ denote the joint distribution of X_1 and X_2, then

$$\begin{aligned}
f(x_1,x_2) &\propto f(x_1)g(x_2) \\
&= h(x_1)\exp\{-\int_0^{x_1} h(u)du\}\frac{{\lambda_{lat}}^{\nu_{lat}}{x_2}^{\nu_{lat}-1}e^{-\lambda_{lat}x_2}}{\Gamma(\nu_{lat})} \\
&\propto h(x_1)\exp\{-\int_0^{x_1} h(u)du\}{x_2}^{\nu_{lat}-1}e^{-\lambda_{lat}x_2} \\
&= h(x_1)\exp\{-\int_0^{t_1} h(u)du - \int_{t_1}^{t_2} h(u)du - \ldots \\
&\qquad\qquad - \int_{t_T}^{x_1} h(u)du - \lambda_{lat}x_2\}{x_2}^{\nu_{lat}-1} \\
&= h(x_1)\exp\{-\sum_{i=0}^{T-1} h_i \times (t_{i+1}-t_i) - h_T\,(x_1 - t_T) - \lambda_{lat}x_2\}{x_2}^{\nu_{lat}-1} \\
&= h_T\,\exp\{-\sum_{i=0}^{T-1} h_i\,(t_{i+1}-t_i) + h_T t_T\}e^{-h_T x_1}e^{-\lambda_{lat}x_2}{x_2}^{\nu_{lat}-1}. \qquad (6.8)
\end{aligned}$$

Let $\Lambda = h_T\,\exp\{-\sum_{i=0}^{T-1} h_i\,(t_{i+1}-t_i) + h_T t_T\}$, which does depend on x_1, since T is defined as the initial time of the ultimate infection partition before time x_1.

Then $f(x_1, x_2) \propto f(x_1)g(x_2) = \Lambda e^{-h_T x_1}e^{-\lambda_{lat}x_2}{x_2}^{\nu_{lat}-1}$.

After rescaling,

$$f(x_1,x_2) = \frac{\Lambda\; e^{-h_T x_1}\; e^{-\lambda_{lat}x_2}\; {x_2}^{\nu_{lat}-1}}{\iint\; \Lambda\; e^{-h_T x_1}\; e^{-\lambda_{lat}x_2}\; {x_2}^{\nu_{lat}-1}\; dx_1 dx_2}. \qquad (6.9)$$

The range of values of x_1 and x_2, and hence the domain of integration, are discussed in the next section.

6.4.2.2 Estimation of expected time to infection and length of latent period

The expected values for X_1 and X_2 are estimated from the joint distribution formulated above. Integrating with respect to x_1 first, the expected values are given by:

$$\begin{aligned}
E[X_i] &= \iint x_i f(x_1,x_2)\;\; dx_1 dx_2\;, \qquad i = 1,2 \\
&= \frac{\iint x_i\;\Lambda\; e^{-h_T x_1}\; e^{-\lambda_{lat}x_2}\; {x_2}^{\nu_{lat}-1}\; dx_1 dx_2}{\iint\; \Lambda\; e^{-h_T x_1}\; e^{-\lambda_{lat}x_2}\; {x_2}^{\nu_{lat}-1}\; dx_1 dx_2}. \qquad (6.10)
\end{aligned}$$

The domain of integration for the double integrals in the probability density function in Equation (6.9) and for expectations in Equation (6.10) needs to be determined. The time to infection, x_1, for an infected individual can take any value between 0 and τ and the latent period x_2 can take any non-negative value between $\tau - 1 - x_1$ and $\tau - x_1$ *i.e.* infection could have taken place at any time between the start of exposure to infection (a long latency) and a time just before τ (a short latency). hence, the length of latent period can be very close to $\tau - x_1$ *i.e.* a long latent period with infectiousness starting just before τ, or very close to $\tau - 1 - x_1$ *i.e.* a short latent period with infectiousness starting just after day $\tau - 1$, the day prior to the first positive test, implying that infectiousness started in the early hours of sampling day $\tau - 1$. The length of latent period has to be non-negative and greater than $\tau - 1 - x_1$, otherwise a positive test would have been obtained on day $\tau - 1$ but the latent period would not be longer than $\tau - x_1$ since otherwise the test on day τ should have been negative. In summary, $0 < x_1 < \tau$ and $\max\{0, \tau - 1 - x_1\} < x_2 < \tau - x_1$. It is assumed that a positive test which indicates presence of live virus implies that the individual is in an infectious state (able to infect others).

Since the time between the start of experiment ($t = 0$) and the time of infection for an infected sheep ($t = x_1$) is partitioned into intervals of constant hazard, the domain of integration is constructed in terms of these partitioned intervals.

Consider an arbitrary time interval (t_T, t) with range less than or equal to 1 day. From the design of the experiment, the maximum range for any partitioned interval is 1 day. Movement of sheep between groups is considered to be an event starting a new interval. Thus in situations where no new infection or removal has occurred over 2 days, the only event is the change of mixing groups which happens on a daily basis.

Considering an infected individual which first tested positive at time τ, assume that its time to infection lies somewhere between time t_T and time t, and then its latent period can take any value between the maximum of 0 and $\tau - 1 - t$ at one extreme and $\tau - t_T$ at the other. That is, if $t_T < x_1 < t$, with $t - t_T \leq 1$, then $\max\{0, \tau - 1 - t\} < x_2 < \tau - t_T$. Figure 6.4 gives a graphical representation of the region of interest over which we have to integrate. The region of integration is divided into 3 parts labelled Area 1, Area 2 and Area 3. The domain of integration for each area is given in Equation (6.11).

	Domain for x_1		Domain for x_2
Area 1 :	$\tau - 1 - x_2 < x_1 < t$	;	$\max\{0, \tau - 1 - t\} < x_2 < \max\{0, \tau - 1 - t_T\}$
Area 2 :	$t_T < x_1 < t$	;	$\max\{0, \tau - 1 - t_T\} < x_2 < \tau - t$
Area 3 :	$t_T < x_1 < \tau - x_2$	;	$\tau - t < x_2 < \tau - t_T$. (6.11)

Figure 6.4: *Sketch of the region of integration for interval* (t_T, t).

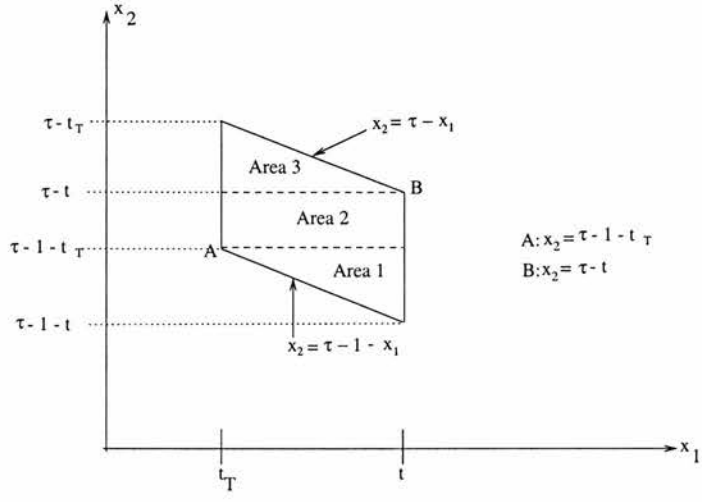

For a given interval (t_T, t), the appropriate domain of integration for each of the 3 parts is obtained. The integral of the joint distribution in interval (t_T, t) is then given by

$$\int\int_{\Omega(t_T,t)} f(x_1, x_2)\, dx_1 dx_2 = \int_{\max\{0,\tau-1-t_T\}}^{\max\{0,\tau-1-t\}} \int_{\tau-1-x_2}^{t} f(x_1, x_2) dx_1 dx_2 +$$

$$\int_{\max\{0,\tau-1-t_T\}}^{\tau-t} \int_{t_T}^{t} f(x_1, x_2)\, dx_1 dx_2 + \int_{\tau-t}^{\tau-t_T} \int_{t_T}^{\tau-x_2} f(x_1, x_2)\, dx_1 dx_2, \quad (6.12)$$

where $f(x_1, x_2)$ is as in Equation (6.9) and $\Omega(t_T, t) \equiv \begin{cases} x_1 \in (t_T, t) \\ x_1 + x_2 \in (\tau - 1, \tau) \end{cases}$.
The 3 double integrals in Equation (6.12) will be referred to as integrals 1 to 3 over areas 1 to 3 respectively.

To evaluate the integral of the joint distribution between the start of the epidemic experiment on day 0 and day τ for a given infected individual, all integrals over the partitioned intervals are summed.

Let $\Omega(t_i, t_j) \equiv \begin{cases} x_1 \in (t_i, t_j) \\ x_1 + x_2 \in (\tau - 1, \tau) \end{cases}$,

then

$$\int\int_{\Omega(0,\tau)} f(x_1,x_2)\,dx_1dx_2 \;=\; \int\int_{\Omega(0,t_1)} f(x_1,x_2)\,dx_1dx_2 \;+$$

$$\int\int_{\Omega(t_1,t_2)} f(x_1,x_2)\,dx_1dx_2 \;+\ldots+\int\int_{\Omega(t_T,\tau)} f(x_1,x_2)\,dx_1dx_2. \tag{6.13}$$

Each double integral in Equation (6.13), for a partioned interval, is composed of 3 double integrals as in Equation (6.12) for the different domains of integration. For instance for interval $(0,t_1)$, where $t_1<\tau$, $t_T\equiv 0$, and $t\equiv t_1$. Thus the limits for the 3 regions for this partitioned interval are:
for Area 1: $\tau-1-x_2<x_1<t_1$ and $\max\{0,\tau-1-t_1\}<x_2<\tau-1-0$
for Area 2: $0<x_1<t_1$ and $\tau-1-0<x_2<\tau-t_1$
for Area 3: $0<x_1<\tau-x_2$ and $\tau-t_1<x_2<\tau-0$.

The expression for the expected values of X_1 and X_2 in Equation (6.10) is then given by

$$E[X_i]=\frac{N(x_i)}{D(x_i)},\quad i\;=\;1,\;2 \tag{6.14}$$

where

$$N(x_i)\;=\;\int\int_{\Omega(0,t_1)} x_i\,k(x_1,x_2)\,dx_1dx_2\;+\;\int\int_{\Omega(t_1,t_2)} x_i\,k(x_1,x_2)\,dx_1dx_2\;+\ldots+$$

$$\int\int_{\Omega(t_T,\tau)} x_i\,k(x_1,x_2)\,dx_1dx_2,$$

$$D(x_i)\;=\;\int\int_{\Omega(0,t_1)} k(x_1,x_2)\,dx_1dx_2\;+\;\int\int_{\Omega(t_1,t_2)} k(x_1,x_2)\,dx_1dx_2\;+\ldots+$$

$$\int\int_{\Omega(t_T,\tau)} k(x_1,x_2)\,dx_1dx_2,$$

and $k(x_1,x_2)=\Lambda\;e^{-h_Tx_1}\;e^{-\lambda_{lat}x_2}\;{x_2}^{\nu_{lat}-1}$.

Each of the 3 integrals 1 to 3 in Equation (6.12) representing the integrals over the 3 areas 1 to 3 is considered separately. Also the denominator and numerator in Equation (6.10) are considered separately for each integral in Equation (6.12) for a given partitioned interval (t_T,t).
Note that the denominator is the same in the expression for the expected time to infection and the expected latent period, only the numerator differs.

6.4.2.3 Expected time to infection, $E[X_1]$

The 3 areas 1 to 3 as outlined in Equation (6.11) are considered separately. Note that for ease of notation, h_T is denoted by h in the expression for the joint distribution and $\tau-1-t_j$ will be used to denote $\max\{0, \tau-1-t_j\}$, where $t_j = t$ or t_τ or x_2.

Numerator integral 1 (for area 1)
In a given interval (t_T, t), the contribution of integral 1 to the numerator $N(x_1)$ of the expected value of X_1, denoted by N_{11} is:

$$\begin{aligned}
N_{11} &= \int_{\tau-1-t}^{\tau-1-t_T} \int_{\tau-1-x_2}^{t} x_1\ \Lambda\ e^{-hx_1}\ e^{-\lambda_{lat}x_2}\ {x_2}^{\nu_{lat}-1}\, dx_1 dx_2 \\
&= \Lambda \int_{\tau-1-t}^{\tau-1-t_T} e^{-\lambda_{lat}x_2}\ {x_2}^{\nu_{lat}-1} \left[\frac{-h\ x_1\ e^{-hx_1} - e^{-hx_1}}{h^2}\right]_{\tau-1-x_2}^{t} dx_2 \\
&= \frac{\Lambda}{h^2}\Big\{-(ht+1)e^{-ht}\int_{\tau-1-t}^{\tau-1-t_T} e^{-\lambda_{lat}x_2}\ {x_2}^{\nu_{lat}-1} dx_2 \\
&\quad + (h(\tau-1)+1)\, e^{-h(\tau-1)}\int_{\tau-1-t}^{\tau-1-t_T} {x_2}^{\nu_{lat}-1} e^{-(\lambda_{lat}-h)x_2}\, dx_2 \\
&\quad - he^{-h(\tau-1)}\int_{\tau-1-t}^{\tau-1-t_T} {x_2}^{\nu_{lat}} e^{-(\lambda_{lat}-h)x_2}\, dx_2\Big\}, \qquad (6.15)
\end{aligned}$$

since Λ is a constant with respect to x_1 in the domain, it is taken outside the integral. This is true for all intergals in this section.

The expression for N_{11} in Equation (6.15) is composed of integrals of gamma densities.

Let $\mathrm{F}_\gamma(t; \nu_{lat}, \lambda_{lat})$ denote the cumulative distribution function up to time t, of a random variable which is gamma distributed with shape parameter ν_{lat} and scale parameter λ_{lat}, *i.e.*

$$\begin{aligned}
\mathrm{F}_\gamma(t; \nu_{lat}, \lambda_{lat}) &= \int_0^t \frac{{\lambda_{lat}}^{\nu_{lat}}}{\Gamma(\nu_{lat})}\, {x_2}^{\nu_{lat}-1}\, e^{-\lambda_{lat}x_2}\, dx_2 \\
\implies \int_0^t {x_2}^{\nu_{lat}-1}\, e^{-\lambda_{lat}x_2}\, dx_2 &= \frac{\Gamma(\nu_{lat})}{{\lambda_{lat}}^{\nu_{lat}}}\, \mathrm{F}_\gamma(t; \nu_{lat}, \lambda_{lat}). \qquad (6.16)
\end{aligned}$$

Substituting the integrals with the equivalent gamma cumulative distribution functions, Equation (6.15) becomes:

$$\begin{aligned}
N_{11} = -\frac{\Lambda(ht+1)e^{-ht}}{h^2}\frac{\Gamma(\nu_{lat})}{{\lambda_{lat}}^{\nu_{lat}}} \times \{&\mathrm{F}_\gamma(\tau-1-t_T; \nu_{lat}, \lambda_{lat}) - \\
&\mathrm{F}_\gamma(\tau-1-t; \nu_{lat}, \lambda_{lat})\}
\end{aligned}$$

$$+ \frac{\Lambda[h(\tau-1)+1]e^{-h(\tau-1)}\Gamma(\nu_{lat})}{h^2(\lambda_{lat}-h)^{\nu_{lat}}} \times \{\mathrm{F}_\gamma(\tau-1-t_T;\nu_{lat},\lambda_{lat}-h) - \mathrm{F}_\gamma(\tau-1-t;\nu_{lat},\lambda_{lat}-h)\}$$

$$- \frac{\Lambda h e^{-h(\tau-1)}}{h^2}\frac{\Gamma(\nu_{lat}+1)}{(\lambda_{lat}-h)^{\nu_{lat}+1}} \times \{\mathrm{F}_\gamma(\tau-1-t_T;\nu_{lat}+1,\lambda_{lat}-h) - \mathrm{F}_\gamma(\tau-1-t;\nu_{lat}+1,\lambda_{lat}-h)\}. \tag{6.17}$$

Numerator integral 2 (for area 2)

In a given interval (t_T, t), the contribution of integral 2 to the numerator $N(x_1)$ of the expected value of X_1, denoted by N_{12}, is:

$$\begin{aligned} N_{12} &= \int_{\tau-1-t_T}^{\tau-t}\int_{t_T}^{t} x_1\ \Lambda\ e^{-hx_1}\ e^{-\lambda_{lat}x_2}\ {x_2}^{\nu_{lat}-1}\ dx_1dx_2 \\ &= \Lambda\int_{\tau-1-t_T}^{\tau-t} e^{-\lambda_{lat}x_2}\ {x_2}^{\nu_{lat}-1}\left[\frac{-h\ x_1\ e^{-hx_1}-e^{-hx_1}}{h^2}\right]_{t_T}^{t} dx_2 \\ &= \frac{\Lambda}{h^2}\left\{(ht_T+1)\ e^{-ht_T}-(ht+1)\ e^{-ht}\right\}\int_{\tau-1-t_T}^{\tau-t} {x_2}^{\nu_{lat}-1}\ e^{-\lambda_{lat}x_2}dx_2. \end{aligned} \tag{6.18}$$

Substituting the integral with the equivalent gamma cumulative distribution function, Equation (6.18) becomes:

$$\begin{aligned} N_{12} &= \frac{\Lambda}{h^2}\left\{\ (ht_T+1)\ e^{-ht_T}-(ht+1)\ e^{-ht}\ \right\}\frac{\Gamma(\nu_{lat})}{{\lambda_{lat}}^{\nu_{lat}}}\times \\ &\quad \{\ \mathrm{F}_\gamma(\tau-t;\nu_{lat},\lambda_{lat})-\mathrm{F}_\gamma(\tau-1-t_T;\nu_{lat},\lambda_{lat})\ \}. \end{aligned} \tag{6.19}$$

Numerator integral 3 (for area 3)

In a given interval (t_T, t), the contribution of integral 3 to the numerator $N(x_1)$ of the expected value of X_1, denoted by N_{13}, is:

$$\begin{aligned} N_{13} &= \int_{\tau-t}^{\tau-t_T}\int_{t_T}^{\tau-x_2} x_1\ \Lambda\ e^{-hx_1}\ e^{-\lambda_{lat}x_2}\ {x_2}^{\nu_{lat}-1}\ dx_1dx_2 \\ &= \Lambda\int_{\tau-t}^{\tau-t_T} e^{-\lambda_{lat}x_2}\ {x_2}^{\nu_{lat}-1}\left[\frac{-h\ x_1\ e^{-hx_1}-e^{-hx_1}}{h^2}\right]_{t_T}^{\tau-x_2} dx_2 \\ &= \frac{\Lambda}{h^2}\Big\{\ (ht_T+1)\ e^{-ht}\int_{\tau-t}^{\tau-t_T} {x_2}^{\nu_{lat}-1}\ e^{-\lambda_{lat}x_2}dx_2 \\ &\quad -\ (h\tau+1)\ e^{-h\tau}\int_{\tau-t}^{\tau-t_T} {x_2}^{\nu_{lat}-1}\ e^{-(\lambda_{lat}-h)x_2}\ dx_2 \\ &\quad +\ h\ e^{-h\tau}\int_{\tau-t}^{\tau-t_T} {x_2}^{\nu_{lat}}\ e^{-(\lambda_{lat}-h)x_2}\ dx_2\Big\}. \end{aligned} \tag{6.20}$$

Integrals in the expression for N_{13} in Equation (6.20) are integrals of gamma densities. Substituting the integrals with the equivalent gamma cumulative distribution functions, Equation (6.20) becomes:

$$\begin{aligned} N_{13} = & \frac{\Lambda(ht_T+1)\ e^{-ht}}{h^2}\ \frac{\Gamma(\nu_{lat})}{{\lambda_{lat}}^{\nu_{lat}}} \times \{\mathrm{F}_\gamma(\tau - t_T; \nu_{lat}, \lambda_{lat}) - \mathrm{F}_\gamma(\tau - t; \nu_{lat}, \lambda_{lat})\} \\ & - \frac{\Lambda\ (h\tau+1)\ e^{-h\tau}}{h^2}\ \frac{\Gamma(\nu_{lat})}{(\lambda_{lat}-h)^{\nu_{lat}}} \times \{\mathrm{F}_\gamma(\tau - t_T; \nu_{lat}, \lambda_{lat} - h) - \\ & \qquad \mathrm{F}_\gamma(\tau - t; \nu_{lat}, \lambda_{lat} - h)\} \\ & + \frac{\Lambda\ h\ e^{-h\tau}}{h^2} \frac{\Gamma(\nu_{lat}+1)}{(\lambda_{lat}-h)^{\nu_{lat}+1}} \times \{\mathrm{F}_\gamma(\tau - t_T; \nu_{lat}+1, \lambda_{lat} - h) - \\ & \qquad \mathrm{F}_\gamma(\tau - t; \nu_{lat}+1, \lambda_{lat} - h)\}\,. \end{aligned} \tag{6.21}$$

Denominator integral 1 (for area 1)

In a given interval (t_T, t), the contribution of integral 1 to the numerator $D(x_1)$ of the expected value of X_1, denoted by D_1 is:

$$\begin{aligned} D_1 &= \int_{\tau-1-t}^{\tau-1-t_T} \int_{\tau-1-x_2}^{t} \Lambda\ e^{-hx_1}\ e^{-\lambda_{lat}x_2}\ {x_2}^{\nu_{lat}-1}\ dx_1 dx_2 \\ &= \Lambda \int_{\tau-1-t}^{\tau-1-t_T} {x_2}^{\nu_{lat}-1}\ e^{-\lambda_{lat}x_2} \left[\frac{-e^{-hx_1}}{h}\right]_{\tau-1-x_2}^{t} dx_2 \\ &= \frac{\Lambda}{h}\Big\{ e^{-h(\tau-1)} \int_{\tau-1-t}^{\tau-1-t_T} {x_2}^{\nu_{lat}-1}\ e^{-(\lambda_{lat}-h)x_2}\ dx_2 \\ &\qquad - e^{-ht} \int_{\tau-1-t}^{\tau-1-t_T} {x_2}^{\nu_{lat}-1}\ e^{-\lambda_{lat}x_2}\ dx_2 \Big\}\,. \end{aligned} \tag{6.22}$$

The expression for D_1 in Equation (6.22) is composed of integrals of gamma densities. Replacing the integral functions with the equivalent expression in terms of the gamma cumulative distribution function, Equation (6.22) becomes:

$$\begin{aligned} D_1 &= \frac{\Lambda e^{-h(\tau-1)}}{h}\ \frac{\Gamma(\nu_{lat})}{(\lambda_{lat}-h)^{\nu_{lat}}} \times \{\mathrm{F}_\gamma(\tau - 1 - t_T; \nu_{lat}, \lambda_{lat} - h) - \\ &\qquad \mathrm{F}_\gamma(\tau - 1 - t; \nu_{lat}, \lambda_{lat} - h)\} \\ &\quad - \frac{\Lambda e^{-ht}}{h}\ \frac{\Gamma(\nu_{lat})}{{\lambda_{lat}}^{\nu_{lat}}} \times \{\mathrm{F}_\gamma(\tau - 1 - t_T; \nu_{lat}, \lambda_{lat}) - \mathrm{F}_\gamma(\tau - 1 - t; \nu_{lat}, \lambda_{lat})\}\,. \end{aligned} \tag{6.23}$$

Denominator integral 2 (for area 2)

In a given interval (t_T, t), the contribution of integral 2 to the numerator $D(x_1)$ of the expected value of X_1, denoted by D_2 is:

$$D_2 = \int_{\tau-1-t_T}^{\tau-t} \int_{t_T}^{t} \Lambda\ e^{-hx_1}\ e^{-\lambda_{lat}x_2}\ {x_2}^{\nu_{lat}-1}\ dx_1 dx_2$$

$$= \Lambda \int_{\tau-1-t_T}^{\tau-t} e^{-\lambda_{lat}x_2}\, {x_2}^{\nu_{lat}-1} \left[\frac{-e^{-hx_1}}{h}\right]_{t_T}^{t} dx_2$$

$$= \frac{\Lambda}{h}\left\{e^{-ht_T} - e^{-ht}\right\} \int_{\tau-1-t_T}^{\tau-t} {x_2}^{\nu_{lat}-1}\, e^{-\lambda_{lat}x_2} dx_2. \qquad (6.24)$$

The integral in the expression for D_2 in Equation (6.24) is an integral of a gamma density. Replacing the integral by the equivalent cumulative distribution function, Equation (6.24) becomes:

$$D_2 = \frac{\Lambda}{h}\left\{e^{-ht_T} - e^{-ht}\right\} \frac{\Gamma(\nu_{lat})}{{\lambda_{lat}}^{\nu_{lat}}} \times \left\{\mathrm{F}_\gamma(\tau - t; \nu_{lat}, \lambda_{lat}) - \mathrm{F}_\gamma(\tau - 1 - t_T; \nu_{lat}, \lambda_{lat})\right\}. \qquad (6.25)$$

Denominator integral 3 (for area 3)

In a given interval (t_T, t), the contribution of integral 3 to the numerator $D(x_1)$ of the expected value of X_1, denoted by D_3, is:

$$D_3 = \int_{\tau-t}^{\tau-t_T} \int_{t_T}^{\tau-x_2} \Lambda\, e^{-hx_1}\, e^{-\lambda_{lat}x_2}\, {x_2}^{\nu_{lat}-1}\, dx_1 dx_2$$

$$= \Lambda \int_{\tau-t}^{\tau-t_T} {x_2}^{\nu_{lat}-1}\, e^{-\lambda_{lat}x_2} \left[\frac{-e^{-hx_1}}{h}\right]_{t_T}^{\tau-x_2} dx_2$$

$$= \frac{\Lambda}{h}\Bigg\{ e^{-ht_T} \int_{\tau-t}^{\tau-t_T} {x_2}^{\nu_{lat}-1}\, e^{-\lambda_{lat}x_2}\, dx_2 - e^{-h\tau} \int_{\tau-t}^{\tau-t_T} {x_2}^{\nu_{lat}-1}\, e^{-(\lambda_{lat}-h)x_2}\, dx_2 \Bigg\}. \qquad (6.26)$$

Replacing the integrals by the equivalent gamma cumulative distribution functions, Equation (6.26) becomes:

$$D_3 = \frac{\Lambda e^{-ht_T}}{h} \frac{\Gamma(\nu_{lat})}{{\lambda_{lat}}^{\nu_{lat}}} \times \left\{\mathrm{F}_\gamma(\tau - t_T; \nu_{lat}, \lambda_{lat}) - \mathrm{F}_\gamma(\tau - t; \nu_{lat}, \lambda_{lat})\right\}$$
$$- \frac{\Lambda e^{-h\tau}}{h} \frac{\Gamma(\nu_{lat})}{(\lambda_{lat} - h)^{\nu_{lat}}} \times \left\{\mathrm{F}_\gamma(\tau - t_T; \nu_{lat}, \lambda_{lat} - h) - \mathrm{F}_\gamma(\tau - t; \nu_{lat}, \lambda_{lat} - h)\right\}. \qquad (6.27)$$

The denominator and numerator integrals for each partitioned interval for the 3 areas are summed over all of the intervals and the expression for calculating the expected time to infection is given by:

$$E[X_1] = \frac{\sum_{\text{all intervals } i} N_{11}(i) + N_{12}(i) + N_{13}(i)}{\sum_{\text{all intervals } i} D_1(i) + D_2(i) + D_3(i)}, \qquad (6.28)$$

where i is any interval $(t_i,\ t_{i+1})$ in $(0, \tau)$.

6.4.2.4 Expected latent period, $E[X_2]$

The denominator in the expression for calculating the expected value of the latent period is the same as that in the expression for calculating the expected value of the time to infection which is given by:

$$\sum_{\text{all intervals } i} D_1(i) + D_2(i) + D_3(i).$$

The numerator in the expression for calculating the expected value of the latent period is calculated in a similar way to the expectation of time to infection by considering the 3 areas, 1 to 3, as outlined in Equation (6.11), separately.

Numerator integral 1 (for area 1)

In a given interval (t_T, t), the contribution of integral 1 to the numerator $N(x_2)$ of the expected value of X_2, denoted by N_{21}, is:

$$\begin{aligned}
N_{21} &= \int_{\tau-1-t}^{\tau-1-t_T} \int_{\tau-1-x_2}^{t} x_2 \, \Lambda \, e^{-hx_1} \, e^{-\lambda_{lat} x_2} \, {x_2}^{\nu_{lat}-1} \, dx_1 dx_2 \\
&= \Lambda \int_{\tau-1-t}^{\tau-1-t_T} {x_2}^{\nu_{lat}} e^{-\lambda_{lat} x_2} \left[\frac{-e^{-hx_1}}{h} \right]_{\tau-1-x_2}^{t} dx_2 \\
&= \frac{\Lambda}{h} \left\{ e^{-h(\tau-1)} \int_{\tau-1-t}^{\tau-1-t_T} {x_2}^{\nu_{lat}} e^{-(\lambda_{lat}-h)x_2} dx_2 \right. \\
&\qquad \left. - \, e^{-ht} \int_{\tau-1-t}^{\tau-1-t_T} {x_2}^{\nu_{lat}} e^{-\lambda_{lat} x_2} dx_2 \right\}. \qquad (6.29)
\end{aligned}$$

Replacing the integrals in 6.29 by the equivalent gamma cumulative distribution functions yields:

$$\begin{aligned}
N_{21} &= \frac{\Lambda e^{-h(\tau-1)}}{h} \frac{\Gamma(\nu_{lat}+1)}{(\lambda_{lat}-h)^{\nu_{lat}+1}} \{ \mathrm{F}_\gamma(\tau-1-t_T; \nu_{lat}+1, \lambda_{lat}-h) - \\
&\qquad \mathrm{F}_\gamma(\tau-1-t; \nu_{lal}+1, \lambda_{lat}-h) \} \\
&\quad - \frac{\Lambda e^{-ht}}{h} \frac{\Gamma(\nu_{lat}+1)}{{\lambda_{lat}}^{\nu_{lat}+1}} \{ \mathrm{F}_\gamma(\tau-1-t_T; \nu_{lat}+1, \lambda_{lat}) - \\
&\qquad \mathrm{F}_\gamma(\tau-1-t; \nu_{lat}+1, \lambda_{lat}) \}. \qquad (6.30)
\end{aligned}$$

Numerator integral 2 (for area 2)

In a given interval (t_T, t), the contribution of integral 2 to the numerator $N(x_2)$ of the expected value of X_2, denoted by N_{22}, is:

$$\begin{aligned}
N_{22} &= \int_{\tau-1-t_T}^{\tau-t} \int_{t_T}^{t} x_2 \, \Lambda \, e^{-hx_1} \, e^{-\lambda_{lat} x_2} \, {x_2}^{\nu_{lat}-1} \, dx_1 dx_2 \\
&= \Lambda \int_{\tau-1-t_T}^{\tau-t} {x_2}^{\nu_{lat}} e^{-\lambda_{lat} x_2} \left[\frac{-e^{-hx_1}}{h} \right]_{t_T}^{t} dx_2 \\
&= \frac{\Lambda}{h} \left(e^{-ht_T} - e^{-ht} \right) \int_{\tau-1-t_T}^{\tau-t} {x_2}^{\nu_{lat}} \, e^{-\lambda_{lat} x_2} dx_2. \qquad (6.31)
\end{aligned}$$

Replacing the integrals by the equivalent gamma cumulative distribution functions in 6.31 yields:

$$N_{22} = \frac{\Lambda}{h}\left(e^{-ht_T} - e^{-ht}\right)\frac{\Gamma(\nu_{lat}+1)}{{\lambda_{lat}}^{\nu_{lat}+1}} \times \{\mathrm{F}_\gamma(\tau - t; \nu_{lat}+1, \lambda_{lat}) - \mathrm{F}_\gamma(\tau - 1 - t_T; \nu_{lat}+1, \lambda_{lat})\}. \quad (6.32)$$

Numerator integral 3 (for area 3)

In a given interval (t_T, t), the contribution of integral 3 to the numerator $N(x_2)$ of the expected value of X_2, denoted by N_{23}, is:

$$\begin{aligned} N_{23} &= \int_{\tau-t}^{\tau-t_T}\int_{t_T}^{\tau-x_2} x_2\ \Lambda\ e^{-hx_1}\ e^{-\lambda_{lat}x_2}\ {x_2}^{\nu_{lat}-1}\, dx_1 dx_2 \\ &= \Lambda \int_{\tau-t}^{\tau-t_T} {x_2}^{\nu_{lat}} e^{-\lambda_{lat}x_2} \left[\frac{-e^{-hx_1}}{h}\right]_{t_T}^{\tau-x_2} dx_2 \\ &= \frac{\Lambda}{h}\left\{e^{-ht_T}\int_{\tau-t}^{\tau-t_T} {x_2}^{\nu_{lat}}\ e^{-\lambda_{lat}x_2}dx_2 - e^{-h\tau}\int_{\tau-t}^{\tau-t_T} {x_2}^{\nu_{lat}}\ e^{-(\lambda_{lat}-h)x_2}dx_2\right\}. \end{aligned} \quad (6.33)$$

Replacing the integrals by the equivalent gamma cumulative distribution functions in Equation (6.33) yields:

$$\begin{aligned} N_{23} = {} & \frac{\Lambda e^{-ht_T}}{h}\frac{\Gamma(\nu_{lat}+1)}{{\lambda_{lat}}^{\nu_{lat}+1}}\{\mathrm{F}_\gamma(\tau - t_T; \nu_{lat}+1, \lambda_{lat}) - \mathrm{F}_\gamma(\tau - t; \nu_{lat}+1, \lambda_{lat})\} \\ & - \frac{\Lambda e^{-h\tau}}{h}\frac{\Gamma(\nu_{lat}+1)}{(\lambda_{lat}-h)^{\nu_{lat}+1}}\{\mathrm{F}_\gamma(\tau - t_T; \nu_{lat}+1, \lambda_{lat}-h) - \\ & \qquad \mathrm{F}_\gamma(\tau - t; \nu_{lat}+1, \lambda_{lat}-h)\}. \end{aligned} \quad (6.34)$$

The numerator in the expression for calculating $E[X_2]$ is attained by summing N_{21}, N_{22}, N_{23} over all intervals and hence the expression for calculating the expected value of the latent period is given by:

$$E[X_2] = \frac{\sum_{\text{all intervals } i} N_{21}(i) + N_{22}(i) + N_{23}(i)}{\sum_{\text{all intervals } i} D_1(i) + D_2(i) + D_3(i)}, \quad (6.35)$$

where i is an interval $(t_i,\ t_{i+1})$.

6.4.2.5 Estimation of infectiousness period

Once estimates for the expected time to infection and the expected length of latent period are obtained, estimates for the expected infectiousness period for each

infected sheep can be calculated, based on the distribution of the infectiousness period. From the estimates of the expected time of infection and expected length of latent period, the time of start of infectiousness and the expected amount of unobserved infectiousness period before τ are estimated. Estimates for the expected length of infectiousness period for infected sheep in groups 2 to 4 are calculated in a similar way to the calculations for group 1 sheep in Section 6.4.1.2. Let t_I denote the expected infectiousness period. The expected infectiousness period for an infected individual given n_e is estimated by:

$$E[T_I|n_e] = \frac{\int_{n_e-1+\hat{T}_\tau}^{n_e+\hat{T}_\tau} t_I f(t_I) dt_I}{\int_{n_e-1+\hat{T}_\tau}^{n_e+\hat{T}_\tau} f(t_I) dt_I}, \tag{6.36}$$

where $f(t_I)$ is the density of the infectiousness distribution which is gamma distributed with shape parameter ν_{inf} and scale parameter λ_{inf}.
The unobserved infectiousness period before τ, T_τ, is the length of time between the end of the latent period and τ and is estimated by $\tau - E[X_1 + X_2]$. Thus for each infected individual, n_e is known and estimates for T_τ and for the expected infectiousness period are obtainable. Hence an estimate for the unobserved expected infectiousness period after ω, T_ω can also be calculated. Thus contributions from each infected individual to the expected total duration of infection exposure for groups of sheep can be calculated and a martingale estimate for β obtained.

6.5 Estimation of rate of infection

In the current chapter, the rate of infection, β_g, acting upon groups 2 to 4 of sheep is estimated using martingale methods. These methods are described in Section 4.3 and the expressions for the estimates of β_g and the corresponding standard error estimates are given in Equation (4.17).

In order to be able to calculate a martingale estimate for β_g, the total expected infection exposure time for each group has to be determined. The exposure time depends on the length of infectiousness periods of infected sheep in a group. For groups where all sheep became infected, an estimate for the expected time of infection of the last sheep to be infected in the group is required to determine the appropriate amount of infection exposure required for the estimate of β_g acting upon such groups. Modelling the entire infection process makes this possible, because estimates for the expected time of infection for all infected individuals are obtained from the model. Thus, through knowledge of the expected times of

infection, a cut-off point is attained for the infection exposure time necessary to calculate the martingale estimate for β acting upon groups where all individuals became infected.

The hazard function, $h(\cdot)$, in the density function for time to infection (Equation (6.1)) involves β. Thus, estimates for the expected infection process characteristics and for the β_g have to be obtained via an iterative scheme as outlined in Section 4.4. The proposed scheme is analogous to the EM algorithm, where in the expectation step, the unobserved infection process characteristics are estimated by expected values conditional on previous estimates, and the equivalent of the maximisation step is an 'estimation step' where the β_g are estimated using either MLE or martingale methods. The scheme is outlined in Algorithm 6.1 below.

6.6 Algorithm for the iterative scheme

Algorithm 6.1

1. Assume the latent period distribution to be a gamma distribution with parameters $\hat{\nu}_{lat}$ and $\hat{\lambda}_{lat}$ as previously estimated.

2. Assume the infectiousness period distribution to be a gamma distribution with parameters $\hat{\nu}_{inf}$ and $\hat{\lambda}_{inf}$ as previously estimated.

3. Initialise the rates of infection, β_2, β_3 and β_4, applying to groups of sheep, to the estimates from the partial model (Chapter 5).

4. Estimate the expected time to infection, expected latent period and expected infectiousness period for each infected individual, according to Equations (6.28), (6.35) and (6.36) respectively, starting with those animals which earliest became infective, and using estimates (from this iteration) of these values where required in the calculations for individuals with later infections.

5. Calculate the estimate for the expected total infection exposure, for each group, by summing the relevant contributions of the estimated expected infectiousness periods.

6. Calculate new martingale based estimates for β_2, β_3 and β_4 according to Equation (4.17).

7. Compare estimates in steps 4 and 6 with estimates from previous iteration or with initial values in the case of the first iteration, if the difference is greater than 10^{-7} go to step 4, else go to step 8.

8. Use the estimates in step 4 and step 6 as the final estimates for the expected infection process characteristics and for the β_g.

9. End.

6.7 Investigation of trend in the rate of infection

The aim of the experiments was to assess whether the rate of infection decreases across groups. The trend in β across groups is measured by a slope calculated from weighted linear regression analyses (Freund and Wilson, 1998, Section 4.3). The β estimates are regressed against the group numbers, with weights given by the square of the reciprocal of the estimated standard error of $\hat{\beta}$ *i.e.* weight $= (\frac{1}{\text{S.e}(\hat{\beta})})^2$. With the estimate for the slope, the regression analysis also gives an estimate of statistical significance ($p-$value). However, because the estimates for the group βs are not independent, due to their underlying dependence on the expected infection process, the $p-$value given by the regression analysis will not be valid. Therefore to test whether the estimate for the slope is significantly less than zero, bootstrap methods (Efron and Tibishirani, 1993, Section 16.2) are employed to calculate a valid $p-$value.

6.7.1 Bootstrap methods

Bootstrap methods involve resampling from the original data either directly or via a fitted model to create replicate data sets from which the variability of the estimates of interest can be assessed. The approach is a computer-intensive method because it involves repeating the original data analysis procedure with many replicate sets of data. In the simplest nonparametric problems, sampling is done from the observed data. A wide range of statistical problems can be tackled this way, rescuing the investigators from the need to over simplify complex problems (Davison and Hinkley, 2000, Chapter 1). Bootstrap methods can also be applied to simple problems to check the adequacy of standard measures of uncertainty, to relax assumptions and to give quick approximate solutions. Even in

situations where one is fairly confident in the suitability of a particular parametric model and the associated standard analysis, it can still be useful to see what can be inferred without making the assumption of a specific parametric model. 200 bootstrap epidemic samples are generated from the simulation model described in Section 2.4.2. In addition to the parameters for the distributions of latent and infectiousness periods and the rate of infection, the model also involves a parameter termed the passage multiplier, which describes the passage effect. For the latent and infectiousness distribution parameters, the parameters estimated from the experimental epidemic data are used. For the rate of infection, a global rate of infection (assuming the same β_g for all groups 2 to 4) is estimated from the experimental data. The passage multiplier is set to 0, since the aim is to generate epidemics under the null hypothesis *i.e.* that the rate of infection is the same for all infected individuals regardless of how far down the infection chain they may be.

6.7.1.1 Global rate of infection (β_{global})

Under the null hypothesis of equal rate of infection acting upon groups of sheep, an equal β_g is assumed for all groups. This is referred to as the global rate of infection, denoted by β_{global}. To estimate β_{global}, information from all groups is combined. A martingale estimate for β_{global} is calculated from the expected total infection exposure time for all groups 2 to 4 and the corresponding values of the B integral, as follows:

$$\begin{aligned}\hat{\beta}_{global} &= \frac{\sum_{g=2}^{4}\int_0^T B_g(x)dN(x)}{\sum_{g=2}^{4}E[\int_0^T \frac{I_g(x)}{n_g(x)}dx]} \\ &= \frac{\sum_{g=2}^{4}\sum_{s=s_g(T)+1}^{8}\frac{1}{s}}{\sum_{g=2}^{4}\text{total expected infection exposure time for each group } g},\end{aligned} \tag{6.37}$$

where T is the stopping time of the experiment, $I_g(x)$ is the number of infectious individuals in group g at time x, $s_g(T)$ is the number of susceptible individuals remaining in group g at the end of the epidemic and $n_g(x)$ is the total number of sheep in the mixing group containing group g at time x.
β_{global} and the expected infection process characteristics are estimated iteratively using Algorithm 6.1, with the different group β_g replaced by β_{global}.

6.7.1.2 The simulation model

Formulation of the simulation model is based on a Susceptible-Latent-Infectious-Removed (SLIR) infection structure, modelling the generational infection of individual sheep (Section 2.4.2) rather than groups of sheep. Group 1 sheep are generation zero infectives and these have an infection potential when exposed to group 2 sheep proportional to the rate $\beta_0 = \hat{\beta}_{global}$. Since the bootstrap epidemics are to be generated under the null hypothesis of no reduction in infectivity with respect to generation number, all infected individuals are assumed to have the same rate of infection, equal to $\hat{\beta}_{global}$.

If the alternative hypothesis that the rate of infection drops with respect to infection generation number is true, then infected individuals in higher groups which will tend to be of higher infection generation number will potentially have lower rate of infection. Thus although it is infection generations of sheep that are being modelled by the simulation model, the alternative hypothesis is equivalent to the rate of infection acting upon groups of sheep dropping across groups. For instance, group 3 individuals are exposed to infected individuals of generation 1 (from group 2) and above and group 4 individuals are exposed to infected individuals of generation two (from group 3) and above.

The simulation model reflects the nature of the experiment, with groups of size 8 and restricted mixing among groups of sheep. A gamma distribution is assumed for the latent and infectiousness processes and the parameters for the distributions are as estimated from the experimental data.

6.7.1.3 Bootstrap epidemic samples

200 bootstrap epidemic samples are generated using the simulation model described in Section 6.7.1.2 above. Using only the information as was observed in the experimental data *i.e.* n_l, τ, n_e, and ω for each individual (refer to Section 5.2), the simulated epidemic data are analysed using methods to model the entire infection process to obtain estimates for β_g, in each of groups 2 to 4. Weighted linear regression analyses are performed by regressing the estimates of β on group number to produce an estimate of the slope as a measure of the trend in the β_g. From the distribution of the 200 estimated slopes, a bootstrap $p-$value (Efron and Tibishirani, 1993, Section 16.2) is obtained. The null hypothesis is equivalent to the estimate of the slope being equal to zero *i.e.* no trend in the β estimates,

and the alternative hypothesis is that the slope is less than 0. If the estimated slope from the experimental data is significantly less than 0, it will be expected to fall outside or at the extreme left of the distribution of the slopes estimated from the bootstrap samples. The $p-$value is formally calculated as follows: Based on the alternative hypothesis of slope decreasing with higher group, the $p-$value is given by:

$$p-\text{value} = \frac{\#\{\text{bootstrap slopes} < \text{observed (estimated) slope}\}}{\text{total number of bootstrap samples}}, \quad (6.38)$$

i.e. count the bootstrap slopes where the slope is less than the estimated slope from the experimental data and divide by the total number of bootstrap samples.

6.8 Implementation of methods

The inferential methods described in previous sections are implemented by programming in C (Kernighan and Ritchie, 1988) and S-Plus (Venables and Ripley, 1994). Programs were developed to model the infection process and the methods were applied to experimental data generated from two identical experiments carried out at the Institute of Animal Health in Pirbright and to simulated data. The experimental data are described and presented in Section 1.3.3 and the simulation models used to generate the simulated data are described in Section 2.4.

6.9 Application of methods to experimental data

6.9.1 Estimates of ν_{lat} and λ_{lat}

Information about group 1 sheep (see Table 5.1) was used to estimate the parameters ν_{lat} and λ_{lat} of the latent period distribution. Group 1 sheep provide more information about the latent period. The time at which these sheep were inoculated is considered as the time of infection. Based on n_l, the number of days that these sheep tested negative after inoculation prior to τ, ML estimates for the distribution parameters were obtained.

Given n_l, for an infected individual, the length of latent period is between n_l and $n_l + 1$. Recall from Section 6.3: if $n_l < x_2 < n_l + 1$, where x_2 is the length of latent period, the log-likelihood function for the latent period is given by:

$$\sum_{\text{all } n_l} (n_l \text{ freq}) \times \ln \left[\int_{n_l}^{n_l+1} \frac{{\lambda_{lat}}^{\nu_{lat}} {x_2}^{\nu_{lat}-1} e^{-\lambda_{lat} x_2}}{\Gamma(\nu_{lat})} \, dx_2 \right]. \quad (6.39)$$

In both experiments, group 1 sheep are observed to have first tested positive either on the first day after inoculation, *i.e.* $n_l = 0$, or on the second day after inoculation, *i.e.* $n_l = 1$. The value of n_l for each of the group 1 sheep from both experiments is given in Table 6.1. In experiment 1, sheep number 3 did not test positive to FMD virus throughout the experiment despite having been inoculated. Therefore in that experiment only data on the remaining 7 sheep are used to model the latent period.

Table 6.1: *Number of negative tests after inoculation prior to the first observed positive test,* n_l.

Sheep ID	1	2	3	4	5	6	7	8
n_l (expt1)	1	0	-*	0	1	0	1	0
n_l (expt2)	1	0	1	1	0	0	0	0

**Sheep did not shed virus*

Using these data the full log-likelihood function given in Equation (6.39) is maximized with respect to ν_{lat} and λ_{lat}, yielding the following estimates:

Experiment 1

The estimate for the shape parameter $\hat{\nu}_{lat} = 32.26$ and the estimate for the scale parameter $\hat{\lambda}_{lat} = 32.95$. Thus the estimate for the mean of the distribution of the latent period for the infected sheep in experiment 1, given by $\frac{\hat{\nu}_{lat}}{\hat{\lambda}_{lat}}$, is 0.98 days with the standard deviation of the distribution given by $\sqrt{\frac{\hat{\nu}_{lat}}{\hat{\lambda}_{lat}^2}}$, equalling 0.172.

Experiment 2

The estimate for the shape parameter $\hat{\nu}_{lat} = 29.99$ and the estimate for the scale parameter $\hat{\lambda}_{lat} = 31.43$. Thus the estimate for the mean of the distribution of the latent period for the infected sheep in experiment 2 is 0.95 days with the standard deviation of the distribution equalling 0.174.

From both experiments, the mean of the distribution for the latent period for infected sheep was estimated to be approximately 1 day (0.98 for experiment 1, 0.95 for experiment 2) with similar variability in latency being seen in both experiments.

The fact that in both experiments there are more sheep that did not test negative after inoculation prior to first testing positive than sheep that tested negative once prior to the day of the first positive test has an effect on the resulting estimate for the mean latent period. Due to the discretization of the time scale,

because sampling is done on a daily basis, n_l takes only values 0 and 1. The resulting likelihood function for the latent distribution is flat and hence there is a wide range of possible values for parameter estimates that maximize the log-likelihood function to a specified tolerance. Different estimates for ν_{lat} and λ_{lat} were obtained depending on the choice of initial values. However, the maximum value of the likelihood was always the same and all values of the estimates gave similar estimates for the mean and standard deviation of the latent period distribution. Only one set of parameter estimates is presented since practical interest is primarily in the mean of the distribution. These estimates are the ones attained after using moment estimates as the initial values for ν_{lat} and λ_{lat}. Using simulated epidemics with an increased group size (*i.e.* 20 sheep per group) similar problems with convergence were encountered for the estimates of the latency parameters. The latent period would still be expected to be between 0 and 2 days, with many individuals presenting at 1 day of latency, assuming that the individuals that test negative once became viraemic shortly after the time of the first negative test and that those that never tested negative before the first positive test started shedding virus shortly before the test was done on the day after inoculation. The use of lognormal and normal distributions (Johnson and Kotz, 1970, Section 4.3) to model the latency variable, did not solve the convergence problem. Sampling more frequently, say on a half day (12 hours) basis would provide more information about the latent process, resulting in an improvement in convergence and possibly better parameter estimates. There is a need to investigate the appropriateness of the gamma distribution as a model for the latent period and further investigation of other choices of distributions for the latent period should be considered, if the experiment is repeated, with a shorter sampling cycle.

6.9.2 Infection process for group 1 sheep

6.9.2.1 Expected latent period

The expected latent period for an infected sheep was estimated conditional on n_l. From Equation (6.5), the expression for the estimate of the expected latent period is given as

$$E[T_L|n_l] = \frac{\int_{n_l}^{n_l+1} t_L f(t_L) dt_L}{\int_{n_l}^{n_l+1} f(t_L) dt_L}. \tag{6.40}$$

Using the properties of the gamma distribution as outlined in Equations (5.4) and (5.5), the expression for the estimate of the expected latent period, in Equation (6.40), becomes:

$$\begin{aligned} E[T_L|n_l] &= \frac{\frac{\nu_{lat}}{\lambda_{lat}} \int_{n_l}^{n_l+1} f_{\nu_{lat}+1,\lambda_{lat}}(t_L)dt_L}{\int_{n_l}^{n_l+1} f_{\nu_{lat},\lambda_{lat}}(t_L)dt_L} \\ &= \frac{\frac{\nu_{lat}}{\lambda_{lat}} [\mathrm{F}_\gamma(n_l+1;\nu_{lat}+1,\lambda_{lat}) - \mathrm{F}_\gamma(n_l;\nu_{lat}+1,\lambda_{lat})]}{\mathrm{F}_\gamma(n_l+1;\nu_{lat},\lambda_{lat}) - \mathrm{F}_\gamma(n_l;\nu_{lat},\lambda_{lat})}. \end{aligned} \tag{6.41}$$

where $f_{\nu_{lat}+1,\lambda_{lat}}(t_L)$ is the density function of a gamma distributed random variable with shape parameter $\nu_{lat}+1$ and scale parameter λ_{lat}. $\mathrm{F}_\gamma(n_l+1;\nu_{lat}+1,\lambda_{lat})$ is the cumulative distribution function up to the point n_l+1 of a gamma distributed random variable with shape parameter $\nu_{lat}+1$ and scale parameter λ_{lat}.

From the expression in Equation (6.41), the estimate for the expected latent period for an infected sheep given n_l was calculated. Sheep with $n_l = 0$ have an estimated expected latent period of 0.86 days for experiment 1 and 0.85 days for experiment 2. Sheep with $n_l = 1$ have an estimated expected latent period of 1.14 days for experiment 1 and 1.13 days for experiment 2. Table 6.2 presents the estimated expected latent period for each of the sheep in group 1 for both experiments. In experiment 1, sheep in group 1 have an estimated average expected latent period of 0.98 days with standard deviation of 0.149. In experiment 2, sheep in group 1 have an estimated average latent period of 0.95 with standard deviation of 0.148. Thus, for both experiments sheep were, on average, estimated to be in the latent state for a period of approximately 1 day.

Table 6.2: *Expected latent period for group 1 sheep given* n_l.

Experiment 1			Experiment 2		
Sheep ID	n_l	Latent period	Sheep ID	n_l	Latent period
1	1	1.14	1	1	1.13
2	0	0.86	2	0	0.85
3*	-	-	3	1	1.13
4	0	0.86	4	1	1.13
5	1	1.14	5	0	0.85
6	0	0.86	6	0	0.85
7	1	1.14	7	0	0.85
8	0	0.86	8	0	0.85

* *sheep did not shed virus*

6.9.2.2 Expected infectiousness period

The expression for calculating the expected infectiousness period given n_e is derived from Equation (6.6), where

$$E[T_I|n_e, n_l] = \frac{\int_{n_e-1+\hat{T}_\tau}^{n_e+\hat{T}_\tau} t_I f(t_I) dt_I}{\int_{n_e-1+\hat{T}_\tau}^{n_e+\hat{T}_\tau} f(t_I) dt_I},$$

where $\hat{T}_\tau$ is the estimated unobserved infectiousness period between the start of infectiousness (end of latency) and τ, and T_I is the expected length of infectiousness period which is assumed to be gamma distributed with shape parameter ν_{inf} and scale parameter λ_{inf} (see Section 5.4.2), and $f(t_I)$ is the corresponding density function.

From the properties of a gamma distribution as outlined in Equations (5.4) and (5.5), the above expression is equivalent to:

$$\begin{aligned} E[T_I|n_e, n_l] &= \frac{\frac{\nu_{inf}}{\lambda_{inf}} \int_a^b f_{\nu_{inf}+1,\lambda_{inf}}(t_I) dt_I}{\int_a^b f_{\nu_{inf},\lambda_{inf}}(t_I) dt_I} \\ &= \frac{\frac{\nu_{inf}}{\lambda_{inf}} \left[\mathrm{F}_\gamma(b; \nu_{inf}+1, \lambda_{inf}) - \mathrm{F}_\gamma(a; \nu_{inf}+1, \lambda_{inf})\right]}{\mathrm{F}_\gamma(b; \nu_{inf}, \lambda_{inf}) - \mathrm{F}_\gamma(b; \nu_{inf}, \lambda_{inf})}, \end{aligned} \tag{6.42}$$

where the limits $a = n_e - 1 + \hat{T}_\tau$ and $b = n_e + \hat{T}_\tau$.

The expected infectiousness period for group 1 sheep is determined conditional on n_e and n_l. Thus sheep with the same n_l and same n_e will have the same expected length of infectiousness period. Using data about n_l and n_e from both experiments, the estimate for the expected length of infectiousness period for each infected sheep in group 1 was calculated based using Equation (6.42). The results are presented in Table 6.3. The estimate for $\hat{T}_\tau$ depends on n_l. In the data set, n_l takes values 0 and 1 (see Table 6.2).

For $n_l = 0$, the estimate of $\hat{T}_\tau$ for experiment 1 is 0.14 days (3.36 hours) *i.e.* in experiment 1, it is estimated that sheep that tested positive on the first day after inoculation were first observed to be excreting virus 3.36 hours after the expected start of virus shedding. For sheep with $n_l = 1$, the estimate of the expected length of unobserved infectiousness before τ is 0.86 days (20.64 hours). It is estimated that these sheep were only observed to be excreting virus more than 20 hours after the expected start of virus shedding.

In experiment 2, the results are similar to those of experiment 1, sheep with $n_l = 0$ had an estimated 0.15 days (3.60 hours) of their infectiousness period unobserved before τ. These sheep were first observed to be excreting virus less than 4 hours after the estimated start of virus shedding. Sheep with $n_l = 1$ had an estimated 0.87 days (20.88 hours) of their estimated infectiousness period unobserved.

In summary, for both experiments, sheep that tested positive on the first testing day after inoculation are estimated to have started to shed virus on average within 4 hours of the test being done. On the other hand, it is estimated that sheep that tested negative once before the first positive test, on average became viraemic within less than 4 hours after the first testing day after inoculation.

With the values of $\hat{T}_\tau$ calculated, the limits of the integrals in the expression for the expected infectiousness period are fully specified. Table 6.3 lists expected lengths of infectiousness period conditional on n_l and n_e.

Table 6.3: *Estimates of the expected lengths of infectiousness period for group 1 sheep given n_l and n_e.*

	Experiment 1		Experiment 2	
n_e	$n_l = 0$	$n_l = 1$	$n_l = 0$	$n_l = 1$
2	1.82[&]	2.40	1.92[&]	2.45
	(0.68)*	(0.54)	(0.77)	(0.58)
3	2.64	3.28	2.66	3.24
	(0.50)	(0.42)	(0.51)	(0.37)
4	3.54	4.22[&]	3.49	4.15[&]
	(0.40)	(0.36)	(0.34)	(0.28)
$\hat{T}_\tau^+$	0.14	0.86	0.15	0.87

[+]$\hat{T}_\tau$ *is the estimated unobserved shedding time before τ given n_l.*
[*]*value in brackets is the estimate of the length of unobserved shedding time after ω.*
[&]*calculated, although no sheep from either experiments was in this category.*

In both experiments, sheep with $n_l = 0$ tested as positive for 3 or 4 days and sheep with $n_l = 1$, tested as positive for 2 or 3 days. This is presumably due to the fact that sheep with $n_l = 1$ had a large portion of their infectiousness period (estimated at 20.60 hours for experiment 1 and 20.88 hours for experiment 2) unobserved before τ Sheep with $n_l = 0$ had a smaller estimated portion of the expected infectiousness period unobserved before τ (3.36 hours for experiment 1 and 3.60 hours for experiment 2). The period of 24 hours between sampling

therefore favoured the observation of positives from sheep that tested positive on the first day of testing. Sheep with a short latent period (less than 24 hours) had their infectiousness observed on the first day of testing after inoculation. However, sheep whose latent period was slightly longer than 1 day (over 24 hours) and became infectious shortly after the first day of testing, because of the 24 hour period between sampling, tended to have fewer positive samples recorded. By the time of next sampling, these sheep were well into their infectiousness state. Comparing columns 2 and 3, for experiment 1 and columns 4 and 5, for experiment 2, of Table 6.3, sheep with the same n_e but with $n_l = 1$, are estimated to have excreted virus, on average, for longer periods than sheep with $n_l = 0$. Thus, given a fixed number of positive observations, n_e, sheep that had an estimated shorter expected latent period (less than 1 day) had a shorter estimated expected infectiousness period.

With estimates for the individual expected infectiousness periods obtained, the expected total unobserved infectiousness period can be obtained. So far, attention has focussed on T_τ, the unobserved infectiousness period before τ. However, after ω, the day of the last positive test, there is an amount of unobserved infectiousness period. It is known that a sheep last tested positive on day ω and tested negative thereafter from day $\omega+1$ on wards. At some point between day ω and day $\omega+1$, infected sheep ceased shedding virus. From the estimates for the expected total infectiousness period and expected start of infectiousness, the expected amount of unobserved infectiousness period after ω can be estimated. This is obtained by subtracting the observed (n_e-1) infectiousness period and $\hat{T}_\tau$ from the estimated expected infectiousness period. Thus $\hat{T}_\omega = E[T_I|n_e, n_l] - (n_e - 1) - \hat{T}_\tau$ and the estimates corresponding to each combination of n_e and n_l are given in Table 6.3. For both experiments and for both $n_l = 0$ and $n_l = 1$, sheep had average estimates of between 8 and 14 hours of unobserved infectiousness after ω. The estimated expected amount of unobserved infectiousness after ω was slightly higher for sheep with $n_l = 0$ when compared to that for sheep with $n_l = 1$.

Table 6.4 shows the estimated total expected unobserved infectiousness period *i.e.* the expected infectiousness period $(E[T|n_e, n_l])$ minus the observed period $(n_e - 1)$, conditional on n_e and n_l. In general, for $n_l = 1$, the estimate is of more than 1 day (between 1.14 and 1.44 days) expected unobserved infectiousness period. Sheep with $n_l = 0$ gave rise to an estimate of less than 1 day (between 0.49 and 0.92 days) of total expected unobserved infectiousness period. In future experiments of this type, the duration between sampling should be smaller to

Table 6.4: *Estimated total expected unobserved infectiousness period (in days) for group 1 sheep.*

	Experiment 1		Experiment 2	
n_e	$n_l = 0$	$n_l = 1$	$n_l = 0$	$n_l = 1$
2	0.82	1.40	0.92	1.45
3	0.64	1.28	0.66	1.24
4	0.54	1.22	0.49	1.15

reduce the amount of unobserved infectiousness period. It appears that a 24 hour sampling interval was not appropriate given the short observed latent periods, and relatively short viraemic periods. In particular, sheep that have an expected latent period of more than a day will have much of their expected infectiousness period unobserved. The results also indicate that for both $n_l = 0$ and $n_l = 1$, the estimated expected unobserved infectiousness period decreases with increasing n_e, as illustrated in Figure 6.5.

Figure 6.5: *Comparison of estimated length of unobserved infectiousness by n_e and n_l.*

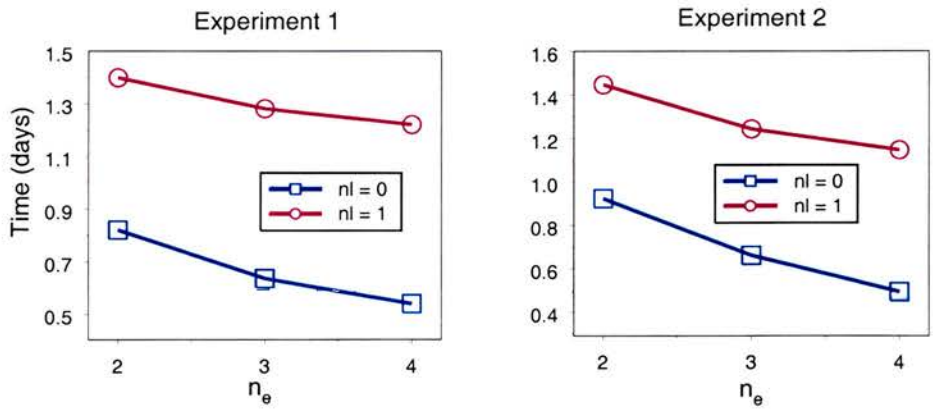

Estimates of the expected infectiousness period for group 1 sheep are included in Table 6.5 for both experiments. In this table, estimates for the entire histories of infection for group 1 sheep, including the expected time of infection (time of inoculation) denoted by 'Inf T', the expected length of latent period, the expected time of start of infectiousness denoted by 'Start inf', the expected time of end of infectiousness denoted by 'End inf' and the expected length of infectiousness period denoted by 'Inf Period' are presented.

Table 6.5: *Estimates for group 1 infection history characteristics, for experiment 1 and 2.*

Experiment	ID	Inf T	Latent	Start inf	Inf Period	End Inf
1	1	0	1.14	1.14	3.28	4.42
	2	0	0.86	0.86	2.64	3.50
	3*	-	-	-	-	-
	4	0	0.86	0.86	2.64	3.50
	5	1	1.14	2.14	2.40	4.54
	6	1	0.86	1.86	2.64	4.50
	7	1	1.14	2.14	2.40	4.54
	8	1	0.86	1.86	3.54	5.40
2	1	0	1.13	1.13	2.45	3.58
	2	0	0.85	0.85	3.49	4.34
	3	0	1.13	1.13	3.24	4.37
	4	0	1.13	1.13	3.24	4.37
	5	1	0.85	1.85	2.66	4.51
	6	1	0.85	1.85	2.66	4.51
	7	1	0.85	1.85	3.49	5.34
	8	1	0.85	1.85	3.49	5.34

**sheep did not shed virus*

Modelling the entire infection history enables appropriate allocation of the contribution of the estimated infectiousness period of each sheep to the respective estimate of the group infection exposure time. For the partial model of the infection process, where only the infectiousness period was modelled, the estimated unobserved infectiousness period was divided into two equal portions, one for the period before τ and the other for the period after ω. By modelling the entire infection process, there is an estimated variable for each of these periods. For instance, sheep number 1 in experiment 1, has an estimated start of infectiousness at $t = 1.14$ *i.e.* after 1 day and 3.3 hours from the start of the experiment; the first observed positive test is on day 2 ($\tau = 2$), the last positive test is on day 4 ($\omega = 4$) and its estimated end of infectiousness occurs at $t = 4.42$, with an expected infectiousness period estimate of 3.28 days. The estimate for T_τ is equal to $2 - 1.14 = 0.86$ days and the estimate for T_ω is $4.42 - 4 = 0.42$ days. The estimate for the total unobserved infectiousness period is $0.86 + 0.42 = 1.28$ days. The equivalent estimate for the unobserved infectiousness period when only the infectiousness period is modelled is 0.92 days, giving 0.46 days to each portion of unobserved infectiousness period before τ and after ω. This implies that infectiousness starts at time 1.46 and ceases at time 4.46, estimating 2.92 days as the expected infectiousness period. The entire infection process model yields estimates with 0.36 days (8.64 hours) of additional infectiousness time compared to the partial model of the infection process.

When estimating the expected total exposure time in order to calculate the estimate for the rate of infection acting upon group 2 sheep, using the full model of the infection process, sheep number 1 from experiment 1 contributes 0.86 days during day 1 when groups 1 and 2 are mixing, compared to 0.46 days estimated from the partial model. The total contribution of sheep number 1 to the estimate for the expected infection exposure time of group 2 in the entire model is $0.86 + 1 = 1.86$ days as compared to 1.46 days. Although the estimate for the total contribution to the expected infection exposure time is not very different, the estimates for T_τ and/or T_ω may be appreciably different as is the case for the estimate of T_τ for sheep number 1, experiment 1. Modelling the entire infection process enables allocation of the appropriate estimated amount of unobserved infectiousness period before τ and after ω, rather than having to assign half of the estimated expected total unobserved infectiousness period to each portion as for the partial model of the infection process. This is no surprise, since the full model takes account of the force of infection applying to individual animals in the run-up to infection.

The infection process for group 1 sheep is now fully specified. Estimates for the expected times at which sheep start and cease to shed virus have been calculated. Using this information plus the observed data *i.e.* τ, n_e and ω, the expected infection history characteristics for sheep in the remaining groups are estimated.

6.9.3 Infection process for sheep from groups 2 to 4

Unlike group 1 sheep, where the time of infection was known (time of inoculation), for infected individuals in the other groups, the time at which infection occurred is not known. The process of time to infection together with the latency process are modelled via a joint distribution of the two variables. From the fully specified infection history for group 1 sheep and using the properties of the latent period distribution estimated from group 1 sheep data, estimates for the expected time to infection and expected latent periods for the infected sheep in groups 2 to 4 are calculated using the expression in Equation (6.14). After deriving estimates for the expected time to infection and the expected latent period, the expected infectiousness period is estimated based on the distribution already fully specified in Section 5.4.2 and Equation (6.36).

For each infected sheep, the period between the start of the experiment and the possible time of infection X_1 is partitioned into intervals with constant hazard,

while taking mixing events into account as described in Section 6.4.2.

Estimates for the expected time to infection X_1 and the expected latent period X_2 are calculated using contributions from all of the partitioned intervals, conditional on τ and n_e and past estimates of infection history from other infective individuals. When calculating estimates for X_1 and X_2, it can be assumed that sheep with the lowest value of τ were the first to be infected. Thus, calculations were done in an ordered way based on the value of τ. In a situation where there was more than 1 sheep with the same value of τ (ties), if the sheep are from the same group, then estimates for X_1 and X_2 will be the same for these sheep (experiment 1: sheep nos. (12 and 14); (18, 19 and 21); (27, 29, 30 and 31)) and if the sheep have the same n_e, they will also have the same estimate for the expected infectiousness period. Because the same distributions for time to infection, latent period and infectiousness period were assumed for every sheep, it is assumed that sheep from the same group with the same τ are unlikely to have contributed to each other's infection exposure. If, however, tied sheep are from different groups, a criterion based on the cumulative force of infection is formulated to choose the group of animals whose infection history components should be calculated first. The cumulative force of infection acting upon each group, using previously estimated infection histories for other infective individuals, is calculated and the group with the largest cumulative force of infection exposure is chosen for initial calculation. If within the chosen group there were more than 1 sheep with the same critical value of τ, then the calculations were performed for one individual and the resulting values adopted for all sheep with the same value of τ and n_e in this group.

After calculating estimates for the expected infection process characteristics, the expected total infection exposure time for each group is calculated by summing contributions from individual infected sheep throughout their estimated expected infectiousness histories. Finally, an estimate for β for each group was calculated based on Equation (4.17), Section 4.3, *i.e.*

$$\hat{\beta} = \frac{\int_0^T B(x)dN(x)}{E[\int_0^T \frac{I(x)J(x)}{n(x)}]dx} \quad \text{and} \quad s.e(\hat{\beta}) = \frac{[\int_0^T B^2(x)dN(x)]^{1/2}}{E[\int_0^T \frac{I(x)J(x)}{n(x)}dx]}.$$

The numerator of $\hat{\beta}$ is the value of the integrals of the B function given in Table 5.8 in Section 5.4.4 and the denominator is an estimate for the expected total infection exposure determined from estimates of the expected infectiousness periods. The numerator for the standard error estimate of $\hat{\beta}$ is calculated from Equation (5.7) of Section 5.4.4.

The procedure of estimating the expected infection process characteristics and the β_g was repeated iteratively until convergence, as outlined in Algorithm 6.1 in Section 6.6.

6.9.3.1 Expected time of infection, latent period and infectiousness period

In Tables 6.6 and 6.7, results for experiments 1 and 2 from the last iteration of the full model of the infection process are presented. The results include estimates for the expected time of infection denoted by 'InfT', expected length of latent period denoted by 'latent', the expected start of infectiousness denoted by 'Start Inf', the expected end of the infectiousness period denoted by 'End Inf', the time of the first positive test τ, the time of the last positive test ω and the expected length of infectiousness period denoted by 'Inf Period'. The estimated entire infection history is presented graphically in Figure 6.6 for the two experiments.

Table 6.6: *Estimated infection process for sheep from groups 2 to 4 (Experiment 1).*

Sheep ID	Inf T	Latent	Start inf	τ	Inf Period	End Inf	ω
9*	-	-	-	-	-	-	-
10	6.52	0.98	7.50	8	2.96	10.45	10
11	3.46	0.99	4.45	5	3.00	7.45	7
12	7.56	0.97	8.53	9	2.93	11.46	11
13	10.48	0.99	11.46	12	2.99	14.45	14
14	7.56	0.97	8.53	9	2.93	11.46	11
15*	-	-	-	-	-	-	-
16	8.65	0.95	9.61	10	2.02	11.62	11
17	9.48	0.99	10.48	11	2.98	13.45	13
18	7.73	0.94	8.67	9	1.97	10.64	10
19	7.73	0.94	8.67	9	2.80	11.47	11
20	9.48	0.99	10.47	11	2.98	13.45	13
21	7.73	0.94	8.67	9	2.80	11.47	11
22	8.63	0.96	9.59	10	3.79	13.38	13
23	6.50	0.98	7.48	8	2.97	10.45	10
24	11.37	1.02	12.39	13	3.05	15.44	15
25*	-	-	-	-	-	-	-
26	9.52	0.98	10.50	11	3.88	14.38	14
27	11.46	0.99	12.44	13	2.15	14.59	14
28	14.43	1.00	15.43	16	3.02	18.45	18
29	11.46	0.99	12.44	13	3.00	15.45	15
30	11.46	0.99	12.44	13	3.00	15.45	15
31	11.46	0.99	12.44	13	3.93	16.37	16
32	12.64	0.96	13.60	14	2.02	15.62	15

**sheep did not shed virus*

Table 6.7: *Estimated infection process for sheep from groups 2 to 4 (Experiment 2).*

Sheep ID	Inf T	Latent	Start inf	τ	Inf Period	End Inf	ω
9	3.49	0.96	4.46	5	2.97	7.43	7
10	5.43	0.98	6.40	7	3.90	10.30	10
11	7.45	0.98	8.42	9	3.00	11.42	11
12	7.45	0.98	8.42	9	2.24	10.66	10
13*	-	-	-	-	-	-	-
14	14.89	1.23	16.11	17	3.26	19.37	19
15*	-	-	-	-	-	-	-
16*	-	-	-	-	-	-	-
17	9.78	0.91	10.69	11	2.78	13.47	13
18	9.78	0.91	10.69	11	2.04	12.73	12
19	8.61	0.94	9.55	10	2.89	12.44	12
20*	-	-	-	-	-	-	-
21	10.54	0.95	11.49	12	2.19	13.68	13
22	12.47	0.97	13.44	14	2.22	15.66	15
23*	-	-	-	-	-	-	-
24	8.61	0.94	9.55	10	2.14	11.69	11
25	13.46	0.97	14.43	15	2.23	16.66	16
26	13.46	0.97	14.43	15	2.23	16.66	16
27	10.86	0.87	11.73	12	2.01	13.74	13
28*	-	-	-	-	-	-	-
29	11.56	0.95	12.51	13	2.93	15.44	15
30*	-	-	-	-	-	-	-
31*	-	-	-	-	-	-	-
32*	-	-	-	-	-	-	-

**sheep did not shed virus*

From Figure 6.6 and Table 6.6, it is observed that for experiment 1, only sheep number 11 is estimated to have been infected during the estimated infectiousness period of group 1 sheep. The rest of group 2 infected sheep are estimated to have been infected after all group 1 sheep had ceased to shed virus. Thus even with 7 infectious sheep in group 1, estimates for the expected infection process characteristics would suggest that only 1 group 2 sheep managed to make an infectious contact with group 1 sheep even though these two groups mixed for a total of 2 days during the estimated expected infectiousness period of group 1 sheep. For experiment 2, the results are similar (Figure 6.6 and Table 6.7); only sheep number 9 from group 2 is estimated to have been infected during the estimated expected infectiousness period of group 1 sheep.

Figure 6.6: *Estimated entire infection history for experiment 1 and 2.*

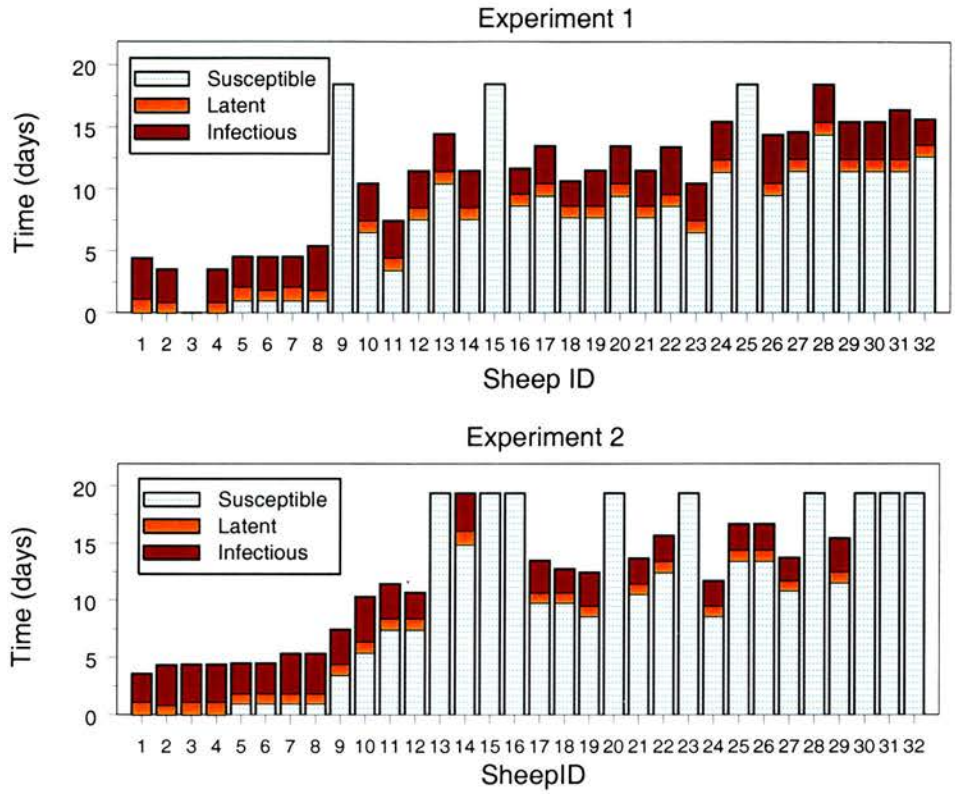

6.9.3.2 Estimates for rate of infection

Estimates of the expected scaled total infection exposure time and estimates for the rates of infection and the corresponding standard error estimates, all derived from the final iteration of the analysis procedure, are presented in Table 6.8. Results from both experiments indicate that the highest rate of infection occurs in group 3 sheep followed by group 4 and then group 2 (the same pattern as was observed for the partial model). It should be noted that the estimate for β_3 in experiment 1 increases relative to the estimate made under the partial model. In this group all sheep were infected, and thus a sizeable amount of infection exposure in this group was 'wasted'. Estimating the expected time of infection for all the sheep enabled identification of the likely last sheep to be infected and the expected time of infection. The estimate for the total expected infection exposure for group 3 was then calculated only up to the estimated expected time of infection of the last sheep in the group to become infected (sheep number 24). After rescaling, the estimated total infection exposure time for group 3 while modelling the full infection process was 1.33 days as compared to 2.65 days under the partial model.

The partial model yielded a severe underestimate for β_3, since all of the time that sheep contributing to the group 3 expected infection exposure time were shedding virus, was included in the estimate for the total expected infection exposure, but the full model would suggest that there were no remaining susceptible sheep to infect in this group after time $t = 11.37$ days. Some individuals in groups 2 to 4 (which contribute to the estimate for the expected exposure time of group 3) were still shedding virus until much later in the experiment with the last sheep shedding virus up to an estimated time of $t = 18.45$, but only time up to 11.37 should contribute to the estimate for the total expected infection exposure for group 3.

Table 6.8: *Estimates for the expected scaled exposure time (in days) and β estimates (per day), from the final iteration of the analysis procedure.*

	Experiment 1			Experiment 2		
Group	Expected Exposure time	β estimates	s.e(β)	Expected Exposure time	β estimates	s.e(β)
2	2.38	0.5116	0.2213	2.16	0.4087	0.1884
3	1.33	2.0469	0.9308	1.68	0.7256	0.3138
4	2.69	0.6377	0.2696	1.36	0.4655	0.2364

Estimates of β_2 and β_4 acting upon groups 2 and 4 of experiment 1 and for all β_g groups in experiment 2, are similar for both the partial and the entire models. For experiment 2, results indicate that the estimated expected scaled exposure time decreases across groups (2.16 days for group 2, 1.68 days for group 3 and 1.36 days for group 4).

Under the experimental hypothesis of reduction in infectivity across groups, group 2 would be expected to have the highest estimate for the rate of infection followed by group 3 and then group 4. However, the results for both experiments indicate a lowest estimated rate of infection applying to group 2, and a highest estimated rate of infection applying to group 3. The estimated rate of infection for group 4 is higher than that for group 2 but lower than that for group 3. Thus, there is an apparent reduction in the estimates for the rate of infection between group 3 and group 4 and as mentioned before it would be interesting to see what would happen if there were to be more than 4 groups. It could be possible that the virus in group 1, which is taken from laboratory stocks, although able to cause infection in group 1 sheep, may lack some factor which promotes infectivity. By contrast,

group 3 and group 4 sheep are exposed only to a natural virus. In Section 6.9.4, a formal test of trend in the rate of infection across groups is performed.

Modelling the entire infection process enabled the expected time of infection for the last sheep in group 3 of experiment 1 to be estimated. The improvement on the β estimate for this group is remarkable. Even though estimates in the other groups are similar for the two methods, modelling the entire infection process allows the use of more information from the experimental data in estimating the rate of infection and in estimation of the expected infection process characteristics *i.e.* time of infection, time of start of infectiousness and removal time for the infection process. Modelling the entire infection process is however, more computationally intensive, whereas modelling of the partial infection process could be implemented using a hand calculator. In Figure 6.7, comparisons of the scaled total time of infection exposure and β_g estimates obtained from both experiments are presented graphically. The graphs indicate that the estimate for the scaled total time of infection exposure and β_g estimates are similar for both methods except in group 3 of experiment 1.

Figure 6.7: *Estimated expected total exposure time (in days) and β estimates (per day) from partial and full infection process models for Experiments 1 and 2.*

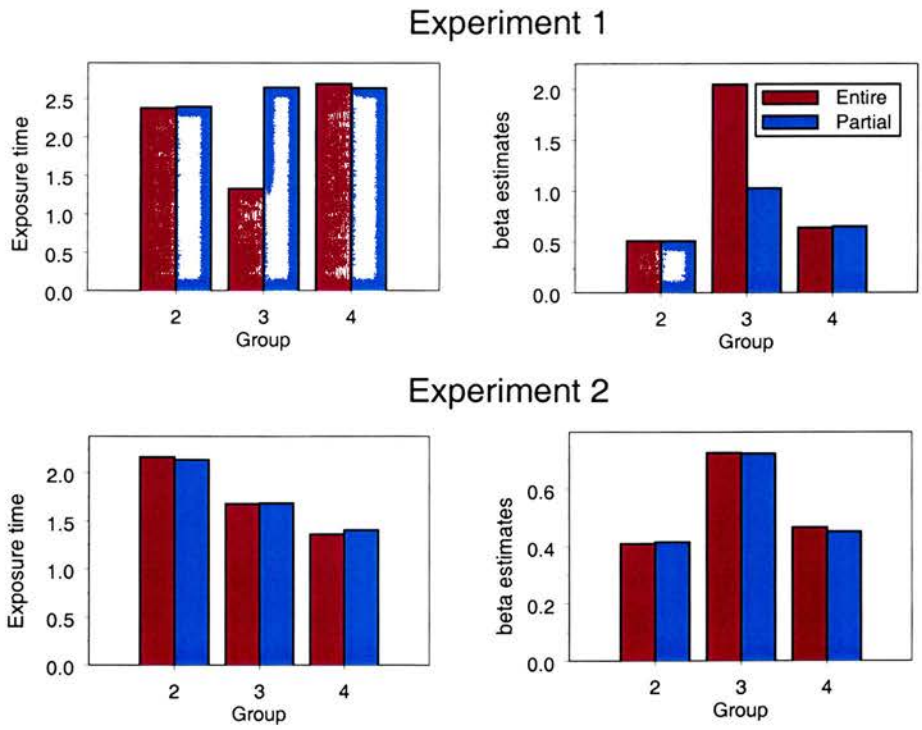

Tables 5.5 and 5.6 present the estimated infectiousness history inferred from the partial model, which can be compared with Tables 6.6 and 6.7 respectively. There is no consistent pattern apparent when comparing the inferred histories from the two models. Estimated infectiousness start times in group 2 individuals tend to be earlier in the full model, but there is one animal where the infectiousness start time comes later. Infectiousness periods vary marginally, but no clear trend is apparent. This is clear from the estimated total exposure times presented in Figure 6.7, where, with the exception of group 3, experiment 1, there are only marginal changes in the summed estimates between the two models. Given the differences seen, for group 3, experiment 1 arises from the imposition of an earlier cut-off point in the full model calculations, rather than from any systematic differences in the estimated infectiousness periods.

6.9.4 Assessment of trend in the rate of infection

To estimate the trend in the rate of infection across groups, weighted linear regression analyses were performed. β_g estimates were regressed against group numbers 2 to 4 with weights given by $(\frac{1}{\text{S.e}(\hat{\beta})})^2$. The model was fitted in the Splus statistical package and the results from both experiments are presented in Table 6.9.

Table 6.9: *Regression results for trend test for both experiments.*

	coefficients:				
		value	std error	t-value	Pr(> |t|)
Expt 1	intercept	0.4060	0.8053	0.5045	0.7026
	groups	0.0728	0.2709	0.2686	0.8330
Expt 2	intercept	0.3699	0.3680	1.0052	0.4984
	groups	0.0405	0.1246	0.3251	0.7999

The regression analysis results indicate a non-zero positive slope for both experiments. Give the $p-$values, there is no evidence of any significant trend in the β estimates. However, because the β estimates are not independent, these regression analysis $p-$values are not correct. It is necessary to calculate a valid $p-$value to test whether the slope for the β estimates is significantly less than that arising under the null hypothesis of no change in infection rate with increased infection generation. This is carried out using bootstrap methods.

6.9.4.1 Testing trend

Bootstrap epidemic samples were generated using the simulation model described in Section 6.7.1.2. For both experiments, a global rate of infection is estimated and this estimate is used as the rate of infection for all infected individuals. 200 bootstrap epidemic samples were generated from the simulation model assuming no trend in the rates of infection *i.e.* the passage multiplier was set to zero.

6.9.4.2 Estimate of global rate of infection (β_{global})

Information from all groups is combined to calculate a martingale based estimate for β_{global} as described in Section 6.7.1.1 using Equation (6.37). Using estimates for the expected total infection exposure for each group (Table 6.8), and values for the B integral (Table 5.8), an initial value for β_{global} is calculated.
For experiment 1 the initial estimate is given by:

$$\hat{\beta}_{global} = \frac{1.2179 + 2.7179 + 1.7179}{2.38 + 1.33 + 2.69} = 0.8834,$$

and for experiment 2 the initial estimate is:

$$\hat{\beta}_{global} = \frac{0.8845 + 1.2179 + 0.6345}{2.16 + 1.68 + 1.36} = 0.5263.$$

β_{global} is then estimated iteratively using Algorithm 6.1, Section 6.5. Estimates for β_{global} and the corresponding estimates for the scaled expected infection exposure time, derived from the final iteration of the fitting procedure, are presented in Table 6.10. For experiment 1, $\hat{\beta}_{global}$ is 0.8818 per day and for experiment 2, $\hat{\beta}_{global}$ is 0.5258 per day.

Table 6.10: *Estimates for global rate of infection for experiments 1 and 2.*

	B-Integral	Overall exposure time	Global β estimate
Experiment 1	5.6537	6.4111	0.8818
Experiment 2	2.7369	5.2056	0.5258

6.9.4.3 Bootstrapping results

Using the estimated latent and infectiousness period gamma distribution parameters for each experiment (*i.e.* estimated mean latent period of 0.98 and estimated

mean infectiousness period of 2.81 days for experiment 1 and estimated mean latent period of 0.95 and estimated mean infectiousness period of 2.79 days for experiment 2), and the estimated global rate of infection for each experiment (0.8818 for experiment 1 and 0.5258 for experiment 2), 200 bootstrap epidemic samples were generated from the simulation model. The resulting epidemic data were analysed using the full model of the infection process, yielding estimates for β_g for groups 2 to 4 for each epidemic realisation. Weighted linear regression analyses were performed on each set of β estimates and estimates for the slopes obtained. Descriptive statistics of the slope distribution are presented in Table 6.11 and histograms of the slopes simulated for each experiment are presented in Figure 6.8.

The aim of the bootstrap exercise was to calculate a $p-$value to test whether the estimated slopes from the experimental data are significantly less than those arising from the null hypothesis. For experiment 1 a total of 139 slopes were less than 0.0728, the estimated slope from the experimental data, yielding a $p-$value of $\frac{139}{200} = 0.695$. For experiment 2, 143 slopes were less than 0.0405, the estimated slope from the experimental data, yielding a $p-$value of 0.715. Thus for both experiments, the estimated slope was not significantly less than those generated under the null hypothesis, leading to the conclusion that there is no significant decreasing trend in the estimated rates of infection across groups. Rather, the estimated slopes from both experiments fall well within the distribution of the bootstrap estimated slopes. For experiment 1, the estimated slope of 0.0728 lies in the right tail of the distribution of the bootstrap slopes at the 70% point. For experiment 2, the estimated slope of 0.0405 also lies in the right tail of the distribution of the bootstrap slopes at the 72% point. If the slopes were significantly less than those arising under the null hypothesis, they would fall at the extreme left ends or outside the distribution of the bootstrap estimated slopes. Hence it is concluded that there is no significant decreasing trend in the estimates for the rates of infection across groups in either experiment.

Table 6.11: *Descriptive statistics for bootstrap slopes.*

variable	N	mean	median	st dev	se mean	min	max	Q_1	Q_3
Slope (Experiment 1)	200	-0.0341	-0.0230	0.3106	0.0220	-1.2058	0.8610	-0.1818	0.1144
Slope (Experiment 2)	200	-0.0407	-0.0156	0.1476	0.0104	-0.5657	0.3224	-0.1467	0.0501

Figure 6.8: *Histograms of slopes from the bootstrap epidemics, the dashed lines denote the observed (estimated) slope of* 0.0728 *for experiment 1 and the observed (estimated) slope of* 0.0405 *for experiment 2.*

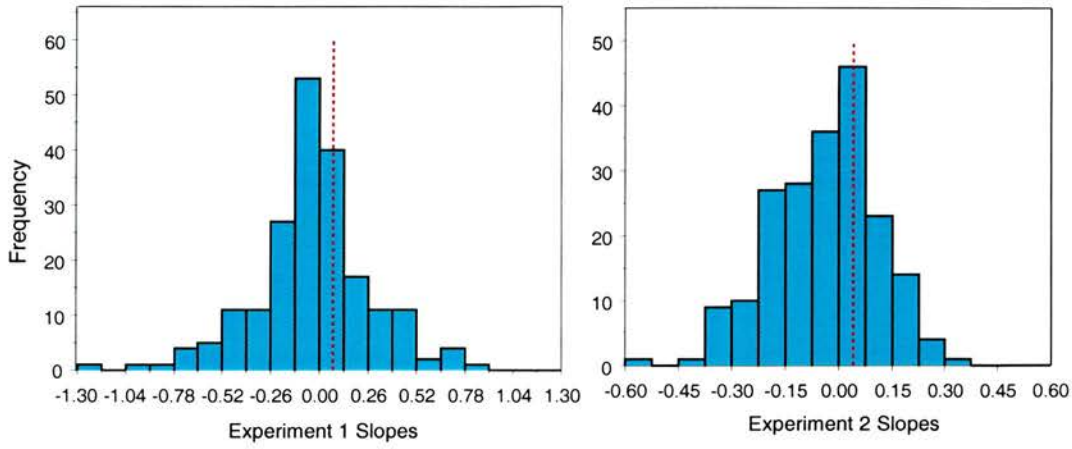

6.10 Summary

Full modelling of the infection process is of crucial importance. Time of infection, length of latent period and length of infectiousness period are all very important components of the infection process as far as infectious diseases are concerned. It is always of interest to know whether individuals have been at high risk of contracting infection when they have been exposed. The methods described in this chapter can be used to model infectious disease data effectively, estimating aspects of the infection history and all of the parameters involved.

Through full modelling of the infection process, estimates for the expected values of the infection process characteristics for each individual were obtained. Using the estimated expected times to infection, a cut-off point was estimated for the expected infection exposure time as is necessary for the calculation of the martingale estimate for β in groups where all individuals become infected. Also, the model no longer necessitated the assignment of an equal amount of estimated unobserved infectiousness period to the two portions of the unobserved infectiousness period before τ and after ω. The results indicate that the expected values of the unobserved infectiousness periods were typically not equal and varied according to the number of observed negative days n_l and the number of positive days n_e.

Considering the results from this analysis, the conclusion may be that there is no

significant trend in the rate of infection across groups. As mentioned previously, it would be of great interest to discover what would happen if there were more than 4 groups, whether the decreasing trend in infectivity would become apparent in later groups (group 3 onwards). Taking into account Home Office regulations, laboratory facilities and other logistic constraints, it unlikely to be feasible to have more groups. An alternative may be to increase the number of sheep in each group, provided that this is logistically possible for the laboratory and acceptable to the regulatory authorities, given the size of the rooms in which sheep are housed.

It could be that a significant trend was not detected because:

1. It did not exist.
2. The inferential methods were not appropriate to the nature of the data.
3. The number of sheep in each group was too small to yield a significant trend, given the size of effect present.

These options are investigated in Chapter 8.

Chapter 7

Full modelling of the infection process: ML estimation methods

7.1 Introduction

As in the previous chapter, the aim of the current chapter is to model the entire infection process by estimating the unobserved infection process characteristics, *i.e.* the times of infection, the length of latent period, the length of infectiousness period and the rate of infection, β_g, acting upon step group g ($g = 2, 3, 4$). In this chapter, the β_g are estimated using MLE methods, in contrast to the martingale methods used in the previous chapter. Two sets of β_g estimates are considered using MLE methods applied to two different models, namely, the unrestricted and restricted models (refer to Section 4.2). Full modelling of the infection history is therefore carried out separately for the two MLE models.

The difference between Chapter 6 and the current chapter lies in the method of estimating β. The assumed distributions for the latent and infectiousness periods and the corresponding parameter estimates, as defined in the previous chapter, will still be utilised. Estimates for the infection process characteristics for group 1 sheep will also be retained, since these are unaffected by the method of estimation of β. The infection process in groups 2 to 4, which is affected by β, will be the considered in this chapter. Using an algorithm similar to Algorithm 6.1, the process of obtaining estimates of the infection process characteristics and of the β_g is carried out with the martingale estimator replaced by the ML estimators. The ML estimators use more of the estimated infection history than was required for the martingale estimators in Chapter 6. It is of interest to see how the two classes of estimator compare.

7.2 Estimation of entire infection process

The model distributions for the length of the latent and infectiousness periods, the corresponding distribution parameter estimates and the estimated infection process characteristics for group 1 sheep, obtained in Chapter 6, are retained. Here, therefore, the focus is on the infection process of sheep in groups 2 to 4.

7.2.1 Infection process for group 2 to 4 sheep

For groups 2 to 4, the time to infection, the length of latent period and length of infectiousness period for all infected sheep are to be estimated. Estimates for the infection process characteristics of any infected animal are obtained conditional on the time of the first observed positive test, τ and the time of the last observed positive test, ω, and on estimates of the infection process characteristics of animals whose infection preceded that of the subject. Estimates of the expected time of infection and expected length of latent period are calculated from a joint distribution of the two variables conditional on τ and the past history of the epidemic, as described in Section 6.4.2.2. Following the calculation of estimates for the expected time to infection and expected length of latent period, estimates for the expected length of infectiousness period are obtained for each infected sheep based on the infectiousness period distribution conditional of the observed number of positive samples (refer to Equation (6.36), Section 6.4.2.5).

7.3 Estimation of rate of infection

In the current chapter, the rate of infection acting upon groups 2 to 4 is to be estimated using MLE methods. These methods are described in Section 4.2. Two sets of ML estimates (unrestricted model and restricted model) are determined. Expressions for the unrestricted model estimators for the β_g and the corresponding standard error estimates are given in Equations (4.3) and (4.4) respectively. The restricted model ML estimates of the β_g depend on whether the estimates fall within or on the boundary of the restricted parameter space, and correspond to distinct scenarios. If the estimates fall within the restricted parameter space, *i.e.* $\hat{\beta}_2 > \hat{\beta}_3 > \hat{\beta}_4$ (Case 1), then the estimates for the β_g are the same as those obtained for the unrestricted model MLE. If, however, the ML estimates fall on the boundary of the parameter space, then there are three possible cases (Cases 2 to 4), to

which the estimates may correspond (Section 4.2.3). In Case 2 ($\hat{\beta}_2 = \hat{\beta}_3 > \hat{\beta}_4$), expressions for the $\hat{\beta}_g$ are given in Equation (4.8) and the corresponding standard error estimates are given in Equations (4.9) and (4.10). In Case 3 ($\hat{\beta}_2 > \hat{\beta}_3 = \hat{\beta}_4$), the estimators for the β_g and the corresponding standard error estimates are as given in Equation (4.11). In Case 4 ($\hat{\beta}_2 = \hat{\beta}_3 = \hat{\beta}_4$), the estimator for the single value of β and the corresponding standard error estimate are given in Equation (4.12). ML estimates for the β_g from the restricted model are obtaining using Algorithm 4.1, Section 4.2.3.

The objective is to estimate the β_g and to investigate whether or not there is a significant decreasing trend in the estimates for β_g across groups. To be able to calculate these estimates, the expected total duration of infection exposure, T_g, for each group of sheep has to be estimated. Modelling the entire infection process makes this possible, because from the estimates of the expected length of infectiousness period, estimates for the durations of infection exposure due to specific infected sheep can be obtained. As a result, T_g, which depends on the expected length of infectiousness period of infected sheep, can be estimated using Equation (4.15).

However, the hazard function, $h(\cdot)$, in the density function for the time to infection (Equation (6.1)) involves β. Thus, estimates of the β_g are obtained alternately with estimates of the expected infection process characteristics, via an iterative scheme. The estimates of T_g required to calculate estimates of the β_g are obtained from the estimated length of infectiousness periods. Taking into account the different estimation method for the β_g and the need to estimate T_g, the equivalent iterative scheme to Algorithm 6.1 is given in Algorithm 7.1 below.

Algorithm 7.1

1. Assume the latent period distribution to be a gamma distribution with parameters $\hat{\nu}_{lat}$ and $\hat{\lambda}_{lat}$ as previously estimated.

2. Assume the infectiousness period distribution to be a gamma distribution with parameters $\hat{\nu}_{inf}$ and $\hat{\lambda}_{inf}$ as previously estimated.

3. Initialise the estimates for the rates of infection, $\hat{\beta}_2$, $\hat{\beta}_3$ and $\hat{\beta}_4$ applying to groups of sheep to the martingale β_g estimates from Chapter 6.

4. Estimate the expected time to infection, expected latent period and expected infectiousness period for each infected individual, according to Equations (6.28), (6.35) and (6.36) respectively, starting with those individuals

which earliest became infective, and using estimates (from this iteration) of these values where required in the calculations for individuals with later infections.

5. Calculate the estimate for the total infection exposure, $\hat{T}_g$, for each group, according to Equation (4.15).

6. Compute new ML estimates for β_2, β_3 and β_4 using Equation (4.3) (unrestricted model MLE) or using Equations (4.3) or (4.8) or (4.11) or (4.12) within Algorithm 4.1 depending on whether the β_g estimates fall within or on the boundary of the parameter space (restricted model MLE).

7. Compare the estimates in Steps 4 and 6 with estimates from previous iteration or with initial values, in the case of the first iteration. If the difference is greater than 10^{-7} go to Step 4, else go to Step 8.

8. Take the estimates in Step 4 and Step 6 as the final estimates of the expected infection process characteristics and of the β_g.

9. End.

7.4 Investigation of trend in ML β estimates

The aim of the FMD experiments was to assess whether or not the rate of infection decreases across groups. For the ML estimates, the method used to assess the trend in the β_g estimates will differ for the two models.

7.4.1 Investigation of trend in the unrestricted model ML β estimates

As in the equivalent case where the β_g are estimated by martingale methods, the trend in the unrestricted model ML β_g estimates is measured by a slope attained from weighted linear regression analysis (Freund and Wilson, 1998, Section 4.3), where the β_g estimates are regressed against group numbers. The significance of the trend is tested using bootstrap methods (Efron and Tibishirani, 1993, Section 16.2), since, as explained in Section 6.7, the p-values obtained from the regression analysis are not valid.

Bootstrap methods involve resampling from the original data either directly or via a fitted parametric model to create replicate data sets from which the variability

of the estimates of interest can be assessed. The methods have been described in Section 6.7.1. Bootstrap epidemic realisations are generated from a simulation model, described in Section 6.7.1.2, based on the estimated infection process parameters and the properties (such as parameters for the latent period) estimated from the experimental data. In particular, the simulation model requires a rate of infection at which infectious individuals make an infectious contact. Since it is necessary to simulate epidemics under the null hypothesis of no trend in the rate of infection, a constant rate of infection acting upon groups of sheep is estimated from the experimental data and used in the simulation model as the rate of infection for infectious individuals.

7.4.1.1 Global rate of infection (β_{global})

Given the null hypothesis of an equal rate of infection from all infected sheep, an equal rate of infection is assumed for all groups and this is referred to as the global rate of infection, denoted by β_{global}. To estimate β_{global}, information from all groups is combined. The assumption that $\beta_2 = \beta_3 = \beta_4$ corresponds to case of estimates for the restricted model MLE. Hence

$$\hat{\beta}_{global} = \frac{I_2 + I_3 + I_4}{T_2 + T_3 + T_4} \quad \text{and} \quad s.e(\hat{\beta}_{global}) = \frac{\sqrt{I_2 + I_3 + I_4}}{T_2 + T_3 + T_4}. \tag{7.1}$$

$\hat{\beta}_{global}$ is obtained alternately with estimates of the expected infection process characteristics, using the iterative scheme outlined in Algorithm 7.1, with all values of β_g replaced by β_{global}.

7.4.1.2 Bootstrap epidemic samples

200 bootstrap epidemic realisations are generated using the simulation model described in Section 6.7.1.2, using model parameters estimated from the experimental data. The generated epidemic realisations are analysed using the methods described in this chapter, to obtain both unrestricted and restricted model ML estimates for the β_g.

Considering the unrestricted model ML estimates, weighted linear regression analyses are performed by regressing the β estimates against group number to generate an estimate of the slope as a measure of the trend in the estimated β_g. From the distribution of the 200 estimated slopes, a bootstrap p-value is obtained. The null hypothesis states that the slope is equal to 0, *i.e.* there is no trend in the

β estimates, while the alternative hypothesis is that the slope is less than 0, *i.e.* there exists a decreasing trend in the β estimates. If the estimated slope from the experimental data is significantly less than 0, it will be expected to fall to the left end of the distribution of the slopes estimated from the bootstrap samples. The one-sided significance probability for the unrestricted model MLE is given by:

$$p\text{-value} = \frac{\#\{\text{bootstrap slopes} < \text{observed (estimated) slope}\}}{\text{total number of bootstrap samples}}. \quad (7.2)$$

7.4.2 Investigation of decrease in the restricted model ML β estimates

With the restricted model, a non-increasing trend is assured for the estimated β_g. The objective of the analysis is to investigate whether there is a significant decrease in the estimated β_g across groups. The size of the decrease in β will be measured by $\hat{d}_{23} = \ln(\hat{\beta}_2) - \ln(\hat{\beta}_3)$, the estimated decrease between the infection rate acting upon group 2 sheep and the infection rate acting upon group 3 sheep and by $\hat{d}_{34} = \ln(\hat{\beta}_3) - \ln(\hat{\beta}_4)$, the estimated decrease between infection rate acting upon group 3 sheep and the infection rate acting upon group 4 sheep. Estimates of the size of any decrease are calculated on the log scale, since the β_g were estimated on a log scale in terms of the α_g (Section 4.2.3), in fact $\hat{d}_{23} = \hat{\alpha}_2 - \hat{\alpha}_3$ and $\hat{d}_{34} = \hat{\alpha}_3 - \hat{\alpha}_4$. In many cases these estimated decreases will equal zero, which would tend to give rise to a poorly fitting regression line. Hence the use of this alternative approach. The statistic selected to summarise the overall decrease will be chosen the more significant of the two quantities $\hat{d}_{23}$ and $\hat{d}_{34}$. The significance is assessed by comparing the quantities $\frac{\hat{d}_{23}}{s.e(\hat{d}_{23})}$ and $\frac{\hat{d}_{34}}{s.e(\hat{d}_{34})}$. The larger value is the more significant and the decrease in β by group will then be summarised by $\hat{d}_{23}$ or $\hat{d}_{34}$, depending on which quantity corresponds to the more significant effect. The decrease in β is also estimated by the sum of $\hat{d}_{23}$ and $\hat{d}_{34}$. The need to choose between the two measures arises only in Case 1 situations where all the three β_g $(\beta_2, \beta_3, \beta_4)$ are estimated. Both measures will be used in assessing the decrease in β across groups. In Case 1 situations, use of the first measure will require standard error estimates for $\hat{d}_{23}$ and $\hat{d}_{34}$. These are calculated, based on the δ-method (Becker, 1989, Appendix), and are given by:

$$s.e(\hat{d}_{23}) = \sqrt{\left(\frac{1}{\hat{\beta}_2}\right)^2 var(\hat{\beta}_2) + \left(\frac{1}{\hat{\beta}_3}\right)^2 var(\hat{\beta}_3)} = \sqrt{\frac{1}{I_2} + \frac{1}{I_3}},$$

$$s.e(\hat{d}_{34}) = \sqrt{\left(\frac{1}{\hat{\beta}_3}\right)^2 var(\hat{\beta}_3) + \left(\frac{1}{\hat{\beta}_4}\right)^2 var(\hat{\beta}_4)} = \sqrt{\frac{1}{I_3} + \frac{1}{I_4}}.$$

In Case 2 situations ($\hat{\beta}_2 = \hat{\beta}_3 > \hat{\beta}_4$) the decrease in β is estimated by $\hat{d}_{34}$ and the associated standard error is estimated by $\sqrt{\frac{1}{I_4} + \frac{1}{I_2+I_3}}$.

In Case 3 situations ($\hat{\beta}_2 > \hat{\beta}_3 = \hat{\beta}_4$) the decrease in β is estimated by $\hat{d}_{23}$ and the associated standard error is estimated by $\sqrt{\frac{1}{I_2} + \frac{1}{I_3+I_4}}$.

In Case 4 situations ($\hat{\beta}_2 = \hat{\beta}_3 = \hat{\beta}_4$) the decrease in β is zero.

7.4.2.1 Testing the significance of a decrease in the restricted model ML β estimates

To test whether an observed decrease in β is significantly greater than 0, bootstrap methods are used. 200 bootstrap epidemics are simulated using the simulation model described in Section 7.4.1.2. The data from each bootstrap epidemic realisation are analysed based on the established model of the entire infection process incorporating restricted model MLE for the β_g. For each bootstrap realisation, the estimate for the decrease in the estimated β_g is determined. The estimated decreases in β are sorted and compared with the estimate of the decrease from the experimental data. If the decrease in β from the experimental data is significantly greater than 0, it lies in the tail/outside the distribution of the estimated bootstrap decreases. The test of significance of decrease is one sided and the p-value for testing the significance of any decrease in β is given by:

$$p\text{-value} = \frac{\#\{\text{bootstrap decreases} > \text{observed (estimated) decrease}\}}{\text{total number of bootstrap samples}}. \quad (7.3)$$

7.5 Application to experimental data

The inferential methods described in the current chapter are implemented by programming in C (Kernighan and Ritchie, 1988) and S-Plus (Venables and Ripley, 1994). Programs were developed to fully model the infection process and the methods were applied to the experimental data generated from the two identical FMD experiments and to simulated data.

The results presented in the current chapter will initially describe the estimated infection histories for group 2 to 4 individuals. Comparisons by method of estimation / choice of model for β (martingale - ML / unrestricted - restricted) will be made for the estimated infection process characteristics and for the β estimates.

7.5.1 Estimates of infection history for sheep from groups 2 to 4

Estimates for the expected infection process characteristics and for the β_g are obtained as described in Sections 7.2.1 and 7.3 respectively. The results from the final iteration of the analysis process are presented.

7.5.1.1 Estimated infection process characteristics

In Table 7.1, estimates of the expected time to infection, expected length of latent period and expected length of infectiousness period for both experiments are presented. Also presented in the same table are the equivalent martingale based estimates. The results presented are: the sheep identity number, 'Sheep ID', estimates of the expected time of infection, 'Exp Inf T', estimates of the expected length of latent period, 'Exp Latent' and estimates of the expected length of infectiousness period, 'Exp Inf P'. To highlight the differences in the estimates, results are presented to 3 decimal places. The estimated entire infection history for both experiments are presented graphically in Figure 7.1 (unrestricted model for β) and Figure 7.2 (restricted model for β).

In experiment 1, from both unrestricted and restricted models, only sheep number 11 has its expected time of infection estimated as occurring during the estimated infectiousness state of group 1 sheep. This is in spite of the fact that, in total, groups 1 and 2 are mixed for an estimated 2.4 days during the estimated typical infectiousness period of group 1 sheep. Hence, it is likely that only 1 group 2 sheep became infected due to group 1 infectious sheep (refer to Table 6.5). Similarly, in experiment 2, only 1 sheep (number 9), has its expected time of infection estimated as occurring during the estimated infectiousness period of group 1 sheep. It appears that the choice of the model for β_g has made little appreciable difference to the estimated expected infection process characteristics, even in group 2 of experiment 1 where it might have been expected that a switch to restricted model MLE would result in changes to the expected pattern of infection. The differences which are present will be discussed in Section 7.5.1.3.

Figure 7.1: *The estimated infection history from unrestricted model MLE.*

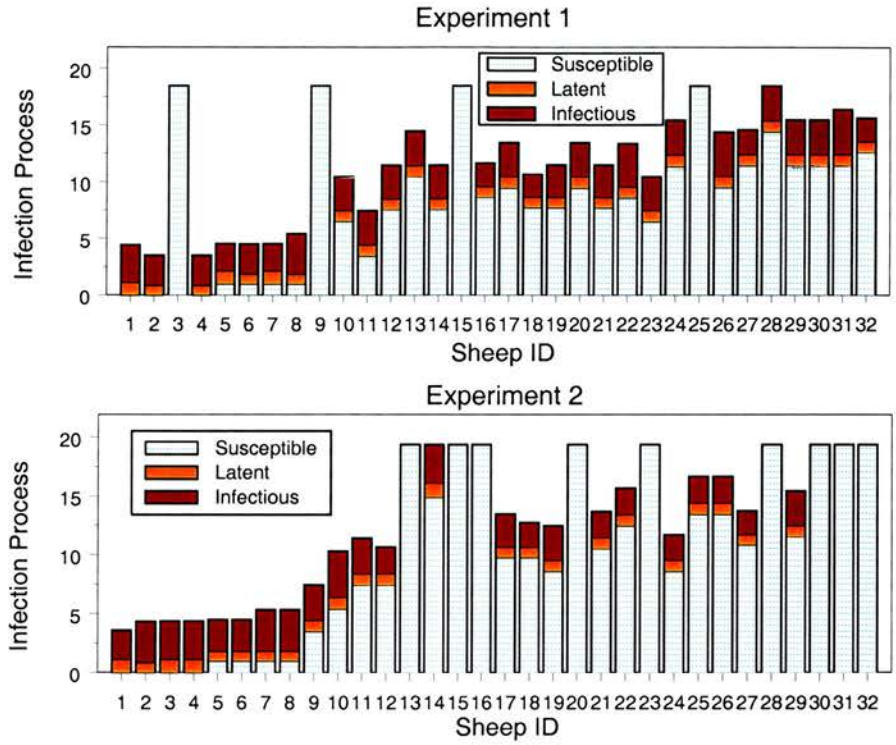

Figure 7.2: *The estimated infection history from restricted model MLE.*

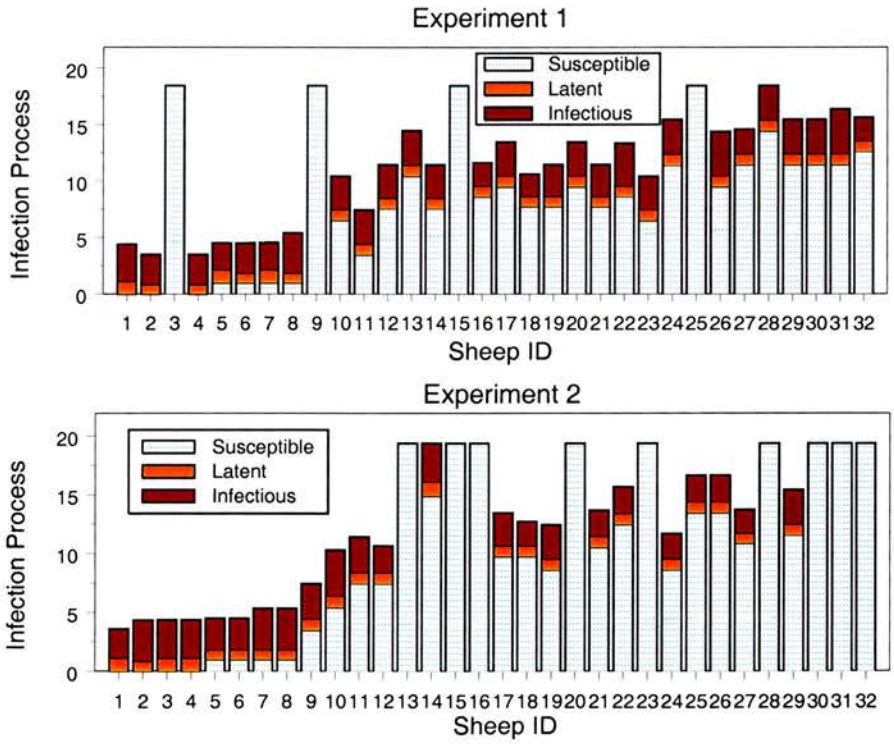

Table 7.1: *Estimates for the expected infection process characteristics, for infected individuals of groups 2 to 4, based on restricted model ML, unrestricted model ML and martingale estimation for β. Sheep numbers 9, 15, 25 (experiment 1) and 13, 15, 16, 20, 23, 28, 30, 31, 32 (experiment 2) did not shed virus.*

		Restricted MLE			Unrestricted MLE			Martingale estimates		
	Sheep ID	Exp Inf T	Exp Latent	Exp Inf P	Exp Inf T	Exp Latent	Exp Inf P	Exp Inf T	Exp Latent	Exp Inf P
	10	6.513	0.981	2.958	6.517	0.980	2.956	6.517	0.980	2.955
	11	3.444	0.990	3.012	3.457	0.988	3.003	3.459	0.987	3.001
	12	7.559	0.967	2.929	7.564	0.966	2.926	7.564	0.966	2.926
	13	10.449	0.994	3.004	10.471	0.989	2.989	10.475	0.988	2.986
E	14	7.559	0.967	2.929	7.564	0.966	2.926	7.564	0.966	2.926
X	16	8.640	0.957	2.026	8.650	0.955	2.019	8.652	0.954	2.018
P	17	9.520	0.982	2.950	9.452	1.003	2.993	9.481	0.994	2.975
E	18	7.735	0.937	1.966	7.724	0.941	1.972	7.729	0.939	1.970
R	19	7.735	0.937	2.800	7.724	0.941	2.807	7.729	0.939	2.804
I	20	9.520	0.982	2.950	9.452	1.003	2.993	9.481	0.994	2.975
M	21	7.735	0.937	2.800	7.724	0.941	2.807	7.729	0.939	2.804
E	22	8.648	0.954	3.780	8.613	0.962	3.805	8.628	0.959	3.795
N	23	6.506	0.980	2.966	6.498	0.981	2.971	6.501	0.981	2.969
T	24	11.409	1.009	3.026	11.345	1.029	3.066	11.372	1.021	3.049
	26	9.518	0.978	3.880	9.518	0.978	3.880	9.523	0.977	3.876
1	27	11.448	0.991	2.151	11.448	0.991	2.151	11.455	0.989	2.147
	28	14.416	1.001	3.027	14.416	1.001	3.027	14.432	0.998	3.016
	29	11.448	0.991	3.007	11.448	0.991	3.007	11.455	0.989	3.003
	30	11.448	0.991	3.007	11.448	0.991	3.007	11.455	0.989	3.003
	31	11.448	0.991	3.934	11.448	0.991	3.934	11.455	0.989	3.929
	32	12.631	0.960	2.031	12.631	0.960	2.031	12.643	0.957	2.024
	9	3.486	0.964	2.975	3.492	0.963	2.970	3.493	0.963	2.970
	10	5.424	0.978	3.896	5.426	0.977	3.895	5.426	0.977	3.895
E	11	7.443	0.978	2.998	7.445	0.977	2.997	7.445	0.977	2.997
X	12	7.443	0.978	2.238	7.445	0.977	2.237	7.445	0.977	2.237
P	14	14.887	1.225	3.259	14.887	1.225	3.259	14.887	1.225	3.259
E	17	9.778	0.909	2.784	9.772	0.911	2.787	9.777	0.909	2.785
R	18	9.778	0.909	2.043	9.772	0.911	2.046	9.777	0.909	2.044
I	19	8.611	0.943	2.890	8.608	0.944	2.892	8.611	0.943	2.890
M	21	10.542	0.953	2.184	10.530	0.956	2.190	10.539	0.954	2.186
E	22	12.475	0.971	2.220	12.464	0.974	2.226	12.472	0.971	2.222
N	24	8.611	0.943	2.141	8.608	0.944	2.143	8.611	0.943	2.141
T	25	13.457	0.975	2.230	13.457	0.975	2.230	13.459	0.974	2.229
	26	13.457	0.975	2.230	13.457	0.975	2.230	13.459	0.974	2.229
2	27	10.855	0.872	2.014	10.855	0.872	2.014	10.856	0.871	2.014
	29	11.558	0.949	2.928	11.558	0.949	2.928	11.561	0.948	2.926

7.5.1.2 Estimates of rate of infection

Recall from Section 4.2.2 (Equation (4.3)) that the estimates for the β_g acting upon groups of sheep from the unrestricted model MLE are given by:

$$\hat{\beta}_g = \frac{I_g}{T_g}, \quad g = 2, 3, 4.$$

For the restricted model MLE, the expressions for the estimates of β depend on the particular case. For the experimental data, the β estimates correspond to Case 2 ($\hat{\beta}_2 = \hat{\beta}_3 > \hat{\beta}_4$) and the β_g estimates are given by:

$$\hat{\beta}_2 = \hat{\beta}_3 = \frac{I_2 + I_3}{T_2 + T_3} \text{ and } \hat{\beta}_4 = \frac{I_4}{T_4},$$

where I_g is the total number of infected individuals in group g and T_g is estimated by the expected total duration of infection exposure determined from Equation (4.15).

Tables 7.2 and 7.3 present estimates for the expected total infection exposure time, estimates for the β acting upon groups 2 to 4 and the corresponding standard error estimates. It should be remembered that these estimates of standard error are likely to be unreliable. For comparison purposes, the corresponding martingale estimates are also included.

Table 7.2: *Estimates of the expected total scaled group exposure time in days (time) and the estimated group rate of infection ($\hat{\beta}$) per day for experiment 1.*

		Restricted ML estimates			Unrestricted ML estimates			Martingale Estimates	
Group	Infs	Time	$\hat{\beta}$	$s.e(\hat{\beta})$	Time	$\hat{\beta}$	$s.e(\hat{\beta})$	$\hat{\beta}$	$s.e(\hat{\beta})$
2	6	9.88	1.0881	0.2908	9.92	0.6051	0.2470	0.5116	0.2213
3	8	2.98	1.0881	0.2908	2.92	2.7388	0.9683	2.0469	0.9308
4	7	7.74	0.9046	0.3419	7.75	0.9032	0.3414	0.6377	0.2696

Table 7.3: *Estimates of the expected total scaled group exposure time in days (time) and the estimated group rate of infection ($\hat{\beta}$) per day for experiment 2.*

		Restricted ML estimates			Unrestricted ML estimates			Martingale Estimates	
Group	Infs	Time	$\hat{\beta}$	$s.e(\hat{\beta})$	Time	$\hat{\beta}$	$s.e(\hat{\beta})$	$\hat{\beta}$	$s.e(\hat{\beta})$
2	5	11.86	0.6220	0.1875	11.86	0.4217	0.1886	0.4087	0.1884
3	6	5.83	0.6220	0.1875	5.82	1.0303	0.4206	0.7256	0.3138
4	4	6.98	0.5728	0.2864	6.99	0.5722	0.2861	0.4655	0.2364

Unrestricted ML estimates

For experiment 1, the results for the unrestricted model ML estimates indicate a similar trend to that seen in the martingale estimates, *i.e.* group 2 has the lowest estimated rate of infection of 0.605 per day with a standard error estimate of 0.247, followed by group 4 with an estimate of 0.903 per day (s.e = 0.341) and group 3 has the highest estimate of 2.739 per day (s.e = 0.968). The unrestricted model ML estimates are, however, higher than the corresponding martingale estimates (Table 7.2). The martingale estimator in Equation (4.17) which uses less information from the inferred historical infection characteristics, produces lower estimates of β_g.

Similarly, the β_g estimates from experiment 2 also depict a trend similar to that seen in the martingale based estimates, with group 2 having the lowest estimated rate of infection of 0.422 per day (s.e = 0.189), followed by group 4 with an estimated rate of infection of 0.572 per day (s.e = 0.286) and group 3 having the highest estimate of 1.030 per day (s.e = 0.421). The estimates for the β_g, as in experiment 1, are consistently higher than the corresponding martingale estimates (Table 7.3).

Restricted ML estimates

For experiment 1, the restricted model MLE results show that group 2 and group 3 have the same estimated rate of infection: $\hat{\beta}_2 = \hat{\beta}_3 = 1.088$ per day (s.e = 0.291). Group 4 has an estimated rate of infection $\hat{\beta}_4 = 0.905$ per day (s.e = 0.342). The results indicate a slightly higher rate of infection acting upon groups 2 and 3 sheep than that acting upon group 4 sheep. However, the difference is unlikely to be statistically significant. The results of experiment 2 depict a similar trend to that displayed by experiment 1 results. Here, $\hat{\beta}_2 = \hat{\beta}_3 = 0.622$ per day (s.e = 0.188) and $\hat{\beta}_4 = 0.573$ per day (s.e = 0.2864). These result indicate a slightly higher estimated rate of infection acting upon groups 2 and 3 sheep than that acting upon group 4 sheep, but again this is unlikely to be statistically significant.

7.5.1.3 Comparisons of estimated times for the three methods

In the two experiments analysed, the effect using restricted model MLE has been to increase the estimated rate of infection acting upon group 2 sheep from $\frac{I_2}{T_2}$ to $\frac{I_2+I_3}{T_2+T_3}$, *i.e.* by a quantity of $\frac{T_2I_3-I_2T_3}{T_2(T_2+T_3)}$. The estimate for the rate of infection acting upon group 3 sheep is, however, reduced from $\frac{I_3}{T_3}$ to $\frac{I_2+I_3}{T_2+T_3}$. Thus the resulting estimate for β_2 from the restricted model is higher than the corresponding β_2 estimate from the unrestricted model. The effect of the restricted model is also reflected in the estimates for the expected infection process characteristics. Although not very different in either experiment, the estimated times of infection for group 2 individuals using the restricted model are earlier than those obtained from the unrestricted model. This is due to the fact that $\hat{\beta}_2$ from the unrestricted model MLE is lower than that from restricted model MLE. Hence individuals in group 2 are estimated as becoming infected earlier in time using the restricted model than when using the unrestricted model estimates. For group 3, the reverse is true; $\hat{\beta}_3$ is higher from unrestricted model MLE than from restricted model MLE. The estimates of the expected times of infection for individuals in this group are earlier using the unrestricted model than when using the restricted

model. For example, in experiment 1, individual number 10 of group 2 has an estimated time of infection of 6.517 days using the unrestricted model compared to 6.513 days using the restricted model, whereas individual number 17 of group 3 has an estimated time of infection of 9.452 days using the unrestricted model compared to 9.520 days using the restricted model. For group 4, the estimates for the expected times of infection are the same for both restricted and unrestricted models except for very minor differences due to the effect of group 3 individuals that contribute to the estimates of group 4 expected infection exposure time.

It should be noted that the differences discussed here generally arise only at third decimal place, *i.e.* in terms of ($\frac{1}{1000^{th}}$ of a day). In general, because the martingale method yields the lowest β estimates for all groups, it leads to later estimates for the expected times of infection. For group 2 individuals, the estimated times of infection are latest using martingale methods, followed by those using the unrestricted model MLE, with those using the restricted model MLE yielding the earliest times. Considering the expected length of latent period and expected length of infectiousness period, the martingale method is associated with the shortest estimates, followed by the unrestricted model, with the restricted model being associated with the longest lengths of time. For group 3 individuals, the restricted model MLE gives rise to the lowest β_3 estimates in both experiments, and is associated with the latest estimates for the expected times of infection, followed by martingale based estimates, while the unrestricted model is associated with the earliest times. The restricted model gives rise to the shortest estimates for the expected length of latent and infectiousness periods, followed by the martingale method, with the unrestricted model generating the largest estimates. Estimates for the three expected infection process characteristics using the unrestricted and restricted models are identical for group 4 individuals. The martingale method gives the lowest β_4 estimates and hence is associated with the latest estimates for the expected times of infection and the shortest estimates for the expected length of latent and infectiousness periods.

7.5.2 Assessment of trend in estimated rates of infection

7.5.2.1 Unrestricted model MLE

The trend in the β_g estimates from unrestricted model MLE is assessed using weighted linear regression. The β_g estimates, with $(\frac{1}{\text{S.e}(\hat{\beta})})^2$ as the weights, are regressed against group numbers. The results are presented in Table 7.4.

Table 7.4: *Weighted linear regression analysis results for experiments 1 and 2.*

	coefficients:				
		value	std error	t-value	Pr(> |t|)
Experiment 1	intercept	0.3125	1.2027	0.2599	0.8381
	groups	0.1771	0.4210	0.4206	0.7465
Experiment 2	intercept	0.2573	0.5558	0.4629	0.7240
	groups	0.1052	0.1990	0.5287	0.6904

The regression analysis yielded an estimated slope of 0.1771 for experiment 1 and 0.1052 for experiment 2. For both experiments, the results indicate an increasing trend in the β_g estimates across groups as opposed to the anticipated decreasing trend. If the alternative hypothesis of decreasing infectivity with higher infection generation were true, a negative estimate for the slope would be expected. There is a need to formally test if the estimated slopes from the experimental data are significantly less than those arising under the null hypothesis. The p-values obtained with the slope estimate are not valid because the β estimates are not independent. Bootstrap methods are used to determine valid p-values.

7.5.2.2 Testing the significance of the estimated slope

Bootstrap epidemic realisations were generated using the simulation model described in Section 6.7.1.2. A global rate of infection, β_{global}, is estimated and the estimate is used as the rate of infection for infected individuals in the simulation model, together with the estimated parameters $\hat{\nu}_{lat}$, $\hat{\lambda}_{lat}$, $\hat{\nu}_{inf}$ and $\hat{\lambda}_{inf}$ for the distributions of latent and infectiousness periods. The parameter for the passage effect, the passage multiplier, is set to zero, corresponding to a null hypothesis of no effect of infection generation on infectivity, and hence no trend in the β_g estimates across groups.

7.5.2.3 Estimate of the global rate of infection (β_{global})

Assuming that the rate of infection in groups of sheep is the same regardless of group, information from all three groups can be combined to determine an estimate for β_{global}. For both unrestricted and restricted model MLE, the expression for $\hat{\beta}_{global}$ is given by Equation (7.1). An initial value for $\hat{\beta}_{global}$ was calculated

from the values of I_g and the final iteration expected values of $\hat{T}_g$, $g = 2, 3, 4$, from the unrestricted model MLE. The values for $\hat{T}_g$ were 9.92, 2.92 and 7.75 days for groups 2, 3 and 4 respectively in experiment 1 and 11.86, 5.82 and 6.99 days for groups 2, 3 and 4 respectively in experiment 2. Thus, for experiment 1, the initial value of $\hat{\beta}_{global}$ was 1.0199 per day and for experiment 2, 0.6080 per day. $\hat{\beta}_{global}$ was obtained alternately with estimates of the expected infection process characteristics, using the iterative scheme outlined in Algorithm 7.1, with all values of β_g replaced by β_{global}.

For experiment 1, the estimate for β_{global} from the final iteration was 1.0195 per day (s.e = 0.2225), with a corresponding estimated total scaled exposure time of 20.60 days (9.89 days for group 2, 2.98 days for group 3 and 7.73 days for group 4). For experiment 2, the estimate for β_{global} from the final iteration was 0.6081 per day (s.e = 0.1570) with an estimated total scaled exposure time of 24.67 days (11.86 days for group 2, 5.83 days for group 3 and 6.98 days for group 4).

7.5.2.4 Bootstrap results

Using $\hat{\beta}_{global}$ as the rate of infection, 200 bootstrap epidemic realisations were generated from the simulation model for each experiment. The bootstrap samples were analysed using the full model for the infection process, yielding estimates for β applying to each group.

Weighted linear regression analyses were performed by regressing the β_g estimates against the group number and estimates for the slope were attained. Descriptive statistics for the slopes are presented in Table 7.5 and histograms are presented in Figure 7.3.

Table 7.5: *Descriptive statistics for bootstrap slopes, where Q_1 and Q_3 are the first and third quantiles.*

variable	N	mean	median	st dev	se mean	min	max	Q_1	Q_3
Slope (Experiment 1)	200	-0.0204	-0.0022	0.2843	0.0201	-0.8370	0.9341	-0.2411	0.1940
Slope (Experiment 2)	200	-0.0231	-0.0258	0.1872	0.0132	-0.6207	0.5235	-0.1628	0.1012

The estimated slopes from the experimental data, 0.1771 for experiment 1 and 0.1052 for experiment 2, do not fall in the tail of the distribution of the bootstrap slopes. If these estimated slopes were significantly less than those arising under the null hypothesis, they would fall in the left end of the distribution of the

Figure 7.3: *Distribution of slopes from the bootstrap epidemic realisations for experiments 1 and 2. The dotted lines indicate the observed (estimated) values for the slopes of* 0.1771 *(experiment 1) and* 0.1052 *(experiment 2).*

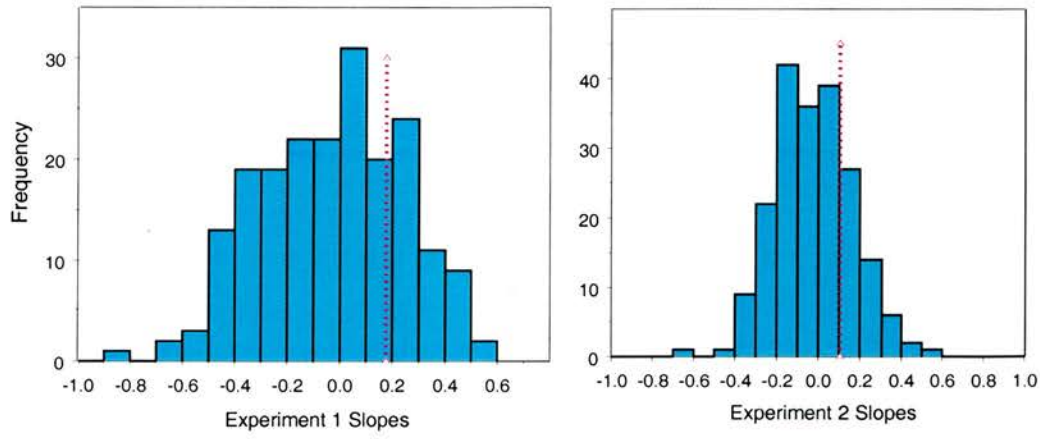

bootstrap slopes which were estimated from realisations assuming zero trend. However, for experiment 1, the slope of 0.1771 falls at the 74.5% point in the right tail of the distribution of bootstrap slopes and for experiment 2, the slope of 0.1052 falls at the 76.5% point in the right tail of the distribution of bootstrap slopes. The observed slopes are well within the distribution of the bootstrap slopes. More formally, the significance of the slopes from the experimental data is tested based on a p-value obtained from Equation (7.2).

For experiment 1, a total of 148 out of 200 estimated bootstrap slopes were less than 0.1771, the estimated slope from the experimental data, giving a p-value of $\frac{148}{200} = 0.74$. For experiment 2, a total of 152 out of 200 estimated bootstrap slopes were less than 0.1052, the estimated slope from the experimental data, giving a p-value of 0.76. It is therefore concluded that the estimated slopes from the experimental data are not significantly lower than those arising under the null hypothesis for both experiments, and hence there is no evidence of any decreasing trend in the estimated rates of infection across groups.

7.5.2.5 Assessment of trend in restricted ML estimates of β

For restricted MLE, two measures of decrease in the $\hat{\beta}_g$ were proposed, one being a choice of $\hat{d}_{23}$ or $\hat{d}_{34}$, whichever was the more statistically significant of the two, and the other being $\hat{d}_{23} + \hat{d}_{34}$. For the experimental data from both experiments,

$\hat{d}_{23} = 0$. Thus the decrease in the estimated rate of infection is measured by $\hat{d}_{34}$ with corresponding standard error estimate given by $\sqrt{\frac{1}{I_2+I_3} + \frac{1}{I_4}}$.

For experiment 1, the decrease in the estimates for the rate of infection across groups is equal to $\hat{d}_{34} = \ln(\hat{\beta}_3) - \ln(\hat{\beta}_4) = 0.1847$, with a standard error estimate of 0.4629. In experiment 2, the decrease in the estimates for the rate of infection across groups is equal to $\hat{d}_{34} = 0.0823$ (s.e = 0.5839).

7.5.2.6 Testing the significance of a decrease in the β_g

For both experiments the estimated decrease in β was greater than zero, *i.e.* 0.1847 for experiment 1 and 0.0823 for experiment 2. It was necessary to test whether these estimated decreases in β were statistically significant. This was done using bootstrap methods. Data from the 200 bootstrap epidemic realisations generated from the simulated model were analysed, with the β_g estimated using restricted model MLE. Estimates for the β_g and estimates for the decreases in β were recorded. Descriptive statistics for the decreases in β for both measures are presented in Table 7.6 and the accompanying histograms are presented in Figure 7.4.

Table 7.6: *Descriptive statistics for the estimated decreases in β from bootstrap epidemic realisations.*

	variable	N	mean	median	st dev	se mean	min	max	Q_1	Q_3
Expt 1	measure 1	200	0.2672	0.1521	0.3406	0.0241	0.0000	1.6418	0.0000	0.4118
	measure 2	200	0.3095	0.1744	0.3934	0.0278	0.0000	1.9632	0.0000	0.4808
Expt 2	measure 1	200	0.2756	0.1306	0.3299	0.0233	0.0000	1.5324	0.0000	0.4522
	measure 2	200	0.3261	0.1306	0.3996	0.0283	0.0000	1.8988	0.0000	0.5541

The estimated decreases in β, 0.1847 for experiment 1 and 0.0823 for experiment 2, fall well within the distribution of the decreases from the bootstrap samples for both experiments and for both measures of decrease (see Figure 7.4). The decrease of 0.1847 lies at the 55% point for the first measure and at the 53% point for the second, and 0.0823 lies at the 43% point for both measures. If the estimated decreases from the experimental data were significantly greater than those arising under the null hypothesis, they would fall at the extreme right of the distribution of the decreases estimated from the bootstrap realisations. The p-values are calculated using Equation (7.3) to formally test the significance of the estimated decreases in β.

Figure 7.4: *Histograms for the estimated decrease in β estimates, for both measures, from the bootstrap epidemic samples. The dotted lines indicate the observed (estimated) decreases of* 0.1847 *(experiment 1) and* 0.0823 *(experiment 2).*

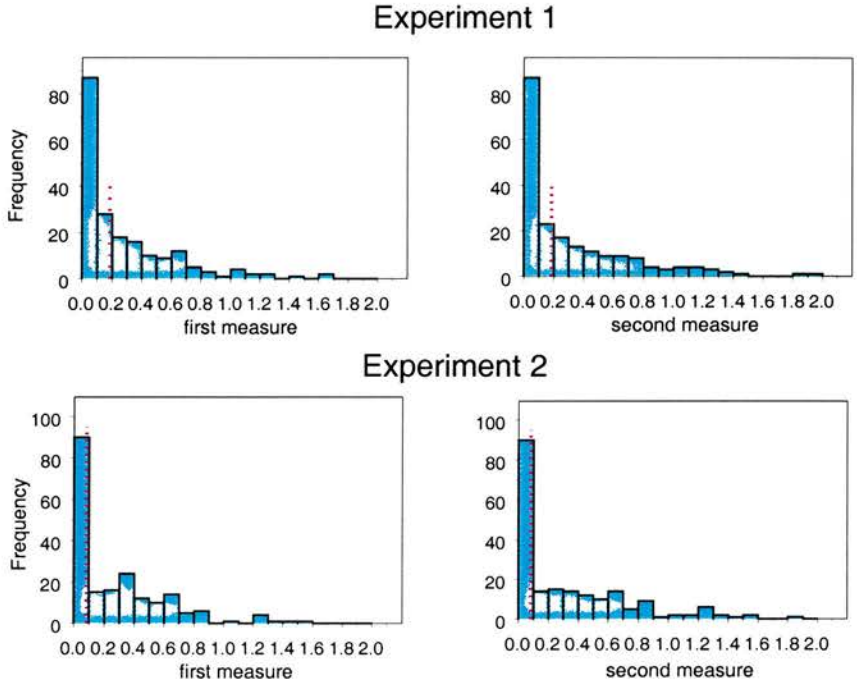

For experiment 1, the following p-values were obtained: $\frac{92}{200} = 0.46$, for the first measure of decrease, and $\frac{96}{200} = 0.48$ for the second measure. For experiment 2, the corresponding values are 0.575 for both measures. The p-values from both experiments indicate that the estimated decrease in β is not significantly greater than those arising under the null hypothesis. Thus, even with a non-increasing model imposed on the estimates, the resulting estimates for the rate of infection do not indicate a significant decreasing trend in β across groups. Indeed, in both experiments, the estimate for group 2 and group 3 is estimated to be identical and the estimate for group 4 is not appreciably smaller than that of groups 2 and 3 (compare 1.0881 versus 0.9046 for experiment 1 and 0.6220 versus 0.5728 for experiment 2).

7.6 Summary

In this chapter, using a full model of the infection process, the expected time of infection, the expected length of latent period, and the expected length of infectiousness period for all infected animals and the rate of infection acting upon

groups of sheep were all estimated. The rate of infection was estimated for both an unrestricted model and a restricted model using MLE methods. Using the unrestricted model MLE, analysis yielded a highest estimated rate of infection acting upon group 3, followed by group 4, with group 2 sheep estimated as having experienced the lowest rate of infection. The restricted model MLE yielded equal estimates for the rate of infection acting upon groups 2 and 3 and this estimate was higher than the estimate acting upon group 4. A test of significance of decreasing trend in the estimated rate of infection was not statistically significant. Hence the MLE based analyses led to the same conclusion, of no significant trend in the estimated rate of infection across groups, as seen in the martingale based analyses. Estimates for the expected infection process characteristics were similar for the restricted and unrestricted models with β fitted using ML estimation methods, with small differences only observed at the 3^{rd} decimal place in the estimates for groups 2 and 3. These differences arose from the nature of the restricted model MLE, where estimates for β_2 and β_3 were effectively pooled, leading to higher estimates in group 2 and lower values in group 3 when compared to those arising from the unrestricted model MLE analysis.

In the results from the analyses for both experiments, the estimates for β_g using the martingale estimator were lower than those for the maximum likelihood estimator from the equivalent (unrestricted) model. This could indicate the presence of a systematic bias in one (or both) of the estimators arising from the dependence on the estimated infection process characteristics. An investigation of the sampling distributions of these estimators would shed light on the matter, but the extensive computing which would be involved places such a project beyond the scope of this thesis.

Chapter 8

Illustrative study based on simulated data

8.1 Introduction

The issues posed in the discussion in Section 6.10, regarding the inferential methods developed in Chapters 5, 6 and 7, are addressed in this chapter. Initial investigations are carried out to find out whether or not the methods are capable of detecting a genuine trend in the rate of infection, β. Using the martingale and restricted model ML estimates of $\hat{\beta}_{global}$ obtained from experiment 1 data, two epidemic realisations are generated from the simulation model described in Chapter 2. A passage multiplier of 0.15 is used to produce a decreasing trend in the rate of infection. The generated data are analysed using the methods developed in Chapters 5, 6 and 7. The martingale approach is used to exemplify the properties of unrestricted model estimators, and the restricted model ML is used as being the more powerful maximum likelihood methodology. Parameters ν_{lat} and λ_{lat} for the latent period and ν_{inf} and λ_{inf} for the infectiousness period distributions, expected values of the infection process characteristics and β_g, the rates of infection acting up on groups of individuals, are estimated from the data. Trends in the $\hat{\beta}_g$ martingale estimates are summarised using weighted linear regression analysis (Freund and Wilson, 1998, Section 4.3), while those in the $\hat{\beta}_g$ restricted model ML estimates are summarised using measures of decrease as in Chapter 7. Bootstrap methods (Efron and Tibshirani, 1993, Section 16.2) are used to test the statistical significance of the estimated summaries of trend.

Further assessment of the methods is performed based on the assumption that the methods developed are appropriate for the data and that it may be a small group size, a small decrease in the β_g and/or a low reproduction ratio (R_0) that is/are

responsible for the failure to reject the null hypothesis of no trend in the β_g in the analysis of the experimental data. For this task, epidemic data are simulated under three scenarios using martingale estimates of β. One scenario models the situation where the passage multiplier is increased to ensure a large decrease in the β_g. Another models the situation where β is boosted from $\hat{\beta}_{global}$ to a higher value with a value of R_0 approximately equal to 10, but with only a small decrease (passage multiplier = 0.15) imposed on the β_g, while a third scenario describes the event where the group size is increased from 8 to 20, retaining a moderate value of β_{global} and a passage multiplier of 0.15. For each of the three scenarios, the parameter estimates for the latent period and infectiousness distributions obtained from experiment 1 data are assumed. The full model for the infection process using the martingale estimation method for the β_g is applied to the data to calculate estimates of the expected infection process characteristics and of the β_g. Trends in the $\hat{\beta}_g$ are summarised and the statistical significance evaluated.

8.2 Ability of methods to detect trend

Two data sets, one based on the martingale $\hat{\beta}_{global}$ estimate and the other based on the restricted model ML $\hat{\beta}_{global}$ estimate, are generated using the simulation model described in Section 2.4.2. The data sets will be referred to as 'martingale based' and 'MLE based' respectively. The specifications of the simulated data are summarised below:

1. Four groups each of size 8 with restricted mixing as in the FMD experiments and as described in Section 2.4.2.

2. The rate of infection for the initial infectives, β_0, set to either the martingale $\hat{\beta}_{global}$ estimate of 0.8818 per day (corresponding to $R_0 = 2.48$) or to the restricted model ML $\hat{\beta}_{global}$ estimate of 1.0195 per day ($R_0 = 2.86$), as estimated from experiment 1 data.

3. A passage multiplier of 0.15 is used to define a trend in β with respect to generation of infection (higher values for the passage multiplier resulted in the failure of the epidemic to reach group 4).

4. A gamma distributed latent period with mean 0.98 days and a gamma distributed infectiousness period with mean 2.81 days are used in the model, the parameters are derived from the experiment 1 data (Sections 5.2.1 and 6.9.1).

Each data set will be analysed using the full model of the infection process using both martingale and restricted model ML estimation methods to generate estimates for the β_g. The simulated data will be analysed as if it were partially observed, making the properties of the simulated data equivalent to those of the experimental observed data.

8.2.1 The data

The martingale based data are presented in Table 8.1, columns 2 to 4 and the MLE based data are presented in Table 8.2, columns 2 to 4. Also presented in these tables are the corresponding estimates of the infection process characteristics obtained from the full model using the two estimation methods for β. Only data from infected individuals is presented. As before, all group 1 individuals (ID numbers 1 to 8) are assumed to be infected at time $t = 0$, the start of the epidemic, and all individuals in the other groups are susceptible at time $t = 0$.
In the martingale based data, there were 7 infecteds in group 2 (ID numbers 9 to 16), 5 in group 3 (ID numbers 17 to 24) and 2 in group 4 (ID numbers 25 to 32). The true infection history for the simulated epidemic is presented graphically in Figure 8.1. The data suggest that if individuals were to be tested for the presence of an infectious agent, the first positive individuals in group 2 would be detected on day 3 (ID 9, 13, 16) and the last positive in this group would be detected on day 10. The respective times are day 6 and 14 for group 3 and day 9 and 14 for group 4. Overall, the last infectious individual ceased to be infectious at time 14.66 (individual 28) and thus the epidemic lasted for a total of 15 days.

In the MLE based data, there were 7 infecteds in group 2, 5 in group 3 and 1 in group 4. The infection history for the simulated epidemic is displayed in Figure 8.2. From these data, assuming the testing of an infectious agent was done on a daily basis, infectious individuals would be detected between day 3 and day 9 for group 2, day 5 and day 17 for group 3 and day 14 and day 16 for group 4. The epidemic lasted up to day 17.9 when individual 23 ceased to be infectious.

Table 8.1: *Martingale based data; the information presented for infected individuals is: ID, time of infection (InfT), latent period (LatP) and infectiousness period (InfP). The table also includes the estimates for these variables from the full model of the infection process using both estimation methods for β.*

	True simulated values			Martingale method			Restricted MLE		
ID	InfT	LatP	InfP	InfT	LatP	InfP	InfT	LatP	InfP
1	0	1.06	2.46	0	1.13	2.43	0	1.13	2.43
2	0	0.94	2.00	0	0.85	1.87	0	0.85	1.87
3	0	0.80	2.12	0	0.85	1.87	0	0.85	1.87
4	0	0.86	2.76	0	0.85	2.67	0	0.85	2.67
5	0	0.85	3.46	0	0.85	3.56	0	0.85	3.56
6	0	1.22	1.82	0	1.13	2.43	0	1.13	2.43
7	0	1.09	2.74	0	1.13	2.43	0	1.13	2.43
8	0	0.95	4.11	0	0.85	4.50	0	0.85	4.50
9	1.98	0.91	3.30	1.51	0.96	3.91	1.51	0.96	3.91
11	3.78	0.80	1.91	3.45	0.97	2.20	3.44	0.97	2.21
12	4.97	0.85	2.74	4.56	0.96	2.96	4.55	0.96	2.96
13	1.44	1.12	3.02	1.51	0.96	3.00	1.51	0.96	3.00
14	4.24	0.77	3.37	4.56	0.96	2.96	4.55	0.96	2.96
15	5.85	1.12	3.57	5.53	0.96	3.89	5.52	0.96	3.90
16	1.37	0.77	3.86	1.51	0.96	3.00	1.51	0.96	3.00
17	6.09	0.98	4.56	6.50	0.96	3.92	6.50	0.96	3.92
18	4.61	1.02	2.32	4.54	0.95	2.14	4.54	0.95	2.14
19	4.09	0.99	3.58	4.54	0.95	2.97	4.54	0.95	2.97
20	7.83	1.15	2.67	7.56	0.95	2.96	7.56	0.95	2.96
24	9.60	0.94	3.83	9.54	0.96	3.89	9.53	0.96	3.89
28	11.05	1.11	2.50	11.35	1.00	2.26	11.35	1.00	2.26
31	7.05	1.22	3.53	7.52	0.96	3.00	7.52	0.96	2.99

8.2.2 Parameter estimates for latent and infectiousness period distributions

Using MLE methods, the scale and shape parameters (ν_{lat} and λ_{lat}) of the distribution of the length of latent period were estimated from n_l, the number of occasions on which group 1 individuals would test as negative after the start of the epidemic before they were first observed to be infectious. Given n_l, parameter estimates were obtained by maximizing the likelihood in Equation (6.3). For both data sets, group 1 individuals had the same generated infection history. Thus the estimates of the parameters for the latent period distribution were the same for both data sets. The distribution of n_l was such that 5 of the 8 group 1 individuals would on no occasion test as negative after time 0 hence the frequency of $n_l = 0$ was 5. The remaining 3 would test as negative once and thus the frequency of $n_l = 1$ was 3.

Table 8.2: *MLE based data; the information presented for infected individuals is: ID, time of infection (InfT), latent period (LatP) and infectiousness period (InfP). The table also includes the estimates for these variables from the full model of the infection process using both estimation methods for β.*

	True simulated values			Martingale method			Restricted MLE		
ID	InfT	LatP	InfP	InfT	LatP	InfP	InfT	LatP	InfP
1	0	1.06	2.46	0	1.13	2.43	0	1.13	2.43
2	0	0.94	2.00	0	0.85	1.86	0	0.85	1.86
3	0	0.80	2.12	0	0.85	1.86	0	0.85	1.86
4	0	0.86	2.76	0	0.85	2.67	0	0.85	2.67
5	0	0.85	3.46	0	0.85	3.55	0	0.85	3.55
6	0	1.22	1.82	0	1.13	2.43	0	1.13	2.43
7	0	1.09	2.74	0	1.13	2.43	0	1.13	2.43
8	0	0.95	4.11	0	0.85	4.49	0	0.85	4.49
9	1.88	0.91	3.30	1.51	0.96	3.90	1.51	0.96	3.91
11	3.53	0.97	2.12	3.45	0.97	2.20	3.44	0.97	2.20
12	5.09	1.12	3.57	5.49	0.97	3.00	5.48	0.97	3.01
13	1.41	1.12	3.02	1.51	0.96	2.99	1.51	0.96	3.00
14	4.78	0.95	4.10	4.59	0.95	3.84	4.58	0.95	3.84
15	3.46	0.94	3.46	3.45	0.97	3.03	3.44	0.97	3.04
16	1.35	0.77	3.86	1.51	0.96	2.99	1.51	0.96	3.00
17	4.65	1.17	2.30	4.59	0.94	2.93	4.59	0.95	2.93
19	6.61	1.18	1.91	6.50	0.96	2.16	6.50	0.96	2.16
20	2.83	1.31	2.86	3.69	0.93	2.86	3.69	0.93	2.86
22	9.35	0.84	4.06	9.24	1.04	4.08	9.24	1.04	4.08
23	14.23	1.04	2.63	14.32	1.01	2.26	14.32	1.01	2.26
31	11.94	1.11	3.35	12.69	0.93	2.86	12.69	0.93	2.86

Considering the distribution of the length of infectiousness period, the scale and shape parameters (ν_{inf} and λ_{inf}) were estimated from n_e, the number of times on which infected individuals would be observed to be infectious. The parameter estimates were obtained by maximising the likelihood in Equation (5.6). The distribution of n_e for both data sets is presented in Table 8.3.

Table 8.3: *Distribution of n_e, the number of times on which individuals would test positive in the simulated data.*

n_e	2	3	4	5	Total
Frequency (martingale based data)	8	8	5	1	22
Frequency (MLE based data)	8	8	4	1	21

The parameter estimates for the latent period and the infectiousness period distributions are presented in Table 8.4. Also presented in the same table are the true parameters which were used in the simulation model when generating the data.

Figure 8.1: *True infection history for martingale based simulated data.*

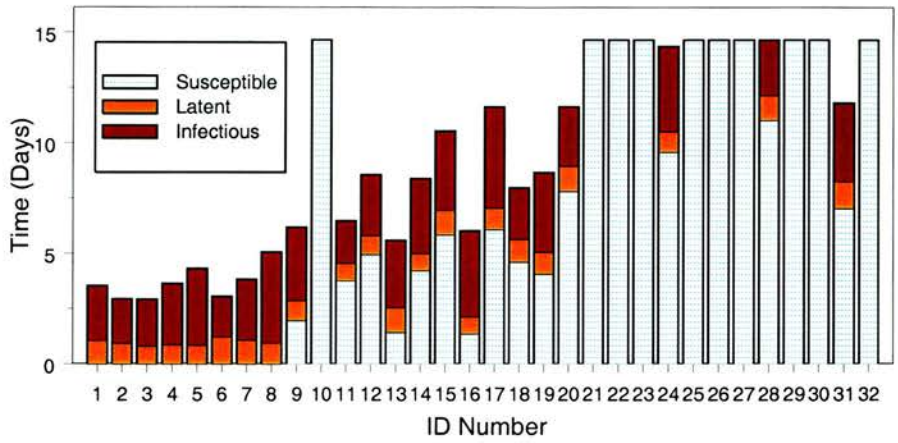

Figure 8.2: *True infection history for MLE based simulated data.*

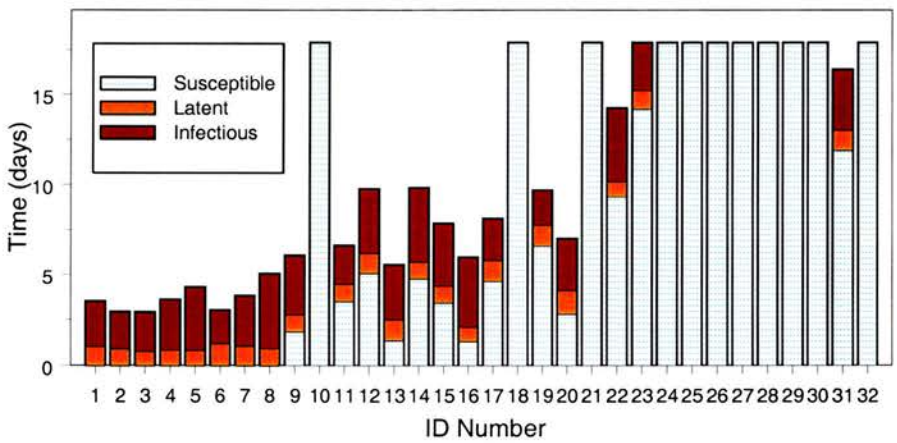

The estimates for the mean and standard deviation of the latent period distribution for both data sets were 0.95 days and 0.175 respectively. These estimates compared well with the true mean of the distribution, 0.98 days, and the true standard deviation, 0.172. The estimated means for the infectiousness distribution from the simulated data (2.96 days for the martingale based data and 2.91 days for the MLE based data) were slightly higher than the original distribution mean of 2.81 days. In general, the latent and infectiousness period distribution parameter estimates were in good agreement with the true parameters, estimating a mean period of approximately 1 day for the latent period and 3 days for the infectiousness period.

Table 8.4: *Estimates for the latent and infectiousness period distribution parameters from martingale based and MLE based simulated data.*

	True data		Martingale based data		MLE based data	
	Latent	Infectious	Latent	Infectious	Latent	Infectious
Scale parameter	32.2594	12.6362	29.5951	14.6637	29.5951	14.7012
Shape parameter	32.9544	4.4952	31.0183	4.9594	31.0183	5.0573
Distribution mean	0.98	2.81	0.95	2.96	0.95	2.91
Distribution SD	0.172	0.791	0.175	0.772	0.175	0.758

8.2.3 Estimated infection process

Using the methods described in Chapter 6 for the martingale estimates and Chapter 7 for the restricted model ML estimates, the simulated data were analysed to yield estimates for the expected infection process characteristics and of the β_g. The estimates of the expected infection process characteristics based on the two β estimation methods are presented in Table 8.1, columns 5 to 10 for the martingale based data and Table 8.2, columns 5 to 10 for the MLE based data. The true and estimated infection histories based on the martingale β estimation method are displayed in Figures 8.3 and 8.4 to allow comparison of the true and estimated values. The summarised averages for the expected lengths of latent and infectiousness period by group are presented in Table 8.5.

Table 8.5: *Mean true and estimated expected length of latent and infectiousness period.*

	Martingale based data				MLE based data			
	True means		Martingale estimated means		True means		Restricted ML estimated means	
Group	Latent	Inf Period	Latent	Inf Period	Latent	Inf Period	Latent	Inf Period
1	0.97	2.68	0.95	2.72	0.97	2.68	0.95	2.72
2	0.90	3.11	0.96	3.13	0.97	3.35	0.97	3.14
3	1.02	3.39	0.96	3.18	1.11	2.75	0.98	2.86
4	1.17	3.02	0.98	2.64	1.11	3.35	0.93	2.86

Figure 8.3: *Comparison of true and estimated infection histories for the martingale based data, for groups 1 and 2.*

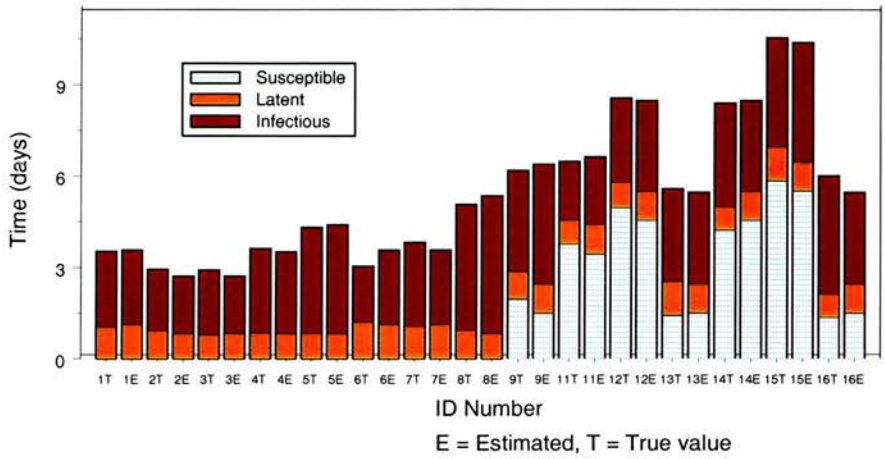

Figure 8.4: *Comparison of true and estimated infection histories for the martingale based data, for groups 3 and 4.*

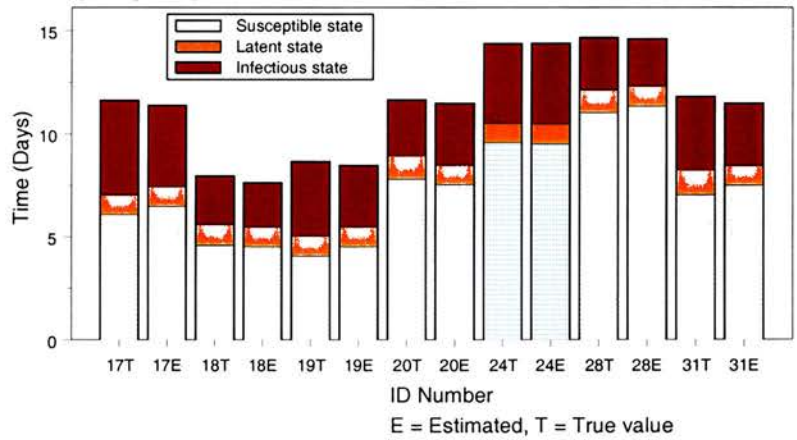

The estimates for the expected infection process characteristics, using both β estimation methods, were comparable to the true simulated data with minor differences. For the martingale based data, the expected length of latent period for group 1 individuals, using the martingale estimation method for β, were slightly underestimated for individuals with $n_l = 0$ and slightly overestimated for individuals with $n_l = 1$. Estimates of the expected length of infectiousness period in group 1 were such that individuals with true infectiousness period greater than 3 days had the expected length of infectiousness period slightly overestimated, while individuals with true infectiousness period between 2 and 3 days had the value underestimated. However, the average estimated length of infectiousness period for group 1 individuals of 2.72 days was very similar to the true average

of 2.68 days (Table 8.5). Examining the plots in Figures 8.3 and 8.4 comparing the estimated to the true infection process characteristics, the length of latent periods were in fairly good agreement while there were only minor differences in the length of infectiousness periods. The average estimated length of latent and infectiousness periods for group 1 individuals were in very close agreement with the average of the true values from both the martingale based data analysed based on martingale β estimation method (Table 8.5, columns 4 and 5) and the MLE based data analysed based on restricted model ML β estimation method (Table 8.5, columns 8 and 9).

For group 2 individuals, estimates of the expected length of latent period from the martingale based simulated data analysis using the martingale estimator for β were slightly higher than the true values except for those from individuals with true length of latent period greater than 1 day (see Table 8.1, column 3 and Figure 8.3). This was reflected in the average length of latent periods. For group 3 and 4 individuals, however, the results indicated slightly lower estimates than the true simulated values. For the infectiousness period, the average of the estimated lengths were similar to the true averages except for group 4 individuals where the average of the estimated lengths was lower than the true average (Table 8.5, column 5).

For the MLE based data, using the restricted model MLE for β, the estimates for the expected length of latent period for group 2 individuals were slightly higher than the true values except for those from individuals with length of latent period greater than 1 day. The mean of the estimated length of latent period was, however, equal to the mean of the true values. For group 3 and 4 individuals, the mean of the estimated lengths of latent periods was lower than the true mean. Considering the infectiousness period, the mean of the estimated periods for group 2 and 4 individuals were lower than the true mean, however, the reverse was true for group 3 individuals.

In general, the means of the estimates of the lengths of latent period were less variable across groups than the true means. The mean estimates of the length of infectiousness periods did not appear to be more or less variable than the true averages on a group-by-group basis, but it is true that the estimates and true means could, on occasion be quite different. More frequent sampling of individuals should reduce the size of these discrepancies (Table 8.5).

8.2.4 Estimates of the rate of infection, β

8.2.4.1 Estimates for the martingale based data

Martingale and restricted model ML estimates for the β_g obtained from analysing the martingale based data are presented in Table 8.6. Also presented in these tables are β_g estimates obtained from the true simulated data. For both estimation methods, the results indicate a consistent drop in the rate of infection across groups.

Table 8.6: *Estimates for expected duration of exposure time (Expo time) and rate of infection (β) using both the martingale estimation method for β and the restricted model MLE method for β, for the martingale based data.*

			Martingale method					
			True simulated data			Estimated history		
Group	Infs	B Integral	Expo time	$\hat{\beta}$	$s.e(\hat{\beta})$	Expo time	$\hat{\beta}$	$s.e(\hat{\beta})$
2	7	1.7179	2.56	0.6709	0.2836	2.62	0.6558	0.2772
3	5	0.8845	1.86	0.4754	0.2192	1.83	0.4823	0.2224
4	2	0.2679	1.17	0.2291	0.1623	1.00	0.2668	0.1891
			Restricted MLE					
			True simulated data			Estimated history		
Group	Infs		Expo time	$\hat{\beta}$	$s.e(\hat{\beta})$	Expo time	$\hat{\beta}$	$s.e(\hat{\beta})$
2	7		8.05	0.8696	0.3287	7.80	0.8974	0.3392
3	5		8.33	0.6001	0.2684	8.52	0.5872	0.2626
4	2		7.78	0.2571	0.1898	6.82	0.2932	0.2073

The analysis using the martingale estimation method for the β_g yielded a consistent decreasing trend for both the $\hat{\beta}_g$ and the estimated scaled total infection exposure time by increasing group number. The $\hat{\beta}_g$ estimates obtained from the estimated infection history compare well with estimates obtained from the true infection history. The $\hat{\beta}_2$ estimate from the true infection history was slightly higher than the estimate from the estimated infection history. The $\hat{\beta}_3$ and $\hat{\beta}_4$ estimates obtained from the estimated infection history were higher than those obtained from the true data. Note that the $\hat{\beta}_2$ estimate in both cases (0.6558 from the estimated history and 0.6709 from true history) was lower than 0.8818, the basic rate of infection which was used to generate the data. This was to be expected where there is reduction of infection potential by increasing generation

of infection, as assumed in the model. It is notable that the martingale estimator for the β_g in Equation (4.17) which uses partial information consistently gave rise to an estimate of $\hat{\beta}_2$ which is less than 0.8818 using both the estimated and true infection histories. However, the ML $\hat{\beta}_2$ estimates were more consistent with the true parameter value.

The restricted model ML β_g estimates obtained from the martingale based data decreased by increasing group number. These estimates were constrained to decrease or stay the same across groups, *i.e.* a non-increasing trend was imposed on them. The estimates from the estimated infection process were in good agreement with those obtained from the true infection history. The restricted model ML estimator (which uses complete information) gave rise to a $\hat{\beta}_2$ estimate close to $\hat{\beta}_{global}$ using the estimated history (compare 0.8974 and 0.8818).

The trend in the martingale $\hat{\beta}_g$ estimates was summarised via a slope estimated by weighted linear regression where the estimates were regressed against group numbers with a weight $(\frac{1}{s.e(\hat{\beta})})^2$. The analysis yielded an estimated slope of -0.1973 (s.e $= 0.0124$). For the restricted model MLE $\hat{\beta}_g$ estimates, where a non-increasing trend was imposed, a decrease in the $\hat{\beta}_g$ was estimated. As described in Chapter 7, the decrease in the β_g was summarised based on two measures: measure 1 being equal to the more significant quantity of $\hat{d}_{23}$ (the estimated decrease between $\hat{\beta}_2$ and $\hat{\beta}_3$) and $\hat{d}_{34}$ (the estimated decrease between $\hat{\beta}_3$ and $\hat{\beta}_4$) and measure 2 being the sum $\hat{d}_{23} + \hat{d}_{34}$ (refer to Section 7.4.2). From the martingale based data, the analysis yielded an estimated decrease of 0.6894 for measure 1 and 1.1187 for measure 2. The statistical significance of the estimated slope and of the estimated decreases was tested using bootstrap methods as described in Chapters 6 and 7.

8.2.4.2 Assessing the significance of the trend in the β_g estimates

To generate bootstrap epidemics to be used in testing the statistical significance of the estimated slope and of the estimated decreases, a martingale estimate and a restricted model ML estimate of β_{global} were obtained from the simulated data using methods from Sections 6.7.1.1 and 7.4.1.1 respectively. The martingale estimate for $\hat{\beta}_{global}$ was 0.5261, corresponding to a scaled total expected exposure time of 5.46 days and a sum of the B integral equal to 2.8702. The restricted model ML estimate for $\hat{\beta}_{global}$ was 0.6050. Using the estimates of $\hat{\beta}_{global}$ and the estimates for the parameters of the latent and infectiousness period distributions for the martingale based data (Table 8.4), for each of the β estimation methods,

200 bootstrap epidemic realisations were simulated under the null hypothesis of no trend in the β_g. The bootstrap samples were analysed to yield martingale and restricted model ML β_g estimates for groups 2 to 4. For each data set, for martingale β estimation, a slope was estimated by weighted linear regression and for restricted model ML β estimation, the decrease in the $\hat{\beta}_g$ was estimated based on the standard measures. Descriptive statistics for the estimated slopes and decreases are presented in Table 8.7 and the histograms of the slopes and of the decreases are presented in Figure 8.5.

Table 8.7: *Descriptive statistics for the estimated slopes from the bootstrap epidemic realisations, where Q_1 is the first quartile and Q_3 is the third quartile.*

variable	N	mean	median	st dev	se mean	min	max	Q_1	Q_3
Estimated slopes	200	-0.0463	-0.0369	0.1762	0.0125	-0.7260	0.8514	-0.1313	0.0344
Measure 1	200	0.3225	0.1851	0.3800	0.0269	0.0000	1.7783	0.0000	0.4972
Measure 2	200	0.3516	0.2104	0.4271	0.0302	0.0000	1.8816	0.0000	0.5193

Figure 8.5: *Histograms for estimated slopes and decreases from the bootstrap epidemic samples, the dotted lines indicate the estimated slope of -0.1973 and estimated decrease 2 of 1.1187 from the martingale based data.*

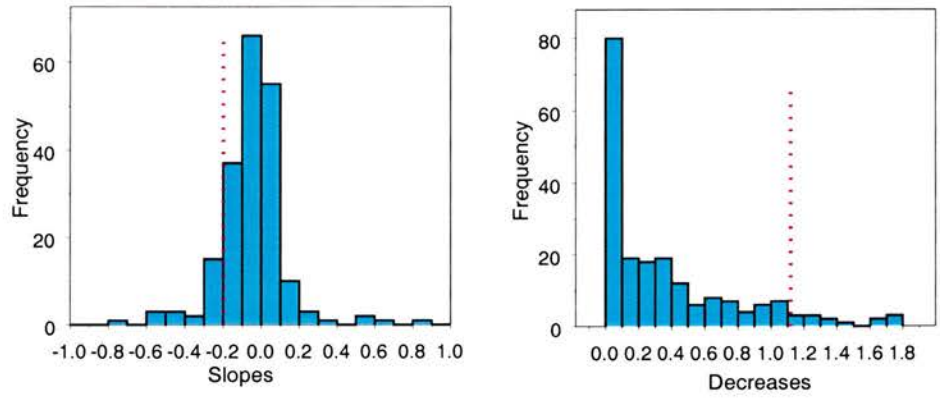

The estimated slopes from the bootstrap samples are fairly symmetrically distributed about 0, with most slopes lying between -0.72 and 0.86, with a mean of -0.0463 and a standard deviation of 0.1762. If significantly less than that arising under the null hypothesis, the estimated slope of -0.1973 from the martingale based data would be expected to fall at the extreme left end of the distribution of the bootstrap estimated slopes. The estimated slope, however, falls at the 12% point in the left tail of the distribution of the bootstrap slopes. A formal test of significance is done through a $p-$value. 24 of the 200 bootstrap slopes were less than -0.1973, yielding a $p-$value of 0.12. For the restricted model ML

based estimates, the estimated decrease in the $\hat{\beta}_g$ for both measures of decrease were not statistically greater than those arising under the null hypothesis with p-values of 0.165 (33 decreases greater than 0.6894) for measure 1 and 0.065 (13 decreases greater than 1.1187) for measure 2. Thus, for the martingale based data, it was concluded that the estimated slope was not statistically significantly less than those arising under the null hypothesis and the estimated decreases were not statistically greater than those arising under the null hypothesis at the 5% significance level. Even though a decreasing trend was imposed on the rates of infection across groups, it was not possible to reject the null hypothesis of no trend in the β_g based on either the martingale or the restricted model ML estimation methods for the rate of infection.

8.2.4.3 Estimates for the MLE based data

Martingale and restricted model ML estimates for the β_g obtained from analysing the MLE based data are presented in Table 8.8. Also presented in these tables are β_g estimates obtained from the true simulated data. For both estimation methods, the results indicate a consistent drop in the rate of infection across groups.

Table 8.8: *Estimates for expected duration of exposure time (Expo time) and rate of infection (β) using both the martingale estimation method for β and the restricted model MLE method for β, for the MLE based data.*

			Martingale method					
			True simulated data			Estimated history		
Group	Infs	B Integral	Expo time	$\hat{\beta}$	$s.e(\hat{\beta})$	Expo time	$\hat{\beta}$	$s.e(\hat{\beta})$
2	7	1.7179	2.64	0.6519	0.2756	2.56	0.6704	0.2834
3	5	0.8845	1.68	0.5265	0.2427	1.68	0.5252	0.2421
4	1	0.1250	0.72	0.1744	0.1709	0.73	0.1709	0.1709
			Restricted MLE					
			True simulated data			Estimated history		
Group	Infs		Expo time	$\hat{\beta}$	$s.e(\hat{\beta})$	Expo time	$\hat{\beta}$	$s.e(\hat{\beta})$
2	7		7.63	0.9175	0.3468	7.52	0.9303	0.3517
3	5		8.66	0.5776	0.2583	8.71	0.5741	0.2567
4	1		5.27	0.1898	0.1898	5.44	0.1838	0.1838

The analysis using the martingale estimation method for the β_g yielded a consistent decreasing trend in both the $\hat{\beta}_g$ and the estimated scaled total infection exposure time by increasing group number. Also, the $\hat{\beta}_g$ estimates obtained from the estimated infection history compare well with estimates obtained from the true infection history. However, the resulting estimates probably underestimate the true rates of infection in all groups.

The restricted model ML estimates for the β_g in groups 2 to 4 were calculated to ensure more power in detecting a genuine trend in the rate of infection across groups. Results from the analysis (Table 8.8) indicate a decreasing trend in the $\hat{\beta}_{global}$ by increasing group number. The estimates obtained from the estimated infection history compared well with those obtained from the true infection history. The $\hat{\beta}_2$ estimate obtained from the estimated infection history is slightly higher than the estimate from the true infection history, though smaller than the basic infection rate used to simulate the data (0.9393 versus 1.0195). The discrepancy can be explained by the presence of generation 3 infections in group 2.

The trend in the martingale $\hat{\beta}_g$ estimates was summarised via a slope estimated using weighted linear regression. The analysis yielded an estimated slope of -0.2653. For the restricted model MLE using decrease measure 1, the analysis yielded an estimated decrease of $\hat{d}_{34} = 1.1383$, which was the more significant estimated decrease. The second measure of $\hat{d}_{23} + \hat{d}_{34}$ yielded an estimated decrease of 1.6216. The estimated slope and the estimated decreases indicate that there was a decreasing trend in the $\hat{\beta}_g$, however, it was still necessary to formally test whether or not the estimated trend summaries were statistically significantly different to those arising under the null hypothesis.

8.2.4.4 Assessing the significance of the trend in the $\hat{\beta}_g$ estimates

To test whether the estimated slope and the estimated decreases were statistically significantly different to those arising under the null hypothesis, bootstrap methods were used. A martingale estimate and a restricted model ML estimate of β_{global} were obtained from the simulated data using methods from Sections 6.7.1.1 and 7.4.1.1 respectively. The martingale estimate for $\hat{\beta}_{global}$ equal to 0.5481 per day and the restricted model ML estimate for $\hat{\beta}_{global}$ was 0.5996 per day. Using the estimates of $\hat{\beta}_{global}$ and the estimates for the parameters of the latent and infectiousness period distributions for the MLE based data (Table 8.4), for each of the β estimation methods, 200 epidemic realisations were simulated under the null hypothesis of no trend in the $\hat{\beta}_g$. The data sets were analysed to yield esti-

mates for the $\hat{\beta}_g$ for both estimation methods. Slopes from the weighted linear regression were obtained from the martingale $\hat{\beta}$ estimates and decreases were estimated from the restricted model ML $\hat{\beta}_g$ estimates. Descriptive summary statistics for the estimated slopes and estimates of the decreases using both measures are presented in Table 8.9 and the histograms for the slopes and measure 2 decreases are presented in Figure 8.6.

Table 8.9: *Descriptive statistics for the estimated decreases in β from the bootstrap epidemic realisations, where Q_1 is the first quartile and Q_3 is the third quartile.*

variable	N	mean	median	st dev	se mean	min	max	Q_1	Q_3
Estimated slopes	200	-0.0387	-0.0295	0.1535	0.0109	-0.7051	0.5262	-0.1155	0.0355
Decrease 1	200	0.2992	0.1600	0.3770	0.0267	0.0000	1.8605	0.0000	0.4729
Decrease 2	200	0.3316	0.1600	0.4248	0.0300	0.0000	1.8942	0.0000	0.5262

Figure 8.6: *Histograms for estimated slopes and measure 2 decreases from the bootstrap epidemic samples, the dotted lines indicate the estimated slope of -0.2652 and estimated decrease measure 2 of 1.6216 from the MLE based data.*

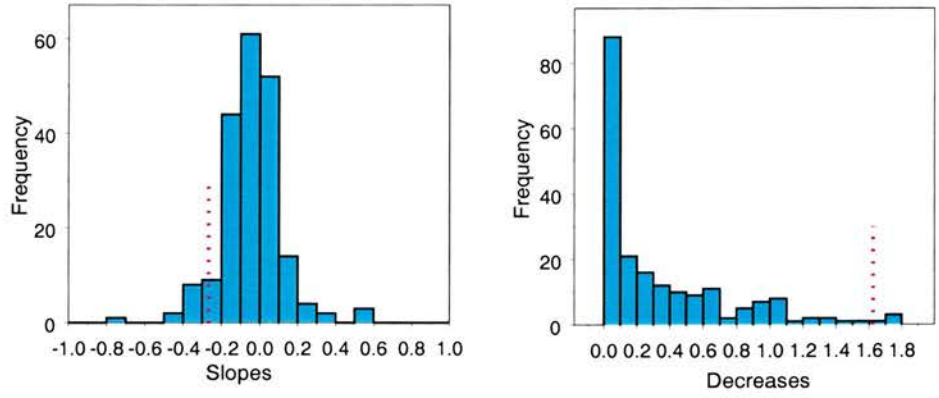

The estimated slope of -0.2653 from the martingale $\hat{\beta}_g$ estimates falls at the 6% point in the left tail of the distribution of the bootstrap slopes with 12 of the bootstrap estimated slopes being less than -0.2653. Thus the bootstrap analysis yielded a p-value of 0.06. Thus at a 5% significance level, the results imply that there is no significant trend in the martingale $\hat{\beta}_g$ estimates across groups. For the restricted model ML $\hat{\beta}_g$, the estimated decrease of 1.1383 arising from measure 1 lies at the 97% point of the distribution of the bootstrap decreases with only 6 of the 200 decreases being greater than 1.1383, which yields a $p-$value of 0.03. For measure 2, the estimated decrease of 1.6216 lies at the 98% point of the distribution of the bootstrap decreases, with a $p-$value of 0.02. The estimated decreases based on both measures lie at the extreme right end of the distribution

of bootstrap decreases. Both measures of decrease are significantly greater than those arising under the null hypothesis, at significance level greater than 3%. Using the restricted model MLE, which is proposed as increasing the power of the test, the methods are able to detect a decrease in the rate of infection when it does indeed exist. Using the martingale methods, however, it was not possible to detect a known existing decrease in the rate of infection at a level of significance less than 5% (although the significance level was very close to 5%, and a greater number if bootstrap realisations might allow a more precise estimate of the p-value). The restricted model MLE yielded $p-$values of 0.02 and 0.03 compared to the martingale methods (unrestricted) which yielded a $p-$value of 0.06. Thus it is evident that the restricted model MLE may have more potential to detect a genuine decreasing trend in the rate of infection than the martingale estimation method for β.

Since the martingale estimation methods for β were unable to formally identify a significant decreasing trend when it indeed existed, for both the martingale based data ($\hat{\beta}_{global} = 0.8818$) and the MLE based data ($\hat{\beta}_{global} = 1.0195$), it appeared worthwhile to investigate the effect of other factors which might influence the power if the test (discussed in Section 6.10). These were, that possibly the decrease was too small to be detected given the group size of 8 or that the group size of 8 was not large enough to enable detection of a significant trend given the specified value of R_0 (which is less than 3). These issues are addressed in the next section.

8.3 Ability of martingale based methods to detect changes in β_g: effect of passage, R_0 and group size

After attaining a non-significant test result for a genuine trend based on martingale estimates, further investigations regarding the appropriateness of the proposed methods are required. In this section, investigations are carried out to test whether or not the developed methods using martingale method of estimation for β, are appropriate for the nature of the data. One would want to know whether it is the smallness of the decrease in the $\hat{\beta}_g$ or low value of R_0 or the group size or a combination of these factors, that is responsible for a genuine trend not being detected as significant. Thus, investigations are carried out for three scenarios, namely:

1. To explore whether a significant trend was not attained because the genuine effect was too small, the passage multiplier is increased from 0.15 to 1.5 to ensure a large decrease in the rate of infection by infection generation. For this purpose, data are generated based on four groups of size 8 (group 1: ID numbers 1 to 8; group 2: ID numbers 9 to 16; group 3: ID numbers 17 to 24 and group 4: ID numbers 25 to 32), with a rate of infection for infected individuals of 0.8818 and passage multiplier of 1.5. These data will be referred to as data set A.

2. To test whether a significant trend was not attained due to a low R_0 in the initial group of infectives, and that a decrease in β corresponding to passage multiplier of 0.15 could have been detectable if R_0 in the initial group of infectives was big enough, R_0 is boosted from 2.48 to approximately 10, corresponding to a rate of infection of 3.57. Data are generated based on four groups of size 8, with a rate of infection for infected individuals of 3.57 and passage multiplier of 0.15. These data will be referred to as data set B.

3. To test whether it was because of small group size that a significant trend was not attained, the group size is increased from 8 to 20. Data are then generated based on four groups of size of 20 (group 1: ID numbers 1 to 20; group 2: ID numbers 21 to 40; group 3: ID numbers 41 to 60 and group 4: ID numbers 61 to 80), with a rate of infection for infected individuals of 0.8818 and passage multiplier of 0.15. These data will be referred to as data set C.

For all scenarios, a gamma distributed latent period with mean 0.98 days (scale parameter equal to 32.26 and shape parameter equal to 32.95) and a gamma distributed infectiousness period with mean 2.81 days (scale parameter equal to 12.64 and shape parameter equal to 4.50) were assumed in the simulation model which was used to generated the data. Also, all group 1 individuals are assumed to be infected at the start of the epidemic, $t = 0$.

8.3.1 The simulated data

Data sets A and B (for infected individuals only) are presented in Table 8.10 and data set C is presented in Table 8.11. For data set A, the epidemic lasted up to day 7 and there were 3 (out of 8) infecteds in group 2 and no infected individuals in groups 3 and 4. For data set B, the epidemic lasted up to day 11 and had all

24 initially susceptible individuals in groups 2 to 4 infected. For data set C, the epidemic lasted up to day 20 and had 19 (out of 20) infecteds in group 2, 14 in group 3 and 6 in group 4.

The three data sets were analysed using methods developed in Chapters 5 and 6 where the β_g were estimated using martingale methods. Parameters for latent and infectiousness period distributions, the expected values of the infection process characteristics and the β_g were estimated from the data. The trends in the $\hat{\beta}_g$ were estimated and bootstrap methods were used to test whether or not the estimated trends were statistically significant.

Table 8.10: *Simulated epidemic data about infected individuals from data set A and data set B, presented is data about identity number (ID), time of infection (Inf time), latent period (Latent) and infectiousness period (Inf period).*

Data A				Data B			
ID	Inf time	Latent	Inf period	ID	Inf time	Latent	Inf period
1	0.00	1.07	2.46	1	0.00	0.77	3.34
2	0.00	0.94	2.00	2	0.00	1.41	1.57
3	0.00	0.80	2.12	3	0.00	1.00	4.11
4	0.00	0.86	2.76	4	0.00	0.84	3.21
5	0.00	0.85	3.46	5	0.00	0.94	3.23
6	0.00	1.22	1.82	6	0.00	1.11	3.17
7	0.00	1.09	2.74	7	0.00	1.03	2.80
8	0.00	0.95	4.11	8	0.00	0.88	3.83
9	1.98	0.91	3.29	9	1.10	0.96	1.75
13	1.44	1.12	3.02	10	1.58	0.93	4.05
16	1.37	0.77	3.86	11	3.60	0.95	3.42
				12	1.35	1.03	4.18
				13	1.08	1.10	3.29
				14	1.13	1.44	4.17
				15	1.14	0.96	3.50
				16	3.01	1.23	2.76
				17	3.98	1.10	2.37
				18	3.39	0.79	2.35
				19	2.14	1.20	1.97
				20	2.53	1.22	1.67
				21	2.99	0.80	1.88
				22	3.75	0.74	4.18
				23	2.70	0.89	2.98
				24	2.90	0.84	3.43
				25	3.87	0.89	1.24
				26	3.80	1.06	3.14
				27	4.00	0.98	2.66
				28	4.76	1.15	2.58
				29	6.11	0.95	3.02
				30	5.33	1.11	3.72
				31	5.22	0.83	2.94
				32	5.41	0.76	2.64

Table 8.11: *Simulated epidemic data about infected individuals from data set C, presented is data about identity number (ID), time of infection (InfT), latent period (Latent) and infectiousness period (InfP).*

Group 1				Group 2				Group 3 and 4			
ID	InfT	Latent	InfP	ID	InfT	Latent	InfP	ID	InfT	Latent	InfP
1	0	0.78	1.83	21	1.22	1.28	2.88	41	4.29	0.92	1.78
2	0	1.07	2.29	22	3.34	1.18	2.38	42	4.87	1.07	1.98
3	0	0.79	2.05	23	1.15	1.18	3.37	43	2.87	0.95	3.18
4	0	0.90	1.36	24	3.36	0.73	3.02	45	8.61	0.74	4.31
5	0	0.87	4.18	25	2.63	1.27	3.40	46	4.59	0.88	1.42
6	0	0.96	4.10	26	1.55	0.76	2.88	47	8.15	0.87	3.57
7	0	1.13	2.13	27	3.60	0.98	3.58	50	13.79	1.14	1.87
8	0	1.02	1.91	28	6.95	1.09	1.91	51	16.61	0.83	1.95
9	0	1.17	2.59	29	1.52	1.08	1.89	52	10.26	1.29	1.20
10	0	1.03	3.01	31	1.70	0.97	1.78	53	10.73	0.94	1.89
11	0	1.32	3.31	32	3.76	1.03	1.96	55	6.66	0.74	3.23
12	0	0.96	3.62	33	1.81	0.92	2.56	57	15.62	0.88	3.47
13	0	1.12	2.35	34	5.03	1.04	1.77	58	7.95	1.06	1.54
14	0	0.99	3.25	35	4.84	1.23	3.04	60	6.21	1.13	2.97
15	0	0.75	3.07	36	1.35	1.06	2.18	63	11.39	0.93	2.37
16	0	0.78	2.12	37	1.91	0.90	2.81	67	13.53	0.65	1.92
17	0	0.93	2.51	38	1.36	0.80	2.33	68	8.70	1.18	2.38
18	0	0.80	3.28	39	1.17	0.89	3.27	69	5.53	0.92	2.60
19	0	1.15	2.56	40	4.03	1.03	3.46	74	10.25	0.99	3.00
20	0	1.17	2.18					76	11.11	1.23	2.16

8.3.2 Parameter estimates for latent and infectiousness distributions

Using MLE methods, the scale and shape parameters (ν_{lat} and λ_{lat}) of the distribution of the length of latent period were estimated from the n_l, the number of times that group 1 individuals would test negative after the start of the epidemic before they are first observed to be infectious. For the distribution of the length of infectiousness period, the scale and shape parameters (ν_{inf} and λ_{inf}) were estimated from n_e, the number of times that infected individuals would be observed to be infectious. The data for n_l and n_e are presented in Table 8.12. For all three data sets, n_l was either 0 or 1, implying that the length of the latent period was between 0 and 2 days. From the distribution of n_e (Table 8.12), it was observed that for data set A, infected individuals would be observed to be infectious at least twice and at most 5 times. For data set B, infected individuals would be observed to be infectious at least once and at most 4 times and for data set C, individuals would be observed to be infectious between 1 and 5 times.

Table 8.12: *Distribution of n_l, the number of times that group 1 individuals would test negative after the start of the epidemic before they are first observed to be infectious, and of n_e, the number of times that infected individuals would be observed to be infectious, for data sets A, B and C.*

		n_l		n_e					
	Data	0	1	1	2	3	4	5	Total
Frequency	A	5	3	0	5	3	2	1	11
	B	4	4	3	8	9	12	0	32
	C	11	9	7	23	20	7	2	59

Given the data for n_l and n_e, the log-likelihood functions for the latent and infectiousness periods in Equations (6.3) and (5.6) respectively, were maximized to yield estimates for the latent and infectiousness period distribution parameters. The resulting estimates are presented in Table 8.13. From data set A, a mean of 0.95 days and standard deviation of 0.175 was obtained for the distribution of the length of latent period and a mean of 2.91 days for the distribution of the length of infectiousness period. For data set B, a mean of 1.01 days was obtained for the distribution of the length of latent period and a mean of 2.94 days for the distribution of the length of infectiousness period. For data set B, a mean of 0.99 days was obtained for the distribution of the length of latent period and a mean of 2.56 days for the distribution of the length of infectiousness period.

Table 8.13: *Estimates for latent and infectiousness period (Inf period) distribution parameters for simulated data sets A, B and C.*

	Input values		Data A		Data B		Data C	
Parameter	Latent	Inf period	Latent	Inf period	Latent	Inf period	Latent	Infperiod
scale	32.26	12.64	29.60	10.53	67.24	9.47	59.80	8.60
shape	32.95	4.50	31.02	3.62	66.90	3.22	60.44	3.36
mean	0.98	2.81	0.95	2.91	1.01	2.94	0.99	2.56
SD	0.172	0.791	0.175	0.897	0.123	0.955	0.128	0.873

For each of the three data sets, estimates for the mean of the distribution of the length of latent period were in good agreement with the model mean of 0.98 days. The estimated means for the distribution of the length of infectiousness period from data set A and data set B were slightly higher than the model distribution mean of 2.81 days. For data set C, the estimated mean of the distribution was lower than the assumed mean and this is mainly because 30 out of the 59 infected individuals in this data set, would have been observed to be infectious on less

than three occasions, forcing the overall estimated mean to drop.

8.3.3 Estimates of the infection history and β

The simulated epidemic data sets A, B and C presented in Tables 8.10 and 8.11 were analysed using the proposed methods of full modelling of the infection process based on martingale estimation methods for β. Estimates for the expected infection process characteristics were calculated alternately with the estimates of the β_g using Algorithm 6.1. The resulting estimates for the β_g from the last iteration are presented in Table 8.14. Also presented in the same table are the β_g estimates based on the true simulated infection history.

Table 8.14: *Estimates for expected duration of exposure time (Time) and the rate of infection (β) for data set A, B and C.*

				True simulated data			Estimated history		
Data	Group	Infecteds	B Integral	Time	$\hat{\beta}$	$s.e(\hat{\beta})$	Time	$\hat{\beta}$	$s.e(\hat{\beta})$
A	2	3	0.43	1.37	0.32	0.185	1.37	0.32	0.184
	3	0	0.00	0.29	0.00	0.000	0.31	0.00	0.000
	4	0	0.00	0.00	0.00	0.000	0.00	0.00	0.000
B	2	8	2.72	1.21	2.25	1.021	0.94	2.90	1.314
	3	8	2.72	0.37	7.41	3.370	0.47	5.74	2.609
	4	8	2.72	0.80	3.41	1.551	0.97	2.81	1.277
C	2	19	2.60	2.44	1.06	0.316	2.43	1.07	0.318
	3	14	1.15	1.70	0.68	0.191	1.64	0.70	0.197
	4	6	0.35	0.98	0.35	0.145	0.95	0.36	0.149

For data set A, the infection did not go beyond group 2, thus the martingale estimate for $\hat{\beta}_3$ and $\hat{\beta}_4$ was 0. For group 2, $\hat{\beta}_2$ was estimated to be 0.32 ($s.e$ = 0.184) in good agreement with the estimate based on true infection history but well below the model rate of infection of 0.8818. This appeared to be anomalous, since it could be assumed that many of the infections occurring in group 2 were generation 1 infections. The martingale estimator underestimates the rate of infection. The slope in the βs across groups was estimated to be equal to -0.1583 ($s.e$ = 0.0914) from regressing the β estimates against the group numbers but with weights of 1 in all groups (since weights defined in terms of $s.e(\hat{\beta})$ could not be assigned for groups 3 and 4). If however, the slope had been estimated based

on comparing the estimated rate of infection in group 2 with that in group 3 only (since β estimates in groups 3 and 4 are 0), then the slope would have been estimated to be equal to -0.3165.

For data set B, all individuals in all groups became infected. The results were such that $\hat{\beta}_4 < \hat{\beta}_2 < \hat{\beta}_3$. However, from the true simulated infection history, results indicated that $\hat{\beta}_2 < \hat{\beta}_3 < \hat{\beta}_4$. It was observed that $\hat{\beta}_g$ estimates from the estimated infection history were different from those obtained from the true infection history. One explanation is that many individuals became infected during the same day and under the estimated infection history, if these individuals had the same value of n_e then their estimated time of infection, estimated length of latent and of infectiousness periods would be the same. Hence the estimated durations of group infection exposure were bound to be different to the true durations. In general, the more vigorous the infection process, the more frequent sampling requires to be, so as to generate enough detail in the data to model fine distinctions in the infection process. In this case, the sampling regime was probably deficient. Again, since all individuals in all groups became infected, a cutoff time based on the time of the last susceptible to become infected had to be determined for the appropriate martingale estimate. In group 2, for example, the true time of infection for the last susceptible was 3.60 whereas the estimated expected time of infection for this individual was 3.31. This imposed a further effect on the resulting estimates compared to estimates based on true data. However, in analyses based on both the true and estimated infection processes, group 3 was estimated to have experienced the highest rate of infection. The weighted linear regression analysis was performed to summarise the trend in the $\hat{\beta}_g$ estimates and an estimate for the slope of -0.0143 ($s.e = 0.4042$) was obtained. The estimate for group 3 was given a very low weight.

For data set C, the results indicated a decreasing trend in the $\hat{\beta}_g$ estimates across groups. These estimates were comparable with those obtained from the true infection history. An estimated slope of -0.5242 ($s.e = 0.0742$) was obtained for the trend in the $\hat{\beta}_g$ estimates.

The significance of the estimated slopes was tested using bootstrap methods as described previously. An martingale estimate for $\hat{\beta}_{global}$ was obtained from each data set A, B and C. The aim was to generate bootstrap epidemics from each of the three simulated epidemics based on the $\hat{\beta}_{global}$ estimate and the parameter estimates for the distributions of the length of latent and infectiousness period for these epidemics. The $\hat{\beta}_{global}$ estimate was calculated as in Section 6.7.1.1 based

on Equation (6.37). For data set A, the resulting estimate for $\hat{\beta}_{global}$ was 0.26 corresponding to overall scaled total expected infection exposure time of 1.68 days. For data set B, the estimate for $\hat{\beta}_{global}$ was 3.39 and an overall scaled total expected infection exposure time of 2.41 days. For data set C, the estimate for $\hat{\beta}_{global}$ was 0.82 and an overall scaled total expected infection exposure time of 5.02 days.

8.3.3.1 Assessing the significance of the trend in the β_g estimates

From each of the simulated epidemics A, B and C, based on the infection process characteristics (latency and infectiousness) for the simulated epidemic and a constant rate of infection equal to the estimated $\hat{\beta}_{global}$, 200 bootstrap epidemics were generated under the null hypothesis that there is no trend in the $\hat{\beta}_g$ estimates. For each of the 200 bootstrap data from epidemics A, B and C, estimates for the $\hat{\beta}_g$ were obtained. Weighted linear regression analyses were performed yielding estimates of slopes for each epidemic sample. In Table 8.15 descriptive summary statistics for the slopes are presented and in Figure 8.7 the histograms for the estimated bootstrap slopes are presented.

Table 8.15: *Descriptive statistics for estimated bootstrap slopes from data sets A, B and C, where Q_1 and Q_3 are the first and third quartiles respectively.*

Slopes for data	N	mean	median	st dev	se mean	min	max	Q_1	Q_3
A	200	0.007	-0.005	0.101	0.007	-0.268	0.281	-0.068	0.082
B	200	0.288	0.281	0.419	0.030	-1.005	1.287	-0.041	0.593
C	200	-0.023	-0.006	0.226	0.016	-0.881	0.548	-0.149	0.127

For data set A, the bootstrap slopes fell between -0.268 and 0.281 and were fairly symmetrical about the mean of 0.007. For data B, the bootstrap slopes were between -1.005 and 1.287 and were fairly symmetrically distributed about the mean of 0.288. For data set C, the bootstrap slopes were between -0.881 and 0.548 and were fairly symmetrically distributed about the mean (-0.023). It was curious that the mean slope simulated for data set B had a positive value significantly different to zero.

For data set A, 7 out of the 200 bootstrap estimated slopes were less than -0.1583, the estimated slope from data set A, yielding a $p-$value of 0.035. Thus the estimated slope from these data was statistically significantly less than 0 at the

Figure 8.7: *Histogram for estimated bootstrap slopes from data sets A, B and C, the dotted lines indicate the estimated slopes from the original data set A of* -0.1583*, data set B estimated slope of* -0.0143 *and data set C estimated slope of* -0.5254.

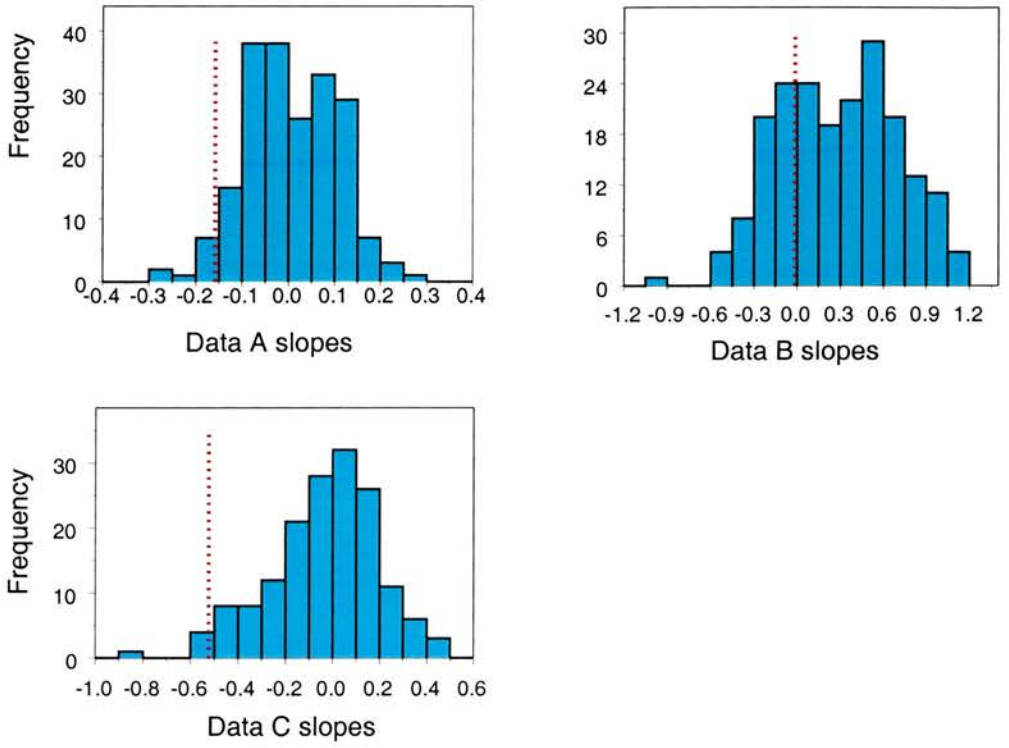

5% significance level. It can therefore be concluded that a genuine decrease in the rate of infection can be detected under the estimated R_0 of 2.48 from experiment 1 and group size of 8 if the decrease was reasonably large.

For data set B, 56 out of the 200 estimated bootstrap slopes were less than the estimated slope of -0.0143, yielding a $p-$value of 0.28. Thus the estimated slope was not statistically significantly less than 0 implying that, with a genuine small decrease in the β_g, with groups of size 8, boosting the value of R_0 in the initial group of infectives would probably not increase the probability of detecting a significant trend.

The effect of a larger value of R_0 on the ability to detect a genuine decrease in the rate of infection was investigated further by considering a larger decrease. A passage multiplier of 1.5 was used in the simulation model, to effect a larger decrease in the rate of infection by generation of infection. Data were generated based on rate of infection of 3.57 (corresponding to $R_0 \simeq 10$), passage multiplier equal to 1.5 and group size 8. The generated data had all 8 group 2 individuals

infected, 4 infecteds in group 3 and 1 infected in group 4. Analysis of these data resulted in a decreasing trend in the estimated $\hat{\beta}_g$ where $\hat{\beta}_2 = 3.38\,(s.e = 1.538)$, $\hat{\beta}_3 = 0.41\,(s.e = 0.209)$ and $\hat{\beta}_4 = 0.20\,(s.e = 0.197)$. Weighted regression analysis was performed and an estimated slope equal to -1.6643 was obtained. Based on the $\hat{\beta}_{global}$ estimate from these data of 1.14, bootstrap epidemics were generated and analysed to yield bootstrap slope estimates. The estimated slope from the original data of -1.6643 was less than all the 200 bootstrap estimated slopes ($p-$value < 0.005). Leading to the conclusion that the estimated slope was statistically significantly less than 0 at the 1% confidence level. Thus, large values of R_0 with groups of size 8 would enable detection of a genuine decrease in the rate of infection, but only if the decrease was substantially large. The larger change in decrease was probably the key factor.

For data set C, 3 out of the 200 estimated bootstrap slopes were less than the estimated slope from data set C of -0.5242 yielding a $p-$value of 0.015. Thus the estimated slope was statistically significantly less than 0 at the 5% confidence level, leading to the conclusion that increasing group size would enable the proposed methods to detect a genuine small decrease in the rate of infection given $R_0 < 3$ in the initial group of infectives.

8.4 Discussion

In the experimental data, the group size of 8 may not have been big enough given the initial dose of virus infection introduced in the group 1 individuals. From both experiments, results showed that the rate of infection for group 2 (the only group that was exposed to group 1 infection) was the lowest of all the three groups (2 to 4). It could be that the amount of infection that group 1 individuals were able to pass on to group 2 individuals was really minimal and/or that group size of 8 was not big enough. It is also possible that a genuine decreasing trend did not actually exist in these data.

In the evaluation of the appropriateness of the proposed methods, simulation methods were used. Data were generated on the basis of the infection process characteristics as estimated from experiment 1. When a small decrease was imposed on the rate of infection, the restricted model MLE based methods were able to detect the decrease as statistically significant for the data set simulated under $\hat{\beta}_{global} > 1$. However, the martingale based methods resulted in the estimate

of a non-significant decrease at the 5% level of significance. This result was in line with the underlying motivation for the development of the restricted model MLE, that this approach would increase the power of the methodology to detect decreases in β with increasing group number. The experiment was designed to investigate a drop in infectivity with increased passage: as discussed earlier, this should be associated with a sampling distribution of decreases with more support on positive variables than the distribution of slopes arising from the null hypothesis of no drop in infectivity. The distribution of decreases arising from the null hypothesis is used to define a critical region for rejection of the hypothesis. A one-sided test for decreased infectivity will equate to a critical region of decreases greater than a particular critical value. It is anticipated that estimating these decreases under the null hypothesis using restricted model ML will give rise to less variable estimates than those arising from unrestricted model ML. Hence, the critical value for the test is likely to be lower in the restricted case than in the unrestricted scenario. By contrast, any test statistic generated under the alternative hypothesis has a high chance of being unaffected by the choice of restricted or unrestricted estimates. If there is a sufficiently large decrease in infectivity, the restricted and unrestricted estimates are likely to be identical. An unchanged test statistic and a lower critical value will give rise to a reduction in the type 2 error. Treatment of restricted estimates (nature of maxima).

The non-significant result for a decreasing trend for the martingale β estimate, prompted further investigations on the martingale based methods. Three situations were considered as discussed in Section 8.3. In investigating whether the martingale based methods would detect a genuine decrease in the rate of infection but that the decrease imposed by initial passage multiplier of 0.15 was too small, a large decrease (multiplier of 1.5) was imposed on the rate of infection and analysis of data based on this criterion yielded a significant decrease. To investigate whether the problem was the initial value of R_0, the value of R_0 in the initial group of infected individuals was boosted to approximately equal to 10, while maintaining use of the other parameters of the infection process, but the analysis of data based on these conditions yielded a non-significant trend. The rate of infection is so high that the decrease is effectively negligible. All individuals still become infected very quickly. More individuals would be required to detect such a trend. When, however, the decrease was increased, the martingale based method was able to detect the decreasing trend in the rate of infection across groups. In the third scenario, the group size was investigated on the assumption that even a small decrease would have been detected if the group size had been greater than

eight. Analysis of data based on group size 20 but with the other infection process characteristics as estimated from experiment 1 yielded a significant decrease in the rate of infection.

In conclusion therefore, the proposed inferential methods have inferential power for the type of epidemic data. The restricted model MLE method is able to detect a small genuine decrease in the rate of infection for groups of size 8. The martingale based methods, however, appear to be able to detect a genuine decrease in the rate of infection in groups of size 8 only if the decrease was reasonably large. Hence, as long as a sizeable decrease is indeed present in the rate of infection across groups, groups of size 8 will probably suffice for the method to formally detect the decrease. Martingale based methods would also be able to detect a small genuine decrease in the rate of infection when $R_0 < 3$ in the initial group of infectives if the group size was large. However, if R_0 was large ($\simeq 10$), a small decrease in the rate of infection would not be detected by martingale based methods, but a large decrease would be detectable.

The results seem to indicate that a group size of 8 is sufficient to detect a genuine existing trend if R_0 in the initial group of infectives is big enough. In Section 8.2, where data were generated based on group size 8 with $R_0 < 3$, martingale based analyses yielded a non-significant trend at a level of significance less than 5%. Boosting R_0 to 10 and imposing a large decrease in the rate of infection but maintaining the group size yielded very significant trend at a 1% level of significance. The results therefore suggest that a genuine trend would be detected in group sizes of eight provided R_0 in the initial group of subjects is big enough and the decrease is large. Increasing the group size to 20 for example, even with a low value of R_0, would allow the methods to detect even a small decrease in the rate of infection. As always, the larger the experiment, the more power it will have to detect an effect of any specified size. Where the alternative hypothesis describes a consistent decline or rise in infectivity, it is probably optimal to use a restricted model MLE method to test the hypothesis. It may be worthwhile to investigate whether the properties of the martingale methodology can be improved through the use of some other summary statistic to summarise any pattern in the βs. Certainly, a more detailed power study is required before it can be stated with confidence that the restricted model MLE based method has more power to detect an effect of a given size than the martingale based method. Given sufficient power, both methods have the potential to successfully fit models to this class of data. The results suggest that the major factor influencing the properties of the

estimators is not the use of the estimated infection history, but the choice of the estimator. It is possible that the martingale estimator consistently underestimates the infection rate.

Any tendency for the distribution of slopes (in the case of unrestricted estimates) under the null hypothesis of no passage effect to exhibit a differential number of negative than positive slopes is very important. In the restricted model ML case, such an effect would correspond to a distribution of drops with a heavier or lighter tail, even under the null hypothesis, and hence, in both cases, a lower or higher power to detect genuine passage effects than might have been expected. Before the analyses were completed, it seemed likely that there might be a tendency of negative slopes, arising from a tendency of the stochastic process to generate less vigorous epidemics in higher number mixing groups. It is possible that such a tendency might arise from threshold properties of non-linear stochastic epidemics. It is well known that the SIR model exhibits threshold behaviour with respect to the reproduction ratio θ (Bailey, 1975, Section 6.5). Where $\theta > 1$, there is a finite probability $(1 - \frac{1}{\theta})$ of a major rather than a minor outbreak, while for $\theta < 1$, all outbreaks are minor. The current model incorporates a latent period, but in so far as this property merely delays the onset of infectivity, it will not greatly affect the stochastic properties of the final size of the epidemic. In the simpler case with no restricted mixing structures, and homogeneous mixing of all individuals, there will be no effect. As discussed in Diekmann and Heesterbeek (2000), Exercise 1.40, for final size, it does not matter by whom an individual is infected, but only whether an individual is infected. In this context, it is easy to formulate an equivalent process, where 'infection' events occur from infectives individually to all other individuals (some of these being so called 'ghost' infections), where it is obvious that the event of any individual being infected at least once in a realisation, is not affected by the latency model. By contrast, the interplay between latency and restricted mixing makes the outcome of a particular realisation dependent on the mixing status of the individual when it becomes infective. The main effect of this will be to increase variability in the final size distribution, the system should still exhibit major and minor outbreaks. Similarly, the use of a gamma distribution to describe the length of infection period will not affect the conclusions.

If each mixing group is thought of as a discrete entity, which is exposed to 'initial' infectives primarily from the preceding mixing group, then the probability of a major outbreak occurring in the group will depend both on the rate of infection β and the mean infectiousness time, but also on the number of 'initial'

infectives. Obviously, if a major outbreak occurs in each mixing group, then the estimates for β in each case will be unbiased and the overall analysis of the 3 estimates will provide information only about the passage parameter. However, should one of the mixing groups undergo only a minor outbreak, β will be underestimated for this group. This in itself has potential to produce a heavy tailed distribution of drops from the restricted model ML case. However, since a minor outbreak, by definition, will be associated with a small number of infectives, the next mixing group will be exposed to a smaller number of 'initial' infectives, with a correspondingly higher probability of a minor outbreak ensuing. Hence, a drop in the perceived value of β, arising only from the stochastic properties of the epidemic in one mixing group, has an enhanced chance of being propagated to subsequent mixing groups, and hence of being summarised by a slope with a negative coefficient.

Examination of the results from Experiment 1 and Experiment 2 suggested that this effect was not having a large effect on the bootstrap estimates. The median of the bootstrap estimated slopes (Table 7.5), although negative in each case, was very close to zero. Examination of the slope distributions for the simulated data provides further evidence that this factor has had little or no effect on the results presented in this chapter. For data set A and C, the distributions are clearly distributed around zero, with medians extremely close to zero. Curiously, the one bootstrap distribution which is clearly not distributed around zero, that for data set B, has a tendency of positive slope values. However, the effect of a minor outbreak may explain the apparently anomalous results presented in Table 8.15, where the estimates for data set A showed a very small estimated infection rate in group 2, followed by extinction. It is, of course, possible that the minor outbreak effect would be more salient in another situation, perhaps where β is small. The tendency of positive slopes in data set B requires a different explanation. It presumably arises from some property of the estimation procedure which fails particularly badly in the case where infectivity is very high and hence all animals become infected very quickly. This is, of course, a particularly difficult situation to model where only partial data is available. Consideration of these possible patterns in β arising under the null hypothesis leads to an important conclusion. It is even more essential that the relationship between the different estimates of β be evaluated using a bootstrap-type approach. Any correlation between epidemics in different mixing groups will give rise to correlations between β estimates which must be allowed for in any hypothesis test.

Further work is required to investigate the potential impact of minor outbreaks on estimates of β. However, if this aspect of the stochastic process does under some circumstances have a large impact on estimates of β, it might be concluded that the bootstrap simulations should perhaps not be based on an estimated β_{global} value, if this may indeed be affected by the inclusion of minor epidemics. The mixing group which is least likely to be subject to a minor outbreak is group 2, and it is arguable that a restricted model ML estimate of the infection rate applying to group 2 is therefore the best estimate of the global infection rate, even when working under the assumption that there is no systematic passage effect.

The nature of estimates for the infection and removal rates of the SIR model arising from minor and major outbreaks is discussed further in Chapter 9.

Chapter 9

Coverage properties of confidence intervals for the reproduction ratio

9.1 Introduction

In the analysis of epidemic data, estimates for infection process parameters (for example the rate of infection, β, and the removal rate, γ), depend on whether the epidemic results in a minor or major outbreak (Bailey, 1975, Section 6.5). In general, for minor outbreaks the size of the population is largely irrelevant because there will be little information regarding infected individuals and, by definition, estimates derived from small outbreaks will tend to underestimate β. For major outbreaks, however, there will be a substantial amount of information regarding the infection process if the population size is large. In parameter estimation, it is crucial that estimated parameters are accompanied by estimates of standard errors and confidence intervals. For a given parameter estimate, once an estimate for the standard error is calculated, a confidence interval can be constructed, justified by Asymptotic Likelihood Theory (ALT), using the central limit theorem (CLT) to approximate the distributional properties of the estimate. Asymptotic ML and martingale estimation methods both give rise to estimates for the standard error of estimates of a given parameter. As a result, the construction of confidence intervals justified by the CLT is very appealing (and is discussed further in Section 9.2). Becker (1989), Section 7.2, uses ALT to construct confidence intervals justified by what he terms the martingale CLT.

Unfortunately, confidence intervals based on ALT are only valid for large epidemics and large population sizes. In many cases this fact has, however, been ignored and researchers have proceeded to construct ALT-based confidence inter-

vals regardless of the epidemic and population sizes. The results obtained from such approximations may be invalid and conclusions based on such results are likely to be unreliable.

In this chapter, the properties of confidence intervals based on ALT will be evaluated. Since it is believed that ALT is not appropriate in situations with small populations or small outbreaks, ways to improve ALT-based confidence limits are discussed and alternative methods of constructing confidence intervals are proposed and evaluated. The properties of ALT-based confidence intervals are compared with those of the percentile based confidence intervals generated by parametric and semi-parametric bootstrap methods. A calibration process is applied to each of these methods with the objective of improving the basic confidence intervals. Simulated data are used to explore the coverage properties of the different confidence intervals for the reproduction ratio, denoted by θ, of a susceptible-infectious-removed (SIR) infection process. The parameter θ equals β times the mean duration of infectiousness period, *i.e.* $\theta = \beta \times \frac{1}{\gamma}$, and measures the average potential of an infective to infect a susceptible. Properties of confidence intervals are assessed with respect to the susceptible population size, the number of secondary infections and the size of the epidemic (minor or major). If the susceptible population is small, there is a limited amount of information available to make inference about the infection process mechanism. If, in addition, the resulting epidemic is minor, there is very little information available regarding the infection process. A strategy to address the effect of minor outbreaks on confidence intervals is proposed, based on the use of a beta-binomial mixture distribution.

Since the main aim of this chapter is to explore the properties of confidence intervals, a simplified SIR simulation model, as described in Section 2.4.1, is used to generate data which is then analysed under the assumption that the infection process is fully observable. The SIR model assumes that there is no latent period and that the length of infectiousness period is exponentially distributed with mean $\frac{1}{\gamma}$. The model further assumes a uniformly homogeneous mixing population. The simulated infection process starts with 1 infectious individual and the rest of the population susceptible. Once an individual becomes infected, it becomes infectious immediately and stays in the infectious state for a random period of time generated from the exponential distribution with mean equal to $\frac{1}{\gamma}$, after which it is removed, *i.e.* it is no longer infectious and is not susceptible to re-infection.

9.2 Estimation of parameters

When generating estimates for β and γ, different methodologies are available to calculate confidence intervals. Those discussed at most length in the statistical literature are those based on the Neyman-Pearson likelihood ratio statistic, those based on the Rao score statistic and those based on the Wald, or maximum likelihood (ML) estimate statistic. These are presented in their multi-dimensional and scalar forms in Barndorff-Nielsen and Cox (1994), Section 3.2. These methods are all equivalent to the first order of approximation, but they have subtly different properties in terms of ease of calculation and of suitability in specific situations. In each case, the calculation of the confidence interval is based on a proof that the distribution of the test statistic converges in probability to a chi-square (multi-dimensional parameter) or normal (scalar parameter) distribution as the size of the data set tends to infinity. The key issue when calculating confidence intervals for $\hat{\beta}$ and $\hat{\gamma}$ is the fact that the likelihood for these parameters is non-zero only on the positive axis. When calculating confidence intervals for $\hat{\theta}$, it should be noted that these estimates are not estimated directly from the data, but rather as a function of estimates of β and γ. Confidence intervals derived from the critical region of the Neyman-Pearson statistic automatically exclude any regions where the likelihood is zero (such as those corresponding to negative values of the parameter). This is not true of the other two statistics (Barndorff-Nielsen and Cox, 1994, Section 4.2). Hence, everything else being equal, a confidence interval based on the chi-square approximation to the log-likelihood ratio might be preferred. However, the ML estimate statistic has computational advantages, since if the information matrix is evaluated at the ML estimate, the confidence interval is fully defined by the point estimate and the second derivatives of the log-likelihood (as illustrated in Section 4.2). In the case of θ, this computational advantage is compounded by an overwhelming practical issue. Both the Neyman-Pearson and Rao methods require direct knowledge of the likelihood function. In the case of θ, no such function is available. However, the use of the ML estimates for β and γ and hence the direct calculation of their estimated variances will allow the calculation of a point estimate and variance for the associated estimate of θ. Hence, for θ, the use of the ML estimate is unavoidable. For ease of computation and comparison, the same methodology is used for β and γ, although it should be stressed that the log-likelihood ratio approach would give better results for these two parameters.

9.2.1 Estimation of rate of infection, β

Let N denote the total number of individuals in the simulated epidemic,

I_0 denote the number of initial infectives, $I_0 = 1$,

I_s denote the total number of secondary infectives in a simulated epidemic, such that $N - 1 - I_s$ is the total number of individuals still susceptible at the end of the epidemic,

$I(t)$ denote the number of infectives at time t,

t_i denote the time of infection of infected individual i, and

t_{max} denote the time of the end of the epidemic.

The likelihood function L from which β is to be estimated is given by

$$\begin{aligned} L &= \prod_{i=1}^{I_s} \left\{ \frac{\beta I(t_i)}{N} e^{-\beta \int_0^{t_i} \frac{I(t)}{N} dt} \right\} \prod_{j=1}^{N-1-I_s} e^{-\beta \int_0^{t_{max}} \frac{I(t)}{N} dt} \\ &= \beta^{I_s} \prod_{i=1}^{I_s} \left(\frac{I(t_i)}{N} \right) e^{-\beta \sum_{i=1}^{I_s} \int_0^{t_i} \frac{I(t)}{N} dt} e^{-\beta (N-1-I_s) \int_0^{t_{max}} \frac{I(t)}{N} dt}. \end{aligned}$$

The log-likelihood l is given by

$$l = I_s \ln(\beta) + \sum_{i=1}^{I_s} ln \left(\frac{I(t_i)}{N} \right) - \beta \sum_{i=1}^{I_s} \int_0^{t_i} \frac{I(t)}{N} dt - \beta (N - 1 - I_s) \int_0^{t_{max}} \frac{I(t)}{N} dt.$$

Taking first and second order derivatives of the log-likelihood with respect to β yields:

$$\begin{aligned} \frac{dl}{d\beta} &= \frac{I_s}{\beta} - \left[\sum_{i=1}^{I_s} \int_0^{t_i} \frac{I(t)}{N} dt + (N - 1 - I_s) \int_0^{t_{max}} \frac{I(t)}{N} dt \right] \\ &= \frac{I_s}{\beta} - \sum_{k=1}^{N-1} \int_0^{\min\{t_k, t_{max}\}} \frac{I(t)}{N} dt \\ &= \frac{I_s}{\beta} - T_e \\ \frac{d^2 l}{d\beta^2} &= -\frac{I_s}{\beta^2} \end{aligned} \tag{9.1}$$

where $T_e = \sum_{k=1}^{N-1} \int_0^{\min\{t_k, t_{max}\}} \frac{I(t)}{N} dt$

is the total scaled exposure time for the $N - 1$ initially susceptible individuals. It should be noted that individuals that remain susceptible at the end of the epidemic have a notional time of infection t_k beyond the time of the end of the epidemic t_{max}, and hence, for such individuals, $\min\{t_k, t_{max}\} = t_{max}$.

From the first order derivative of the log-likelihood, the estimate for β is determined:

$$\frac{dl}{d\beta} = 0 \Rightarrow \hat{\beta} = \frac{I_s}{T_e}. \tag{9.2}$$

From the second order derivative of l, the estimate for the standard error of β is determined:

$$s.e(\hat{\beta}) \simeq \sqrt{\left[-\frac{d^2l}{d\beta^2}\right]^{-1}_{\beta=\hat{\beta}}} = \frac{\hat{\beta}}{\sqrt{I_s}} = \frac{\sqrt{I_s}}{T_e}. \tag{9.3}$$

Assuming the asymptotic normality of the estimator, the $(1-\alpha)100\%$ confidence interval for $\hat{\beta}$ is given by

$$[\,\hat{\beta} - s.e(\hat{\beta})\, z_{1-\frac{\alpha}{2}},\ \hat{\beta} + s.e(\hat{\beta})\, z_{1-\frac{\alpha}{2}}\,],$$

where z_α is the standard normal value such that $\Phi(z_\alpha) = \alpha$.

9.2.2 Estimation of rate of removal, γ

The SIR model assumes a negative exponentially distributed infectiousness period with mean $\frac{1}{\gamma}$. Thus the length of infectiousness period for the i^{th} infected individual, denoted by X_i, is negative exponentially distributed with mean $\frac{1}{\gamma}$, for all i. The aim is to estimate γ.
Let I_t denote the total number of infected individuals during the epidemic *i.e.* $I_t = I_0 + I_s$, and $f_X(x_i;\, \gamma)$ denote the probability density function of X_i, then

$$f_X(x_i,\, \gamma) = \gamma\, e^{-\gamma x_i}.$$

The likelihood function of the infectiousness period of infected individuals is given by

$$L = \prod_{i=1}^{I_t} \gamma\, e^{-\gamma x_i} = \gamma^{I_t}\, e^{-\gamma \sum_{i=1}^{I_t} x_i}$$

and the log-likelihood function is given by

$$l = ln(L) = I_t\, ln(\gamma) - \gamma \sum_{i=1}^{I_t} x_i.$$

Taking first and second order derivatives of l with respect to γ yields:

$$\frac{dl}{d\gamma} = \frac{I_t}{\gamma} - \sum_{i=1}^{I_t} x_i; \quad \text{and} \quad \frac{d^2l}{d\gamma^2} = -\frac{I_t}{\gamma^2}. \tag{9.4}$$

Estimates for γ and the associated standard error are determined from the log-likelihood derivatives as follows:

$$\begin{aligned} \frac{dl}{d\gamma} &= 0 \Rightarrow \hat{\gamma} = \frac{I_t}{\sum_{i=1}^{I_t} x_i} = \frac{I_t}{T_p} \quad \text{and} \\ s.e(\hat{\gamma}) &= \sqrt{\left[-\frac{d^2 l}{d\gamma^2}\right]_{\hat{\gamma}}^{-1}} = \frac{\hat{\gamma}}{\sqrt{I_t}} = \frac{\sqrt{I_t}}{T_p}, \end{aligned} \tag{9.5}$$

where $T_p = \sum_{i=1}^{I_t} x_i$ is the total infectiousness period of all I_t infectives.

Assuming the asymptotic normality of the estimator, the $(1-\alpha)100\,\%$ confidence interval for $\hat{\gamma}$ is given by

$$[\,\hat{\gamma} - s.e(\hat{\gamma})\, z_{1-\frac{\alpha}{2}},\ \hat{\gamma} + s.e(\hat{\gamma})\, z_{1-\frac{\alpha}{2}}\,].$$

9.2.3 Estimation of the reproduction ratio, θ

Since θ is given by $\frac{\beta}{\gamma}$, an estimate of $\hat{\theta}$ and an estimate of the standard error of $\hat{\theta}$ can be determined from the estimates of β and γ and the corresponding estimates for their standard errors. From expressions for the estimates of β and γ in Equations 9.2 and 9.5, the estimate for θ is given by:

$$\hat{\theta} = \frac{\hat{\beta}}{\hat{\gamma}} = \frac{I_s\, T_p}{I_t\, T_e} = \frac{I_s\, T_p}{(I_s+1)\, T_e}, \quad \text{since} \quad I_t = I_s + I_0. \tag{9.6}$$

Examining the estimator of θ, simulation results suggest that minimal non-zero values of $\hat{\theta}$ will occur where $I_s = 1$. Let x_1 denote the infectiousness period of the initial infective, x_2 denote the infectiousness period of the only secondary infection and E_2 denote the scaled duration of exposure for the secondary infection. It should be noted that $E_2 = \frac{x_1^*}{N}$, where x_1^* $(x_1^* \leq x_1)$, is the duration of exposure that caused the secondary infective to became infected. Then the total duration of infection exposure T_e is given by:

$$T_e = (N - I_s - 1)\frac{(x_1+x_2)}{N} + \frac{x_1^*}{N} = (N-2)\frac{(x_1+x_2)}{N} + \frac{x_1^*}{N}$$

and

$$\begin{aligned} \hat{\theta} &= \frac{x_1+x_2}{2\left[(N-2)\frac{(x_1+x_2)}{N} + \frac{x_1^*}{N}\right]} = \frac{N\,(x_1+x_2)}{2\,[(N-2)(x_1+x_2) + x_1^*]} \\ &\geq \frac{N\,(x_1+x_2)}{2\,[(N-2)(x_1+x_2) + (x_1+x_2)]} = \frac{N}{2\,[N-1]}. \end{aligned} \tag{9.7}$$

Hence, $\hat{\theta}$ is bounded below by $\frac{N}{2(N-1)}$, a monotonically decreasing function in N. As $N \to \infty$, $\frac{N}{2(N-1)} \to \frac{1}{2}$.

Using the δ method (Becker, 1989, Appendix), the variance of $\hat{\theta}$ can be estimated as follows:
Let $g(\beta, \gamma) = \theta = \frac{\beta}{\gamma}$, then

$$\begin{aligned} var(\hat{\theta}) &\simeq \left(\frac{d}{d\,\beta} g(\beta, \gamma)\right)^2 \Big|_{\hat{\beta},\hat{\gamma}} var(\hat{\beta}) + \left(\frac{d}{d\,\gamma} g(\beta, \gamma)\right)^2 \Big|_{\hat{\beta},\hat{\gamma}} var(\hat{\gamma}) \\ &\quad + 2\left(\frac{d}{d\,\beta} g(\beta, \gamma)\right)\left(\frac{d}{d\,\gamma} g(\beta, \gamma)\right)\Big|_{\hat{\beta},\hat{\gamma}} cov(\hat{\beta}, \hat{\gamma}) \\ &= \left(\frac{1}{\hat{\gamma}}\right)^2 var(\hat{\beta}) + \left(\frac{-\hat{\beta}}{\hat{\gamma}^2}\right)^2 var(\hat{\gamma}) - 2\frac{1}{\hat{\gamma}}\frac{\hat{\beta}}{\hat{\gamma}^2} cov(\hat{\beta}, \hat{\gamma}) \\ &= \frac{1}{\hat{\gamma}^2}\left[var(\hat{\beta}) + \hat{\theta}^2\, var(\hat{\gamma})\right] \text{ conditional on } cov(\hat{\beta}, \hat{\gamma}) = 0 \end{aligned}$$

$$\text{thus } s.e(\hat{\theta}) = \sqrt{var(\hat{\theta})} = \frac{1}{\hat{\gamma}}\sqrt{\left[var(\hat{\beta}) + \hat{\theta}^2\, var(\hat{\gamma})\right]}. \tag{9.8}$$

The joint likelihood for β and γ can be factored into two parts, one a function of β alone and the other a function of γ alone. Hence the ML estimates are independent. Assuming the asymptotic normality of the estimator, the confidence interval for $\hat{\theta}$ is given by

$$[\,\hat{\theta} - s.e(\hat{\theta})\, z_{1-\frac{\alpha}{2}},\ \hat{\theta} + s.e(\hat{\theta})\, z_{1-\frac{\alpha}{2}}\,]. \tag{9.9}$$

9.3 Evaluation of confidence intervals based on the asymptotic properties of the ML estimate statistic

ALT-based confidence intervals for $\hat{\theta}$, which are based on the standard error estimates for $\hat{\theta}$, depend on the variance estimates of $\hat{\beta}$ and $\hat{\gamma}$. It is therefore important to explore the properties of $\hat{\beta}$ and $\hat{\gamma}$ and their variance estimators to evaluate their effect on estimates of the standard errors of $\hat{\theta}$. For this task, epidemics are simulated assuming a SIR infection process with parameters β and γ. Estimates of $\hat{\beta}$ and $\hat{\gamma}$ and their corresponding standard errors are determined for each simulated epidemic sample. Epidemics are repeatedly simulated based on population sizes (n) of 10 and 50, each with $\beta = 2$ and $\gamma = 1$. It is well known

that the SIR model exhibits threshold behavior with respect to the reproduction ratio θ (Bailey, 1975, Section 6.5). Where $\theta > 1$, there is a finite probability $(1 - \frac{1}{\theta})$ of a major rather than a minor outbreak, while for $\theta < 1$, all outbreaks are minor. It therefore seems reasonable to attempt to fit a model to the observed (simulated) number of secondary infections which assumes the existence of two separate underlying distributions, one of which can be thought of as arising from minor outbreaks, and the other from major outbreaks. For each population size, outbreaks are categorized into minor and major outbreaks using a beta-binomial mixture distribution as described below.

Let s denote the number of initial susceptibles in the population and I_s the number of secondary infectives, with i_s the observed value of I_s. The probability density function of I_s assuming a beta-binomial mixture distribution, is given by:

$$\begin{aligned} \mathrm{P}(I_s = i_s) &= \mathrm{P}(\text{minor}) \binom{s}{i_s} \frac{\Gamma(\alpha_1+\beta_1)}{\Gamma(\alpha_1)\Gamma(\beta_1)} \frac{\Gamma(i_s+\alpha_1)\Gamma(s-i_s+\beta_1)}{\Gamma(\alpha_1+\beta_1+s)} \\ &+ (1 - \mathrm{P}(\text{minor})) \binom{s}{i_s} \frac{\Gamma(\alpha_2+\beta_2)}{\Gamma(\alpha_2)\Gamma(\beta_2)} \frac{\Gamma(i_s+\alpha_2)\Gamma(s-i_s+\beta_2)}{\Gamma(\alpha_2+\beta_2+s)}, \end{aligned} \tag{9.10}$$

where P(minor) is the probability of I_s arising from a minor outbreak, 1 - P(minor) is the probability of I_s arising from a major outbreak, α_1 and β_1 are the scale and shape parameters respectively for the minor outbreak beta distribution, and α_2 and β_2 are the scale and shape parameters respectively for the major outbreak beta distribution.

For an observed outbreak with i_s observed secondary infectives, the quantity

$$\left\{ \frac{\Gamma(\alpha_1+\beta_1)}{\Gamma(\alpha_1)\Gamma(\beta_1)} \frac{\Gamma(i_s+\alpha_1)\Gamma(s-i_s+\beta_1)}{\Gamma(\alpha_1+\beta_1+s)} \right\} \left\{ \frac{\Gamma(\alpha_2+\beta_2)}{\Gamma(\alpha_2)\Gamma(\beta_2)} \frac{\Gamma(i_s+\alpha_2)\Gamma(s-i_s+\beta_2)}{\Gamma(\alpha_2+\beta_2+s)} \right\}^{-1} \tag{9.11}$$

is used to categorize i_s as a minor or major outbreak, depending on whether this function is greater than or less than unity.

The likelihood of I_s for each class of simulated data sets (specified by population size and parameter choice) was maximised and estimates of parameters for the beta-binomial mixture distribution were obtained. It was then possible to obtain critical values of I_s against which to classify epidemics as minor or major outbreaks. For the $n = 10$ epidemics, the partition was taken to be such that outbreaks with 1 to 3 secondary infectives are minor outbreaks and outbreaks with 4 to 9 secondary infectives are major (on the balance of likelihood). For

$n = 50$ epidemics, the partition was taken to be such that epidemics with 1 to 20 secondary infectives are minor outbreaks while the observation of 21 to 49 secondary infections implies a major outbreak.

The first and second order properties of $\hat{\beta}$ and $\hat{\gamma}$ estimators are explored based on the simulated epidemics. For $n = 10$, 3249 non-trivial epidemic samples (*i.e.* with $I_s > 0$) were generated and from these, 984 were categorized as minor outbreaks. For $n = 50$, 3285 non-trivial epidemic samples were generated and 1064 were categorized as minor outbreaks. These data are used, in a later section, to explore the properties of $\hat{\beta}$ and $\hat{\gamma}$ and the associated standard errors. For each epidemic sample, $\hat{\beta}$ and $\hat{\gamma}$ and the associated standard errors are estimated based on Equations 9.2, 9.3 and 9.5.

The goodness of fit of the beta-binomial mixture distribution was assessed by fitting the model to smaller simulated data sets containing 100 realisations, for populations sizes 10 and 50 and parameters $\theta = 2\,(\beta = 1, \gamma = 0.5)$. These realisations were all non-trivial and hence the likelihood was conditioned on the observation of non-zero random variables. For both population sizes, the analysis showed good fits of the beta-binomial mixture distribution to the data; chi-square values of 2.7903 with 8 degrees of freedom (p-value = 0.947) for $n = 10$ and chi-square values of 11.5476 with 14 degrees of freedom (p-value = 0.643) for $n = 50$. The fitted distributions are displayed in Figure 9.1.

Figure 9.1: *Plot of mixture distribution for epidemics from population sizes* 10 *and* 50.

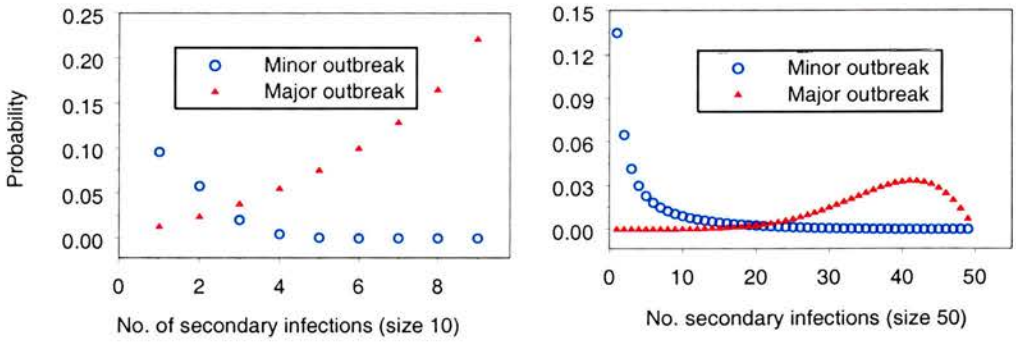

Examining the plots for the fitted mixture distributions, it is clear that the classification of epidemics as minor and major outbreaks is possible and that the distinction between these classes becomes more obvious with increased population size. For $n = 10$, there seems to be a region of outcomes where, given the

number of secondary infections, there is an appreciable probability of an outbreak arising from either category. Where $n = 50$ there is a very clear partition between the two categories of outbreak.

9.3.1 Exploring the properties of the estimate of β

To explore the properties of the estimated β, the estimates of $\hat{\beta}$ are plotted against the number of secondary infections I_s as is the mean of $\hat{\beta}$. The plots are displayed in Figure 9.2 for population sizes 10 and 50.

Figure 9.2: *Plot of estimates of* β $(\beta = 2)$ *and the mean of estimates of* β *against the number of secondary infections* I_s *for* (*a*) *population size* 10 *and* (*b*) *population size* 50.

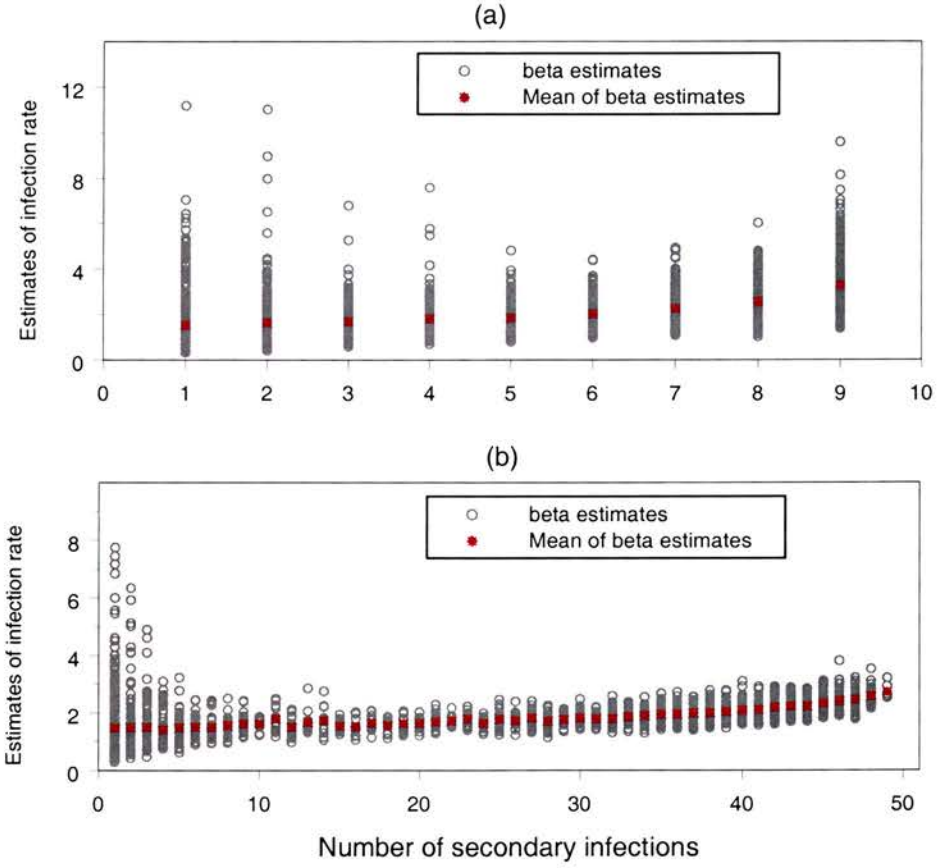

The plots indicate a non-linear relationship between estimates of β and the number of secondary infections. This is to be expected from the nature of the estimator for β ($\hat{\beta} = \frac{I_s}{\sum_{i=1}^{N-1} T_i}$), since the expected value of $\hat{\beta}$ given by

$E(\hat{\beta}) = I_s E\left[\frac{1}{\sum_{i=1}^{N-1} T_i}\right]$ is non-linear in I_s, where T_i is the duration of infection exposure for individual i. From the plots it is observed that variability first decreases and then increases with I_s (this is more obvious in the case $n = 10$). There is more information in the data as the epidemic size increases, however, for large I_s, there is scope for more variability in the estimators as the epidemic exhausts itself and changes in the observed exposure durations are not matched by changes in I_s. For small I_s, infection exposure is calculated by summing a small number of random variables, with an associated lack of ability to average out variability in T_i. Hence variability will be high in β estimates for small and large values of I_s but lower for median values of I_s. It is also notable that the mean of $\hat{\beta}$ increases with I_s and it is consistently below the true value for small values of I_s, *i.e.* for all minor outbreaks.

To explore the properties of the variance estimator, estimates of standard errors for $\hat{\beta}$ are plotted against the number of secondary infections (I_s). The plot is displayed in Figure 9.3. The figure also includes plots of estimated standard errors derived from the standard deviation of the simulated estimates (blue line), the asymptotic standard error of the ML estimator conditional on the number of observed infections (green line) and the asymptotic standard error of the ML estimator in the case of a large outbreak (red line).

The asymptotic variance estimate for $\hat{\beta}$ is derived from the second order derivative of the log-likelihood in Equation (9.1) as follows:

$$\begin{aligned} \frac{d^2l}{d\beta^2} &= -\frac{I_s}{\beta^2} \Rightarrow E\left[\frac{d^2l}{d\beta^2}\right] = -\frac{E[I_s]}{\beta^2} \\ &\Rightarrow var(\hat{\beta}) \simeq \left[E\left(-\frac{d^2l}{d\beta^2}\right)\right]^{-1} = \frac{\beta^2}{E(I_s)}. \end{aligned}$$

Conditional on $I_s = i_s$, the asymptotic standard error of $\hat{\beta}$ is therefore by:

$$\sqrt{var(\hat{\beta}|i_s)} = \sqrt{\frac{\beta^2}{E(I_s)}} = \frac{\beta}{\sqrt{i_s}},$$

and the asymptotic standard error of $\hat{\beta}$ in case of a large outbreak is given by:

$$\sqrt{var(\hat{\beta}|\text{major})} = \sqrt{\frac{\beta^2}{E(I_s|\text{major})}} = \frac{\beta}{\sqrt{E(I_s|\text{major})}},$$

where $E(I_s|\text{major})$ is estimated from the simulated data.

Figure 9.3: *Plot of estimates of standard errors of $\hat{\beta}$ against the number of secondary infections I_s for (a) population size 10 overall, (b) population size 10 major outbreaks ($I_s \geq 4$), (c) population size 50 minor outbreaks ($I_s \leq 20$) and (d) population size 50 major outbreaks ($I_s > 20$).*

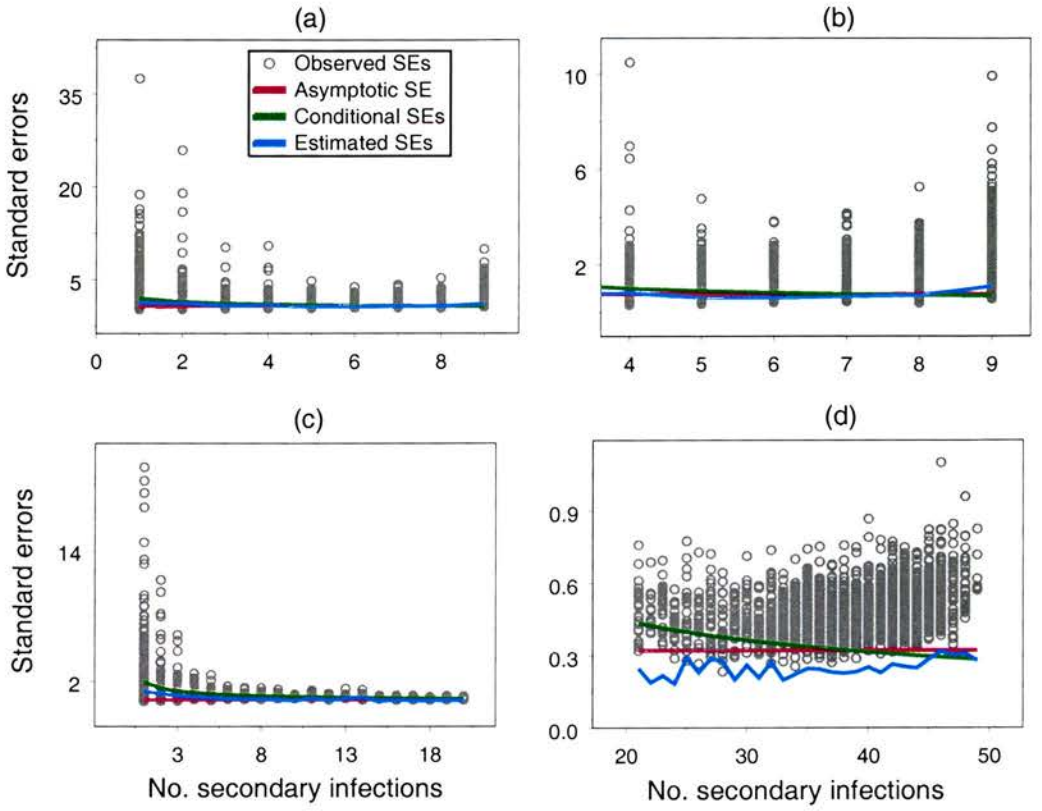

For outbreaks for population size 10, the calculated estimates of the standard errors (termed observed SEs on the plot) have a high variability for lower values of I_s but this decreases as I_s increases, for $I_s < 7$ but increases again for larger I_s. For population size 50, the trend in variability of estimates of standard errors of $\hat{\beta}$ is similar to that for population size 10 where variability tends to be high for small values of I_s but tends to decrease with increasing I_s in minor outbreaks (see Figure 9.3(c)). For major outbreaks ($I_s > 20$), the variability in calculated estimates of standard errors seems to slightly increase with increasing I_s. The explanation for this is as earlier given, that changes in the infection exposure time will not necessarily be matched by changes in I_s where the epidemic exhausts the susceptible population.

When I_s is very small, comparing the 'observed' standard errors with the theoretical standard errors (asymptotic SEs and estimates from standard deviations)

is inappropriate. This is because the theoretical values plotted are not valid since they are based on asymptotic large sample properties of the likelihood. Comparisons between the calculated estimates and estimates of standard error calculated from the standard deviation of the simulated values of $\hat{\beta}$, suggest that there is no consistent bias in the calculated standard error estimators. This is true for both the large and small population scenarios. However, estimates of $\hat{\beta}$ from small outbreaks will tend to be biased downwards. For larger outbreaks, the calculated ('observed') standard errors tend to overestimate the theoretical variability of the estimator, and the resulting confidence intervals will therefore be liberal. It should be noted that for cases with large numbers of secondary infections, the theoretical (ML-based) values (red) are close to the estimated values (blue), indicating that the ML estimates are a good approximation. However the estimates of these values are poor. The combination of these effects ensures that it is unlikely that the true coverage of a notional confidence interval will be correct. This is reflected in an evaluation of the coverage properties of the nominal 90% confidence intervals for β derived from ALT.

For the $n = 10$ epidemic, the number of confidence intervals containing the true value of $\beta = 2$ was 2996 out of 3249 yielding an estimated confidence of 92% with a 95% confidence interval for the true confidence of $(0.91, 0.93)$. This estimated coverage probability is statistically significantly greater than 0.90, but not very different in absolute terms. However, as might be expected, this global estimate is misleading given the divergent behavior of the estimates in the two underlying groups. Out of the 3249 simulated epidemics, 984 were classed as minor and of these, 777 confidence intervals contained the true value of β, *i.e.* an estimated confidence of 79% with a 95% confidence interval for the true confidence of $(0.76, 0.81)$. Hence the true confidence in this class is much less than 90%. By contrast, among the 2265 major epidemics, the number of confidence intervals containing the true value of β was 2219, giving an estimated confidence of 98% with a 95% confidence interval for the true confidence of $(0.97, 0.99)$. As expected, the notional 90% confidence interval is extremely liberal for major outbreaks.

For the $n = 50$ epidemic, the number of confidence intervals containing the true value of β was 3011 out of 3285, *i.e.* an estimated confidence of 92% with a 95% confidence interval for the true confidence of $(0.91, 0.93)$. This estimated coverage probability is again statistically significantly greater than 0.90, but not very different in absolute terms. However, once again, this global estimate is misleading given the divergent behavior of the estimates in the two underlying

groups. 1064 simulated epidemics out of 3285 were classified as minor and of these, 831 gave rise to confidence intervals containing the true value of β, *i.e.* an estimated confidence of 78% with a 95% confidence interval for the true confidence of $(0.75, 0.81)$. Hence the true confidence in this class is much less than 90%. By contrast, among the 2221 major epidemics, 2180 confidence intervals contained the true value of β giving a 98% estimated confidence with a 95% confidence interval for the true confidence of $(0.98, 0.99)$. Thus, the notional 90% confidence interval is consistently liberal for major outbreaks. These results are consistent with the earlier review of the properties of standard errors for $\hat{\beta}$.

9.3.2 Exploring the properties of the estimate of γ

Estimates of γ and the mean of these estimates are plotted against the number of secondary infections I_s, and the plots are displayed in Figure 9.4 for population sizes 10 and 50.

For population size 10, variability in the estimates of γ is high in minor epidemics ($I_s < 4$) but is smaller in major outbreaks. This can be explained from the definition of the estimator. The bigger I_s is, the more information is present in the data regarding the infection process. It can indeed be observed from the plots that variability in the estimates decreases with increasing number of secondary infections. The mean of $\hat{\gamma}$ decreases with increasing I_s and there seems to be a nonlinear relationship between $\hat{\gamma}$ and I_s. It should be noted from the equation for the estimator of γ ($\hat{\gamma} = \frac{I_t}{\sum_{i=1}^{I_t} x_i}$), that the expected value of $\hat{\gamma}$ ($E(\hat{\gamma}) = I_t\, E\left[\frac{1}{\sum_{i=1}^{I_t} x_i}\right]$) is not linear in I_t. The trend is similar for population size 50 with variability in estimates being higher for minor outbreaks ($I_s < 10$). For larger outbreaks, the variability in the estimates is minimal and most estimates are tightly concentrated around the mean for each I_s and around the true value of $\gamma = 1$. In general, the variability in the estimates is higher for those simulated with population size 10 compared to those with population size 50.

To explore the properties of the estimator of the standard error for $\hat{\gamma}$, estimates of the standard errors of $\hat{\gamma}$ are plotted against the number of secondary infections (I_s) and these are displayed in Figure 9.5 for populations of size 10 and 50. Also included on the plots are estimated standard errors derived from the standard deviation of the simulated estimates (blue line), the asymptotic standard error of the ML estimator conditional on the number of observed infections (green line)

Figure 9.4: *Plot of estimate of removal rate* $\hat{\gamma}$ *(*$\gamma = 1$*) and the mean of estimates of* γ *against the number of secondary infections* I_s *for* (*a*) *population size* 10 *and* (*b*) *population size* 50.

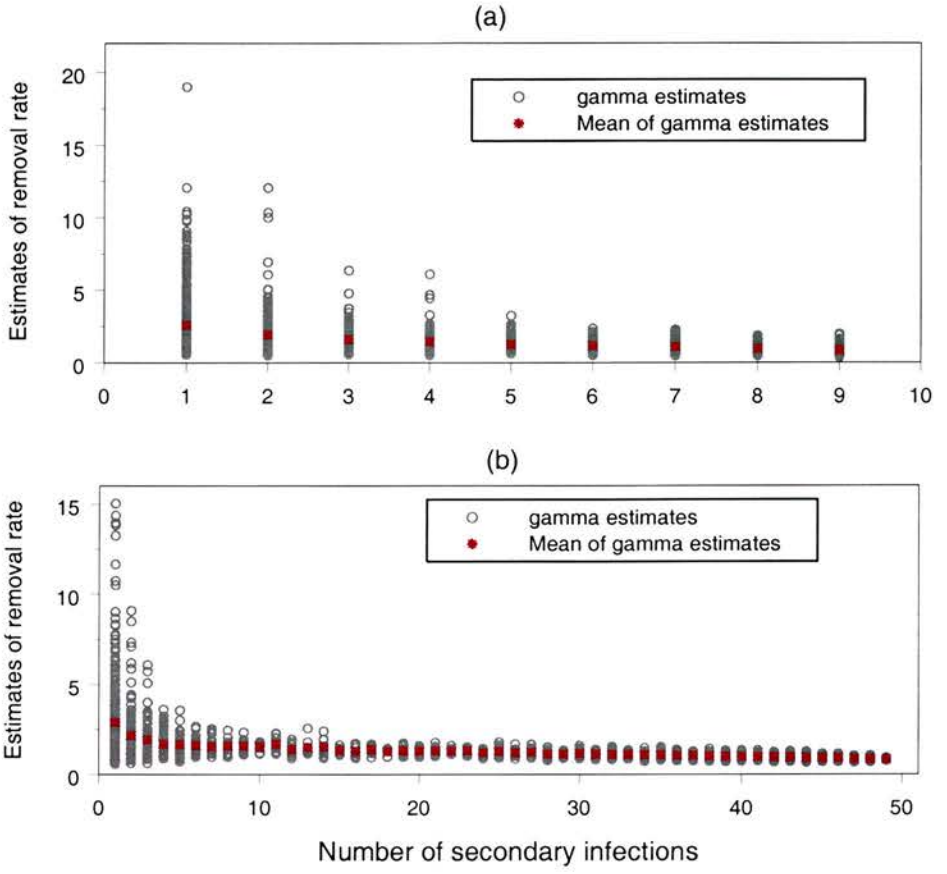

and the asymptotic standard error of the ML estimator in the case of a large outbreak (red line).

The asymptotic variance estimate of $\hat{\gamma}$ is derived from the second order derivative of the log-likelihood in Equation (9.4) as follows:

$$\begin{aligned} \frac{d^2l}{d\gamma^2} &= -\frac{I_t}{\gamma^2} \Rightarrow E\left[\frac{d^2l}{d\gamma^2}\right] = -\frac{E[I_t]}{\gamma^2} \\ &\Rightarrow var(\hat{\gamma}) \simeq \left[E\left(-\frac{d^2l}{d\gamma^2}\right)\right]^{-1} = \frac{\gamma^2}{E(I_t)}. \end{aligned}$$

The asymptotic standard error of $\hat{\gamma}$ conditional on the number of observed infections $I_t = i_t$ is therefore given by:

$$\sqrt{var(\hat{\gamma}|i_t)} = \sqrt{\frac{\gamma^2}{E(I_t)}} = \frac{\gamma}{\sqrt{i_t}},$$

Figure 9.5: *Plot of estimates of standard errors of $\hat{\gamma}$ against the number of secondary infections I_s for (a) population size 10 overall, (b) population size 10 major outbreaks ($I_s \geq 4$), (c) population size 50 minor outbreaks ($I_s < 21$) and (d) population size 50 major outbreaks ($I_s \geq 21$).*

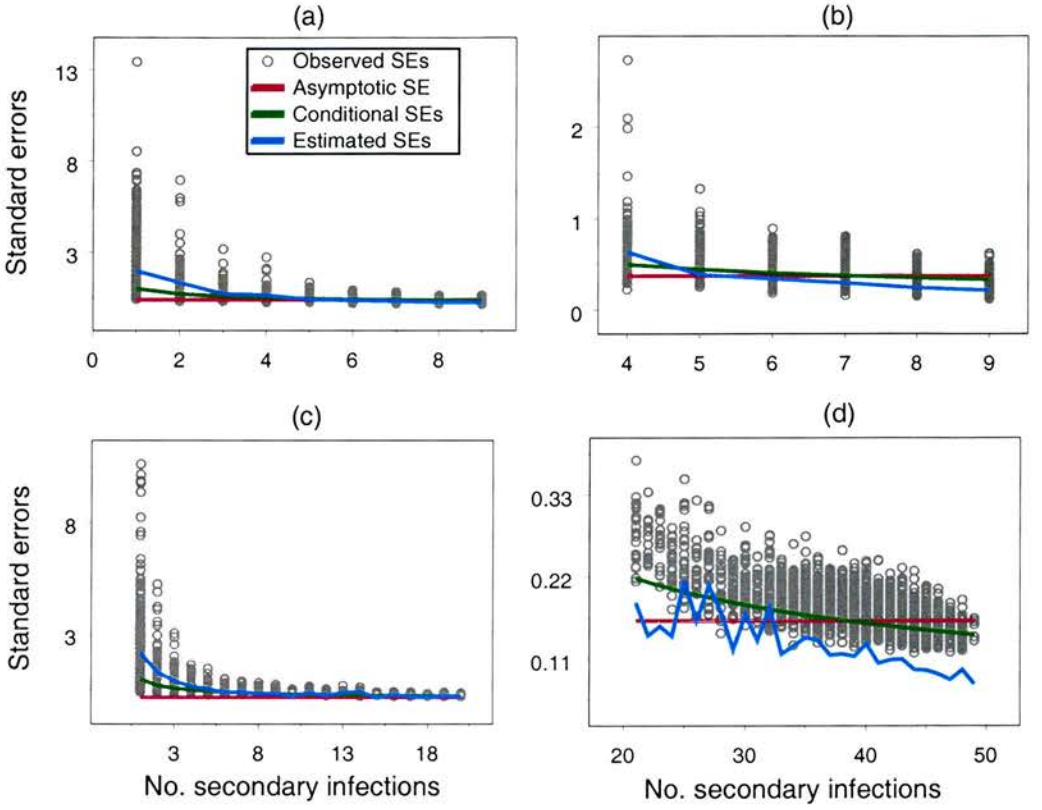

and the asymptotic standard error of $\hat{\gamma}$ in case of a large outbreak is given by:

$$\sqrt{var(\hat{\gamma}|\text{major})} = \sqrt{\frac{\gamma^2}{E(I_t|\text{major})}} = \frac{\gamma}{\sqrt{E(I_t|\text{major})}},$$

where $E(I_t|\text{major})$ is estimated from the simulated data.

For all classes of outbreaks, the calculated estimates of the standard errors of $\hat{\gamma}$ (termed 'observed' standard errors in Figure 9.5) decrease with increasing I_s. When comparing these estimates with the theoretical standard errors, the pattern is clearest in the case of $n = 50$. Where I_s is very small, the theoretical values plotted are meaningless as they assume asymptotic large sample properties of the likelihood, however, comparisons between the calculated estimates and estimates of standard errors calculated from the standard deviation of simulated values of $\hat{\gamma}$, suggest that there is no consistent bias in the variance estimator, and if anything, there is a tendency for the asymptotic standard errors to underestimate the vari-

ability in the simulated estimates in minor outbreaks. However, as I_s increases, the calculated standard errors tend to overestimate the theoretical variability of the estimator. Hence, even in the situation where we have a large outbreak, and might have thought that there was a sufficient volume of information to allow the use of the ML estimates and the use of ALT-based on a large sample, the coverage properties of the confidence intervals may be poor.

The properties of the estimator can be explored by evaluating the true coverage properties of the notional 90% confidence interval. For the $n = 10$ case, out of 3249 simulated epidemics, 3036 of the estimated confidence intervals contained the true value of $\gamma = 1$, *i.e.*, a 93% confidence with a 95% confidence interval of the true confidence of $(0.93, 0.94)$. For the case where $n = 50$, from 3285 simulated epidemics, 3146 of the estimated confidence intervals contained the true value of γ, *i.e.*, an estimated confidence of 96% with a 95% confidence interval for the true confidence of $(0.95, 0.96)$. The results indicate some liberality in confidence interval coverage relative to the notional 90% confidence level. However, it is more informative to consider the results for minor and major outbreaks separately. For the $n = 10$ case, from 984 minor outbreaks, 982 of the estimated confidence intervals contained the true value *i.e* an estimated confidence of 99.8% with a 95% confidence interval for the true confidence of $(0.99, 0.9998)$. From 2265 major outbreaks, 2054 of the estimated confidence intervals contained the true value, *i.e.*, a 91% estimated confidence with a 95% confidence interval for the true confidence of $(0.89, 0.92)$. For the $n = 50$ case, from 1064 minor outbreaks, 1035 of the estimated confidence intervals contained the true value of γ, *i.e.*, an estimated confidence of 97% with a 95% confidence interval for the true confidence of $(0.96, 0.98)$. In 2221 major outbreaks, 2111 of the confidence intervals contained the true value of γ, giving a 95% estimated confidence with a 95% confidence interval for the true confidence of $(0.94, 0.96)$.

From the above results it can be concluded that the use of asymptotic results, as applied to the estimation of $\hat{\gamma}$, may produce appreciably liberal or conservative confidence intervals. Minor outbreaks seem likely to give rise to liberal confidence intervals, while major outbreaks may give rise to conservative results.

9.3.3 Exploring the effect of variance estimates of $\hat{\beta}$ and $\hat{\gamma}$ on the properties of $\hat{\theta}$

The estimate of the standard error of $\hat{\theta}$ is calculated on the assumption that the correlation between $\hat{\beta}$ and $\hat{\gamma}$ is zero. Again, this is a large sample assumption, and it is typical to observe correlation between the two parameter estimates. Estimated values of $\hat{\beta}$ are plotted against values of $\hat{\gamma}$. The plots are displayed in Figure 9.6 for all epidemics, for minor outbreaks and for major outbreaks based on population sizes 10 and 50.

Figure 9.6: *Plot of estimates of γ against estimates of β for (a) population size 10 overall, (b) population size 10 minor outbreaks i.e. $I_s \leq 3$, (c) population size 10 major outbreaks i.e. $I_s > 3$, (d) population size 50 overall, (e) population size 50 minor outbreaks i.e. $I_s \leq 20$ and (f) population size 50 major outbreaks i.e. $I_s > 20$. Note: Different colours indicate different values of I_s, with blue indicating the smallest I_s value.*

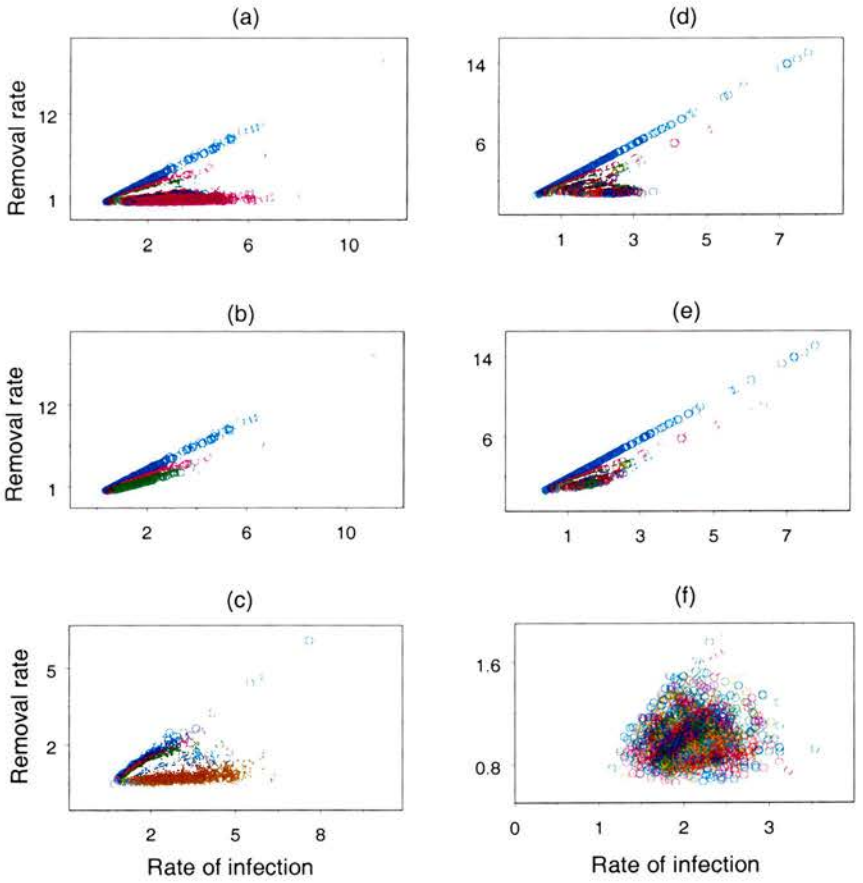

For small values of I_s, the linear nature of the relationship between $\hat{\beta}$ and $\hat{\gamma}$ is obvious with correlation coefficient $r = 0.999$ (p-value < 0.001) for $I_s = 1$, $n = 10$

and $r = 1$ (p-value < 0.001) for $I_s = 1$, $n = 50$. The correlations are appreciable for the $(\hat{\beta}, \hat{\gamma})$ pairs as a whole ($r = 0.298$ (p-value < 0.001) for $n = 10$ and $r = 0.38$ (p-value < 0.001) for $n = 50$) although it should be stressed that in these cases, given the clear non-linear structures present in the data, the actual correlation values are meaningless. Considering only major outbreaks, the correlation is significantly greater than zero ($r = 0.226$ (p-value < 0.001) for $I_s > 3$, $n = 10$ and $r = 0.083$ (p-value < 0.001) for $I_s > 20$, $n = 50$). The correlation for $n = 50$ is small in absolute terms, however, for $n = 10$, $r = 0.226$ is still an appreciable correlation. Thus the assumption that the correlation between $\hat{\beta}$ and $\hat{\gamma}$ is zero is likely to be inaccurate, and this assumption will affect the coverage properties of the confidence intervals for $\hat{\theta}$.

The ALT-based confidence interval for $\hat{\theta}$ is calculated using Equation (9.9) where $s.e(\hat{\theta})$ depends on the variance estimates for $\hat{\beta}$ and $\hat{\gamma}$ and the assumption that $cov(\hat{\beta}, \hat{\gamma}) = 0$. Hence underestimates or overestimates of the true variability of $\hat{\beta}$ and $\hat{\gamma}$ and the assumption of non-zero correlation between $\hat{\beta}$ and $\hat{\gamma}$ will affect the coverage of the resulting confidence interval for $\hat{\theta}$. The properties of the interval will also be affected by the accuracy of the δ method approximation which is used to estimate the variance of $\hat{\theta}$ and the variability of the assumption of asymptotic normality for $\hat{\theta}$. The exact effect of underestimates and overestimates in estimating the second order properties of $\hat{\beta}$ and $\hat{\gamma}$ on $s.e(\hat{\theta})$ will depend on the means of the estimates and the relative sizes of the variance estimates. Hence, these will vary for different values of β and γ. The effect of inadequacies in the estimation of β, γ and the associated variance estimates on $\hat{\theta}$ and $s.e(\hat{\theta})$ is evaluated using simulations.

The 3249 and 3285 epidemic samples for $n = 10$ and $n = 50$ analysed in the previous sections were evaluated relative to the true parameter value of $\theta = 2$ ($\beta = 2, \gamma = 1$). Estimates of $\hat{\theta}$ and estimates of the standard errors of $\hat{\theta}$ were obtained and ALT-based confidence intervals constructed. In Table 9.1, results for the estimated confidence of the confidence intervals for all epidemics and for categorised minor and major outbreaks are presented.

The results indicate that the true confidence for non-categorised epidemics (overall) decreases with increased population size with a 90% estimated confidence for $n = 10$ and a 74% estimated confidence for $n = 50$, which is a curious result. It is therefore vital to review the properties of the confidence intervals separately for minor and major outbreaks. It should be stressed that the fact that the overall coverage may occasionally be close to 90% (as in the case of $n = 10$) does not

Table 9.1: *Summary of results for ALT-based confidence intervals for* $\hat{\theta}$.

Size (n)	Outbreak type	Estimated confidence	95% CI for for confidence	$\hat{\beta}$ confidence	$\hat{\gamma}$ confidence
10	overall	0.90	(0.89, 0.91)	0.92	0.93
	minor	0.67	(0.64, 0.70)	0.79	0.998
	major	1.00	(0.95, 1.00)	0.98	0.91
50	overall	0.74	(0.73, 0.76)	0.92	0.96
	minor	0.21	(0.19, 0.24)	0.78	0.97
	major	0.997	(0.995, 0.999)	0.98	0.95

imply that the statistical methodology is working well, when this is the average of two distinct populations with very different properties. This explains the apparently paradoxical result that the overall coverage properties become poorer as the population size increases. Considering the coverage properties of confidence intervals for θ separately for minor and major outbreaks, the results reveal that minor outbreaks consistently have poor coverage, with estimated confidences well below the nominal 90% confidence level and with properties which deteriorate with increasing population, given the 21% estimated confidence for $n = 50$. For major outbreaks, however, coverage is very high as can also be observed from Figure 9.7, with a 100% estimated confidence for $n = 10$ and 99.7% for $n = 50$. For $n = 10$, all of the confidence intervals that did not include the true value of θ were from minor outbreaks. For $n = 50$, 99% of the confidence intervals that did not include the true θ were from minor outbreaks. Thus, the overall poor estimated confidence is largely due to the effect of minor outbreaks. From the previously estimated confidences for $\hat{\beta}$ and $\hat{\gamma}$ (refer to columns 5 and 6 of Table 9.1), it should be noted that though the methodology provides reasonably good estimates for $\hat{\beta}$, $s.e(\hat{\beta})$, $\hat{\gamma}$ and $s.e(\hat{\gamma})$, this is not reflected in the confidence estimates for $\hat{\theta}$, particularly for minor outbreaks.

From the plot of confidence intervals against $\hat{\theta}$ presented in Figure 9.7, it can be observed that there is a consistent trend for confidence intervals from major outbreaks to be wide and those for minor outbreaks to be narrower, illustrating the liberal and conservative nature of the confidence intervals arising from major and minor outbreaks respectively. Hence, estimates of $\hat{\theta}$ from minor outbreaks are unlikely to cover the true value with the specified, notional confidence. The true confidence is likely to be much less. This may be due to the properties of the estimator of the standard error, especially the biased nature of $\hat{\beta}$ estimates from minor epidemics. Confidence intervals from major epidemics, by contrast are likely to be liberal.

Figure 9.7: *Plots of* 90% *confidence intervals of* $\hat{\theta}$ *against* $\hat{\theta}$ *from population sizes* (*a*) 10 *and* (*b*) 50.

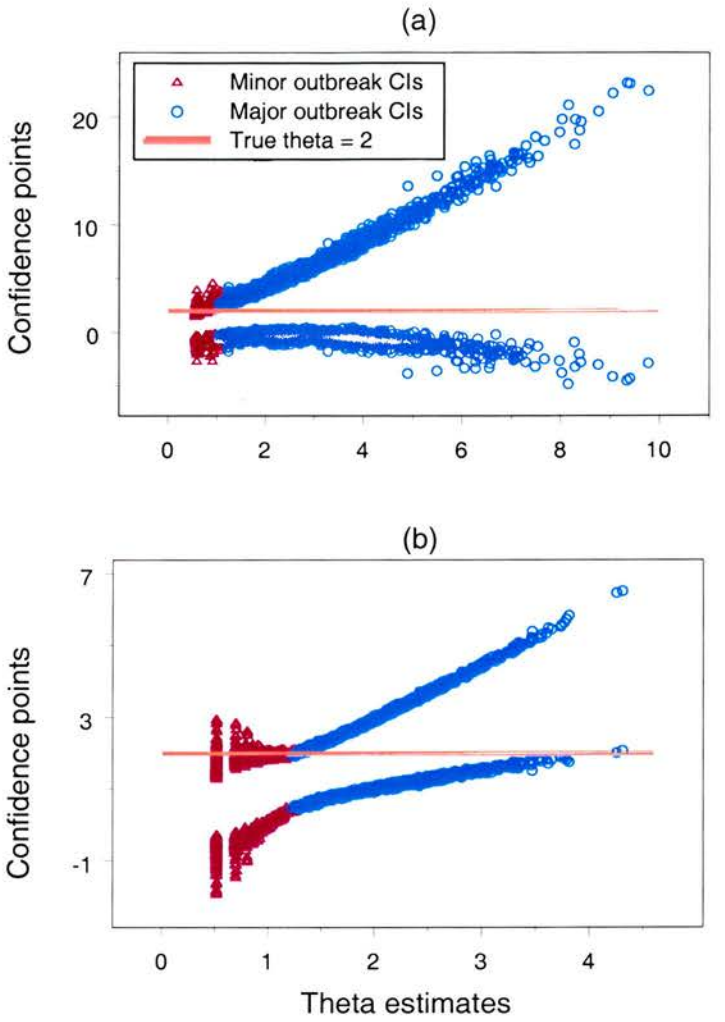

In conclusion, results from the use of the maximum likelihood estimate statistic, assuming asymptotic normality of the estimator, indicate that it is a poor methodology for the construction of confidence intervals in the context of the epidemic data. Therefore, alternative methods of constructing confidence intervals are explored, using bootstrap methods which have the advantage of not depending on large sample assumptions about the nature of the likelihood.

9.4 Epidemic bootstrapping and calibration

9.4.1 The procedure

In this section bootstrap methods, as applied to the epidemic simulations, are described. Two methods are used, namely, the parametric bootstrap (Efron and Tibshirani, 1993, Sections 6.5) and the semi-parametric bootstrap. From the simulated epidemics, confidence intervals are constructed based on ALT, percentile parametric bootstrap and percentile semi-parametric bootstrap methods. Calibration is performed on the confidence limits generated by the three methods. Below is an outline of the procedure that will be followed in simulating and bootstrapping epidemics and calibrating the resulting parameter estimates.

Step 1: Generate an epidemic based on the SIR infection process, this requires parameters β and γ.

Step 2: Check if realization is non-trivial, *i.e.*, whether the number of secondary infections is greater than zero, if non-trivial go to step 3 otherwise go to step 1.

Step 3: Calculate parameter estimates $\hat{\beta}$, $\hat{\gamma}$, $\hat{\theta}$ and the associated standard errors using the expressions outlined in Equations (9.2), (9.3), (9.5), (9.6) and (9.8) and an construct ALT-based confidence interval for $\hat{\theta}$ as in Equation (9.9).

Step 4: Generate 200 valid bootstrap epidemics using both parametric and semi-parametric bootstrap methods. The bootstrap methods are described in the next section.

Step 5: Calculate parameter estimates $\hat{\beta}$, $\hat{\gamma}$, $\hat{\theta}$, and the associated standard errors as in step 3 for the 200 bootstrapped epidemic samples based on both parametric and semi-parametric bootstrap methods.

Step 6: Construct confidence intervals based on the percentiles of the 200 $\hat{\theta}$ bootstrap estimates from Step 5, for each of the parametric and semi-parametric approaches.

Step 7: Perform calibration of confidence points for ALT-based confidence points, parametric bootstrap percentile confidence points and semi-parametric bootstrap percentile confidence points.

9.4.2 Bootstrap methods

Parametric and semi-parametric bootstrap methods are used to generate epidemic samples based on the observed infection history of the simulated epidemic from Step 1 of Section 9.4.1.

9.4.2.1 Parametric bootstrap methods

During the parametric bootstrap procedure, epidemics are generated by simulation of the SIR infection process as in Step 1 but with the $\hat{\beta}$ and $\hat{\gamma}$ obtained in Step 3 as the input parameters.

9.4.2.2 Semi-parametric bootstrap methods

From the infection process generated by the SIR simulation model based on parameters β and γ, it is possible to generate bootstrap infection processes (epidemic pseudo-realisations) using semi-parametric methods. For each individual in the initial infection process, an infection profile is created, *i.e*, the duration of infection exposure (exposure threshold), the time of infection if it were infected, and its duration of infectiousness period are calculated. Based on these profiles, bootstrap epidemics may be generated. There may be up to are three types of individual in the observed process, namely, the initial infective, any secondary infectives and any susceptibles at the end of the epidemic. The bootstrapped epidemics are generated based on one initial infective, *i.e.*, $I_0 = 1$, as in the 'parent' epidemic process. For the initial infective, all that is required for the simulation is a length of infectiousness to specify a removal time, since the time of infection for this individual is set to zero, the start of the epidemic. An infectiousness period is randomly assigned to the initial infective from the existing pool of infectiousness periods from the profiles of infected individuals from the initial infection process. For the remaining $N - 1$ individuals, a new infection profile is determined by assigning exposure thresholds. These will be used to determine any times of infection. The process of generating a new infection profile and creating a bootstrap epidemic realisation is described.

From the initial generated epidemic, the number of secondary infectives, I_s, is determined. The infection exposure thresholds for all $N - 1$ individuals are determined from the initial epidemic as follows:
Let E_i denote the exposure threshold for infected individual i, then

$$E_i = \int_0^{t_i} \frac{I(t)}{N}\, dt.$$

where t_i is the time of infection for individual i, $I(t)$ is the number of infectious individuals at time t and N is the total number of individuals.
For individuals that remain susceptible at the end of the epidemic, the exposure threshold is unknown, but will be greater than $\int_0^{t_{max}} \frac{I(t)}{N}\, dt$.

Sampling with replacement from the I_s observed infection exposure thresholds E_i associated with the infected individuals in the parent epidemic, would give rise to an epidemic with a bias towards individuals which became infected easily. Rather, an individual among the $N-1$ is assigned an exposure threshold based on the following criteria:
For each individual i of the $N-1$ initial susceptibles, generate a uniform random variable u_i from the uniform distribution $U(0,\ 1)$.

- If $u_i \leq \frac{I_s}{N-1}$, sample from the exposure thresholds of infected individuals and assign the threshold to this individual. This corresponds to a non-parametric sampling of a threshold from an infected individual.

- If $u_i > \frac{I_s}{N-1}$, do not assign a threshold from the pool of E_i, instead calculate a new E_i as follows:

  Generate a further uniform $U(0,1)$ random variable u_{i2} and scale this to a uniform random number u_j from the uniform distribution $U(0,\ e^{-\hat{\beta}\int_0^{tmax}\frac{I(t)}{N}dt})$ such that

  $$u_j \ = \ u_{i2}\, e^{-\hat{\beta}\int_0^{tmax}\frac{I(t)}{N}dt}.$$

  Based on u_j, the exposure threshold for the individual is given by

  $$E_j \ = \ -\frac{\ln(u_j)}{\hat{\beta}}.$$

  This corresponds to a parametric sampling of a threshold for an individual that had not become infected by the end of the epidemic.

With each of the $N-1$ individuals assigned an exposure threshold E_i, each individual is randomly assigned an infectiousness period from the set of observed infectiousness periods, sampling with replacement. The new infection process is sorted by exposure threshold. From the sorted exposure thresholds and corresponding infectiousness periods, where these become relevant, a new epidemic is generated where individuals become infected and infectious if and only if the associated threshold is surpassed by the summed scaled exposure. The new epidemic is analysed from which parameter estimates $\hat{\beta}$, $\hat{\gamma}$ and $\hat{\theta}$ are to be generated.

9.4.2.3 Generation of epidemic realisations by the semi-parametric bootstrap

Based on the sorted exposure thresholds and corresponding infectiousness periods, new epidemics are generated in what is termed the semi-parametric bootstrap. It is semi-parametric because it involves β in the calculation of the exposure thresholds for individuals with u_i is greater than $\frac{I_s}{N-1}$ rather than merely sampling with replacement from the generated exposure thresholds.

At time $t = 0$, the start of the infection process, the number of initial infections is set to 1 where the initial infective has an exposure threshold of zero ($E_{(1)} = 0$) and a randomly assigned infectiousness period from the pool of infectiousness periods from the infection process of the original (simulated) epidemic. The removal time, R_1, of the initial infective is given by infection time 0 plus the infectiousness period. From $E_{(2)}$, the first non-zero exposure threshold among the sorted thresholds, $t_{(2)}$, the time of infection for the individual associated with exposure threshold $E_{(2)}$, is calculated as follows:

$$E_{(2)} = \int_0^{t_{(2)}} \frac{I(t)}{N}\, dt \;\Rightarrow\; \frac{I(0)}{N}\,(t_{(2)} - 0) \;=\; E_{(2)} \;\Rightarrow\; t_{(2)} = \frac{N\,E_{(2)}}{I(0)} \;=\; N\,E_{(2)}.$$

Hence the time of the next event, whether a new infection or a removal is determined by the minimum of R_1 and $t_{(2)}$. If R_1 is the minimum of the two quantities, then the next event is a removal of the initial infective at time R_1. In this case the epidemic ends with no secondary infectives. If $t_{(2)}$ is the minimum, then the next event is a new infection with time of infection $t_{(2)}$ and removal time R_2 equal to $t_{(2)}$ plus the associated infectiousness period. The number of individuals in each state of SIR is updated at the times 0, $t_{(2)}$ and a cumulative exposure denoted by $CumE_{(2)}$ is determined up to time $t_{(2)}$. For the next step, the minimum removal time, min_R, among the removal times for currently infected individuals is determined. Then the next time of infection, corresponding to the next exposure threshold, $E_{(next)}$, is determined as follows:

$$\begin{aligned} E_{(next)} \;&=\; CumE_{(next-1)} \;+\; \frac{I(t_{next-1})}{N}[\,t_{next} - t_{next-1}\,] \\ \Rightarrow\; t_{next} \;&=\; \frac{N\,[\,E_{(next)} - CumE_{(next-1)}\,] \;+\; t_{next-1}\,I(t_{next-1})}{I(t_{next-1})}. \end{aligned}$$

The time of next event is determined by the minimum of min_R and t_{next}. If min_R is the minimum, then the next event is a removal occurring at time min_R. If t_{next} is the minimum, then the next event is a new infection occurring at time t_{next} with

its removal time given by t_{next} plus the length of the corresponding infectiousness period. The number of individuals in each of the SIR states at the next event time is updated and the cumulative exposure threshold up to this time is determined. Subsequently, the time of infection corresponding to the next exposure threshold (which could be the same exposure threshold as in the previous iteration if the preceding event was a removal) is determined. It is compared with the minimum among the current non-zero removal times and the time of the next event and the nature of the event are determined. The process is repeated until there are no infectious individuals remaining in the system *i.e.* $I(t_{max}) = 0$. If there are any susceptibles left at the end of the epidemic, their exposure threshold is equal to the cumulative exposure threshold at the end of the epidemic, at time t_{max}. Hence, a new epidemic has been generated and the parameters of interest can then be estimated based on the infection history of the generated epidemic for those non-trivial epidemic realisations having at least 1 secondary infection.

9.4.3 Calibration of confidence points

In this section, the method of calibration of confidence points is described (Efron and Tibshirani, 1993, Section 18.3). Consider a statistical estimator $\hat{\theta}_\lambda(x)$ which depends on an adjustable parameter λ. In order to apply the estimator to data, a value of λ is needed. Bootstrap methods can be used to assess the performance of $\hat{\theta}_\lambda(x)$ for each fixed value of λ and based on the assessment, the value λ that optimizes the performance of $\hat{\theta}_\lambda(x)$ can be chosen. This process is called adaptive estimation. If the process is applied to confidence interval procedures, it is referred to as calibration. In this thesis the calibration process will be applied to the ALT based confidence points, and both the parametric and the semi parametric bootstrap percentile confidence points. This process will result in calibrated confidence points for each of the three types of confidence intervals. Theory suggests that such calibrated confidence points will be second order accurate, improving the performance of the confidence intervals relative to the uncalibrated intervals.

9.4.3.1 Calibration of a confidence point

Suppose $\hat{\theta}[\alpha]$ is an estimate of the lower α level confidence point for a parameter θ, *i.e.*

$$\Pr\left\{\theta \leq \hat{\theta}[\alpha]\right\} = \alpha. \tag{9.12}$$

For a maximum likelihood estimate statistic, assuming asymptotic normality of the estimate, the confidence interval $\hat{\theta}[\alpha]$ is the standard normal point $\hat{\theta} - z_{1-\frac{\alpha}{2}}\, s.e(\hat{\theta})$ and in the case of a bootstrap percentile-based confidence interval, $\hat{\theta}[\alpha]$ is the bootstrap percentile point at the $\frac{\alpha}{2}\%$ point in the sorted list of estimated values of θ derived from the bootstrap realisations. Since the actual confidence of a confidence procedure is rarely equal to the desired confidence α and is sometimes even substantially different, one way to think about the properties of a confidence procedure is in terms of a calibration . That is, for each α, if $\Pr\{\theta \leq \hat{\theta}[\alpha]\} \neq \alpha$, perhaps the equality will hold for $\hat{\theta}[\lambda]$ where $\lambda \neq \alpha$. For example, if the desired α in Equation (9.12) is 5 % perhaps it can be achieved by using the 3 % confidence point. If the mapping $\alpha \longrightarrow \lambda$ was known, then a confidence procedure with exactly the desired property could be constructed, but the mapping is not known, hence the need to perform a calibration. The bootstrap is used to carry out the calibration as follows.
Let $\hat{\theta}[\lambda]$ denote a family of confidence points, where the objective is to find a value λ such that

$$\hat{p}(\lambda) \;=\; \text{Prob}\left\{\theta \leq \hat{\theta}[\lambda]\right\} = \alpha. \tag{9.13}$$

If the procedure is calibrated correctly, then (9.13) holds exactly with $\lambda = \alpha$. Let $\hat{p}(\lambda)$ denote the bootstrap estimate of $p(\lambda)$ and let $\hat{p}(\lambda)$ be equal to $\text{Prob}\{\hat{\theta} \leq \hat{\theta}_b[\lambda]\}$ where $\hat{\theta}$ is the estimate for which a confidence interval is required and $\hat{\theta}_b$ is the estimate of θ calculated from bootstrap sample b. To approximate $\hat{p}(\lambda)$, a number of bootstrap realisations (200 in this case) are generated. For each realisation $\hat{\theta}_b$ is determined and $\hat{p}(\lambda)$ is given by

$$\hat{p}(\lambda) = \frac{\#\{\hat{\theta} \leq \hat{\theta}_b[\lambda]\}}{\text{number of bootstrap samples}}.$$

The process of estimating $\hat{p}(\lambda)$ is carried out over a wide range of values of λ using the same bootstrap samples. The calibrated confidence point is then given by $\hat{\theta}[\hat{\lambda}_\alpha]$, where $\hat{\lambda}_\alpha$ is the value of λ satisfying $\hat{p}(\lambda) = \alpha$. In this project a range of λ values in the interval $(0, 1]$, in steps of $\frac{1}{200}$ is used, such that λ takes values $0.005, 0.01, \ldots, 0.995, 1$. The algorithms for the calibration process of the ALT-based confidence points and the bootstrap percentile confidence points are outlined in the following sections. 200 bootstrap realisations are used as the minimum required to give rise to reasonable results. The decision to use only 200 bootstrap realisations was driven by the use of the double bootstrap in the calibration of bootstrap confidence intervals, where the total number of bootstrap realisations required, at 200^2, is already extremely large. In practice,

higher numbers should be used. In each case the aim is to construct a calibrated confidence interval for $\hat{\theta} = \frac{\hat{\beta}}{\hat{\gamma}}$, estimated from the 'parent' simulated epidemic sample.

9.4.3.2 Calibration of an ALT-based confidence point via the bootstrap

The ALT-based confidence interval is calibrated as follows:

Step 1: Using $\hat{\beta}$ and $\hat{\gamma}$ estimated from a 'parent' simulated epidemic sample, generate 200 bootstrap samples $b = 1, 2, \ldots, 200$ and for each sample, estimate $\hat{\theta}_b$ and the associated standard error.

Step 2: Sort the set of 200 $\hat{\theta}_b$.
For the lower confidence point , $\hat{p}(\lambda)$ is computed from

$$\hat{p}(\lambda) = \frac{\#\{\hat{\theta} \leq \hat{\theta}_b - |z^L_{1-\lambda}|\, s.e(\hat{\theta}_b)\}}{200},$$

and the aim is to find $\hat{\lambda}$ such that $\hat{p}(\hat{\lambda}) = \frac{\alpha}{2}$.
For the upper confidence point $\hat{p}(\lambda)$ is computed from

$$\hat{p}(\lambda) = \frac{\#\{\hat{\theta} \leq \hat{\theta}_b + |z^U_{1-\lambda}|\, \mathrm{se}(\hat{\theta}_i)\}}{200},$$

with the aim of finding $\hat{\lambda}$ such that $\hat{p}(\hat{\lambda}) = 1 - \frac{\alpha}{2}$.

Evaluation of $\hat{p}(\lambda)$ requires a $z_{1-\lambda}$ value. The computation of $\hat{p}(\lambda)$ is equivalent to determining a $z_{1-\lambda}$ value ($z^L_{1-\lambda}$ for the lower limit and $z^U_{1-\lambda}$ for the upper limit) for which $\hat{p}(\lambda)$ is equal to the desired α-level confidence probability. The calibrated confidence interval will then be given by $[\hat{\theta} - |z^L_{1-\lambda}|\, s.e(\hat{\theta}),\ \hat{\theta} + |z^U_{1-\lambda}|\, s.e(\hat{\theta})]$.

For the lower confidence point, the threshold occurs at $\hat{\theta} = \hat{\theta}_b - |z^L_{1-\lambda}|\, s.e(\hat{\theta}_b)$

$$\Rightarrow -|z^L_{1-\lambda}| = \frac{\hat{\theta} - \hat{\theta}_b}{s.e(\hat{\theta}_b)} \ \Rightarrow\ |z^L_{1-\lambda}| = \frac{\hat{\theta}_b - \theta}{s.e(\hat{\theta}_b)}, \text{ where } \hat{\theta}_b > \theta.$$

Calculate $z^L_{1-\lambda_{(b)}} = \frac{\hat{\theta}_b - \hat{\theta}}{s.e(\hat{\theta}_b)}$ from the 200 estimated values of $\hat{\theta}_b$.
It should be noted that the expression is only meaningful in cases where it gives rise to a positive value. The required $z^L_{1-\lambda}$ value, equivalent to $\hat{p}(\lambda) = \alpha$, can be determined from the sorted list of the calculated $z^L_{1-\lambda_{(b)}}$ values, by choosing the $(1 - \frac{\alpha}{2})\,100\%$ point value in the list, conditional on it being positive.

For the upper confidence point, the threshold occurs at $\hat{\theta} = \hat{\theta}_b + |z^U_{1-\lambda}|\, s.e(\hat{\theta}_b)$

$$\Rightarrow |z^U_{1-\lambda}| = \frac{\hat{\theta} - \hat{\theta}_b}{s.e(\hat{\theta}_b)}.$$

Again, calculations of $\frac{\hat{\theta}-\hat{\theta}_b}{s.e(\hat{\theta}_b)}$ are only meaningful in cases where they give rise to a positive value. The $z^U_{1-\lambda(b)}$ values are computed from the bootstrap samples , yielding z-values corresponding to the 200 realisations. The required $z^U_{1-\lambda}$ value equivalent to $\hat{p}(\lambda) = \alpha$ is determined from the sorted list of the calculated $z^U_{1-\lambda_{(b)}}$ values by choosing the $(1 - \frac{\alpha}{2})\,100\%$ point value in the list, conditional on it being positive.

In practice, it is easier to operate simply in terms of $z_{1-\lambda} = \frac{\hat{\theta}-\hat{\theta}_b}{s.e(\hat{\theta}_b)}$. For instance, for a 90% confidence interval, the lower confidence point will require a $z_{1-\lambda}$ value which corresponds to $\hat{p}(\lambda) = 0.05$, *i.e.* $z_{0.95}$. This z-value is the $z_{1-\lambda}$ value in the 10^{th} position from the bottom *i.e.* the 191^{th} ranked $z_{1-\lambda}$ value, conditional on this value being negative. Then the lower calibrated confidence point is given by $\hat{\theta} + z_{1-\lambda}[191]\, s.e(\hat{\theta})$. The upper confidence point will require a $z_{1-\lambda}$ value which corresponds to $\hat{p}(\lambda) = 0.95$, *i.e.* $z_{0.05}$. This z-value is the $z_{1-\lambda}$ value in the 10^{th} ranked value in the list of the $z_{1-\lambda}$ sorted values, conditional on this being positive. Thus the resulting upper calibrated confidence point is given by $\hat{\theta} + z_{1-\lambda}[10]\, s.e(\hat{\theta})$.

9.4.3.3 Calibration of a bootstrap percentile confidence point

Percentile confidence intervals are calibrated as follows:

Step 1: Generate 200 bootstrap samples based on $\hat{\beta}$ and $\hat{\gamma}$ (the same realisations as used for calibration of the ALT-based confidence point) and for each realisation b obtain estimates $\hat{\beta}_b$, $\hat{\gamma}_b$, $\hat{\theta}_b$ and the associated standard errors.

Step 2: For each bootstrap realisation $b = 1, 2, \ldots, 200$, using $\hat{\beta}_b$ and $\hat{\gamma}_b$ generate 200 calibration bootstrap samples $c = 1, 2, \ldots, 200$ and obtain estimates $\hat{\beta}_{bc}$, $\hat{\gamma}_{bc}$, $\hat{\theta}_{bc}$ and the associated standard errors.
It should be noted that calibration of a bootstrap percentile confidence point will require bootstrap sampling making the overall calibration a nested computation, sometimes called a "double bootstrap " (Efron and Tibshirani, 1993, Section 18.3). Construction of a calibrated bootstrap percentile confidence interval for a single estimate of $\hat{\theta}$, will require a total of $200 \times 200 = 40,000$ bootstrap realisations each for both parametric and semi-parametric methods.

Step 3: Sort the 200 calibrated $\hat{\theta}_{bc}$ estimates and denote the sorted estimates by $\hat{\theta}^*_\lambda(b)$, corresponding to bootstrap realisation b. Each of the $\hat{\theta}^*_\lambda(b)$ corresponds to a value of λ in $0.005, \ldots, 1$.

Step 4: For each λ, compute the number of estimated bootstrap θ_b that are greater than or equal to $\hat{\theta}$, for $b = 1, 2, \ldots, 200$ and define

$$\hat{p}(\lambda) = \frac{\#\{\hat{\theta} \leq \hat{\theta}^*_\lambda(b)\}}{200}.$$

The computation of $\hat{p}(\lambda)$ is illustrated in Table 9.2.

Table 9.2: *Illustration of a computation of $\hat{p}(\lambda)$ for calibration of a bootstrap percentile confidence point. The body of the table contains the output of indicator functions, specifying whether or not $\hat{\theta} \leq \hat{\theta}^*_\lambda(b)$ for sample b and confidence coefficient λ.*

	λ							
bootstrap sample b	0.005	0.010	0.015	...	...	0.990	0.995	1
1	0	0	0	...	...	0	1	1
2	0	0	1	...	...	1	1	1
3	0	0	1	...	...	1	1	1
⋮	⋮	⋮	⋮	...	...	⋮	⋮	⋮
200	0	0	1	...	...	1	1	1
$\#\{\hat{\theta} \leq \hat{\theta}^*_\lambda(b)\}$	0	0	3	...	...	199	200	200
$\hat{p}(\lambda)$	0	0	0.015	...	...	0.995	1	1

Step 5: Find the value of λ ($\lambda_L \equiv$ lower, $\lambda_U \equiv$ upper confidence points) satisfying $\hat{p}(\lambda) = \alpha$, for each of the lower and upper confidence points.

The calibrated confidence interval for $\hat{\theta}$ is given by $\left[\hat{\theta}[\lambda_L], \hat{\theta}[\lambda_U]\right]$. For a 90 % confidence interval, it is necessary to find λ such that $\hat{p}(\lambda) = 0.05$ for the lower confidence point and $\hat{p}(\lambda) = 0.95$ for the upper confidence point. The 200 bootstrap $\hat{\theta}_b$ in Step 1 are sorted and a 90% confidence interval is determined by selecting the λ_L% and λ_U% points (rather than the 5 % and 95 % points) of the bootstrap distribution for $\hat{\theta}$.

However, because a discretised set of λ is used, it is possible that there will be no value of λ for which $\hat{p}(\lambda) = 0.05$ or $\hat{p}(\lambda) = 0.95$ exactly. Various other situations may instead arise, for instance, there may be several λ for which $\hat{p}(\lambda) = 0.05$

or $\hat{p}(\lambda) = 0.95$. Alternatively, there may be a situation where $\hat{p}(\lambda_{(1)}) < 0.05$ and $\hat{p}(\lambda_{(1)} + \frac{1}{200}) > 0.05$. Another situation that might arise due to the number of calibrated samples being insufficient is a situation where $\hat{p}(\lambda_{(1)}) > 0.05$ or $\hat{p}(\lambda_{(200)}) < 0.95$, or even situations where all of the estimated calibrated θ_{bc} are greater than the original $\hat{\theta}$, such that $\hat{p}(\lambda) = 1$ for all values of λ. The following criteria to select λ will therefore be followed:
For the lower confidence point choose λ such that

$$\lambda = \begin{cases} \max_\lambda\{\hat{p}(\lambda) \leq 0.05\} & \text{if } \hat{p}(\lambda_{(1)}) \leq 0.05 \\ \lambda_{(1)} & \text{if } 0.05, < \hat{p}(\lambda_{(1)}) < 1 \end{cases}$$

and for the upper confidence point, choose λ such that

$$\lambda = \begin{cases} \min_\lambda\{\hat{p}(\lambda) \geq 0.95\} & \text{if } \hat{p}(\lambda_{(1)}) \leq 0.95, \text{ and } \hat{p}(\lambda_{(200)}) \geq 0.95, \\ \lambda_{(200)} & \text{if } \hat{p}(\lambda_{(200)}) < 0.95. \end{cases}$$

In situations where all the calibrated $\hat{\theta}_{bc}$ are greater than $\hat{\theta}$, such that $\hat{p}(\lambda) = 1$ for all λ, both the lower and upper limits of the confidence interval of $\hat{\theta}$ will be set to the estimated value of $\hat{\theta}$, to indicate that in this pathological case the methodology has failed.

The advantage in calibration of confidence points is that it produces confidence intervals that are second order accurate provided that the confidence points being calibrated are first order accurate. This is true of both the asymptotic likelihood and the bootstrap percentile point methods. Hence, the calibrated interval will enjoy the same accuracy as the BCa procedure which is recommended for the improvement of accuracy of confidence intervals in many cases (Efron and Tibshirani, 1993, Section 18.4). The BCa methodology was believed inappropriate in the epidemic bootstrap case, since it relies on an assumption of smoothness in the functional relationship between the estimator ($\hat{\theta}$) and the underlying data. Small changes in the data (*i.e.*, times of infection and removal times) should result in only a small change in $\hat{\theta}$. This is not true in this case, hence the use of bootstrap calibration as an alternative. Because of the property of second order accuracy, calibration should produce superior confidence points.

9.5 Evaluation of bootstrap confidence intervals

Bootstrap methods do not depend on large sample assumptions, and hence where data is lacking, they should generate better estimates of variability in estimates.

However, these methods can do nothing about any bias arising in estimates from minor outbreaks. When calibrating ALT-based confidence points, the effect of simulated minor outbreaks will be to create problems caused by spurious values of λ which will tend to suggest that the confidence intervals need to be wider. This is illustrated by the diagram in Figure 9.8. If the distribution of the bootstrapped $\hat{\theta}_b$ is as in Figure 9.8(a), the estimate of the upper ALT-based confidence limit $\hat{\theta}_b + s.e(\hat{\theta}_b)\, z_{1-\frac{\alpha}{2}}$ will have a high proportion of cases which fail to cover $\hat{\theta}$ because of the presence of the minor outbreaks. Hence the notional value of λ which gives the desired α level will tend to be reduced inappropriately, giving rise to wider confidence intervals.

Figure 9.8: *Illustration of distribution of estimated bootstrapped $\hat{\theta}_b$s.*

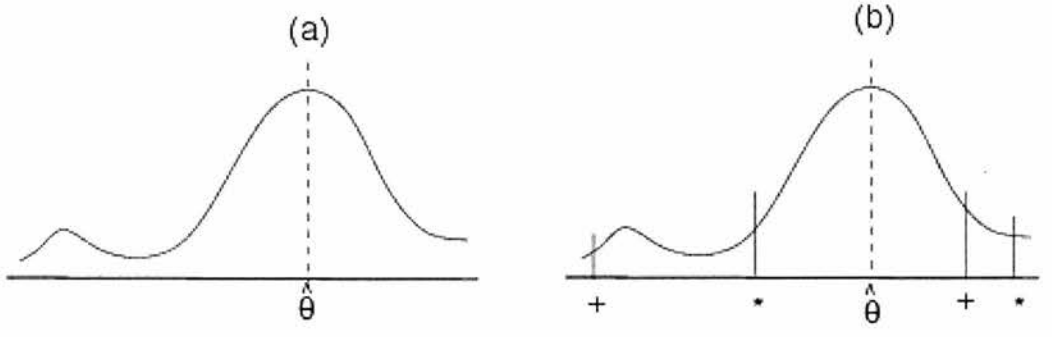

In the case of bootstrap percentile confidence intervals, the effect of minor outbreaks will be to extend the basic percentile confidence intervals by the inclusion of results from minor outbreaks, while the calibration which follows will be affected by the generation of λ_b associated with the properties of estimators of θ from minor epidemics. Focusing only on major outbreaks, the bootstrap confidence intervals should be as specified by the $'*'$ values in Figure 9.8(b). If minor outbreaks are, however, included in the process, the estimated confidence intervals will potentially move to the alternative values indicated by $'+'$ on the same figure. Hence the effect will be to spuriously increase the width of the confidence interval and in particular to make the lower limit much lower. The calibration scheme will not succeed in improving these confidence intervals since many of the values of λ will be calculated based on simulations of sub-threshold epidemics which will have properties different to those of major outbreaks. There is no reason to believe that these will be identical to the properties of those from major epidemics, leaving aside the particular issues which arise in the estimation

of small values of θ to be discussed in a later section. First, however, results obtained from the calibration process are examined.

9.5.1 Evaluation of ALT-based confidence intervals

In the calibration process for the ALT-based confidence limits, 100 initial simulated epidemics are generated with $\beta = 1$ and $\gamma = 0.5$ *i.e.* with $\theta = 2$, for population sizes $n = 10$, 30 and 50. It should be noted that the simulated epidemics analysed here are different from those analysed in earlier sections. Based on estimates of β and γ, from the simulated epidemics, for each realisation, 200 bootstrap epidemic realisations are generated. Basic ALT-based and ALT calibrated confidence intervals for $\hat{\theta}$ are constructed for each of the 100 θ estimates. The results, presented in terms of all epidemics (overall) and of epidemics classified as minor or major outbreaks, are presented in Table 9.3. Partitioning was carried out for the cases $n = 10$ and $n = 50$ on the same basis as described in Section 9.3. In the case of $n = 30$, a beta-binomial mixture distribution was fitted and on the balance of likelihood, outbreaks with fewer than 10 secondary infections were defined as minor, while those with 10 or more secondary infections were defined to be major.

Table 9.3: *Summary of results for* 90% *ALT and calibrated ALT confidence intervals for* $\hat{\theta}$.

Size(n)	Outbreak	Estimated basic confidence	95% CI for basic confidence	Estimated calibrated confidence	95% CI for calibrated confidence
10	Overall	0.84	(0.75, 0.91)	0.66	(0.56, 0.75)
	Minor	0.43	(0.24, 0.63)	0.00	(0.00, 0.12)
	Major	1.00	(0.95, 1.00)	0.92	(0.83, 0.97)
30	Overall	0.65	(0.55, 0.74)	0.60	(0.50, 0.70)
	Minor	0.00	(0.00, 0.11)	0.00	(0.00, 0.11)
	Major	0.96	(0.88, 0.99)	0.88	(0.78, 0.95)
50	Overall	0.64	(0.55, 0.74)	0.59	(0.49, 0.69)
	Minor	0.03	(0.001, 0.16)	0.00	(0.00, 0.11)
	Major	0.96	(0.87, 0.99)	0.88	(0.78, 0.95)

The results for the basic ALT-based confidence intervals are comparable with earlier results (refer to Table 9.1), but have wider confidence intervals for the true confidence due to the smaller number of realizations. Minor outbreaks give rise to estimates with poor confidence intervals for all population sizes. For major

outbreaks, for population size 10, basic ALT-based confidence intervals are liberal, while for larger population sizes, the point estimate for the coverage is always greater than 90%, and the failure for the estimated coverage to be statistically significantly different to 90% (see the 95% confidence intervals for the estimated confidences) can be explained by the smaller number of realisations.

Considering the ALT-based calibrated confidence intervals, the properties of confidence intervals arising from minor outbreaks are still poor (coverage less than 90%) for each of the three population sizes. This is inevitable given the bias in the estimates. Among major epidemics, the estimated confidence has consistently moved to be closer to 90%.

The significance of the improvement in the confidence interval through calibration was assessed by fitting a generalized linear mixed model (GLMM)(Brown and Prescott, 1999, Section 3.2). The response variable was a binary random variable indicating whether a confidence interval did or did not cover the true θ for both the basic and calibrated ALT-based intervals. For major epidemics with population size $n = 10$, modelling the responses as Bernoulli random variables with a logit link function and fitting epidemic realisation as a random effect with dispersion fixed to one, yielded an estimate of -3.052 ($s.e = 1.163$); $p-$value < 0.01, for the difference in the calibrated and basic confidence intervals. Hence, for $n = 10$, the estimated confidence for the calibrated ALT-based confidence intervals in major outbreaks is significantly lower than the estimated confidence of the basic ALT-based confidence intervals. For $n = 30$ and $n = 50$, results from the GLMM indicated drops in the estimated confidence of the calibrated ALT compared to those from the basic ALT confidence intervals for major outbreaks, but the differences were not statistically significant.

Where $n = 10$, plotting the basic and calibrated ALT based confidence intervals against θ estimates (Figure 9.9(a)), shows that the calibrated intervals are mostly wider, although their estimated confidence is lower. It is also observed that although the lower limits of the calibrated scheme may be rather low, they are still being adjusted upwards relative to the basic ALT-based limits. In particular, the calibration removes the spurious negative values of the basic confidence intervals. Plotting the basic and calibrated ALT-based confidence points against each other (Figures 9.9(b) and 9.9(c)), the plots indicate that there is a smooth relationship between the associated confidence points. Hence, for this case ($n = 10, \beta = 1, \gamma = 0.5$) there is some evidence that the calibration method does improve the properties of the ALT-based confidence intervals, and that it operates in a

Figure 9.9: *Comparison of basic ALT and calibrated ALT-based confidence intervals for the case of* $n = 10$, (*a*) *Confidence points plotted against* θ *estimates,* (*b*) *Relationship between lower limits and* (*c*) *Relationship between upper limits.*

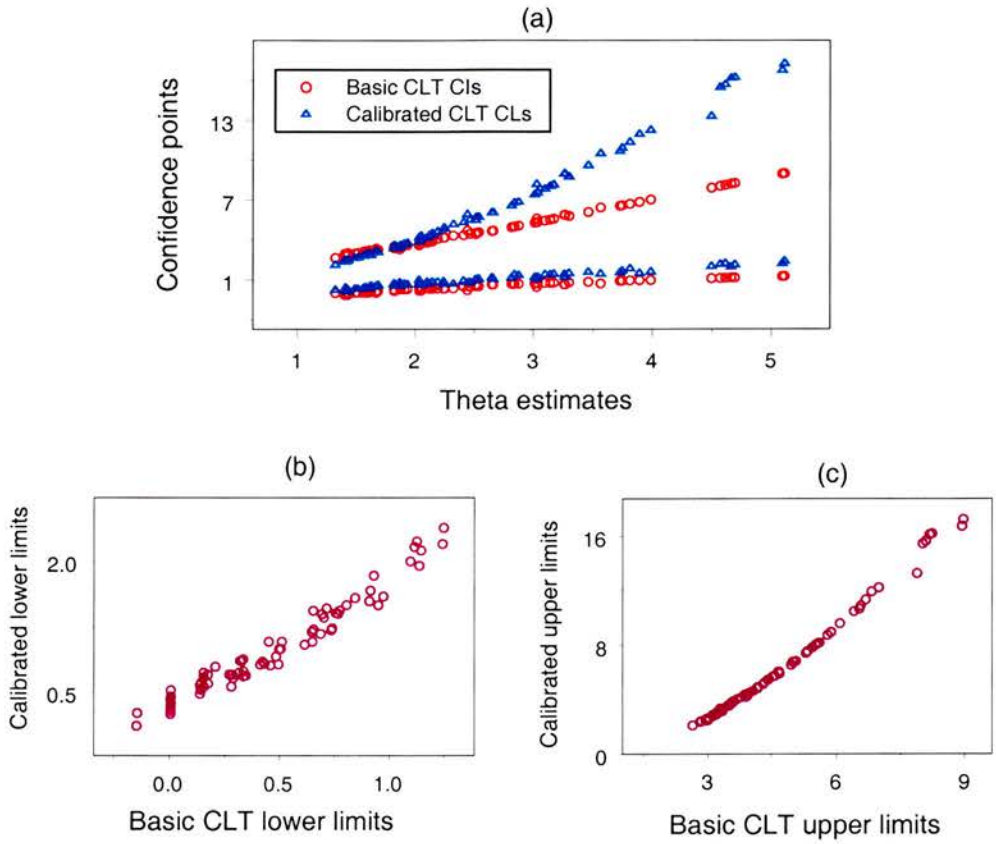

consistent fashion. However, the fact that one can be fairly sure that the calibration procedure is not working properly (Section 9.5) means that this observation should not be generalised in an assumption that this result applies for any values of β and γ. Before examining the effect of calibration on the bootstrap percentile confidence points, the effect of an estimation problem on the calibration of ALT-based confidence points in situations where the true θ is below the lower bound of $\hat{\theta}$ is examined.

9.5.1.1 Evaluation of the calibration method for ALT-based confidence intervals when the true value of $\theta = 0.5$

A problem will arise in the calibration of the ALT-based confidence points in the case where the true θ is below the lower bound for $\hat{\theta}$ (refer to Equation (9.7)), since it immediately follows that the true value of θ will be consistently lower than

all of the bootstrap estimates that are generated. This will clearly have an effect on the coverage properties of the confidence interval. However, $\hat{\theta}$ cannot be lower than all the bootstrap estimates which are generated since, by definition, $\hat{\theta}$ and $\hat{\theta}_b$ are all estimated. Hence, the bootstrap calibration is incapable of modelling an important component of the relationship between θ and $\hat{\theta}$ which must cast doubt on the ability of the procedure to recalibrate the confidence interval in an appropriate fashion.

Using $\theta = 0.5$ ($\beta = 0.167$ and $\gamma = 0.334$), epidemics were simulated with $n = 10, 30$ and 50. The resulting data were analysed and 90% basic and calibrated ALT-based confidence intervals were constructed for $\hat{\theta}$. The estimated properties of the confidence intervals are presented in Table 9.4. It should be noted that since the true value of θ was small, categorizing of epidemics was not necessary as the generated epidemics would, by definition, result in minor outbreaks.

Table 9.4: *Summary of results for* 100 *ALT-based confidence intervals for* $\hat{\theta}$ *when the true value of* $\theta = 0.5$ *i.e is below lower bound for* $\hat{\theta}$.

Size(n)	Estimated basic confidence	95% CI for basic confidence	Estimated calibrated confidence	95% CI for calibrated confidence
10	1.00	(0.96, 1.00)	0.98	(0.93, 0.998)
30	0.98	(0.93, 0.998)	0.98	(0.93, 0.998)
50	0.99	(0.95, 1.00)	0.92	(0.85, 0.96)

The estimated confidences for both basic and calibrated confidence intervals are greater than the notional 90% with the basic ALT-based intervals being consistently liberal for all three population sizes. The calibration procedure gives rise to a drop in the confidence estimate towards the theoretical value of 90% for $n = 50$ but not where $n = 10$ or $n = 30$ where the estimated calibrated confidences are significantly higher than 90%. Fitting a generalised linear mixed model to examine the effect of calibration for $n = 10$ and $n = 30$ confirmed that the drop in confidence due to calibration was not statistically significant ($p-$value $= 0.29$). For $n = 50$, the GLMM fit indicates a significant drop in coverage, of -1.52 ($s.e = 0.6171$) with a p-value $= 0.01$, due to the calibration relative to the basic ALT method.

It was observed that the realisations which generated ALT-based confidence intervals which covered the true value of θ but calibrated ALT-based confidence intervals which did not cover θ (and hence are causing the drop in confidence

level), were exclusively those with observed $\hat{\theta} > 1$. The bootstrap calibration for these intervals was therefore based on values of λ which were generated from distributions for $\hat{\theta}$ which contained a sizeable number of estimates derived from major outbreak data, and as established earlier, the bootstrap calibration has some ability to recalibrate major outbreaks. However, it seems unlikely that these λ will be particularly appropriate for use in calibrating the estimate for a minor outbreak. Hence, it is likely that the apparent drop in the true confidence level is not based on any reliable re-calibration and would therefore be unlikely to be a general result for all β and γ.

9.5.2 Evaluation of percentile bootstrap confidence intervals

The bootstrap percentile confidence points, based on the 100 test simulations and the associated 200 bootstrap epidemic realisations for each of the 100 initial simulations (as in Section 9.5.1), were calibrated. For each of the 200 bootstrapped realisations, 200 calibration realisations were generated. Bootstrap percentile confidence intervals were obtained for both parametric and semi-parametric bootstrap methods. From the calibration samples, values of λ were obtained, from which calibrated percentile confidence intervals were constructed for both bootstrap methods and for population sizes of 10, 30, and 50 individuals. Estimated confidences were generally poor and only confidence intervals for major outbreaks are presented in Table 9.5.

Table 9.5: *Summary of results for major outbreaks from* 100 *bootstrap based confidence intervals for* $\hat{\theta}$ *where* $\theta = 2$.

	Semi-parametric bootstrap estimates				Parametric bootstrap estimates			
Size (n)	Basic confidence	95% CI for basic confidence	Calibrated confidence	95% CI for Calibrated confidence	Basic confidence	95% CI for basic confidence	calibrated confidence	95% CI for calibrated confidence
10	0.97	(0.90, 0.997)	1.00	(0.95, 1.00)	1.00	(0.95, 1.00)	1.00	(0.95, 1.00)
30	0.98	(0.90, 1.00)	0.98	(0.90, 1.00)	0.98	(0.90, 1.00)	0.96	(0.90,1.00)
50	1.00	(0.95, 1.00)	1.00	(0.95, 1.00)	0.94	(0.85, 0.98)	1.00	(0.95,1.00)

The basic bootstrap confidence intervals are liberal, and the calibration process shows no signs of improving their properties, as might have been expected from the theoretical consideration of the effects of minor outbreak realisations on the exercise. Reviewing the properties of the calibration process, it is noticeable that

many of the λ which were applied to the calibration of major outbreak estimates were pathological *i.e.* $\lambda = 1$. Many of the upper limit λ were set to one, which corresponds to a case where it was impossible to set the upper value of λ equal to any of the (discrete) λ values available because the largest available value of λ, $\lambda_{(200)}$ corresponded to $\hat{p}(\lambda)$ being less than the desired α value of 0.95. Most typically, this problem would be associated with the use of an overly small number of bootstrap samples and hence an unacceptably crude discretisation of λ. However, in this case, it is more likely that the problem is associated with minor outbreaks skewing the distribution of the estimated λ.

It has been observed from earlier analyses that the properties of all methods are distorted and in some cases ruined by the occurrence of minor outbreaks in the bootstrap realisations of epidemics. The problems that arise due to minor outbreaks can potentially be addressed by what we term the weighted bootstrap approach.

9.5.3 The weighted bootstrap approach

If the data suggest that θ is greater than one, one solution might be to condition on the occurrence of large outbreaks, using bootstrapped information only in so far as it is consistent with having arisen from a major outbreak. Two quantities are readily available to assess whether a simulated epidemic falls into the minor or major class. These are the number of secondary infections and the estimated value of θ. It might seem attractive to use the estimated value of θ, but the true (unknown) sampling distribution for this variable, although dependent on θ, is complicated by its functional dependence on discrete and continuous random variables. A simple distributional model for $\hat{\theta}$ would be unlikely to adequately fit this complex distribution. By contrast, the number of secondary infections is a discrete distribution on a bounded set of integers. It seems likely that a fairly simple model for this class of data might suffice to summarise the differences between minor and major outbreaks. As described in Section 9.3 (Equations (9.10) and (9.11)), a beta-binomial mixture distribution can be used to define epidemics as major or minor outbreaks.

Thus the bootstrap approach could be extended to what we term the weighted bootstrap to condition on the presence of major or minor outbreaks. The standard bootstrap approach works on the basis of an equal weighting of $\frac{1}{B}$, where

B is the number of bootstrap samples, in the construction of percentile confidence intervals, and in the calibration process, $\hat{p}(\lambda)$ increases in steps of $\frac{1}{B}$. The weighted bootstrap approach would instead give a weight (summing to one over the distribution) which reflected the relative likelihood of an observation coming from a major or minor outbreak (Equation (9.11)). In the case where every observation is assumed to come from the distribution of interest, the standard bootstrap method is recovered. In the theoretical case, where a perfect partitioning is possible, minor epidemics will not affect the calculations and the weighted approach is equivalent to a standard bootstrap applied only to the major outbreaks. In reality, where no such perfect partitioning is possible, it is hoped that the weighted bootstrap would allow bootstrap confidence intervals to be calculated and bootstrap calibration to be applied successfully.

9.6 Summary

The initial exploration of the properties of bootstrap confidence intervals and bootstrap calibrated intervals indicates that the effect of minor outbreak realisations severely undermines the approach in most cases. There is weak evidence that when analysing a major outbreak it might be worthwhile to apply bootstrap calibration to any confidence intervals estimated using ALT. However, this latter conclusion is provisional and would require to be tested against a wider range of super threshold values of β and γ. The problems all arise from the occurrence of minor outbreaks. If the data suggest that θ is greater than 1, a solution might be to condition on large outbreaks, using bootstrapped information only in so far as it is consistent with having arisen from a major outbreak.

Should the weighted bootstrap prove successful in facilitating the calculation of valid bootstrap confidence intervals and valid calibration, the resulting confidence intervals will, of course, not be useful in establishing whether θ is significantly greater than 1. The weighted bootstrap, by conditioning on the existence of major outbreaks, implicitly assumes that θ is greater than 1. However, where there is a super-threshold outbreak, the methodology outlined in this chapter could give better bounds on the range of likely values of θ, and hence facilitate decisions about the severity of intervention required to bring θ down to sub-threshold levels.

Chapter 10

Conclusions and further work

10.1 Methods employed

The main aim of this thesis was to investigate methods of statistical inference for veterinary infectious disease data. This was pursued by fitting epidemic models to data obtained from experimental FMD virus infections in sheep and simulated data. The main contribution of this work is the estimation of expected infection history characteristics for infected individuals. To investigate the experimental hypothesis of intrinsic diminution in the infectivity of infected sheep during the course of successive naturally transmitted infections of FMD virus, the infection process for FMD virus in sheep was modelled in two ways: one based on infection generation information for individual sheep and the other based on the estimated infection rate applying to groups of sheep. Considering infection generation models, chain binomial and generalised linear models were used to estimate the rate of infection from each generation of infectives. In the analysis based on groups of sheep, an iterative algorithm was used to estimate values for the unobservable aspects of the infection history and the rates of infection acting upon groups 2 to 4 of sheep under a SLIR infection process. A gamma distribution was assumed for the latent and infectiousness periods and the distribution parameters were estimated from the observed experimental data. The rates of infection acting upon groups of sheep were estimated based on maximum likelihood and martingale estimation methods. The former approach being applied to two models: an unrestricted model, where the estimated rates of infection could take any values, and a restricted model, where the estimated rates of infection were constrained to be non-increasing. The trend in the estimated rates of infection was summarized by a slope in the case of the martingale and unrestricted model ML estimates and by a measure of decrease between groups 2 and 3 and between groups 3 and 4 in case of the restricted model ML β_g estimates. The significance of any decreasing

trend in the estimated rates of infection was tested using bootstrap methods. An illustrative study using simulated data was carried out to investigate the appropriateness of these methods to the observed type of highly structured epidemic data. Finally, the coverage properties of confidence intervals for the reproduction ratio were explored using simulated SIR infection processes.

10.2 Conclusions for analyses using infection generations

A re-parameterisation proposed (in a different context) by de Jong et al. (1996), was used to describe the infection model. The method also assumes that the infection pathway is known: in practice, it is assumed that the analyst can 're-construct' a likely path, which is then used as the basis of the analysis. Together, the re-parameterisation and the specification of an infection pathway allow infection rate parameters to be estimated from a standard Generalised linear model.

Generalised linear model

- The results indicated that the inoculated sheep had a low potential to cause infection in group 2 individuals.
- The estimated rate of infection increased by infection generation from generation 0 to generation 2, but a drop in infectivity was observed between generations 2 and 3, suggesting a possible drop in infectivity in naturally infected sheep.
- Evaluation of the method using simulated data led to the conclusion that the proposed re-parameterisation was not appropriate for epidemic data where there are likely to be more than one infection generation of individuals in the system on any day during the experiment. In particular, the re-parameterisation was not appropriate for the particular situation arising from the experimental design and especially not where the aim was to estimate more than 2 parameters.
- The method relies heavily on the assumption of knowledge of the infection pathway.

Chain binomial model

The chain binomial formulation of infection models, as presented in the literature was reviewed, and extended to apply to the type of structured mixing seen in the experimental data.

- The chain binomial model formulation yielded a complicated likelihood because of the many unobserved aspects of the infection process. It was appreciated that such a likelihood would be difficult to be maximise in a situation involving groups of size 8.

10.3 Conclusions for analyses using infection rates applying to groups of sheep

The latent and infectiousness periods of individual sheep were modelled as gamma random variables, and parameters for these distributions were estimated from the observed data set using maximum likelihood

Latent and infectiousness periods

- For both experiments, the mean length of latent period was estimated to be equal to approximately 1 day and the mean length of infectiousness period was estimated to be 2.9 days.

Rate of infection acting upon groups of sheep

The estimation of the β_g was done using unrestricted and restricted models. For the unrestricted model, both the martingale and the unrestricted ML estimation methods were used. For the restricted model, the β_g were estimated using MLE methods. The estimation of the β_g requires unobserved information about the infection history. The unobserved history was estimated using conditional estimates of the expectation of unobserved quantities, followed by estimation of the β_g, using an iterative procedure to convergence. Trends in the β_g were summarised and their significance tested using bootstrap methods.

- Martingale and unrestricted model ML-based estimates suggested that group 2 experienced the lowest rate of infection, while group 3 experienced the highest rate of infection, with an observed decline in the rate of infection between group 3 and 4.

- β_g estimates based on the restricted model MLE suggested that groups 2 and 3 experienced an equal estimated rate of infection (estimates on the boundary of restricted parameter space) and that there was a lower estimated rate of infection in group 4.

- The martingale and unrestricted model ML estimates yielded positive estimated slopes, contrary to the experimental hypothesis of a decreasing trend. The restricted model MLE method yielded estimated decreases greater than zero. However, these estimates were not found to be statistically significant (p-value = 0.46 for experiment 1, and p-value = 0.48 for experiment 2).

- In analysis the experimental data, the conclusion was that there was no significant trend in the rate of infection across groups. For both experiments, the results suggested that the rate of infection for group 2 was the lowest of that from all the three groups, 2 to 4. It could be that group 1 individuals were able to pass on only a limited amount of infection to group 2 individuals. Alternatively, the group size of 8 may not have been sufficient, given the initial dose of virus infection inoculated into group 1 individuals, to enable the detection of a significant trend in the rate of infection acting upon the groups of sheep.

- The martingale estimator used in this thesis is of interest because it makes minimal use of the estimated infection history characteristics, when compared to the ML estimates for the unrestricted β_g model. However, the results of Chapters 6 and 7 are consistent with the hypothesis that the martingale estimator consistently produces lower estimates of β_g than the ML estimator.

Illustrative study based on simulated data

Using the martingale and restricted model ML estimates of $\hat{\beta}_{global}$ obtained from experiment 1 data, two epidemic realisations were generated. The initial aim was to find out whether or not the methods are capable of detecting a genuine trend in the rate of infection, β. A passage multiplier of 0.15 was used to produce a small decreasing trend in the rate of infection. The generated data were analysed using the martingale approach to exemplify the properties of unrestricted estimators, and the restricted model ML as the more powerful maximum likelihood method.

- From the data generated using $\hat{\beta}_{global} = 0.8188$ (the martingale estimate from experiment 1), both estimation methods resulted into a non-significant decrease. From the data generated using the restricted model ML estimate of $\hat{\beta}_{global} = 1.0195$, the restricted MLE based methods were able to detect the small decrease. However, the martingale based methods resulted into a non-significant decrease.

The properties of the martingale-based methodology were illustrated using further simulated data sets.

- A data set was simulated assuming a large decrease in the rate of infection with successive infection generations. The martingale analysis yielded evidence of a significant decrease in infectivity.
- A data set was simulated assuming a large R_0 and a small decrease in the rate of infection on each infection generation. The martingale analysis estimated a non-significant trend. A further data set was simulated assuming a large R_0 and a large decrease in the rate of infection on each infection generation. The martingale analysis detected a statistically significantly decreasing trend in the rate of infection across groups.
- A data set was simulated assuming group size of 20. The martingale analysis yielded evidence of a statistically significant decrease in the rate of infection across groups.

General conclusions

- The inferential methods were appropriate for the type of highly structured epidemic data.
- MLE based methods for the restricted model have some ability to detect a small genuine decrease in the rate of infection for groups of size 8. Martingale based methods (unrestricted model) may detect a genuine decrease in the rate of infection in groups of size 8 if the decrease is reasonably large.
- As long as a sizeable genuine decrease is present in the rate of infection across groups, a group size of 8 is likely to suffice for the methods to be able to detect the decrease.
- Results using the martingale estimator suggest that it would be desirable to increase the group size as this would enhance the ability of the method to detect a small genuine trend in the rate of infection across groups.

10.4 Conclusions from the review of properties of asymptotic likelihood-based confidence intervals

In exploring the properties of confidence intervals for the reproduction ratio based on the asymptotic properties of the maximum likelihood estimate statistic, it was

concluded that:

- Construction of confidence intervals for R_0 based on the asymptotic properties of the likelihood is likely to yield overly wide confidence intervals.

A methodology was proposed to produce semi-parametric and parametric bootstrap realisations of an epidemic. These bootstrap realisations were used to generate bootstrap confidence intervals and for calibration purposes.

- Both the bootstrap confidence intervals and the calibrated intervals exhibited problems arising from the occurrence of minor outbreaks among the bootstrap realisations.

10.5 Further work

10.5.1 Experimental work

After analysing data from simulated experiments, the results indicated that a group size of 8 is likely to be sufficient to detect a genuine trend if R_0 in the initial group of infectives is large and the decrease in the rates of infection is substantial. In practice, these are properties of the infection, rather than of the experiment. Increase in group size is proposed, as the results indicated that a larger group size would be likely to increase the power of the methodology to detect a genuine trend even if the decrease in the rates of infection with increased infection generation number was small.

Analyses from experimental data yielded a lower estimate for the rate of infection in group 4 compared to that applying to group 3. It would be worthwhile to investigate any decrease in rate of infection by comparing only the estimates for groups 3 and 4 since only sheep in these groups were only exposed to naturally acquired infection. When evaluating the rate of infection estimates from the unrestricted model, another summary of trend other than the slope could be investigated. It would be interesting to investigate if the decreasing trend between groups 3 and 4 is maintained in further groups by increasing the number of groups of subjects in the study.

The maximisation of the latent period likelihood suffered from convergence problems. Although the estimated mean and standard deviation of the distribution was stable, individual shape and scale parameter estimates varied substantially during the estimation process. More detailed data must allow some exploration

of which distributions, other than gamma, are suitable models for the length of latent period.

Before any further experiments which are similar in structure to the FMD experiments are carried out, substantial work should be carried out to evaluate the design of the experiments. The statistical design of studies involving infectious diseases is an important topic, especially when the results from the experiments are of vital importance in understanding the infection mechanisms. There is a need for a power study to consider the effect of group size, number of groups, the sampling time scale (which should probably be less than 24 hours) and also the mixing pattern and length of time for which groups should mix. It is important to ensure that the design, both in structure and size is suitable given the objectives of the study. It is possible that, for some infections, small and relatively inexpensive changes (such as a shorter sampling time scale) could dramatically increase the information available from the experiment. Considerations of cost-efficiency and of ethics necessitate an attempt to maximise the output of information while minimising the number of animals used in the experiment. In an extreme case, where power calculations suggest that more animals are required in an experiment than can logistically be included, the experiment should not proceed at all. Only a thorough power study can justify the choice of animal numbers and experimental design in such an extensive experiment.

10.5.2 Methodological work

Application of MCMC methods to model the infection process is a possible area of further research for these data. Previously studies where these methods have been applied to epidemic modelling have been discussed in Section 4.5. These methods could be used to model the individual based infection process, for example, by modelling the epidemic chains so that infection pathways are estimated along with the other unobserved infection process characteristics. MCMC methods could also be used to model the infection process based on groups of sheep to explore how the results compare with those obtained in this thesis.

It is arguable that the characteristics of the infection process in group 1 individuals is different to that in individuals from groups 2 to 4, however, estimation of the latent period distribution parameters was based only on data summarising the number of occasions on which group 1 individuals tested negative before the first positive test after inoculation (n_l). MCMC methods would facilitate the estimation of the latent period distribution separately for the two categories of sheep,

i.e. inoculated and natural infectives, although estimates of the latent period for natural infectives would be likely to be somewhat variable. The assumption that all inoculated animals become infected as a result of their inoculation could also be relaxed, with the model allowing infections between group 1 individuals. In general, it would be useful to investigate the use of MCMC methods, even when applied to the group rate estimation problem, since use of this methodology would avoid many of the *a*d hoc assumptions required in Chapters 6 and 7 to estimate the aspects of the unobserved infection history. It might also be useful to revise the model for the infection process by allowing individuals to exhibit variability in susceptibility.

The martingale estimator consistently produced lower estimates of β_g than the ML estimator, It would therefore be of interest to study the sampling distribution of the two (martingale and ML) estimators to investigate what bias may be present in the estimators and how this may relate to the dependency of the $\hat{\beta}_g$ on the infection history characteristics, given the *a*d hoc nature of the iterative estimation process.

Statistical significance of trend was tested using bootstrap methods, however, further work is required to investigate the potential impact of simulated minor outbreaks on estimates of the rate of infection. If this aspect of the stochastic process does, under some circumstances, have a large impact on estimates of the rate of infection, it might be concluded that the bootstrap simulations should perhaps not be based on an estimated β_{global}, if this may indeed be affected by the inclusion of minor epidemics. The mixing group which is least likely to be subject to a minor outbreak is group 2, and it is arguable that a restricted model ML estimate of the infection rate applying to group 2 is therefore the best estimate of the global infection rate, even when working under the assumption that there is no systematic passage effect.

In chapter 9, the nature of estimates of the rate of infection, removal rate and R_0 of the SIR model arising from realised minor and major outbreaks was explored. The results suggested that the presence of realised minor outbreaks affected the estimated confidence intervals of these parameters. To address this problem, a weighted bootstrap approach was proposed. It would be worthwhile to carry out to carry out further work using the weighted bootstrap approach to estimate confidence intervals conditional on observations coming from major outbreaks. It is hoped that the weighted bootstrap would allow the bootstrap calibration method described in Chapter 9 to be applied successfully.

References

Addy, C. L., Longini, I. M., and Haber, M. (1991). A generalized stochastic model for the analysis of infectious disease final size data. *Biometrics*, **47** (3), 961–974.

Alexandersen, S., Kitching, R. P., Mansley, L. M., and Donaldson, A. I. (2003). Clinical and laboratory investigations of five outbreaks of foot-and-mouth disease during the 2001 epidemic in the United Kingdom. *The Veterinary Record*, **152** (16), 489–496.

Alsaif, N. and Brazier, J. S. (1996). The distribution of clostridium difficile in the environment of south wales. *Journal of Microbiology*, **45** (2), 133–137.

Andersen, P. K. and Borgan, O. (1985). Counting process models for life history data: a review. *Scandinavian Journal of Statistics*, **12**, 97–158.

Anderson, R. M., Donnelly, C. A., Ferguson, N. M., Woolhouse, M. E. J., Watt, C. J., Udy, H. J., MaWhinney, S., Dunstan, S. P., Southwood, T. R. E., Wilesmith, J. W., Ryan, J. B. M., Hoinville, L. J., Hillerton, J. E., Austin, A. R., and Wells, G. A. H. (1996). Transmission dynamics and epidemiology of BSE in british cattle. *Nature*, **382** (6594), 779–788.

Anderson, R. M. and May, R. M. (1991). *Infectious Diseases of Humans, Dynamics and Control.* Oxford University Press, Oxford.

Anonymous (2003). Government responds on animal experiments. *The Veterinary Record*, **152** (5), page 124.

Armitage, P. and Berry, G. (1994). *Statistical Methods in Medical Research.* Blackwell Science Ltd., Oxford.

Azzalini, A. (1996). *Statistical Inference - Based on the likelihood.* Chapman and Hall, London.

Bailey, N. T. J. (1953a). The total size of a general stochastic epidemic. *Biometrika*, **40** (1/2), 177–185.

Bailey, N. T. J. (1953b). The use of chain-binomials with a variable chance of infection for the analysis of intra-household epidemics. *Biometrika*, **40** (3/4), 279–286.

Bailey, N. T. J. (1956a). On estimating the latent and infectious periods of measles: I. Families with two susceptibles only. *Biometrika*, **43** (1/2), 15–22.

Bailey, N. T. J. (1956b). On estimating the latent and infectious periods of Measles: II. Families with three or more susceptibles. *Biometrika*, **43** (3/4), 322–331.

Bailey, N. T. J. (1956c). Significance tests for a variable chance of infection in chain-binomial theory. *Biometrika*, **43** (3/4), 332–336.

Bailey, N. T. J. (1975). *The Mathematical Theory of Infectious Diseases and its Applications.* Charles Griffin & Company limited, London.

Bailey, N. T. J. and Alff-Steinberger, C. (1970). Improvements in the estimation of the latent and infectious periods of contagious disease. *Biometrika*, **57** (1), 141–153.

Baker, H. F. and Ridley, R. M. (1996). What went wrong in BSE? From prion to public disaster. *Brain Research Bulletin*, **40** (4), 237–244.

Ball, F. (1986). A note on the total size distribution of epidemic models. *Journal of Applied Probability*, **23** (3), 832–836.

Ball, F. and Clancy, D. (1995). The final outcome of an epidemic model with several different types of infective in a large population. *Journal of Applied Probability*, **32** (2), 579–590.

Ball, F. and O'Neill, P. (1999). The distribution of general final state random variables for stochastic epidemic models. *Journal of Applied Probability*, **36** (2), 473–491.

Barkema, H. W., Schukken, Y. H., Lam, T. J. G. M., Beiboer, M. L., Benedictus, G., and Brand, A. (1999). Management practices associated with the incidence rate of clinical mastitis. *Journal of Dairy Science*, **82** (8), 1643–1654.

Barndorff-Nielsen, O. E. and Cox, D. R. (1994). *Inference and Asymptotics.* Chapman and Hall, London.

Bartely, L. M., Donnelly, C. A., and Anderson, R. M. (2002). Review of foot-and-mouth disease virus survival in animal excretions and on fomites. *The Veterinary Record*, **151**, 667–669.

Bartlett, M. S. (1949). Some evolutionary stochastic processes. *Journal of the Royal Statistical Society, Series B-Statistical Methodology*, **11**, 211–229.

Becker, N. G. (1968). The spread of an epidemic to fixed groups within the population. *Biometrics*, **24** (4), 1007–1014.

Becker, N. G. (1977). On a general stochastic epidemic model. *Theoretical Population Biology*, **11** (1), 23–36.

Becker, N. G. (1979). An estimation procedure for household disease data. *Biometrika*, **66** (2), 271–277.

Becker, N. G. (1981). The infectiousness of a disease within households. *Biometrika*, **68** (1), 133–141.

Becker, N. G. (1982). Estimation in models for the spread of infectious diseases. In *Proceedings of the XIth International Biometric Conference*, pages 145–151.

Becker, N. G. (1989). *Analysis of Infectious Disease Data.* Chapman and Hall, London.

Becker, N. G. (1993a). Martingale methods for the analysis of epidemic data. *Statistical Methods in Medical Research*, **2**, 93–112.

Becker, N. G. (1993b). Parametric inference for epidemic models. *Mathematical Biosciences*, **117** (1–2), 239–251.

Becker, N. G. (1995). Statistical challenges of epidemic data. In *Epidemic Models: Their Structure and Relation to Data*, (ed. D. Mollison), pages 339–349. Cambridge University Press, Cambridge.

Becker, N. G. (1997). Uses of EM algorithm in the analysis of data on HIV/AIDS and other infectious diseases. *Statistical Methods in Medical Research*, **6** (1), 24–37.

Becker, N. G. and Angulo, J. (1981). On estimating the contagiousness of a disease transmitted from person to person. *Mathematical Biosciences*, **54**, 137–154.

Becker, N. G. and Britton, T. (2001). Design issues for studies of infectious diseases. *Journal of Statistical planning and Inference*, **96** (1), 41–66.

Becker, N. G. and Dietz, K. (1995). The effect of household distribution on transmission and control of highly infectious diseases. *Mathematical Biosciences*, **127** (2), 207–219.

Becker, N. G. and Hall, R. (1996). Immunization levels for preventing epidemics in a community of households made up of individuals of various types. *Mathematical Biosciences*, **132** (2), 205–216.

Becker, N. G. and Hasofer, A. M. (1997). Estimation in epidemics with incomplete observations. *Journal of the Royal Statistical Society, Series B- Statistical Methodology*, **59** (2), 415–429.

Becker, N. G. and Hasofer, A. M. (1998). Estimating the transmission rate for a highly infectious disease. *Biometrics*, **54**, 730–738.

Becker, N. G. and Hopper, J. L. (1983). The infectiousness of a disease in a community of households. *Biometrika*, **70** (1), 29–39.

Becker, N. G. and Utev, S. (1998). The effect of community structure on the immunity coverage required to prevent epidemics. *Mathematical Biosciences*, **147** (1), 23–39.

Becker, N. G. and Yip, P. (1989). Analysis of variations in an infection rate. *Australian Journal of Statistics*, **31** (1), 42–52.

Begon, M., Bennett, M., Bowers, R. G., French, N. P., Hazel, S. M., and Turner, J. (2002). A clarification of transmission terms in host-microparasite models: numbers, densities and areas. *Epidemiology and Infection*, **129** (1), 147–153.

Blanco, E., Romero, L. J., el Harrach, M., and Sanchez-Vizcaino, J. M. (2002). Serological evidence of FMD subclinical infection in sheep population during the 1999 epidemic in Morocco. *Veterinary Microbiology*, **85** (1), 13–21.

Borchers, K. (2002). Transmissible spongiform encephalopathies (TSE): Old diseases with new importance. *Berliner und Muncherner Tierarztliche Wochenschrift*, **115** (3-4), 81–90.

Bouvet, J., Bavia, C., Rossel, R., le Roux, A., Montet, M. P., Ray-Gueniot, S., Mazuy, C., Arquilliere, C., and Vernozy-Rozand, C. (2001). Prevalence of verotoxin-producing Escherichia coli and E-coli O157:H7 in pig carcasses from

three french slaughterhouses. *International Journal of Food Microbiology*, **71** (2-3), 249–255.

Britton, T. (1998). Estimation in multitype epidemics. *Journal of the Royal Statistical Society, Series B- Statistical Methodology*, **60** (4), 663–679.

Britton, T. and O'Neill, P. D. (2002). Bayesian inference for stochastic epidemics in populations with random social structure. *Scandinavian Journal of Statistics*, **29** (3), 375–390.

Brooks, S. P. (1998). Markov chain monte carlo method and its application. *The Statistician*, **47** (1), 69–100.

Brown, H. and Prescott, R. (1999). *Applied Mixed Models in Medicine*. John Wiley & sons, Ltd, Chichester.

Bruckner, G. K., Vosloo, W., du Plessis, B. J. A., Kloeck, P. E. L. G., Connoway, L., Ekron, M. D., Weaver, D. B., Dickason, C. J., Schreuder, F. J., Marais, T., and Mogajane, M. E. (2002). Foot and mouth disease: the experience of South Africa. *Revue Scientifique et Technique del Office International des Epizooties*, **21** (3), 751–764.

Bruggemann, H., Baumer, S., Fricke, W. F., Wiezer, A., Liesegang, H., Decker, I., Herzberg, C., Martinez-Arias, R., Merkl, R., Henne, A., and Gottschalk, G. (2003). The genome sequence of clostridium tetani, the causative agent of tetanus disease. *Proceedings of the National Academy of Sciences of the United States of America*, **100** (3), 1316–1321.

Caley, P. and Ramsey, D. (2001). Estimating disease transmission in wildlife, with emphasis on leptospirosis and bovine tuberculosis in possums, and effects of fertility control. *Journal of Applied Ecology*, **38** (6), 1362–1370.

Cassagne, M. H. (2002). Managing compensation for economic losses in areas surrounding foot and mouth disease outbreaks: the response of France. *Revue Scientifique et Technique del Office International des Epizooties*, **21** (3), 823–829.

Chapman, P. A., Malo, A. T. C., Ellin, M., Ashton, R., and Harkin, M. A. (2001). Escherichia coli O157 in cattle and sheep at slaughter, on beef and lamb carcasses and in raw beef and lamb products in South Yorkshire, UK. *International Journal of Food Microbiology*, **64** (1-2), 139–150.

Chapman, P. A., Siddons, C. A., Wright, D. J., Norman, P., Fox, J., and Crick, E. (1993). Cattle as a possible source of verocytotoxin-producing Escherichia coli O157 infections in man. *Epidemiology and Infection*, **111**, 439–447.

Clifton-Hadley, F. A. (2000). Detection and diagnosis of Escherichia coli O157 and other verocytotoxigenic E-coli in animal faeces. *Reviews in Medical Microbiology*, **11** (1), 47–58.

Clough, H. E., Clancy, D., O'Neill, P. D., and French, N. P. (2003). Bayesian methods for estimating pathogen prevalence within groups of animals from faecal-pat sampling. *Preventive Veterinary Medicine*, **58** (3-4), 145–169.

Cobbold, R. and Desmarchelier, P. (2001). Characterisation and clonal relationships of shiga-toxigenic Escherichia coli (STEC) isolated from australian dairy cattle. *Veterinary Microbiology*, **79** (4), 323–335.

Collett, D. (1994). *Modelling Survival Data in Medical Research.* Chapman and Hall, London.

Cornick, N. A., Booher, S. L., Casey, T. A., and Moon, H. W. (2000). Persistent colonization of sheep by Escherichia coli O157:H7 and other E-coli pathotypes. *Applied and Environmental Microbiology*, **66** (11), 4926.

Coutinho, F. A. B., Lopez, L. F., Burattini, M. N., and E, E. M. (2001). Modelling the natural history of HIV infection in individuals and its epidemiological implications. *Bulletin of Mathematical Biology*, **63** (6), 1041–1062.

Davies, G. (2002). The foot and mouth disease (FMD) epidemic in the United Kingdom 2001. *Comparative Immunology Microbiology and Infectious Diseases*, **25** (5-6), 331–343.

Davison, A. C. and Hinkley, D. V. (2000). *Bootstrap Methods and their Application.* Cambridge University Press, Cambridge.

de Clercq, K. (2002). Vaccination as a tool to control foot-and-mouth disease. *Annales de Medecine Veterinaire*, **146** (3), 155–160.

de Jong, M. C. M. (1995). Mathematical modelling in veterinary epidemiology: why model building is important. *Preventive Veterinary Medicine*, **25** (2), 183–193.

de Jong, M. C. M., Diekmann, O., and Heesterbeek, H. (1995). How does transmission of infection depend on population size. In *Epidemic Models: Their*

Structure and Relation to Data, (ed. D. Mollison), pages 84–94. Cambridge University Press, Cambridge.

de Jong, M. C. M. and Kimman, T. G. (1994). Experimental quantification of vaccine induced reduction in virus transmission. *Vaccine*, **12** (8), 761–766.

de Jong, M. C. M., van der Poel, W. H. M., Kramps, J. A., Brand, A., and van Oirschot, J. T. (1996). Quantitative investigation of population persistence and recurrent outbreaks of bovine respiratory syncytial virus on dairy farms. *American Journal of Veterinary Research*, **57** (5), 628–633.

Dekker, A. and Terpstra, C. (1999). Foot-and-mouth disease: Clinical signs, epizootiology and diagnosis. *Tijdschrift voor Economische en Sociale Geografie*, **124** (3), 74–79.

Dempster, A. P., Laird, N. M., and Rubin, D. B. (1977). Maximum likelihood from incomplete data via the EM algorithm. *Journal of the Royal Statistical Society, Series B- Statistical Methodology*, **39** (1), 1–38.

Dexter, N. (2003). Stochastic models of foot and mouth disease in feral pigs in the Australian semi-arid rangelands. *Journal of Applied Ecology*, **40** (2), 293–306.

Diekmann, O. and Heesterbeek, H. (2000). *Mathematical Epidemiology of Infectious Diseases : Model Building, Analysis, and Interpretation.* Wiley, Chichester.

Donaldson, A. I. (1997). Risks of spreading foot and mouth disease through milk and dairy products. *Revue Scientifique et Technique del Office International des Epizooties*, **16** (1), 117–124.

Donnelly, C. A., MaWhinney, S., and Anderson, R. M. (1999). A review of the BSE epidemic in british cattle. *Ecosystem Health*, **5** (3), 164–173.

Durand, B. and Mahul, O. (2000). An extended state-transition model for foot-and-mouth disease epidemics in France. *Preventive Veterinary Medicine*, **47** (1-2), 121–139.

Efron, B. and Tibishirani, R. J. (1993). *An Introduction to the Bootstrap.* Chapman and Hall, London.

Erstad, B. L. (2002). Implications of prion-induced diseases for animal-derived pharmaceutical products. *American Journal of Health-System Pharmacy*, **59** (3), 254–260.

Ferguson, N. M., Donnelly, C. A., and Anderson, R. M. (2001a). The foot-and-Mouth Epidemic in Great Britain: Pattern of Spread and Impact of Interventions. *Science*, **292** (5519), 1155–1160.

Ferguson, N. M., Donnelly, C. A., and Anderson, R. M. (2001b). Transmission intensity and impact of control policies on the foot and mouth epidemic in Great Britain. *Nature*, **414** (6861), 329–329.

Ferguson, N. M., Donnelly, C. A., and Anderson, R. M. (2001c). Transmission intensity and impact of control policies on the foot and mouth epidemic in Great Britain. *Nature*, **413** (6855), 542–548.

Ferguson, N. M., Donnelly, C. A., Woolhouse, M. E. J., and Anderson, R. M. (1997). The epidemiology of BSE in cattle herds in Great Britain .2. model construction and analysis of transmission dynamics. *Philosophical Transactions of the Royal Society of London, Series B-Biological Sciences*, **352** (1355), 803–838.

Ferguson, N. M., Donnelly, C. A., Woolhouse, M. E. J., and Anderson, R. M. (1999). Estimation of the basic reproduction number of BSE: the intensity of transmission in british cattle. *Proceedings of the Royal Society of London, Series B-Biological Sciences*, **266** (1414), 23–32.

French, N. P., Clancy, D., Davison, H. C., and Trees, A. J. (1999). Mathematical models of neospora caninum infection in dairy cattle: transmission and options for control. *International Journal of Parasitology*, **29**, 1691–1704.

Freund, R. J. and Wilson, W. J. (1998). *Regression Analysis: Statistical Modelling of a Response Variable.* Academic Press, London.

Gallagher, E., Ryan, J., Kelly, L., Leforban, Y., and Wooldridge, M. (2002). Estimating the risk of importation of foot-and-mouth disease into Europe. *The Veterinary Record*, **150** (25), 769–772.

Gamerman, D. (1997). *Markov Chain Monte Carlo: Stochastic Simulation for Bayesian Inference.* Chapman and Hall, London.

Ganiere, J. P., Ruvoen, N., and Andre-Fontaine, G. (2001). Infectious zoonoses of livestock. *Medecine et Maladies Infectieuses*, **31**, 143S–158S.

Garner, M. G., Fisher, B. S., and Murray, J. G. (2002). Economic aspects of foot and mouth disease: perspectives of a free country, Australia. *Revue Scientifique et Technique del Office International des Epizooties*, **21** (3), 625–635.

Geffray, L. and Paris, C. (2001). Infectious risks associated with pets. *Medecine et Maladies Infectieuses*, **31**, 126S–142S.

Genstat 5 Committee (1993). *Genstat 5 Release 3 Reference Manual.* Clarendon Press, Oxford.

Gibson, G. J. (1997). Markov Chain Monte Carlo Methods for fitting spatiotemporal stochastic models in plant epidemiology. *Journal of the Royal Statistical Society, Series C- Applied Statistics*, **46** (2), 215–233.

Gibson, G. J. and Renshaw, E. (1998). Estimating parameters in stochastic compartmental models using markov chain methods. *IMA Journal of Mathematics Applied in Medicine and Biology*, **15** (1), 19–40.

Gilks, W. R., Richardson, S., and Spiegelhalter, D. J. (1996). *Markov Chain Monte Carlo in Practice.* Chapman and Hall, London.

Green, L. E. and Medley, G. F. (2002). Mathematical modelling of the foot and mouth disease epidemic of 2001: strengths and weaknesses. *Research in Veterinary Science*, **73**, 201–205.

Greenhalgh, D. and Hay, G. (1997). Mathematical modelling of the spread of HIV/AIDS amongst injecting drug users. *IMA Journal of Mathematics Applied in Medicine and Biology*, **14** (1), 11–38.

Greenwood, M. (1931). On the statistical measure of infectiousness. *Journal of Hygiene*, **31**, 336–351.

Halloran, M. E., Haber, M., and Longini, I. M. (1992). Interpretation and estimation of vaccine efficacy under heterogeneity. *American Journal of Epidemiology*, **136** (3), 328–343.

Hatton, M. D. (1977). *Mathematical Analysis.* Hodder and Stoughton Ltd., London.

Hay, R. K. (1998). Science and the Scottish Parliament. *Proceedings of a Symposium of the Edinburgh International Science Festival, 7th April 1998, organised by the Scottish Agricultural Science Agency.*

Haydon, D. T. and Woolhouse, M. E. J. (1997). An analysis of foot-and-mouth-disease epidemics in the UK. *IMA Journal of Mathematics Applied in Medicine and Biology*, **14** (1), 1–9.

Heuvelink, A. E., van den Biggelaar, F. L. A. M., de Boer, E., Herbes, R. G., Melchers, W. J. G., Huis, J. H. J., and Monnens, L. A. H. (1998). Isolation and characterization of verocytotoxin-producing Escherichia coli O157 strains from Dutch cattle and sheep. *Journal of Clinical Microbiology*, **36** (4), 878–882.

Hinton, M. (1993). Spoilage and pathogenic microorganisms in animal feed. *International Biodeterioration and Biodegradation*, **32** (1-3), 67–74.

Howard, S. C. and Donnelly, C. A. (2000a). Estimation of a time-varying force of infection and basic reproduction number with application to an outbreak of classical swine fever. *Journal of Epidemiology and Biostatistics*, **5** (3), 161–168.

Howard, S. C. and Donnelly, C. A. (2000b). The importance of immediate destruction in epidemics of foot and mouth disease. *Research in Veterinary Science*, **69** (2), 189–196.

Hu, Y., Zhang, Q., and Meitzler, J. C. (1999). Rapid and sensitive detection of Escherichia coli O157:H7 in bovine faeces by a multiplex PCR. *Journal of Applied Microbiology*, **87** (6), 867–876.

Hughes, G. J. (2001). *Modelling the maintenance and transmission of foot-and-mouth disease virus in sheep.* PhD thesis, The University of Edinburgh.

Hughes, G. J., Mioulet, V., Haydon, D. T., Kitching, R. P., Donaldson, A. I., and Woolhouse, M. E. J. (2002a). Serial passage of foot-and-mouth disease virus in sheep reveals declining levels of viraemia through time. *Journal of General Virology (submitted)*, **83** (8), 1907–1914.

Hughes, G. J., Mioulet, V., Kitching, R. P., Woolhouse, M. E. J., Alexandersen, S., and Donaldson, A. I. (2002b). Foot-and-mouth disease virus infection of sheep: implications for diagnosis and control. *The Veterinary Record*, **150** (23), 724–727.

Hunter, A. (1996). *Animal Health.* MacMillan, London.

Hutber, A. M., Kitching, R. P., and Conway, D. A. (1999). Predicting the level of herd infection for outbreaks of foot-and-mouth disease in vaccinated herds. *Epidemiology and Infection*, **122** (3), 539–544.

Jalvingh, A. W., Nielen, M., Maurice, H., Stegeman, A. J., Elbers, A. R. W., and Dijkhuizen, A. A. (1999). Spatial and stochastic simulation to evaluate the impact of events and control measures on the 1997-1998 classical swine fever

epidemic in The Netherlands. I. Description of simulation model. *Preventive Veterinary Medicine*, **42** (3-4), 271–295.

Jemmi, T., Danuser, J., and Griot, C. (2000). Zoonoses as a risk when handling livestock or animal products. *Schweizer Archiv fur Tierheilkunde*, **142** (12), 665–671.

Johnson, N. L. and Kotz, S. (1970). *Distributions in Statistics: Continuous Univariate Distributions.* Houghton Mifflin, New York.

Jones, P. N. and McLachlan, G. J. (1991). Fitting mixture distributions to Phenylthiocarbamide (PTC) sensitivity. *American Journal of Human Genetics*, **48** (1), 117–120.

Karakulska, J. and Nawrotek, P. (1999). Identification and virulence determination of cytotoxigenic E-coli strains by conventional methods and PCR. *Medycyna Weterynaryjna*, **55** (2), 129–133.

Keeling, M. J., Woolhouse, M. E. J., Shaw, D. J., Matthews, L., Chase-Topping, M., Haydon, D. T., Cornell, S. J., Kappey, J., Wilesmith, J., and Grenfell, B. T. (2001). Dynamics of the 2001 UK Foot and Mouth Epidemic: Stochastic Dispersal in a Heterogeneous Landscape. *Science*, **294** (5543), 813–817.

Kermack, W. O. and McKendrick, A. G. (1927). A contribution to the mathematical theory of epidemics. *Proceedings of the Royal Society of London, Series A-Mathematical and physical sciences*, **115**, 700–721.

Kernighan, B. W. and Ritchie, D. M. (1988). *The C Programming Language.* Prentice Hall, Englewood Cliffs, N.J.

Kolarova, M., Kolarova, L., Perina, A., and Chalupa, P. (2002). Animal products and selected human infectious diseases. *Czech Journal of Animal Science*, **47** (7), 297–307.

Kretzschmar, H. A. and Lederer, R. M. (2002). Prion diseases. *Ernahrungs-Umschau*, **49** (6), 216–216.

Kruze, J. (1998). The milking routine and its role in mastitis control programmes. *Archivos de Medicina Veterinaria*, **30** (2), 7–16.

Law, A. M. and Kelton, W. D. (2000). *Simulation Modeling and Analysis.* McGraw-Hill, London.

le Corfec, E., Rouzioux, C., and Costagliola, D. (2000). HIV-1 quantitive dynamics in vivo: a review of mathematical models. *Revue d Epidemiologie et de Sante Publique*, **48** (2), 168–181.

Leslie, J. (1996). Simulation of the transmission of salmonella enteritidis phage type 4 in a flock of laying hens. *The Veterinary Record*, **139**, 388–391.

Levett, P. N. (1986). Clostridium-difficile in habitats other than the human gastrointestinal-tract. *Journal of Infection*, **12** (3), 253–263.

Liang, Z., Jaszczak, R. J., and Coleman, R. E. (1992). Parameter-estimation of finite mixtures using the EM algorithm and information criteria with application to medical image-processing. *IEEE Transactions on Nuclear Science*, **39** (4), 1126–1133.

Longini, I. M. and Koopman, J. S. (1982). Household and community transmission parameters from final distributions of infections in households. *Biometrics*, **38** (1), 115–126.

MacDonald, G. (1965). The dynamics of helminth infections, with special reference to schistosomes. *Transactions of the Royal Society of Tropical Medicine and Hygiene*, **59**, 489–506.

MacKenzie, K. and Bishop, C. (2001). Developing stochastic epidemiology models to quantify the dynamics of infectious disease in domestic livestock. *Journal of Animal Science*, **79** (8), 2047–2056.

Matfield, M. (2002). Animal experiments are important for Britain, and for the future of science. *The Times*, page 18. 25^{th} July.

MathSoft (1987–1999). *S-Plus 2000 User's Guide*. Data Analysis Products Division.

Matthews, L., Coen, P. G., Foster, J. D., Hunter, N., and Woolhouse, M. E. J. (2001). Population dynamics of a scrapie outbreak. *Archives in Virology*, **146** (6), 1173–1186.

McLachlan, G. J. and Krishnan, T. (1997). *The EM Algorithm and Extensions*. Wiley, New York.

McLachlan, G. J., Peel, D., and Whiten, W. J. (1996). Maximum likelihood clustering via normal mixture models. *Signal processing-image communication*, **8** (2), 105–111.

Mead, P. S. and Griffin, P. M. (1998). Escherichia coli O157:H7. *Lancet*, **352** (9135), 1207–1212.

Mepham, B. (2001). Foot and Mouth Disease and British agriculture: Ethics in a crisis. *Journal of Agricultural & Environmental Ethics*, **14** (3), 339–347.

Moennig, V. and Kramer, M. (2002). Fmd: Basic rules for the prevention of spread of the disease. *Praktische Tierarzt*, **83** (5), 450–455.

Morgan, B. J. T. (1984). *Elements of Simulation*. Chapman and Hall, London.

Morris, R. S., Wilesmith, J. W., Stern, M. W., Sanson, R. L., and Stevenson, M. A. (2001). Predictive spatial modelling of alternative control strategies for the foot-and-mouth disease epidemic in Great Britain, 2001. *The Veterinary Record*, **149** (5), 137–144.

Ng, S. K. and McLachlan, G. J. (1998). On modifications to the long-term survival mixture model in the presence of competing risks. *Journal of Statistical computation and simulation*, **61** (1-2), 77–96.

Ng, S. K., McLachlan, G. J., McGiffin, D. C., and O'Brien, M. F. (1999). Constrained mixture models in competing risks problems. *Environmetrics*, **10** (6), 753–767.

Nodelijk, G., de Jong, M. C. M., van Nes, A., Vernooy, J. C. M., van Leengoed, L. A. M. G., Pol, J. M. A., and Verheijden, J. H. M. (2000). Introduction, persistence and fade-out of porcine reproductive and respiratory syndrome virus in a Dutch breeding herd: a mathematical analysis. *Epidemiology and Infection*, **124** (1), 173–182.

O'Neill, P. D. (2002). A tutorial introduction to bayesian inference for stochastic epidemic models using markov chain monte carlo methods. *Mathematical Biosciences*, **180**, 103–114.

O'Neill, P. D., Balding, D. J., Becker, N. G., Eerola, M., and Mollison, D. (2000). Analyses of infectious disease data from household outbreaks by markov chain monte carlo methods. *Journal of the Royal Statistical Society, Series C- Applied Statistics*, **49** (4), 517–542.

O'Neill, P. D. and Becker, N. G. (2001). Inference for an epidemic when susceptibility varies. *Biostatistics*, **2** (1), 99–108.

O'Neill, P. D. and Roberts, G. O. (1999). Bayesian inference for partially observed stochastic epidemics. *Journal of the Royal Statistical Society, Series A-Statistics in Society*, **162** (1), 121–129.

Osek, J. (1999). Escherichia coli O157 - a dangerous pathogen with a broad spectrum of illnesses. *Medycyna Weterynaryjna*, **55** (4), 215–221.

Paarlberg, P. L. and Lee, J. G. (1998). Import restrictions in the presence of a health risk: An illustration using FMD. *American Journal of Agricultural Economics*, **80** (1), 175–183.

Paton, A. W. and Paton, J. C. (1998). Detection and characterization of shiga toxigenic Escherichia coli by using multiplex PCR assays for stx(1), stx(2), eaeA, enterohemorrhagic E-coli hly A, rfb(O111), and rfb(O157). *Journal of Clinical Microbiology*, **36** (2), 598–602.

Pennington Group (1997). Report on the circumstances leading to the 1996 outbreak of infection with E.coli O157 in central scotland, the implications for food safety and the lessons to be learned. The Stationary Office, Edinburgh.

Phillips, A. D., Navabpour, S., Hicks, S., Dougan, G., Wallis, T., and Frankel, G. (2000). Enterohaemorrhagic Escherichia coli O157:H7 target Peyer's patches in humans and cause attaching/effacing lesions in both human and bovine intestine. *GUT*, **47** (3), 377–381.

Press, W. H., Teukolsky, S. A., Vetterling, W. T., and Flannery, B. P. (1992). *Numerical Recipes in C.* Cambridge University Press, Cambridge.

Reid, S. M., Ferris, N. P., Hutchings, G. H., de Clercq, K., Newman, B. J., Knowles, N. J., and Samuel, A. R. (2001). Diagnosis of foot-and-mouth disease by RT-PCR: use of phylogenetic data to evaluate primers for the typing of viral RNA in clinical samples. *Archives of Virology*, **146** (12), 2421–2434.

Reid, S. M., Ferris, N. P., Hutchings, G. H., Zhang, Z. D., Belsham, G. J., and Alexandersen, S. (2002). Detection of all seven serotypes of foot-and-mouth disease virus by real-time, fluorogenic reverse transcription polymerase chain reaction assay. *Journal of Virological Methods*, **105** (1), 67–80.

Reid, S. M., Grierson, S. S., Ferris, N. P., Hutchings, G. H., and Alexandersen, S. (2003). Evaluation of automated RT-PCR to accelerate the laboratory diagnosis of foot-and-mouth disease virus. *Journal of Virological Methods*, **107** (2), 129–139.

Remme, H., Alley, S., and Plaisier, A. (1995). Estimation and prediction in tropical disease control: the example of onchocerciasis. In *Epidemic Models: Their Structure and Relation to Data*, (ed. D. Mollison), pages 372–393. Cambridge University Press, Cambridge.

Renshaw, E. (1991). *Modelling Biological Populations in Space and Time*. Cambridge University Press, Cambridge.

Renshaw, E. and Gibson, G. J. (1998). Can Markov Chain Monte Carlo be usefully applied to stochastic processes with hidden birth times? *Inverse Problems*, **14** (6), 1581–1606.

Richter, H., Klie, H., Timm, M., Gallien, P., Steinruck, H., Perlberg, K. W., and Protz, D. (1997). Verotoxin-producing E-coli (VTEC) in faeces from cattle slaughtered in Germany. *Berliner und Muncherner Tierarztliche Wochenschrift*, **110** (4), 121–127.

Royal Society (2002). *Infectious Diseases in Livestock*. The Royal Society, London, U. K.

Salomon, J. A. and Murray, C. J. L. (2001). Modelling HIV/AIDS epidemics in sub-saharan africa using seroprevalence data from antenatal clinics. *Bulletin of the World Health Organisation*, **79** (7), 596–607.

Sanson, R. L. (1994). The epidemiology of foot-and-mouth-disease - implications for new-zealand. *New Zealand Veterinary Journal*, **42** (2), 41–53.

Scudamore, J. M., Trevelyan, G. M., Tas, M. V., Varley, E. M., and Hickman, G. A. W. (2002). Carcass disposal: lessons from Great Britain following the foot and mouth disease outbreaks of 2001. *Revue Scientifique et Technique del Office International des Epizooties*, **21** (3), 775–787.

Shinoda, S., Yamamoto, S., Tomochika, K., and Miyoshi, S. (1997). Enterohemorrhagic Escherichia coli O157:H7 infection. *Japanese Journal of Toxicology and Environmental Health*, **43** (1), 1–14.

Shoukri, M. M. and McLachlan, G. J. (1994). Parameter estimation in a genetic mixture model with application to nuclear family data. *Biometrics*, **50** (1), 128–139.

Slasor, P. and Laird, N. (2003). Joint models for efficient estimation in proportional hazards regression models. *Statistics in Medicine*, **22** (13), 2137–2148.

Stegeman, A., Elbers, A. R. W., Bouma, A., de Smit, H., and de Jong, M. C. M. (1999). Transmission of classical swine fever virus within herds during the 1997-1998 epidemic in The Netherlands. *Preventive Veterinary Medicine*, **42** (3-4), 201–218.

Stringer, S. M., Hunter, N., and Woolhouse, M. E. J. (1998). A mathematical model of the dynamics of scrapie in a sheep flock. *Mathematical Biosciences*, **153** (2), 79–98.

Synge, B. A., Gunn, G., Ternent, H. E., Thomson-Carter, F., Foster, G., and McKendrick, I. J. (2000). Preliminary results from epidemiological studies in cattle in scotland, in zoonotic infections in livestock and the risk to public health. *Royal College of Physicians of Edinburgh, Edinburgh*, pages 10–11. June 28th.

Taylor, K. C. (2002). Environmental impacts of the foot and mouth disease outbreak in Great Britain in 2001: the use of risk analysis to manage the risks in the countryside. *Revue Scientifique et Technique del Office International des Epizooties*, **21** (3), 797–813.

Taylor, L. H., Latham, S. M., and Woolhouse, M. E. J. (2001). Risk factors for human disease emergence. *Philosophical Transactions of the Royal Society of London, Series B-Biological sciences*, **356** (1411), 983–989.

Thompson, D., Muriel, P., Russell, D., Osborne, P., Bromley, A., Rowland, M., Creigh-Tyte, S., and Brown, C. (2002). Economic costs of the foot and mouth disease outbreak in the United Kingdom in 2001. *Revue Scientifique et Technique del Office International des Epizooties*, **21** (3), 675–687.

Thrusfield, M. V. (1995). *Veterinary Epidemiology.* Blackwell Science, Oxford.

Valleron, A. J. (2000). Roles of mathematical modelling in epidemiology. *Comptes Rendus de l Academie des Sciences Serie III-Sciences de la vie-Life Sciences*, **323** (5), 429–433.

van Nes, A., de Jong, M. C. M., Buijtels, J. A. A. M., , and Verheijden, J. H. M. (1998). Implications derived from a mathematical model for eradication of pseudorabies virus. *Preventive Veterinary Medicine*, **33** (1–4), 39–58.

van Nes, A., de Jong, M. C. M., Kersten, A. J., Kimman, T. G., and Verheijden, J. H. M. (2001). An analysis of a presumed major outbreak of pseudorabies virus in a vaccinated sow herd. *Epidemiology and Infection*, **126** (1), 119–128.

Venables, W. N. and Ripley, B. D. (1994). *Modern Applied Statistics with S-Plus.* Springer-Verlag, New York, Inc.

Watson, Y. (2001). Zoonotic Escherichia coli. *ACTA Veterinaria Scandinavica*, pages 79–84.

Weber, T., Otto, M., Bodemer, M., and Zerr, I. (1997). Diagnosis of Creutzfeldt-Jakob disease and related human spongiform encephalopathies. *Biomedicine and Pharmacotherapy*, **51** (9), 381–387.

Weiss, R. A. (2001). The leeuwenhoek lecture 2001. animal origins of human infectious disease. *Philosophical Transactions of the Royal Society of london, Series B-Biological sciences*, **356** (1410), 957–977.

Woolhouse, M. E. J. (2003). Foot-and-mouth disease in the UK: What should we do next time? *Journal of Applied Microbiology*, **94**, 126S–130S.

Woolhouse, M. E. J., Haydon, D. T., Pearson, A., and Kitching, R. P. (1996). Failure of vaccination to prevent outbreaks of foot-and-mouth disease. *Epidemiology and Infection*, **116** (3), 363–371.

Woolhouse, M. E. J., Matthews, L., Coen, P., Stringer, S. M., Foster, J. D., and Hunter, N. (1999). Population dynamics of scrapie in a sheep flock. *Philosophical Transactions of the Royal Society of London, Series B-Biological sciences*, **354** (1384), 751–756.

Woolhouse, M. E. J., Stringer, S. M., Matthews, L., Hunter, N., and Anderson, R. M. (1998). Epidemiology and control of scrapie within a sheep flock. *Proceedings of the Royal Society of London, Series B-Biological Sciences*, **265** (1402), 1205–1210.

Zwingmann, W. and Fiedler, J. (2001). FMD and international trade relations - conditions and consequences. *Deutsche Tierarztliche Wochenschrift*, **108** (12), 518–521.